

Technical Report

Title: *Borehole DGR-3 and DGR-4 Porewater Investigations*

Document ID: TR-08-40


Authors: Monique Hobbs, Antoine de Haller,
Margarita Koroleva, Martin Mazurek, Jorge
Spangenberg, Urs Mäder and Dimitri Meier
Rock Water Interaction (RWI),
University of Bern

Revision: 0

Date: March 31, 2011

DGR Site Characterization Document
Geofirma Engineering Project 08-200



Intera Engineering DGR Site Characterization Document	
Title:	Borehole DGR-3 and DGR-4 Porewater Investigations
Document ID:	TR-08-40
Revision Number:	0 Date: March 31, 2011
Authors:	Monique Hobbs, Antoine de Haller, Margarita Koroleva, Martin Mazurek, Jorge Spangenberg, Urs Mäder and Dimitri Meier, Rock Water Interaction (RWI), University of Bern
Technical Review:	Richard Jackson, Dru Heagle, Kenneth Raven; Ian Clark (University of Ottawa); Laura Kennell (NWMO)
QA Review:	John Avis
Approved by:	 Kenneth Raven

Document Revision History		
Revision	Effective Date	Description of Changes
0	March 31, 2011	Initial issue

**Institute of Geological Sciences
University of Bern, Switzerland**

RWI Technical Report TR 10-01

**Borehole DGR-3 and DGR-4
Porewater investigations**

**Monique Y. Hobbs¹, Antoine de Haller¹, Margarita Koroleva², Martin
Mazurek¹, Jorge Spangenberg³, Urs Mäder¹ and Dimitri Meier¹**

¹Rock-Water Interaction (RWI), Institute of Geological Sciences, University of Bern, Switzerland

²Now at the Department of Earth Sciences, University of Hamburg, Germany.

³Institute of Mineralogy and Geochemistry, University of Lausanne, Switzerland

Revision: February 2011



u^b

^b
UNIVERSITÄT
BERN

Contents

CONTENTS.....	I
LIST OF TABLES.....	III
LIST OF FIGURES.....	VI
1 INTRODUCTION.....	12
2 METHOD ADVANCES.....	13
2.1 Petrophysical properties.....	13
2.1.1 Gravimetric water content.....	13
2.1.3 Measurement of bulk dry density.....	14
2.2 Aqueous Leaching.....	14
2.3 Ethanol-water extractions.....	15
2.4 Water isotope diffusive-exchange technique.....	15
2.4.1 Approach for DGR3 samples.....	16
2.4.2 Approach for DGR4 samples.....	16
2.5 Advective Displacement.....	16
2.5.1 Experimental setup and sampling procedures.....	17
3 ROCK MINERALOGY.....	19
3.1 Litho-stratigraphy and petrography.....	19
3.2 Mineralogy of the whole rock.....	20
DGR-3 samples.....	20
DGR-4 samples.....	20
4 POREWATER AND PETROPHYSICAL PARAMETERS.....	43
4.1 Water activity.....	43
4.2 Water and porewater contents.....	47
4.2.1 Water content.....	47
4.2.2 Porewater contents.....	53
4.3 Densities.....	65
4.4 Physical and porewater-loss porosity.....	69
5 STABLE ISOTOPES OF POREWATER ($\delta^{18}\text{O}$ AND $\delta^2\text{H}$).....	77
5.1 Methodological improvements and data screening.....	77
5.2 Water contents.....	81
5.3 Stable isotopic composition of porewater.....	83
5.4 Evaluation of the adapted diffusive isotope-exchange method applied to DGR samples and comparison with other databases.....	84
6 AQUEOUS EXTRACTIONS.....	98
6.1 Evidence for mineral dissolution.....	110
6.1.1 Halite.....	110
6.1.2 Sulphate minerals.....	114
6.1.3 Carbonate minerals.....	116
6.2 Data screening for soluble salts.....	118
6.3 Additional screening from scaling to water content.....	130
6.3.1 Scaling to water content.....	130
6.3.2 Speciation modelling to predict saturation indices.....	134
7 ETHANOL-WATER EXTRACTIONS.....	140
7.1 Behaviour of ethanol-water mixtures.....	140

II

7.2	Extractions with minerals	141
7.3	Extractions with DGR-3 samples	142
8	OUT-DIFFUSION EXPERIMENTS	153
8.1	Time-series Cl ⁻ concentrations	154
8.2	Final solutions	155
8.2.1	<i>Chemical compositions</i>	155
8.2.2	<i>Carbon isotopic compositions</i>	162
8.3	Porosity	163
8.4	Constraints on Cl ⁻ concentration of porewaters.....	164
8.5	Estimation of Cl ⁻ pore diffusion coefficient (D _p)	165
9	ADVECTIVE DISPLACEMENT – INITIAL RESULTS	169
10	POREWATER CHARACTERISATION – STATUS.....	172
10.1	Defining porewater chemical composition.....	172
10.2	Apparent porewater ion concentrations.....	176
10.2.1	<i>Apparent ion molalities in porewater</i>	176
10.2.2	<i>A starting point to account for ion-accessible porosity</i>	188
10.3	Reconstructive geochemical modelling.....	193
10.3.1	<i>How does current information measure up?</i>	194
10.4	Porewater characterisation - recommendations	198
11	SUMMARY AND CONCLUSIONS.....	199
11.1	Evidence for the saturation state of DGR samples	199
11.2	Chemical composition of porewaters	200
11.3	Testing of other methodologies for porewater extractions.....	202
11.3	<i>Stable isotope composition of porewaters</i>	202
	ACKNOWLEDGEMENTS	204
	REFERENCES	201
	APPENDIX A: SUPPLEMENTARY INFORMATION FOR THE DIFFUSIVE EXCHANGE TECHNIQUE	205
A1.0	Diffusive Isotope Exchange Technique.....	206
A1.1	<i>Isotopic composition of porewater</i>	206
A1.2	<i>Water content by the diffusive isotope-exchange technique</i>	207
A1.3	<i>Error calculation</i>	208
A2.0	Protocol for the adapted diffusive-isotope exchange technique (saline porewaters).....	208
A2.1	<i>Protocol for analysis of oxygen and hydrogen isotopes in saline waters</i>	209
A2.2	<i>Data screening criteria for the adapted diffusive isotope exchange technique</i>	211
	APPENDIX B: SUPPLEMENTARY INFORMATION ON GRAVIMETRIC WATER CONTENT	
	MEASUREMENTS	227
	APPENDIX C: RESULTS FOR DUPLICATE AQUEOUS EXTRACTIONS, DGR-3 AND DGR-4	
	SAMPLES.....	235
	APPENDIX D: SUPPORTING PETROPHYSICAL DATA, UNIVERSITY OF NEW BRUNSWICK	
	SAMPLES.....	241
	APPENDIX E: REVISED DGR-2 DATA.....	245

List of Tables

Table 1: Petrography of DGR-3 samples	22
Table 2: Petrography of DGR-4 samples	24
Table 3: Mineralogy of DGR-3 whole rock samples based on X-Ray diffraction and CS-Mat IR spectroscopy	26
Table 4: Mineralogy of DGR-4 whole rock samples based on X-Ray diffraction and CS-Mat IR spectroscopy	27
Table 5: Summary of DGR-3 samples containing soluble minerals	28
Table 6: Summary of DGR-4 samples containing soluble minerals	28
Table 7: Measured water activities of samples from DGR-3	45
Table 8: Measured water activities of samples from DGR-4	46
Table 9: Average gravimetric water contents ($WC_{Grav.}$) of DGR-3 samples determined by drying to constant mass at different temperatures. The water contents are calculated relative to the wet ($WC_{Grav. wet}$) or dry ($WC_{Grav. dry}$) mass of the rock sample	49
Table 10: Average gravimetric water content ($WC_{Grav.wet}$) of DGR-4 samples calculated relative to the wet mass of the rock sample. Water contents were determined by drying to constant mass at 40 °C or 105 °C	51
Table 11: Average gravimetric water content ($WC_{Grav.dry}$) of DGR-4 samples calculated relative to the dry mass of the rock sample. Water contents were determined by drying to constant mass at 40 °C or 105 °C	52
Table 12: Solutions used as estimates of porewater salinity over the sedimentary sequence (Bass Islands through to the Cambrian)	56
Table 13: Porewater contents for DGR-3 samples calculated relative to wet ($PWC_{Grav.wet}$) or dry ($PWC_{Grav.dry}$) mass of rock	58
Table 14: Porewater contents for DGR-4 samples calculated relative to wet ($PWC_{Grav.wet}$) or dry ($PWC_{Grav.dry}$) mass of rock	60
Table 15: Comparison of porewater contents for DGR-3 samples calculated relative to wet ($PWC_{Grav.wet}$) mass of rock using estimated porewater salinities and densities from this study and from Intera, 2010a	61
Table 16: Comparison of porewater contents for DGR-4 samples calculated relative to wet ($PWC_{Grav.wet}$) mass of rock using estimated porewater salinities and densities from this study and from Intera, 2010a	63
Table 17: Bulk and grain densities determined for DGR-3 samples	67
Table 18: Bulk and grain densities determined for DGR-4 samples	68
Table 19: Calculated porewater-loss (ϕ_{PWL}) and physical porosities (ϕ_{tot}) of DGR-3 samples	70
Table 20: Calculated porewater-loss (ϕ_{PWL}) and physical porosities (ϕ_{tot}) of DGR-4 samples	72
Table 21: Summary of data screening procedure for experiments with DGR-3 samples	78
Table 22: Summary of data screening performed for experiments with DGR-4 samples	79
Table 23: Borehole DGR-3. Isotope Diffusive Exchange Experiments: Measured isotopic compositions of the test solutions and calculated porewater compositions	92

IV

Table 24:	Borehole DGR-3. Water contents calculated from isotope diffusive exchange data and measured by oven-drying.....	94
Table 25:	Borehole DGR-4. Isotope Diffusive Exchange Experiments: Measured isotopic composition of the test solutions and calculated porewater compositions.	96
Table 26:	Borehole DGR-4. Water contents calculated from isotope diffusive exchange data and determined by oven-drying.....	97
Table 27:	Borehole DGR-3: Chemical composition of aqueous extract solutions from experiments conducted at a solid:liquid ratio of 1:1. Reported values are the average of two replicates. 100	100
Table 28:	Borehole DGR-4: Chemical composition of aqueous extract solutions from experiments conducted at a solid:liquid ratio of 1:1. Reported values are the average of two replicates. 102	102
Table 29:	Comparison of Br ⁻ concentrations determined in aqueous extract solutions for samples from boreholes DGR-3 and DGR-4 using IC and ICP-MS analyses.	103
Table 30:	Borehole DGR-3: Concentration of ions in meq/kg _{rock} calculated from the chemical compositions of aqueous extract solutions. Reported values are the average of two replicates. 104	104
Table 31:	Borehole DGR-4: Concentration of ions in meq/kg _{rock} calculated from the chemical compositions of aqueous extract solutions. Reported values are the average of two replicates. 106	106
Table 32:	Borehole DGR-3: Saturation indices (SI) calculated for aqueous extraction solutions. Shading indicates SI values ≈ 0.0.	107
Table 33:	Borehole DGR-4. Saturation indices (SI) calculated for aqueous extraction solutions. Shading indicates SI values ≈ 0.0.	109
Table 34:	Evidence suggesting the presence of presence of soluble salts in samples from DGR-3 and DGR-4; Evidence for DGR-2 samples is primarily from Koroleva et al. (2009).	120
Table 35:	Dataset of DGR-3 and DGR-4 samples for further evaluation showing dominant ions in solution.	121
Table 36:	Millimolalties of ions for aqueous extract solutions from DGR-3 scaled to water content (WC _{Grav.dry}).	132
Table 37:	Millimolalties of ions for aqueous extract solutions for samples from DGR-4 scaled to water content (WC _{Grav.dry}).	133
Table 38:	DGR-3 - Saturation indices for selected minerals, calculated using the scaled aqueous extract solutions and PhreeQC with pitzer thermodynamic database.....	137
Table 39:	DGR-4 - Saturation indices for selccted minerals, calculated using the scaled aqueous extract solutions and PhreeQC with the pitzer thermodynamic database.....	138
Table 40:	Amount of Na ⁺ and Cl ⁻ dissolved in ethanol-water solutions during extraction experiments with halite and for two different reaction times (units are mg per kg of halite).	142
Table 41:	Results of ethanol-water extractions conducted at multiple ethanol:water ratios (mg/kg of dry rock). Concentrations determined in the aqueous extractions (0% ethanol) are also shown for comparison.	145
Table 42:	Results of ethanol-water extractions conducted at one ethanol:water ratio chosen to replicate the original water content of the rock. Results are reported in mg/kg of dry rock.	149

Table 43: Comparison between the quantity of Br ⁻ and Cl ⁻ determined using aqueous extraction and an ethanol-water extraction in which the quantity of water added was matched to the original water content of the sample.	151
Table 44: DGR-4 samples and experimental parameters used in the out-diffusion experiments..	153
Table 45: Chemical and isotopic composition of initial test solution used in the out-diffusion experiments.	154
Table 46: Chemical and isotopic data for the final experimental solutions from out-diffusion experiments conducted on samples from borehole DGR-4.....	158
Table 47: Modelled parameters for the final experiment solutions from out-diffusion experiments conducted on samples from borehole DGR-4.....	159
Table 48: Isotope composition ($\delta^{13}\text{C}$ and $\delta^{18}\text{O}$) of matrix carbonate (calcite and/or dolomite) in DGR-4 samples used in out-diffusion experiments.....	162
Table 49: Water content and water-loss porosity of samples used for out-diffusion experiments from boreholes DGR-1 and DGR-2. The data are uncorrected for mineral dissolution effects during the experiment.	164
Table 50: Apparent concentrations of Cl ⁻ in the porewater calculated based on corrected Cl ⁻ concentrations in final experimental solution (out-diffusion), the mass of test solution added and the water content ($\text{WC}_{\text{Grav.wet}}$) of the samples determined at the end of the experiment.	165
Table 51: Estimated pore diffusion coefficient for chloride (parallel to bedding as determined at 45 °C), obtained from modelling the concentration time-series of out-diffusion experiments assuming radial diffusion.....	166
Table 52: Assessment of the sources of extractable cations determined using aqueous extraction for the select dataset (i.e. subset in which evidence for the presence of soluble salts was not observed).....	174
Table 53: Assessment of the sources of extractable anions determined using aqueous extraction for the select dataset (i.e. subset in which evidence for the presence of soluble salts was not observed).....	175
Table 54: Select dataset for DGR-3 in which presence of soluble salts was not observed petrographically. Apparent porewater concentrations (mmol/kgH ₂ O) have been calculated using water contents determined gravimetrically at 105 °C ($\text{WC}_{\text{Grav.dry}}$).....	178
Table 55: Select dataset for DGR-4 in which presence of soluble salts was not observed petrographically. Apparent porewater concentrations (mmol/kgH ₂ O) have been calculated using water contents determined gravimetrically at 105 °C ($\text{WC}_{\text{Grav.dry}}$).....	179
Table 56: Select dataset for DGR-3 in which presence of soluble salts was not observed petrographically. Apparent porewater concentrations in mmol/L of porewater, calculated using bulk dry densities and porewater-loss porosity.....	190
Table 57: Select dataset for DGR-3 in which presence of soluble salts was not observed petrographically. Apparent porewater concentrations in mmol/L of porewater, calculated using bulk dry densities and porewater-loss porosity.....	191
Table 58: Apparent porewater concentrations of Cl ⁻ in shale samples from DGR-3 and -4 calculated using ion accessible porosity.....	192
Table 59: Potential constraints on major elements for the next stage in exploratory modelling of apparent porewater compositions.	197

List of Figures

- Figure 1: Sample DGR-3 380.88 (Salina A1 Evaporite). A and B: Massive evaporite rock essentially composed of anhydrite, with minor dolomite and traces of pyrite. C to E: Traces of aluminosilicate minerals have been found in very small veinlets (<10 μ thickness). This silicate mineral could not be identified because of its small size, which results in the EDS analysis being perturbed by the matrix (part or all of the S, Ca, Mg and Fe signals can be related to the surrounding dolomite and anhydrite). The position of the EDS analysis given in E is shown in D. All pictures are back-scattered electron views of uncoated thin sections. 29
- Figure 2: Sample DGR-3 484.58 (Queenston). A and B (B is a detailed view of A): Anhydrite-celestite nodule in Queenston Formation. Celestite appears as mm-sized crystals enclosed in finely crystallized anhydrite. C: Nodules of anhydrite-celestite in shale. Celestite crystals are cut at the border of the nodule, indicating reworking after crystallization. It is unclear if this reworking is synsedimentary, diagenetic or tectonic. Cl has been detected with the EDS in the shaly matrix, but not in the sulphate nodules. Due to the small grain size, no Cl-bearing phase could be identified. D and E: Celestite crystal in anhydrite, and EDS analysis of the celestite, showing minor amounts of Ba replacing Sr. Pictures A and B are crossed nicols views in transmitted light, while pictures C and D are back-scattered electron views of uncoated, freshly broken rock chips. 30
- Figure 3: Sample DGR-3 531.65 (Georgian Bay). A and B: Anhydrite cement in sandy beds. C: Anhydrite patch in a sandy bed near a shaly horizon. All pictures are taken under crossed nicols transmitted light. The identification of anhydrite has been confirmed by Raman microprobe. 31
- Figure 4a: Sample DGR-3 391.34 (Guelph). A: Vein in dolomitised rock filled by dolomite crystals and paragenetically later halite. Black areas correspond to remaining porosity. The host rock contains traces of disseminated pyrite (white dots). B: EDS analysis of the point indicated in A, corresponding to halite. The small peaks of Ca, Mg, and O are due to the matrix effect of the nearby dolomite. C to F: Small veinlet (about 50 μ m thick) filled by dolomite and later calcite and halite. Black areas are remaining porosity. E: EDS analysis of the point shown in F, corresponding to calcite. The small peaks of Mg, Cl, and Na are due to the nearby presence of halite and dolomite. All pictures are back-scattered electron views of uncoated thin sections. 32
- Figure 5: Sample DGR-3 270.06 (Salina-C). Dolomitic shale showing clusters of small pores (<100 μ m). View B is a detailed view of A and C is a detailed view of B. The interstitial clay is chlorite (view C). No halite was found in the pore spaces observed in the thin section. View E: 50 μ m thick vein of halite cutting the rock. View F: EDS analysis of the halite vein shown in E. All pictures are back-scattered electron views of an uncoated thin section (A to D) or a freshly broken rock chip (E). 34
- Figure 6: Sample DGR-3 856.06 (Cambrian). View A and B (B is a detailed view of A): Rhombohedral hydrothermal adularia (grey birefringence) in Cambrian sandy dolostone. Both pictures under crossed nicols. 35
- Figure 7: Sample DGR4-189.16 (Salina-F). Grey-blue dolomitic silty shale cut by gypsum veins. Gypsum contains tiny inclusions of anhydrite (higher birefringence order). View A is under parallel and view B is under crossed nicols transmitted light. 35

VII

- Figure 8: Sample DGR4-229.32 (Salina - E). Silty dolomitic shale cut by veins filled with fluidized rock flour and gypsum crystals (apparently grown in situ). The bedding of the host rock is visible on both sides of the vein structure. View A is under parallel and B under crossed nicols transmitted light. 36
- Figure 9: Sample DGR4-847.48 (Cambrian). Sandy medium grained dolostone. The carbonate fraction of the rock is completely recrystallised to dolomite, but the primary oolitic texture is still preserved. View A is under parallel and B under crossed nicols transmitted light. In A, the brightest grains are quartz. 36
- Figure 10: Depth profiles of calcite and dolomite-ankerite contents. Samples that plot at zero are below the detection limit (see Table 3 and Table 4, and Figure 11). 37
- Figure 11: Depth profiles of dolomitisation, expressed as $100 \cdot \text{dolomite} / (\text{dolomite} + \text{calcite})$. In this calculation, the sum of the dolomite and ankerite contents is used as a proxy for dolomite (see Table 3 and Table 4, and Figure 10). 38
- Figure 12: Depth profiles of siliciclastic minerals and total clay content (assumed to correspond closely to the sum of sheet silicates). Samples that plot at zero are below the detection limit (see Table 3 and Table 4). 39
- Figure 13: Depth profiles of the total sulphur content as determined by CS-Mat (see Table 3 and Table 4).
40
- Figure 14: Depth profiles of sulphur-bearing mineral contents. For the Salina-A2 Evaporite samples, these contents were calculated from the total sulphur content measured by CS-Mat and from XRD data (Table 3 and Table 4). In the other samples, all the sulphur was attributed to the main sulphur-bearing phase observed by optical microscopy. In samples for which a sulphur-bearing mineral content of zero is indicated, the mineral was either not detected or was present in negligible amounts (based on microscopic observations). 41
- Figure 15: Depth profile of the C_{org} content by CS-Mat (see Table 3 and Table 4). 42
- Figure 16: Water activity measured for samples from DGR-2, DGR-3 and DGR-4 as a function of depth (data for DGR-2 samples are from Koroleva et al. 2009). Error bars illustrate the measurement accuracy of the water activities (± 0.015). For samples from DGR-3 and -4, depths have been corrected relative to boreholes DGR-1/-2 (see Table 7 and Table 8). 44
- Figure 17: Porewater content ($\text{PWC}_{\text{Grav.wet}}$) plotted as a function of depth below ground surface in boreholes DGR-2, -3 and -4. Error bars show the uncertainty in the calculated porewater contents. Depths for samples from DGR-3 and -4 are corrected relative to DGR-1/2. 57
- Figure 18: Total sheet silicate content (or clay content) versus calculated porewater content ($\text{PWC}_{\text{Grav.wet}}$) for select samples for which mineralogy was determined. Samples plotting at zero had a sheet silicate content that was below detection ($< 1 \text{ wt.}\%$). 64
- Figure 19: Comparison between calculated and measured bulk densities for DGR-4 samples. Error bars indicate the calculated uncertainty in each parameter. 65
- Figure 20: Porewater-loss porosity versus physical (or total) porosity for samples from boreholes DGR-2, -3 and -4. For clarity, the errors associated with both porosities are not shown on this compilation plot, but are included in Figure 21 and Figure 22. 73
- Figure 21: Porewater-loss porosity versus physical porosity for samples from DGR-2. The error bars show the calculated uncertainty in both parameters. 74
- Figure 22: Plots showing porewater-loss porosity versus physical porosity for samples from DGR-3 (upper) and -4 (lower), including error bars showing the uncertainty in both parameters.

VIII

- Figure 23: Comparison between sample water activity (a_w) and test water a_w in DGR-3 and DGR-4 samples. In these diagrams, the a_w of each individual test water is calculated from its salinity, based on the recorded amount of salt and standard water added to prepare the test water. For DGR-3, the salinities of the test waters are not known exactly, because the masses of salts and standard waters added were not recorded. The calculated salinities and water activities are, therefore, based on the target concentrations (e.g. 5M NaCl). For two samples from DGR-4 (DGR-4-472.78, Queenston Formation; DGR-4-717.12, Sherman Fall Formation), a 3 molal CaCl_2 was used when a 4 molal solution would have provided a better match to the sample water activity. This resulted in a mismatch in a_w of approximately 0.1 between the rock samples and test solutions..... 80
- Figure 24: Water content (WC) by isotopic exchange and drying methods. Values of $\text{WC}_{\delta^{18}\text{O}}$ and $\text{WC}_{\delta^2\text{H}}$ are shown only for samples that passed the screening procedure. If not visible, error bars are smaller than the symbol. Gravimetric water contents ($\text{WC}_{\text{Grav.wei}}$) were measured only at 105°C in DGR-3 LAB and TEW samples (a correction for mass transfer during experiments was applied, as described in section 2.1.1). Error bars on the gravimetric data correspond to the absolute difference between the values measured on the LAB and TEW subsamples. 82
- Figure 25: Profiles showing calculated $\delta^{18}\text{O}$ values of porewater and groundwater versus depth along borehole for samples from boreholes DGR-3 and DGR-4 (groundwater values are from Intera 2009). When not visible, error bars are smaller than the symbols..... 86
- Figure 26: Profiles showing calculated $\delta^2\text{H}$ values of porewater and groundwater versus depth along borehole for samples from boreholes DGR-3 and DGR-4 (groundwater data are from Intera 2009). When not visible, error bars are smaller than the symbols..... 87
- Figure 27: Plot of $\delta^2\text{H}$ versus $\delta^{18}\text{O}$ values of porewaters and groundwaters obtained from samples from DGR-3 and DGR-4 drillholes. The global meteoric water line (GMWL) is also shown. 88
- Figure 28: Comparison of the stable isotope compositions of porewaters determined by the University of Bern (UniBe) and University of Ottawa (UniO) versus depth. Values for groundwater samples from DGR-1 to DGR-4 are also shown for comparison. In the legend, PW indicates porewater and GW indicates groundwater. Depths of DGR-3 and DGR-4 samples were corrected relative to the DGR-1/2 borehole (UniBe: DGR-3 sample depths -14.46m; DGR-4 sample depths -1.05m)..... 89
- Figure 29: $\delta^2\text{H}$ versus $\delta^{18}\text{O}$ plot of DGR-3 and DGR-4 isotope diffusive exchange results (UniBe) compared to DGR-1 to 4 data by University Ottawa (UniO) and groundwater isotopic compositions from boreholes DGR-1 to 4 (Intera, 2008c; 2009a). GMWL = global meteoric water line. In the legend: PW indicates porewater and GW indicates groundwater. In DGR-3 and DGR-4, groundwaters were sampled in the Salina A1, Guelph and in the Cambrian, whereas in DGR-2, groundwater was sampled in the Cambrian. The lithostratigraphic units to which each UniBern sample belongs are shown in Figure 27..... 90
- Figure 30: Data for groundwaters from Southern Ontario (Hobbs et al., 2008). 91
- Figure 31: Concentrations in milliequivalents of Na^+ and Cl^- extracted per kilogram of dry rock at a S:L ratio of 1:1. Error bars indicate analytical uncertainty in concentrations measured in aqueous extract solutions (max. $\pm 10\%$). In several samples, the Na:Cl ratio is 1:1, within the analytical uncertainty, suggesting halite dissolution (in situ or during the extraction) could be the source of these ions..... 111

- Figure 32: Na/Cl ratio (mol/mol) for samples from boreholes DGR-2, DGR-3 and DGR-4 plotted versus depth in meters (relative to DGR-1/2). Error bars indicate the maximum analytical uncertainty in the measured ion concentrations in the aqueous extracts ($\pm 10\%$). 111
- Figure 33: Concentrations in meq/kg_{rock} of Br⁻ and Cl⁻ in aqueous extracts at a S:L ratio of 1:1. Data for DGR-2 samples is from Koroleva et al. (2009). Error bars indicate analytical uncertainty in Br⁻ and Cl⁻ concentrations (max. $\pm 10\%$) measured in aqueous extract solution. 112
- Figure 34: Br/Cl ratio (mol/mol) for samples from boreholes DGR-2, DGR-3 and DGR-4 plotted versus depth in meters. Error bars indicate analytical uncertainty in Cl⁻ concentrations of $\pm 10\%$. Depths for samples from DGR-3 and DGR-4 are corrected relative to DGR-1/2. The Br/Cl ratio of seawater is also shown (dashed line)..... 113
- Figure 35: Sulphate concentration in meq/kg_{rock} plotted as a function of depth as determined for samples from DGR-3, DGR-4 (solid symbols) and DGR-2 (open squares) by aqueous extraction at a S:L ratio of 1:1. Data for DGR-2 samples is from Koroleva et al. (2009). 114
- Figure 36: Concentration of SO₄²⁻ versus Ca²⁺ in meq/kg_{rock} determined by aqueous extraction at a S:L ratio of 1:1. Data for DGR-2 samples is from Koroleva et al. (2009). Error bars indicate analytical uncertainty (max. $\pm 10\%$). 115
- Figure 37: Concentrations of Mg²⁺ versus Ca²⁺ in extract solutions per kg rock for experiments conducted at a S:L ratio of 1:1. The dashed line represents the Ca/Mg activity ratio at equilibrium with both calcite and dolomite (1.34). 117
- Figure 38: Cl⁻ concentration determined using aqueous extraction plotted versus A) porewater content (PWC_{Grav.wet}), and B) water content (WC_{Grav.wet}) for samples in which soluble salts were not identified (see Table 35). BI = Bass Islands, Q = Queenston, Kf = Kirkfield, SF = Sherman Fall. Error bars show the analytical uncertainty in Cl⁻ of $\pm 10\%$, the standard deviation observed in the water content determinations and the calculated uncertainty in the porewater contents (see section 4.2 for details). When the extracted ion concentrations are scaled to porewater content (section 6.3.2), several samples are predicted to be close to saturation with respect to halite (SI of approximately ± 0.3), as indicated in B). 122
- Figure 39: Br⁻ concentration determined by aqueous extraction plotted against A) porewater content in wt.% (PWC_{Grav.wet}) and B) Cl⁻ concentration, for samples in which soluble salts were not identified (see Table 35). C = Cambrian, GB = Georgian Bay formations. The dashed line shows the linear correlation coefficient, $r^2=0.97$, calculated for all plotted data points (i.e. including labelled samples). 123
- Figure 40: Na⁺ concentration determined by aqueous extraction plotted against A) porewater content in wt.% (PWC_{Grav.wet}) and B) Cl⁻ concentration, for samples in which soluble salts were not identified (see Table 35). CH = Cabot Head, Q = Queenston, Cm = Cambrian. The dashed line shows the linear correlation coefficient $r^2=0.96$ calculated for all plotted data points (i.e. including labelled samples). 124
- Figure 41: Ca²⁺ concentration determined by aqueous extraction plotted against A) porewater content in wt.% (PWC_{Grav.wet}) and B) Cl⁻ concentration, for samples in which soluble salts were not identified (see Table 35). CH = Cabot Head Formation. The dashed line shows the linear correlation ($r^2=0.98$) calculated for all plotted data points (i.e. including labelled samples).
124
- Figure 42: Mg²⁺ concentration determined by aqueous extraction plotted against A) porewater content in wt.% (PWC_{Grav.wet}) and B) Cl⁻ concentration, for samples in which soluble salts were not identified (see Table 35). 125

- Figure 43: Sr^{2+} concentration determined by aqueous extraction plotted against A) porewater content in wt.% ($\text{PWC}_{\text{Grav.wet}}$) and B) Cl^- concentration, for samples in which soluble salts were not identified (see Table 35). Q = Queenston, GB = Georgian Bay, Cc = Coboconk, SL = Shadow Lake, Cm = Cambrian. 126
- Figure 44: Concentration of A) Mg^{2+} and B) Sr^{2+} extracted from samples from DGR-2, -3 and -4 plotted as a function of depth. Depths of DGR-3 and DGR-4 samples are plotted as a function of depth relative to boreholes DGR-1/2. Data for DGR-2 samples are from Koroleva et al. (2009). 127
- Figure 45: K^+ concentration determined by aqueous extraction plotted against A) porewater content in wt.% ($\text{PWC}_{\text{Grav.wet}}$) and B) Cl^- concentration, for samples in which soluble salts were not identified (see Table 35). BI = Bass Islands, Mn = Manitoulin, Q = Queenston, SL = Shadow Lake, Cm = Cambrian, Pc = Precambrian. 129
- Figure 46: SO_4^{2-} concentration determined by aqueous extraction plotted against A) porewater content in wt.% ($\text{PWC}_{\text{Grav.wet}}$) and B) Cl^- concentration, for samples in which soluble salts were not identified (see Table 35). Q = Queenston, GB = Georgian Bay, Co = Cobourg, GR = Gull River. 129
- Figure 47: Saturation indices of halite calculated for scaled aqueous extract solutions from DGR-3 and DGR-4 samples. Data are plotted as a function of depth relative to boreholes DGR-1/2. Data for DGR-2 samples are from Koroleva et al. (2009). 139
- Figure 48: Extracted major ion concentrations in $\text{mg/kg}_{\text{rock}}$ with increasing ethanol in solution from 0 to over 99 vol.%. Results are shown for two samples in which halite was identified. Error bars show the approximate analytical uncertainty of $\pm 15\%$ in the concentrations determined using ethanol-water extractions. 147
- Figure 49: Extracted major ion concentrations in $\text{mg/kg}_{\text{rock}}$ with increasing ethanol in solution from 0 to over 99 vol.%. Results are shown for selected samples where no evidence for halite was found (anhydrite was identified in DGR-3 531.65). Error bars show the estimated analytical uncertainty of $\pm 15\%$ in the concentrations determined using ethanol-water extraction. 148
- Figure 50: Cl^- concentrations in the experimental solutions as a function of time in the out-diffusion experiments; conducted on DGR-4 core samples from the Salina F Unit (DGR-4 189.16), Georgian Bay (DGR-4 520.42), Cobourg (DGR-4 665.41) and Kirkfield formations (DGR-4 730.07). 156
- Figure 51: Photographs of the sample of the Georgian Bay Formation (DGR-4 520.42) taken after termination of the out-diffusion experiment and water content determinations (105°C). A) Both sides of the parting along which the sample split during the out-diffusion experiments are shown. Alteration products (iron oxyhydroxides) were visible on the outside rims after several days of drying at 40°C . B) Parting in larger, intact piece of core after the out-diffusion experiments. 157
- Figure 52: Sample from the Salina F Unit (DGR-4 189.16) used in the out-diffusion experiment showing gypsum vein (length of core sample is 11 cm). Photographs were taken after 110 days of submersion in the out-diffusion experiment and drying to constant mass at 105°C 160
- Figure 53: Comparison of ion concentrations in the aqueous extract solutions (solid:liquid = 1:1; values are average of 2 replicates) with the final concentrations determined in the final solutions from the out-diffusion experiments, normalized to a solid:liquid ratio of 1:1. Error bars show the maximum analytical uncertainty of $\pm 10\%$ in the measured ion concentrations. 161
- Figure 54: Fit of estimated Cl^- pore diffusion coefficient (solid line) to time series data using a radial diffusion model. The complete profile is shown in the left-hand diagram; the right-hand

- diagram shows the fit to early-time data. The uncertainty range for D_p Cl⁻ is given by the dashed lines and represents values that are smaller and larger by a factor of 1.41 (square root of 2) corresponding to a factor of 2 in the diffusion time. 167
- Figure 55: Photographs showing A) core sample DGR-4 679.95 with its perimeter encapsulated in resin; B) after placement of a porous, Teflon disk on each end and titanium couplings; C) after wrapping core and edge of titanium couplings in Teflon and rubber-shrink tube sleeve to isolate the core from the confining medium; and D) start of experiment with core installed in advective displacement rig..... 169
- Figure 56: Plots showing the infiltration and confining pressures during the first two months of the advective displacement experiment conducted with an argillaceous limestone sample from the Cobourg Formation (DGR-4 697.95) and using TCE as the infiltrating fluid. 170
- Figure 57: Apparent porewater concentration of Cl⁻ (mmol/kg_{H2O}) and Br/Cl ratio as a function of depth for select dataset (Br/Cl ratio of modern seawater is also shown). Depths of DGR-3 and -4 samples are plotted relative to DGR-1/2. Depth positions in boreholes DGR-2 and DGR-3 where halite was observed petrographically are also shown (note that Cl⁻ concentrations and Br/Cl ratios plotted for these samples are meaningless). 180
- Figure 58: Apparent porewater concentration of Br⁻ (mmol/kg_{H2O}) and Br/Cl ratio as a function of depth for select dataset (Br/Cl ratio of modern seawater is also shown). Depths of DGR-3 and -4 samples are plotted relative to DGR-1/2. Depth positions in boreholes DGR-2 and DGR-3 where halite was observed petrographically are also shown (note that Br⁻ concentrations and Br/Cl ratios plotted for these samples are meaningless). 181
- Figure 59: Apparent porewater concentration of Na⁺ (mmol/kg_{H2O}) and Na/Cl ratio as a function of depth for select dataset. Depths of DGR-3 and DGR-4 samples are plotted relative to DGR-1/2. Depth positions in boreholes DGR-2 and DGR-3 where halite was observed petrographically are also shown (note that Na⁺ concentrations plotted for these samples are meaningless). 182
- Figure 60: Apparent porewater concentrations of Ca²⁺ (mmol/kg_{H2O}) and Ca/Cl ratio as a function of depth for select dataset. Depths of DGR-3 and -4 samples are plotted relative to DGR-1/2. 183
- Figure 61: Na/Ca ratio and δ¹⁸O determined for porewaters as a function of depth in boreholes DGR-1/2, DGR-3 and DGR-4 (see section 5.4 for additional details on stable isotope profiles).185
- Figure 62: Apparent porewater concentration of K⁺ (mmol/kg_{H2O}) and Na/K ratio as a function of depth for select dataset. Depths of DGR-3 and -4 samples are plotted relative to DGR-1/2.188

1 Introduction

Intra Engineering has been contracted by the Nuclear Waste Management Organization on behalf of Ontario Power Generation (OPG) to implement the Geoscientific Site Characterization Plan (GSCP) for the Bruce site located on Lake Huron, Ontario. The GSCP is described by Intra Engineering Ltd. (Intra, 2006; 2008a). The purpose of the site characterization work is to assess the suitability of the Bruce site to construct a Deep Geologic Repository (DGR) to store low-level and intermediate-level radioactive waste.

This Technical Report (TR) presents the results of porewaters investigations conducted on formations sampled in boreholes DGR-3 and DGR-4. These results are integrated with porewater characterization work conducted on DGR-2 samples (Koroleva et al., 2009), building on the understanding obtained from this earlier research. The work described in this report was completed by the Rock-Water Interaction Group, University of Bern, Switzerland, under contract to Intra Engineering Ltd.

In low porosity and permeability formations in the Palaeozoic sedimentary sequence at the Bruce site, direct sampling of porewaters is not feasible. Investigating the chemical composition of porewaters requires application of a suite of indirect techniques, each of which provides partial information. The understanding of porewater composition gained from the application of these techniques can be augmented with geochemical modelling.

To determine the isotopic composition of the porewaters, the diffusive exchange technique originally developed and applied by Rubel et al. (2002) has been adapted by RWI over the course of DGR site characterization activities for application to formations containing highly saline porewaters. This method was initially developed for rocks containing pore water with salinities up to seawater. Significant developments were required to adapt the method to high salinity pore waters (e.g. Waber et al., 2007; de Haller et al., 2008; Koroleva et al., 2009). The most recent and complete adaptation of this method was applied to samples from DGR-4.

To obtain information on the chemical compositions of the porewaters, results of aqueous extractions were evaluated together with mineralogical and petrophysical data to assess whether the extracted ions are predominantly from porewater or significantly influenced by water-rock reactions during the extractions. Where applicable, apparent porewater compositions were derived. As part of research on samples from DGR-3, ethanol-water extractions were also investigated as a potential technique for extracting porewater while minimizing mineral-water interactions during the extraction. The results of initial testing including extractions on pure mineral phases and on DGR-3 samples are presented in this report. Out-diffusion experiments have been performed on select formations, providing information on the pore diffusion coefficients for Cl⁻. Estimates of apparent Cl⁻ porewater concentrations from these experiments are compared to those determined for aliquots of the same samples using aqueous extraction. The advective displacement technique (e.g. Mäder et al., 2004; Mäder, 2005) was also tested as a direct method for the extraction of porewater from a sample of the Cobourg Formation; the results to date are summarized in this report. In the final section of the report, the status of our understanding of the chemical and isotopic composition of porewaters is evaluated and an approach for reconstructing porewater compositions using geochemical equilibrium modelling is presented.

2 Method Advances

The detailed methodologies for the experimental work conducted on DGR-3 and DGR-4 core are generally the same as those applied to DGR-2 core samples and are described in detail by Koroleva et al. (2009). Methods that are new or have undergone substantial development are described below.

2.1 Petrophysical properties

2.1.1 Gravimetric water content

For samples from DGR-4, a comprehensive examination of the analytical uncertainty in the water content determinations at both 40 and 105 °C was made by maintaining detailed records of the mass change as a function of time during drying. Samples were cooled to room temperature over silica desiccant for 3.5 (40 °C) or 4.5 (105 °C) hours prior to weighing. The criterion used for attainment of constant mass during gravimetric measurements was a mass change of less than 0.005 wt.% over a 14-day drying interval.

As described by Koroleva et al. (2009), two aliquots of rock material are prepared for water content determination during initial core sampling. In addition, the aliquots of rock material used in the water isotope diffusive exchange experiments were transferred to glass dishes after completion and their water contents were determined gravimetrically. In total, 4 gravimetric water content measurements are made for each sample. These same procedures were used in DGR-3 and DGR-4. However, water isotope diffusive exchange experiments are based on equilibration through the vapour phase between the pore water and a test water of known isotopic composition. It was noted that in cases where the activity of the test solution is not identical to that of the porewater during the diffusive exchange experiments, there is a small transfer of water between the test solution and rock material. This change in the water content of the sample during the diffusive exchange experiment is quantified using the difference between the initial and final masses of the rock material at the start and of the end of the experiment, respectively. To determine the initial water content of the aliquots at the beginning of the experiment, the water content determined gravimetrically is corrected using the following expression:

$$WC_{\text{grav. (wet or dry)}} = WC_{\text{end}} + \Delta WC_{\text{DEX}} \quad (1)$$

where the gravimetric water content of the initial rock material ($WC_{\text{grav. wet or dry}}$) is equal to the water content determined on the material at the end of the experiment (WC_{end}) plus the change in the water content (ΔWC_{DEX}) during the experiment. The analytical uncertainty associated with this correction is also accounted for in the error propagation.

This correction is an improvement in methodology from borehole DGR-2 and was applied to water content determinations reported for samples from DGR-3 and DGR-4. The DGR-2 water content data for sample aliquots from the diffusive exchange experiments have also been corrected using equation 1. The corrected data for individual replicates and for average water content values are included in Appendix E.

2.1.3 Measurement of bulk dry density

For samples from DGR-4, bulk dry density ($\rho_{b,dry}$) was measured in duplicate using the paraffin displacement method (this method is also used to measure bulk wet density ($\rho_{b,wei}$) as described in Koroleva et al., 2009). The principle of the method is the calculation of bulk dry density from sample mass and volume making use of Archimedes' principle.

Two separate, homogeneous rock pieces of a volume of approx. 1.5-2 cm³ each were taken from the sample aliquots that had been dried to constant mass at 105 °C for determination of gravimetric water content. The volume of each was determined by weighing the rock in air and during immersion into paraffin ($\rho_p = 0.86$ g/cm³ at 20 °C) using a density accessory kit (Mettler Toledo). The bulk dry density was calculated according to:

$$\rho_{b,dry} = \frac{\rho_p * m_{dry,rock}}{m_{dry,rock} - m_{(dry,rock)P}}, \quad (2)$$

where $m_{dry,rock}$ is the mass of the dry rock in air and $m_{(dry,rock)P}$ is the mass of the dry rock in paraffin.

2.2 Aqueous Leaching

The aqueous leaching protocol applied to the DGR-3 and DGR-4 samples is adapted from that used for the DGR-2 samples (Koroleva et al., 2009) and incorporates the following changes:

- i) The leaching or reaction time between the solid and water was reduced from 48 hours to 10 minutes, in an attempt to minimize the dissolution of minerals during leaching;
- ii) The solid:liquid ratio in all aqueous extractions performed on DGR-3 and DGR-4 samples was 1:1; 30 grams of dry, powdered solid was leached with 30 ml of doubly-deionized water. As for DGR-2 samples, all extractions were conducted in duplicate. The concentrations of both cations and anions in the extraction solutions were measured using ion chromatography; and
- iii) pH and alkalinity measurements were performed outside of the glovebox under atmospheric conditions;

In the protocol applied to the DGR-2 samples, both the pH measurements and alkalinity titrations were performed in the glovebox under a nitrogen atmosphere (Koroleva et al. 2009). It was suggested that the calculated supersaturation with respect to calcite observed in DGR-2 aqueous extracts could be a result of out-gassing of CO₂ from the extracts, resulting in higher measured pH values and supersaturation with respect to calcite in the extract solutions. In order to test this hypothesis, the protocol was adapted for DGR-3 and DGR-4 aqueous extractions, as described above (iii).

2.3 Ethanol-water extractions

The ethanol-water extraction technique was developed with the objective of extracting ions present in the porewater while minimizing the dissolution of any soluble minerals (in particular, anhydrite/gypsum and halite) during the extraction procedure. The method was developed and the first tests of the method were conducted on pure mineral phases (halite, gypsum and celestite) and on a suite of samples from DGR-3. The extraction procedure is described below. For the majority of samples examined from DGR-3, multiple extractions were conducted using solutions containing between 70 and 99.9% ethanol by volume.

Sufficient crushed rock material from the inner part of each core sample was dried for both aqueous and ethanol-water extraction (≈ 180 g). The material is dried in a glovebox under an N_2 -atmosphere in desiccators using granular phosphorous pentoxide (P_2O_5 -desiccant). The drying procedure requires between 4 and 8 weeks. Once dry, the samples were removed from the glovebox, powdered and returned to the glove box where the extractions were conducted. A powdered sample (6 g) was weighed in a polypropylene tube and 15 ml of ethanol-water solution was added. The suspension was shaken by hand for 2 minutes. The supernatant was then filtered through a paper filter (4 - 12 μm) and rinsed with pure ethanol in order to remove traces of dissolved salts. The filtered solution was dried at 40 °C on a sand bath located in a fume hood. The dried sediment was dissolved with distilled water (5-10 ml) and analysed by IC for major cations and anions.

2.4 Water isotope diffusive-exchange technique

The underlying theory and development of the water isotope diffusive exchange technique (Rübel et al., 2002) are given in Appendix A. This method was initially developed for rocks containing pore water with salinities up to seawater, and important changes of the protocol are needed to adapt the method to high salinity pore waters (see Waber et al., 2007; Koroleva et al., 2009; de Haller et al., 2008). In particular, to prevent mass transfers and isotopic fractionation (e.g. Horita et al., 1993a and b) between the test water and the pore water of the rock through desiccation-condensation mechanisms, the activity of the test water must be adjusted to fit the rock sample water activity, which depends on the type and concentration of salts and on the proportion of bound water (Sposito, 1990). The activity of pure water is 1, while water activities of brines saturated with NaCl and $CaCl_2$ are 0.75 and 0.32 at 25 °C, respectively (Robinson & Stokes, 1959). Therefore, NaCl can be added to the test water to fit pore water activities down to 0.75, but $CaCl_2$ has to be used if pore water activity is below this value. Most of DGR samples show water activities between 0.55 and 0.7, thus requiring $CaCl_2$ addition to the test waters.

For technical reasons previously discussed in de Haller et al. (2008), the direct measurement of the isotopic composition of saline waters is not possible. Alternative indirect methods are possible but they require the use of correction factors (Horita et al., 1993a and b) and are not adapted for small samples containing 3 to 5 ml of water, as in the case of the test waters used in the diffusive exchange technique.

Methodology development performed in the framework of the DGR project at the Universities of Bern and Lausanne (Switzerland) included the testing of different distillation procedures applied to saline solutions of known isotopic composition. If all the water could be recovered from the brine (i.e. complete drying of the salt), the salt-induced isotopic fractionation would be cancelled and the water composition could be measured with conventional methods (de Haller et al., 2008). Because high temperature (~ 500 °C) distillation was determined to be unreliable (Koroleva et al., 2009), all saline test waters used with DGR-3

and -4 samples were distilled at 120°C after isotopic equilibration. This method was known to give good results for NaCl brines but needed further development to be applicable to CaCl₂ brines. The detailed description of the distillation procedure is given in Appendix A. Due to advances in the methodology, the approach used for DGR-4 samples is different from DGR-3 samples, as described below.

2.4.1 Approach for DGR3 samples

At the time of DGR-3 sample preparation, the 120 °C distillation procedure worked well for NaCl standard solutions but not for CaCl₂ standard solutions (CaCl₂ cannot be fully dehydrated at 120°C). For this reason, only NaCl solutions were used in diffusive exchange experiments with DGR-3 samples. Consequently, for rock samples with measured water activities below 0.75 (NaCl-saturated solution), the activities of the test solutions were not closely matched to the rock samples.

2.4.2 Approach for DGR4 samples

Before the DGR-4 campaign began, a procedure was developed in which CaCl₂ test solutions are treated with NaF to remove the Ca⁺⁺ as CaF₂ (insoluble fluorite). The resulting NaCl solutions can then be distilled at 120°C prior to stable isotope analysis, following the same procedure as for DGR-3 samples, with excellent results (see Appendix A). This allowed the test solutions used in the experiments to be more closely matched to the water activities measured for rock samples by addition of either NaCl for samples with water activities > 0.75 (NaCl-saturated solution) or CaCl₂ to achieve $a_w < 0.75$. NaF was added to the equilibrated CaCl₂ test solutions prior to distillation. This methodological improvement had significant impact on the quality of the DGR-4 data compared to DGR-3.

2.5 Advective Displacement

The objective of this technique is to obtain a sample of porewater subject to relatively minor experimental artefacts by displacing it with an artificial porewater using forced advection. The method requires a saturated core sample that has been processed immediately after drilling and stored protected from atmosphere. Successful displacement of porewater using this method hinges on the presence of sufficient connected porosity, the absence of preferred flow paths, and the ability to induce a relatively homogeneous advective-dispersive displacement front between the injected artificial porewater and the displaced in situ porewater from within the core. Ideally, a number of subsequent small aliquots can be sampled in which the artificial porewater is a minor component. Passive tracer components contained in the artificial porewater are used to monitor the proportion of artificial porewater contained in the extracted porewater (e.g., Br⁻, NO₃⁻, D₂O).

The lower practical limit of hydraulic conductivity for a core sample for the method to work is approximately 10⁻¹⁴ m/s. The hydraulic conductivity K [m/s] of the sample can be calculated for each sampling interval from the average volumetric flow rate Q [m³/s], the sample length l [m] and cross section A [m²], and the difference in hydraulic head h [m_{H2O}] applied during infiltration:

$$K = \frac{Ql}{Ah} \quad (3)$$

Only small sample aliquots (0.5-2 ml) are commonly sampled from low-permeability rocks. This is especially true when the flow-active porosity is small and therefore a relatively fast breakthrough of the injected artificial porewater is to be expected. Typical durations for extracting a few samples from low-permeability rocks range from weeks to months.

The method with applications to indurated claystones is summarized in Mäder et al. (2004) and described in detail by Mäder (2005). An initial test of the method for application to limestone was conducted on an argillaceous limestone sample from the Cobourg Formation, St. Mary's Quarry, Ontario, Canada by Waber et al. (2007). In this experiment, the extraction flow rate gradually decreased during the first 9 days and then decreased abruptly to a no flow condition. This may suggest that due to reactions between the infiltrating artificial porewater, the porewater contained within the core and/or water-mineral interactions, mineral precipitation occurred that sealed pore spaces and caused a rapid decrease in the hydraulic conductivity of the core. In the current study, further development of the advective displacement method for application to rocks containing highly saline porewaters was undertaken. In an effort to minimize interactions between the infiltrating fluid and the porewater within the core, the experiment was conducted using trichloroethylene (TCE) as the infiltrating fluid.

2.5.1 Experimental setup and sampling procedures

As described by Waber et al. (2007), in the initial tests with a limestone sample from the Cobourg Formation, difficulties were encountered during sample preparation when cutting the ends of the core sample to create a sample with smooth, parallel ends. Extensive and irregular fracturing of the core segment occurred subparallel to bedding during cutting (discing). This problem was addressed by first moulding a section of the core in SIKADUR-52 two-component resin to provide stability for cutting. A mould was made from HDPE tubing with an inner diameter of 81 mm. Within this epoxy mould, the core could then be cut accurately. In this study, the same procedure was applied to the core sample from DGR-4 (DGR-4 679.95) used in the advective displacement experiment. A section of the core was removed and used for gravimetric water content measurements. The remainder of the core was sealed in an epoxy resin prior to cutting, as described above. The final dimensions of the core sample used in the experiment were 76 mm diameter (not including epoxy seal) and 90 mm length, having a volume of 407 cm³.

The apparatus used for the experiment comprises a pressure vessel within which a drill core sample can be subject to a hydraulic confining pressure. The core sample is wrapped in Teflon and then placed in a rubber-shrink tubing sleeve to isolate the core from the confining medium. A porous Teflon disc (1 mm thickness) was placed on each end, followed by the titanium couplings that connect via PEEK capillary tubing (1/16" OD) and a PEEK injection valve to an infiltration system. A hydraulic confining pressure of 6.9 MPa was applied. The displacing fluid, TCE, was infiltrated from a Teflon-coated stainless steel sampling cylinder pressurized by helium at an infiltration pressure of 5.0 MPa. The infiltration system guides the gas-pressurized TCE to the surface of the core sample where it is distributed by the porous titanium disc. Similarly, the pore water forced out of the core sample is collected by a porous disc and guided through PEEK capillary tubing to a sampling device. Small syringes connected by luer adapters to the capillary are used as sampling containers.

The experiment is carried out at ambient temperature. Temperature, infiltration and confining pressures are monitored on a routine basis (daily to weekly). In-line measurements of electrochemical parameters such as pH, Eh, and electric conductivity by means of microelectrode flow-through cells are possible with the experimental apparatus, but were not attempted for this experiment due to difficulties in measuring these parameters at the expected high salinities. Sample aliquots are refrigerated in capped syringes or are di-

luted and/or preserved, if required. The analytical program is tailored the size of porewater sample(s) extracted.

3 Rock Mineralogy

3.1 Litho-stratigraphy and petrography

The lithostratigraphic and petrographic descriptions of DGR-3 and DGR-4 samples are given in Table 1 and Table 2, respectively. The petrographic description is based on both macro- and microscopic observations for samples where thin sections were prepared. For samples where the presence of chloride and/or sulphate minerals was suspected, optical determinations were improved by SEM-EDS, whole rock X-ray diffraction (see section 3.2, Table 3 (DGR-3) and Table 4 (DGR-4)) and Raman microprobe (only for DGR-3 samples). A list of the samples containing soluble chloride and/or sulphate minerals is given in Table 5 (DGR-3) and Table 6 (DGR-4).

In DGR-3 samples, sulphate minerals (gypsum, anhydrite, and/or celestite) were documented as veins fillings in the Salina Formation and in the Kirkfield Formation, as massive evaporitic beds in the Salina Formation (Figure 1), as nodules in the Queenston Formation (Figure 2), or as patchy cement in the Georgian Bay Formation (Figure 3). Gypsum occurs preferentially as veins, while anhydrite is dominant in evaporitic beds, and as nodules or patchy cement. Halite was detected by XRD (10 wt.% of the rock, see Table 2) and observed as vein fillings in the Guelph Formation (Figure 4a and Figure 4b), where it overgrows vein dolomite-ankerite and quartz and is therefore paragenetically later. In the Salina Formation, halite was identified by XRD and a halite vein was documented by SEM-EDS on a broken rock chip (Figure 5). The presence of halite could not be confirmed in the Queenston Formation, but small μm size Cl-rich spots were observed by SEM-EDS in the clay-rich matrix (not in the anhydrite-celestite nodules) of freshly broken rock chips. Patchy efflorescences of halite have been observed on the surface of sample DGR-3 453.41 of the Manitoulin Formation (limestone), but the presence of primary (true rock-forming mineral; not porewater evaporation product) halite in this sample was not investigated. Sulphide minerals (pyrite and/or sphalerite) are present in trace amounts in every lithology except in those that are heavily oxidized (rusty color; i.e., Salina-C shale and Queenston shale). Small amounts of disseminated hydrothermal adularia were found in the Cambrian (sample DGR-3 856.06; Figure 6).

In DGR-4 samples, sulphate minerals (gypsum and anhydrite) were documented as veins fillings (Figure 7 and Figure 8) and as massive evaporitic beds in the Salina Formation. Gypsum occurs preferentially in veins while anhydrite is a major phase in evaporitic beds. Halite was observed by SEM-EDS filling a very thin veinlet ($< 50\mu\text{m}$ thick) in a rock chip of sandy dolostone of the Cambrian, but it is not clear if this is a primary feature or if this halite results from the drying of the saline porewater. This sandy dolostone shows well-preserved relicts of oolitic textures (Figure 9) and is cut by calcite-quartz veins (locally drusy texture).

Clear evidence of the past circulation of hydrothermal fluids is recorded by the presence of dolomite-ankerite-quartz-adularia-halite veins in the Guelph Formation (DGR-3) and by calcite-quartz veins (DGR-4) and disseminated adularia (DGR-3) in the Cambrian. These hydrothermal mineralizations are probably related to the regionally recognized hydrothermal event linked to dolomitization and MVT deposits, which is thought to have happened between 350 and 250 Ma (e.g. Hobbs et al., 2008).

3.2 Mineralogy of the whole rock

The whole rock mineralogical compositions obtained by X-ray diffraction (XRD) and CS-Mat for DGR-3 and DGR-4 boreholes are listed in Table 3 and Table 4, respectively. Results are consistent with the petrographic observations (see section 3.1). In both boreholes, carbonate minerals consist of calcite and dolomite-ankerite, whereas siderite is below detection for all the samples and is therefore not reported in the data tables. The degree of dolomitisation expressed in percent is calculated according to equation 3:

$$\text{Dolomitisation (\%)} = (\text{wt.\% dolomite}/(\text{wt.\% dolomite} + \text{calcite})) * 100 \quad (3)$$

where the dolomite content also includes the ankerite fraction (see Table 3 and Table 4).

Anhydrite, gypsum, and minor pyrite were detected by XRD (but not celestite and sphalerite, see section 3.1). The relative contents of these sulphur minerals were calculated from the total sulphur content obtained by CS-Mat or from RIR (relative intensity ratio of XRD peaks). Only pyrite, anhydrite and gypsum were considered in these calculations. Except when RIR was possible, all the sulphur was attributed to the main sulphur-bearing phase observed with optical microscopy.

DGR-3 samples

All samples contain carbonate minerals, with the exception of a sample from the Shadow Lake Formation (Figure 10). All carbonate-bearing samples are dolomitised, between 26 and 100% of the bulk carbonate content (Figure 11). The total clay mineral content varies between less than 1 wt.% in the Salina-A2 Evaporite and the Guelph dolostone to approximately 50 wt.% in the Queenston and Shadow Lake Formations (Figure 12). Where present, quartz occurs in greater amounts than K-feldspar; albite is only present in trace amounts in a few samples. Sulphur-bearing minerals occur as accessory minerals in most formations but are a major constituent of the evaporite beds (Figure 13 and Figure 14). A vertical zoning of the Ca-sulphate minerals is observed in the depth profile, with gypsum in the upper part of the profile (no anhydrite), followed by anhydrite with minor gypsum and then by anhydrite (no gypsum) at greater depths. The total C_{org} is below 0.5 wt.% for all the samples and below the detection limit of 0.1 wt.% in red oxidized rocks (Cabot Head and Queenston formations), evaporites (Salina Formation) and in the Cambrian sandstone (Figure 15).

DGR-4 samples

All samples contain carbonate minerals, with the exception of a red oxidized silty shale sample from the Cabot Head Formation (Figure 10). Aside from two adjacent samples from the Salina-A2 Evaporite and from the top of the Salina-A1 limestone that contain only calcite, all the other carbonate-bearing samples are dolomitised, between 74 and 100% of the bulk carbonate content (Figure 11). The total clay mineral content varies between less than 1 wt.% in the Salina-A2 Evaporite and the Salina-A1 limestone to approximately 78 wt.% (including iron oxides and hydroxides) in a red oxidized silty shale sample of the Cabot Head Formation (Figure 12). Where present, and with the exception of a Shadow Lake sample, quartz always occurs in greater amounts than K-feldspar. Albite is essentially at or below detection limit in all the samples. Gypsum as veins and anhydrite as evaporite beds are major rock constituents in the Salina Formation, from Salina-A2 upward (Figure 13 and Figure 14). Below the Salina-A2 evaporite, sulphur-bearing minerals are only present as accessory minerals, and absent in heavily oxidized rocks of the Cabot Head and Queenston Formations. The total C_{org} is below 0.5 wt.% for all the samples (Figure 15).

Table 1: Petrography of DGR-3 samples

Sample ID (NWMO)	Depth (m BGS)	Formation	Lithology ¹	Petrography ²	Series
DGR-3 198.72	198.72	Salina – F Unit	Dolomitic shale with gypsum	Silty calcareous shale with veins of white and orange gypsum. The rock consists of clay, carbonate and quartz with traces of fine-grained pyrite. The veins show boudinage textures and their origin (tectonic versus diagenetic) is unclear.	U. Silurian
DGR-3 208.41	208.41	Salina - F Unit	Dolomitic shale with gypsum	No thin section. White and orange gypsum veins.	U. Silurian
DGR-3 248.71	248.71	Salina – E Unit	Dolomitic shale with white gypsum veins	No thin section.	U. Silurian
DGR-3 270.06	270.06	Salina - C Unit	Dolomitic shale	Red oxidized silty calcareous shale consisting of detrital quartz, feldspar, and muscovite, cemented by carbonate minerals (dolomite). The red colour is due to the presence of iron (hydr-) oxides. Sulphide minerals were not observed. Halite has been detected by X-ray diffraction and SEM-EDS (as veinlet). Rare gypsum (anhydrite) veinlets.	U. Silurian
DGR-3 289.36	289.36	Salina – B Unit	Argillaceous dolostone with white gypsum veins	No thin section.	U. Silurian
DGR-3 312.53	312.53	Salina - A2 Unit	Dolostone	No thin section	U. Silurian
DGR-3 335.22	335.22	Salina – A2 Evaporite	Anhydrite	Massive anhydrite with inclusions of idiomorphic gypsum crystals. Minor idiomorphic dolomite (<5%) and non-idiomorphic carbonate (calcite?) (<5%). Traces of pyrite.	U. Silurian
DGR-3 344.06	344.06	Salina -A1 Unit	Dolostone	No thin section.	U. Silurian
DGR-3 380.88	380.88	A1 Evaporite	Anhydrite	Massive anhydrite with minor idiomorphic dolomite and traces of pyrite. No Cl-bearing phases were found with SEM-EDS	U. Silurian
DGR-3 391.34	391.34	Guelph	Dolostone (veined)	Veined brown dolostone. The rock is composed of dolomite with minor, fine grained, disseminated pyrite. Veins are partially filled with hydrothermal dolomite (ankerite) with minor quartz, traces of adularia, and abundant paragenetically later halite (SEM-EDS). Residual vein porosity is high.	M. Silurian
DGR-3 435.62	435.62	Cabot Head	Dolostone ± shale	No thin section. Bedded rock.	L. Silurian
DGR-3 453.41	453.41	Manitoulin	Limestone	No thin section. Bioclastic limestone. Patches of salt efflorescences on the drill core surface.	L. Silurian
DGR-3 468.76	468.76	Queenston	Shale	No thin section. Oxidized shale.	U. Ordovician

¹ Consistent with stratigraphic descriptions in Intera 2009, but includes only those aspects which apply to the specific core sample examined.

² Mineralogical determinations were conducted using optical microscopy (transmitted and reflected light), Raman microprobe, X-ray diffraction, and SEM-EDS.

Table 1 (Cont'd): Petrography of DGR-3 samples.

Sample ID (NWMO)	Depth (m BGS)	Formation	Lithology ¹	Petrography ²	Series
DGR-3 484.58	484.58	Queenston	Shale	Silty, oxidised, dolomitic shale with anhydrite-celestite nodules. Celestite appears as large crystals (few mm) in the fine-grained anhydrite. No opaque minerals. No Cl detected (SEM-EDS) in the anhydrite-celestite nodules, but µm-size Cl spots detected in the clay-rich matrix.	U. Ordovician
DGR-3 502.55	502.55	Queenston	Shale	No thin section. Oxidized rock.	U. Ordovician
DGR-3 531.65	531.65	Georgian Bay	Shale / sandstone	Bedded calcareous shale/sandstone. Textures of diagenetic dewatering are present (sandstone fluidization). Sandy layers are composed of quartz, feldspar, dolomite, anhydrite, and minor muscovite. Shaly beds consist of clay, quartz, muscovite, and dolomite. Traces of disseminated sphalerite.	U. Ordovician
DGR-3 581.47	581.47	Georgian Bay	Shale	No thin section.	U. Ordovician
DGR-3 621.63	621.63	Blue Mountain	Shale	No thin section.	U. Ordovician
DGR-3 646.29	646.29	Blue Mountain	Shale	No thin section.	U. Ordovician
DGR-3 665.29	665.29	Cobourg – Collingwood Member	Argillaceous limestone	No thin section.	M. Ordovician
DGR-3 673.00	673.00	Cobourg – L. M.	Limestone	No thin section.	M. Ordovician
DGR-3 676.21	676.21	Cobourg – L. M.	Limestone	No thin section.	M. Ordovician
DGR-3 678.92	678.92	Cobourg – L. M.	Limestone	Bioclastic limestone. The rock is slightly dolomitised and contains traces of pyrite.	M. Ordovician
DGR-3 685.52	685.52	Cobourg – L. M.	Limestone	No thin section.	M. Ordovician
DGR-3 690.12	690.12	Cobourg – L. M.	Argillaceous limestone	No thin section.	M. Ordovician
DGR-3 692.82	692.82	Cobourg – L. M.	Argillaceous limestone	No thin section.	M. Ordovician
DGR-3 697.94	697.94	Cobourg – L. M.	Argillaceous limestone	No thin section.	M. Ordovician
DGR-3 710.38	710.38	Sherman Fall	Argillaceous limestone	No thin section.	M. Ordovician

¹ Consistent with stratigraphic descriptions in Intera 2009, but includes only those aspects which apply to the specific core sample examined.

² Mineralogical determinations were conducted using optical microscopy (transmitted and reflected light), Raman microprobe, X-ray diffraction, and SEM-EDS.

Table 2: Petrography of DGR-4 samples

Sample ID (NWMO)	Depth (m BGS)	Formation	Lithology ¹	Petrography ²	Series
DGR-4 154.60	154.60	Bass Islands	Dolomitic shale with Ca-sulphate	No thin section.	U. Silurian
DGR-4 189.16	189.16	Salina - F	Grey-blue dolomitic shale with Ca-sulphate	Grey-blue dolomitic silty shale crosscut by gypsum (traces of anhydrite?) veins. Disseminated pyrite and sphalerite.	U. Silurian
DGR-4 229.32	229.32	Salina - E	Dolomitic shale with Ca-sulphate	Silty dolomitic shale cut by veins broadly perpendicular to the bedding filled with fluidized rock flour and gypsum crystals (grown in situ). The rock is composed of clay (detrital muscovite, and chlorite), carbonate, and silty quartz. Most of the minor pyrite occurs in vein structures.	U. Silurian
DGR-4 322.68	322.68	A2 Evaporite	Massive Ca-sulphate	Massive finely to medium grained anhydrite containing disseminated up to 10 mm diameter nodules made up of broadly idiomorphic gypsum crystals with inclusions of anhydrite. Some subordinate disseminated calcite. Trace amount of disseminated pyrite.	U. Silurian
DGR-4 332.13	332.13	Salina - A1	Micritic limestone	Micritic limestone cut by minor carbonate veins. Disseminated pyrite.	U. Silurian
DGR-4 369.43	369.43	A1 Evaporite	Anhydritic dolostone	No thin section.	U. Silurian
DGR-4 422.21	422.21	Cabot Head	Red silty shale	Red oxidized shale with thin silty beds. The bedding is crosscut by veins filled with coarser silty material (fluidized rock flour). The rock is composed of clays, silty quartz, hematite (and hydrated iron oxides) and minor feldspar.	L. Silurian
DGR-4 472.78	472.78	Queenston	Red-green shale with carbonate beds	Pale red-green oxidized dolomitic shale containing subordinate silty quartz. Rare thin (<0.5 mm) fractures filled with anhydrite. No pyrite.	U. Ordovician
DGR-4 520.42	520.42	Georgian Bay	Shale with sandstone / siltstone / limestone beds	No thin section.	U. Ordovician
DGR-4 662.83	662.83	Cobourg – L. M.	Bioclastic limestone and argillaceous limestone	No thin section.	M. Ordovician
DGR-4 665.41	665.41	Cobourg – L. M.	Bioclastic limestone and argillaceous limestone	No thin section.	M. Ordovician
DGR-4 672.85	672.85	Cobourg – L. M.	Bioclastic limestone and argillaceous limestone	No thin section.	M. Ordovician

¹ Consistent with stratigraphic descriptions in Intera 2009, but includes only those aspects which apply to the specific core sample examined.

² Mineralogical determinations were conducted using optical microscopy (transmitted and reflected light), X-ray diffraction, and SEM-EDS.

Table 2 (Cont.'d): Petrography of DGR-4 samples

Sample ID (NWMO)	Depth (m BGS)	Formation	Lithology ¹	Petrography ²	Series
DGR-4 685.14	685.14	Cobourg – L. M.	Bioclastic limestone and argillaceous limestone	No thin section.	M. Ordovi- cian
DGR-4 717.12	717.12	Sherman Fall	Bedded argillaceous lime- stone and calcareous shale	No thin section.	M. Ordovi- cian
DGR-4 730.07	730.07	Kirkfield	Limestone with shale beds	No thin section.	M. Ordovi- cian
DGR-4 841.06	841.06	Shadow Lake	Sandy mudstone, siltstone and sandstone	Sandy dolostone beds alternating with finely bedded (up to few mm) dolomitized sandstone, sandy micritic limestone, and black shale. Sandy material consists of detrital quartz and K-feldspar, with minor dolomite. Sandy mudstone beds are dominated by dolomite with minor quartz and K-feldspar. Black shale layers correspond at least in part to stylolite structures. Disseminated pyrite and sphalerite.	M. Ordovi- cian
DGR-4 847.48	847.48	Cambrian	Sandstone / dolostone	Sandy medium-grained dolostone. The rims of quartz and K-feldspar clasts are hydrothermally overgrown, and tend to be idiomorphic. The carbonate fraction of the rock is completely recrystallized to dolomite, but the primary oolitic texture is still clearly visible. Spots of green chlorite (probably hydrothermal). Minor disseminate pyrite. The rock is cut by quartz-calcite veins. Locally, minor fractures are filled with halite, but it is difficult to assess if it is a primary feature (SEM observation on rock chip).	Cambrian

¹ Consistent with stratigraphic descriptions in Intera 2009, but includes only those aspects which apply to the specific core sample examined.

² Mineralogical determinations were conducted using optical microscopy (transmitted and reflected light), X-ray diffraction, and SEM-EDS.

Table 3: Mineralogy of DGR-3 whole rock samples based on X-Ray diffraction and CS-Mat IR spectroscopy

Method		CS-Mat						XRD + CS-Mat		XRD				Others (qualitative)
Sample ID (NWMO)	Formation	S wt%	C _{org.} wt%	C _{inorg.} wt%	Pyrite wt%	Gyp. wt%	Anh. wt%	Calcite wt%	Dol. & Ank. wt%	Quartz Wt%	Albite wt%	K- feldspar wt%	Sheet- Silicates wt%	
DGR-3 198.72	Salina – F Unit	2.9	0.3	4.5	--	18.3	--	<1	36	10	<1	3	33	Muscovite/illite, chlorite.
DGR-3 270.06	Salina - C Unit	<0.1	<0.1	3.3	--	--	--	<1	26	20	5	5	44	Muscovite/illite, chlorite, halite.
DGR-3 335.22	Salina – A2 Evaporite	23.4	<0.1	1.1	--	3	90	5	3	<1	<1	<1	<1	Anhydrite, gypsum, ankerite.
DGR-3 391.34	Guelph	0.2	0.3	11.1	0.4	--	--	1	86	2	<1	<1	<1	Halite (10 wt. %, calculated by difference with the total of other phases), ankerite.
DGR-3 484.58	Queenston	1.3	<0.1	4.7	--	--	5.5	29	10	7	<1	1	48	Muscovite/illite, chlorite, anhy- drite.
DGR-3 531.65	Georgian Bay	0.1	0.4	4.5	--	--	0.4	19	18	25	<1	8	30	Muscovite/illite, chlorite.
DGR-3 852.18	Shadow Lake	1.0	0.3	0.6	1.9	--	--	<1	<1	28	2	16	52	Muscovite/illite, pyrite.
DGR-3 856.06	Cambrian	0.1	<0.1	9.4	0.2	--	--	<1	74	8	<1	7	11	Ankerite.

Notes: gyp. = gypsum, anh. = anhydrite, dol. = dolomite, ank. = ankerite. The sheet silicates column corresponds to the amount (= 100 - total of other phases) of clay and mica minerals. The wt% of pyrite, gypsum, or anhydrite where calculated from the S content, and supported by petrographic and X-ray diffraction results. In the case of sample DGR3-335.22, the ratio of anhydrite to gypsum was calculated from the X-ray diffraction data. In the case of sample DGR-3-484.58 (Queenston), the calculated amount of anhydrite also includes minor celestite (observed in thin sections).

Table 4: Mineralogy of DGR-4 whole rock samples based on X-Ray diffraction and CS-Mat IR spectroscopy

Method		CS-Mat						XRD + CS-Mat		XRD				Others (qualitative)
Sample ID (NWMO)	Formation	S wt%	C _{org.} wt%	C _{inorg.} wt%	Pyrite wt%	Gyp. wt%	Anh. wt%	Calcite wt%	Dol. & Ank. wt%	Quartz wt%	Albite wt%	K-feldspar wt%	Sheet-Silicates wt%	
DGR-4 189.16	Salina - F	4.8	0.2	3.6	--	26	--	3	26	16	1	6	22	Muscovite/illite, gypsum Muscovite/illite, chlorite, gypsum, bassanite (this last mineral is probably an artefact of the milling process).
DGR-4 229.32	Salina - E	11.2	0.1	2.6	--	60	--	2	19	7	<1	<1	12	
DGR-4 322.68	Salina – A2 Evaporite	24.1	<0.1	0.6	--	3	94	5	<1	<1	<1	<1	<1	Anhydrite(94%), gypsum (3%) (% by relative intensity ratios)
DGR-4 332.13	Salina - A1	<0.1	<0.1	12.5	<1	<1	<1	97	1	2.0	<1	0.0	<1	Muscovite/illite, pyrite
DGR-4 422.21	Cabot Head	0.4	<0.1	0.1	1	--	--	<1	<1	19	<1	2	78	Muscovite/illite, hematite
DGR-4 472.78	Queenston	<0.1	0.5	4.5	<1	<1	<1	9	27	13	<1	1	50	Muscovite/illite, chlorite, anhydrite
DGR-4 841.06	Shadow Lake	<0.1	0.6	8.2	<1	<1	<1	<1	65	7	<1	9	19	Muscovite/illite
DGR-4 847.48	Cambrian	<0.1	0.5	10.6	<1	<1	<1	12	72	8	<1	1	6	

Notes: gyp. = gypsum, anh. = anhydrite, dol. = dolomite, ank. = ankerite. The sheet silicates column corresponds to the amount (= 100 - total of other phases) of clay and mica minerals. The wt% of pyrite, gypsum, or anhydrite were calculated from the S content, and supported by petrographic and X-ray diffraction results. In the case of sample DGR4-322.68, the amounts of anhydrite and gypsum were calculated from the X-ray diffraction data. In the case of samples DGR4-229.32 and DGR4-332.13, the calculated amount of gypsum also includes minor pyrite (observed in thin sections). The value for the sheet-silicates content of sample DGR-4 422.21 is a maximum, because it includes also hematite and Fe-hydroxides. No sulphur-bearing mineral has been observed in thin sections in sample DGR-4 422.21 that could explain the 0.4 wt% sulphur obtained by CS-Mat. Therefore, the reported 1 wt% pyrite is hypothetical.

Table 5: Summary of DGR-3 samples containing soluble minerals.

Sample ID (NWMO)	Depth (m BGS)	Formation	Soluble Minerals
DGR-3 198.72	198.72	Salina – F Unit	Gypsum
DGR-3 208.41	208.41	Salina - F Unit	Gypsum
DGR-3 248.71	248.71	Salina – E Unit	Gypsum
DGR-3 270.06	270.06	Salina - C Unit	Halite, gypsum, anhydrite
DGR-3 289.36	289.36	Salina – B Unit	Gypsum
DGR-3 335.22	335.22	Salina – A2 Evaporite	Anhydrite, gypsum
DGR-3 380.88	380.88	A1 Evaporite	Anhydrite
DGR-3 391.34	391.34	Guelph	Halite
DGR-3 484.58	484.58	Queenston	Anhydrite, celestite
DGR-3 531.65	531.65	Georgian Bay	Anhydrite
DGR-3 761.56	761.56	Kirkfield	Anhydrite

Note: trace amounts of sulphide minerals (pyrite, sphalerite) are found in every lithology except in those that are heavily oxidized (rusty color; i.e., Salina-C Unit and Queenston Formation).

Table 6: Summary of DGR-4 samples containing soluble minerals.

Sample ID (NWMO)	Depth (m BGS)	Formation	Soluble Minerals
DGR-4 189.16	189.16	Salina - F	Gypsum, anhydrite
DGR-4 229.32	229.32	Salina - E	Gypsum
DGR-4 322.68	322.68	Salina - A2 Evaporite	Anhydrite, gypsum
DGR-4 472.78	472.78	Queenston	Anhydrite
DGR-4 847.48	847.48	Cambrian	Halite (from pore- water evapora- tion?)

Note: trace amounts of sulphide minerals (pyrite, sphalerite) are observed in every lithology except in those that are heavily oxidized (Queenston and Cabot Head formations).

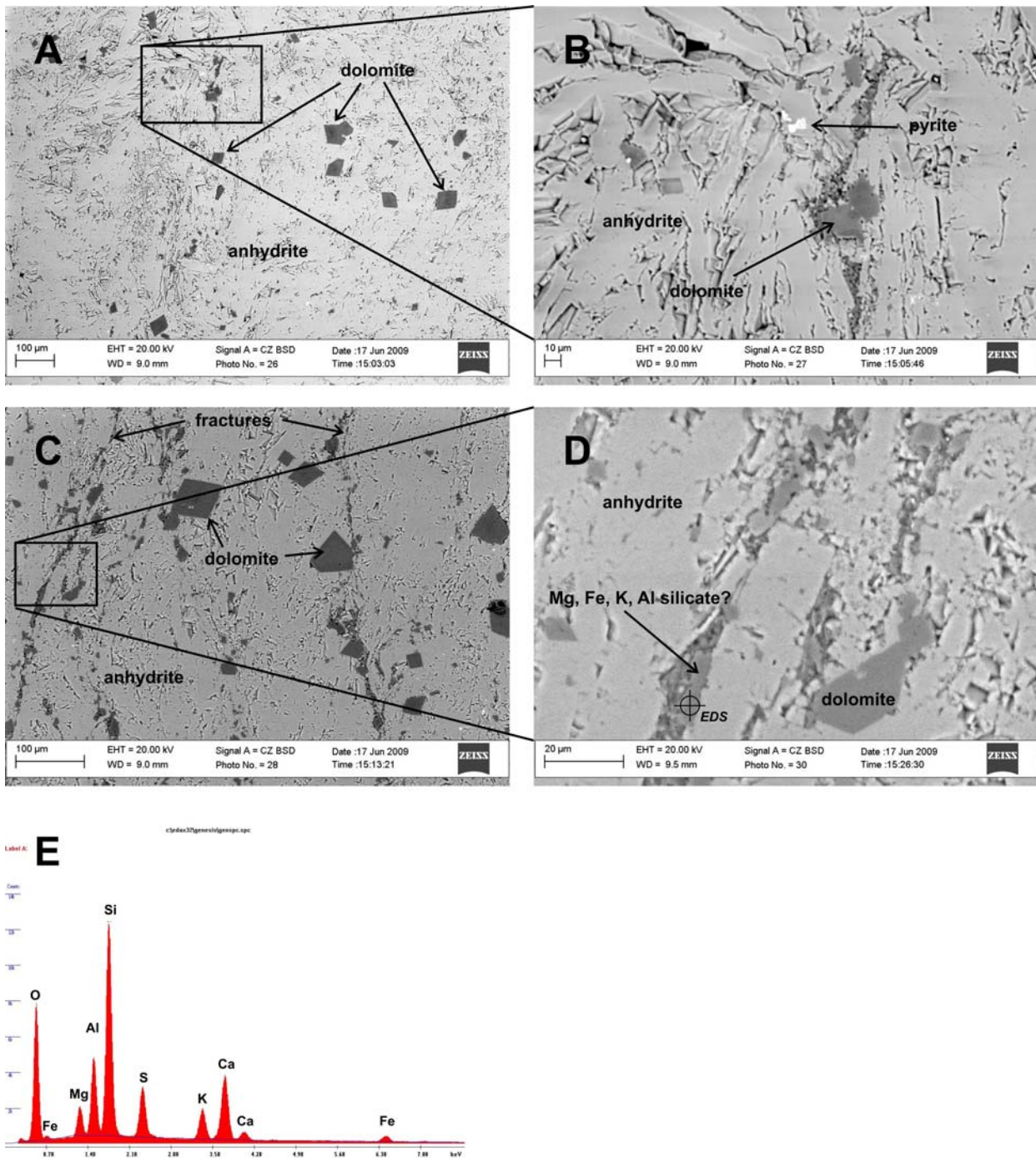


Figure 1: Sample DGR-3 380.88 (Salina A1 Evaporite). A and B: Massive evaporite rock essentially composed of anhydrite, with minor dolomite and traces of pyrite. C to E: Traces of alumino-silicate minerals have been found in very small veinlets (<10μ thickness). This silicate mineral could not be identified because of its small size, which results in the EDS analysis being perturbed by the matrix (part or all of the S, Ca, Mg and Fe signals can be related to the surrounding dolomite and anhydrite). The position of the EDS analysis given in E is shown in D. All pictures are back-scattered electron views of uncoated thin sections.

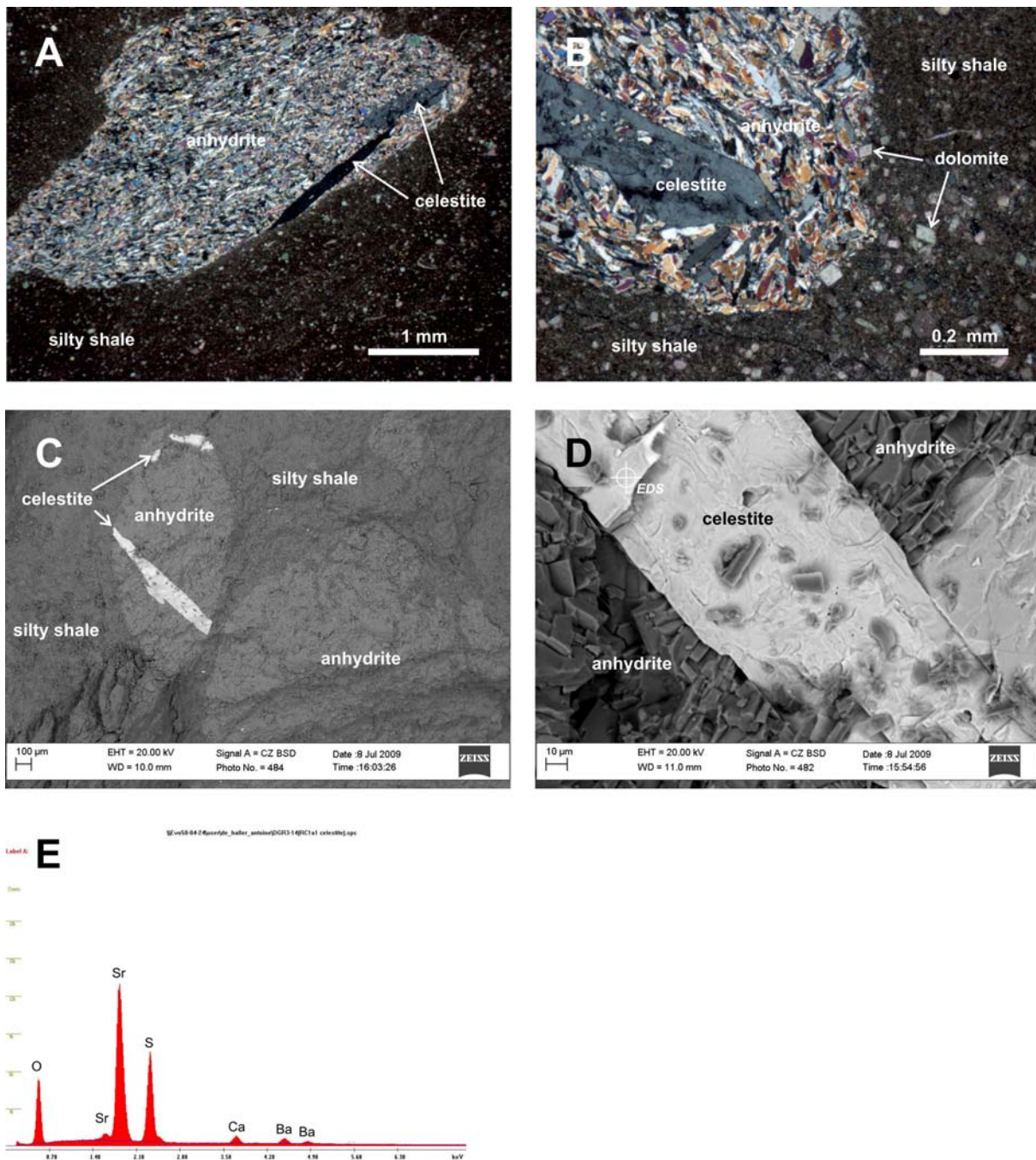


Figure 2: Sample DGR-3 484.58 (Queenston). A and B (B is a detailed view of A): Anhydrite-celestite nodule in Queenston Formation. Celestite appears as mm-sized crystals enclosed in finely crystallized anhydrite. C: Nodules of anhydrite-celestite in shale. Celestite crystals are cut at the border of the nodule, indicating reworking after crystallization. It is unclear if this reworking is syndepositional, diagenetic or tectonic. Cl has been detected with the EDS in the shaly matrix, but not in the sulphate nodules. Due to the small grain size, no Cl-bearing phase could be identified. D and E: Celestite crystal in anhydrite, and EDS analysis of the celestite, showing minor amounts of Ba replacing Sr. Pictures A and B are crossed nicols views in transmitted light, while pictures C and D are back-scattered electron views of uncoated, freshly broken rock chips.

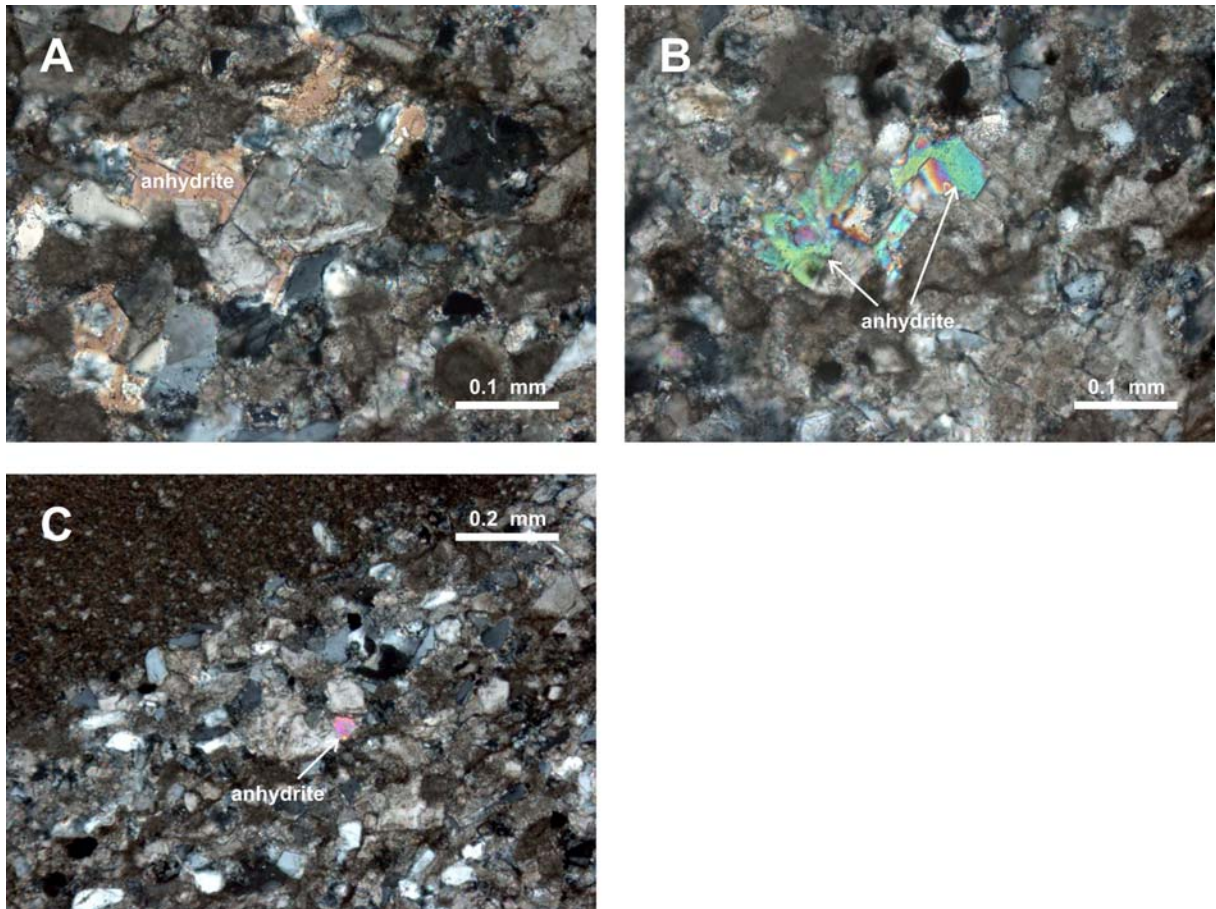


Figure 3: Sample DGR-3 531.65 (Georgian Bay). A and B: Anhydrite cement in sandy beds. C: Anhydrite patch in a sandy bed near a shaly horizon. All pictures are taken under crossed nicols transmitted light. The identification of anhydrite has been confirmed by Raman microprobe.

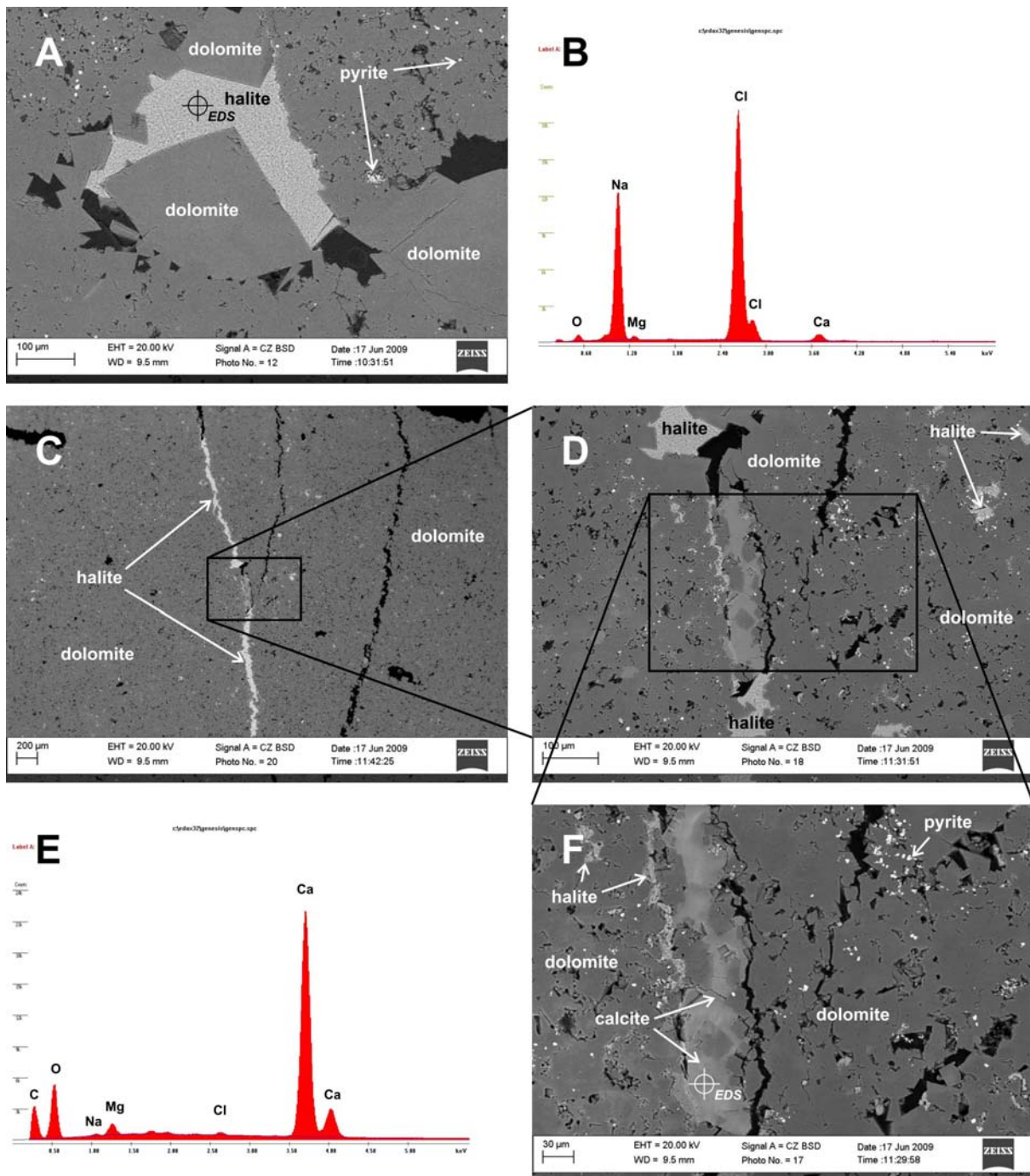


Figure 4a: Sample DGR-3 391.34 (Guelph). A: Vein in dolomitised rock filled by dolomite crystals and paragenetically later halite. Black areas correspond to remaining porosity. The host rock contains traces of disseminated pyrite (white dots). **B:** EDS analysis of the point indicated in A, corresponding to halite. The small peaks of Ca, Mg, and O are due to the matrix effect of the nearby dolomite. **C to F:** Small veinlet (about 50 μm thick) filled by dolomite and later calcite and halite. Black areas are remaining porosity. **E:** EDS analysis of the point shown in F, corresponding to calcite. The small peaks of Mg, Cl, and Na are due to the nearby presence of halite and dolomite. All pictures are back-scattered electron views of uncoated thin sections.

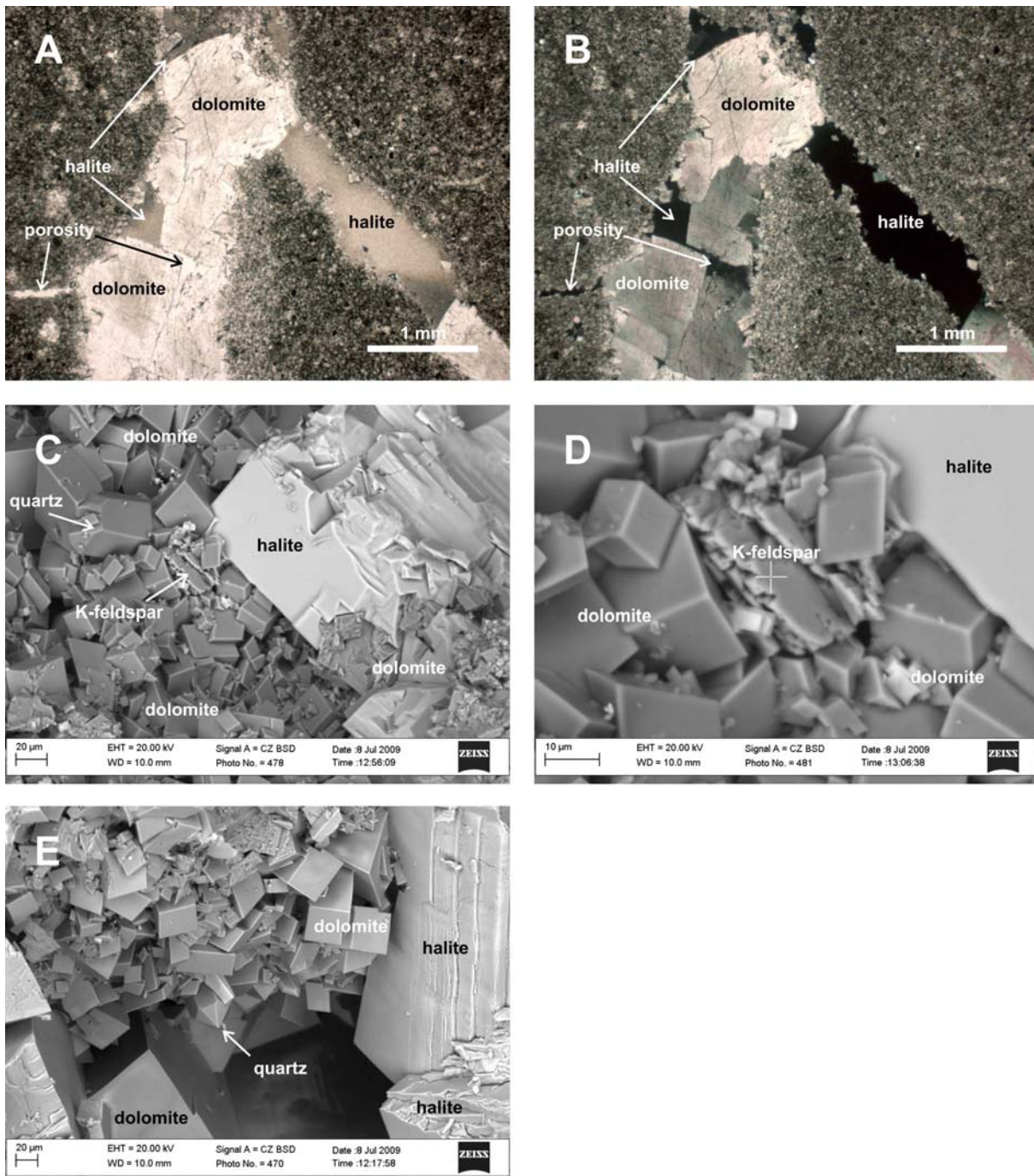


Figure 4b: Sample DGR-3 391.34 (Guelph). A and B: Veined dolostone: transmitted light thin section microphotographs (respectively under parallel and crossed polarizer). Halite polishes poorly and appears brownish under parallel nicols. In contrast, porosity (filled with resin) is clear. C and D: D is a detailed view of C, showing well-crystallized dolomite, quartz, halite, and K-feldspar in an open vein. Halite is later than dolomite. E: Open vein with dolomite, quartz, and halite crystals. Pictures C to E are back-scattered electron views of uncoated, freshly broken rock chips.

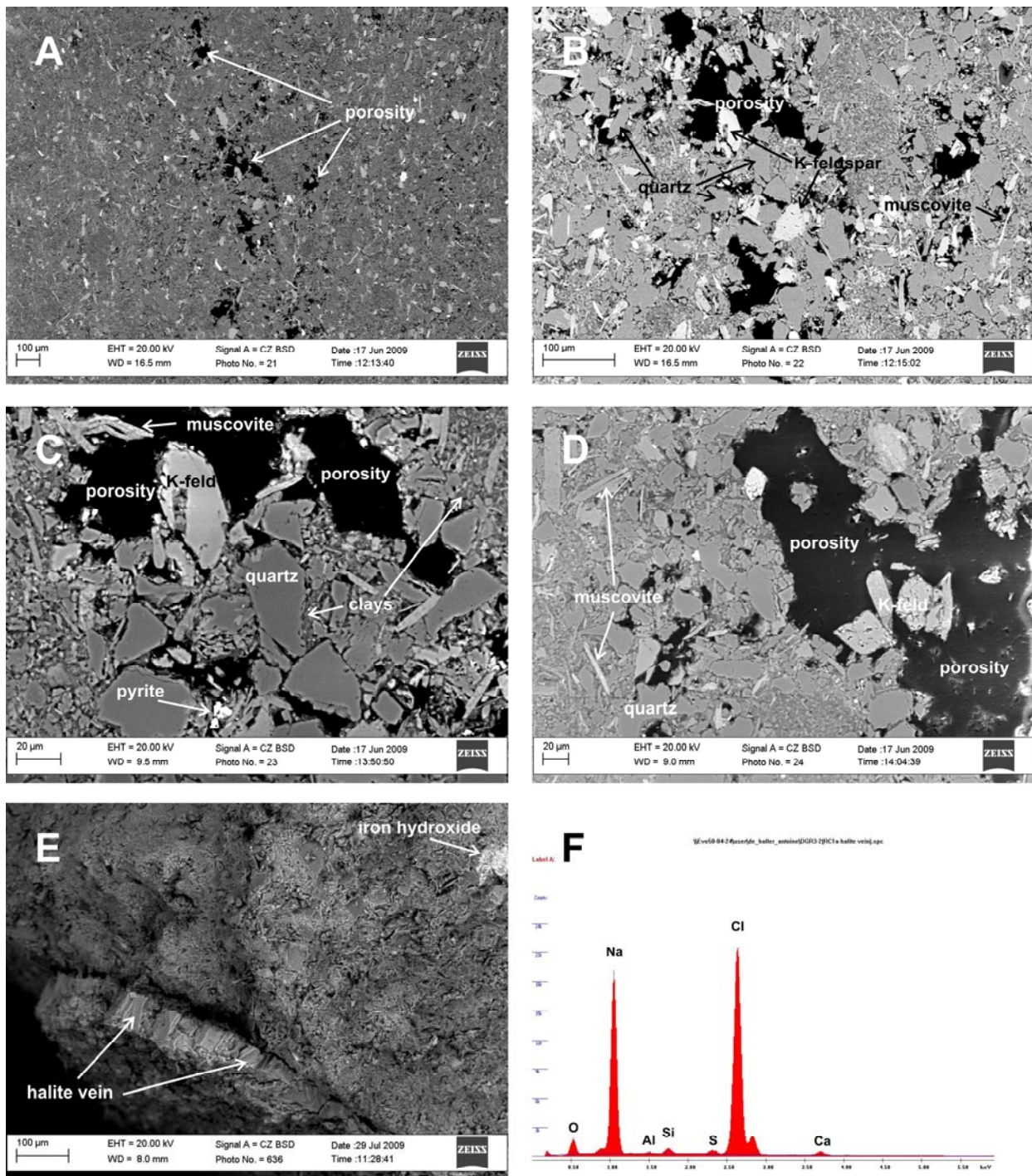


Figure 5: Sample DGR-3 270.06 (Salina-C). Dolomitic shale showing clusters of small pores (<100µm). View B is a detailed view of A and C is a detailed view of B. The interstitial clay is chlorite (view C). No halite was found in the pore spaces observed in the thin section. View E: 50 µm thick vein of halite cutting the rock. View F: EDS analysis of the halite vein shown in E. All pictures are back-scattered electron views of an uncoated thin section (A to D) or a freshly broken rock chip (E).

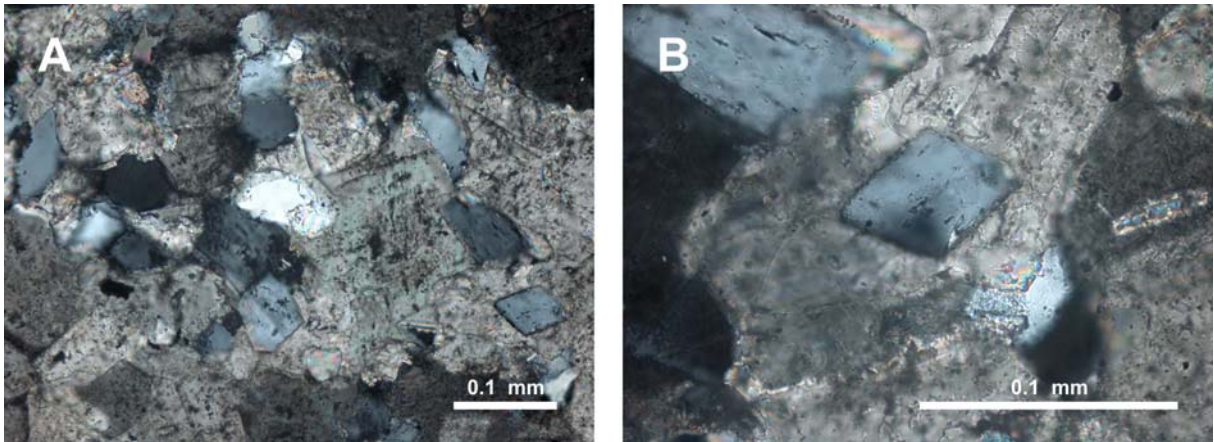


Figure 6: Sample DGR-3 856.06 (Cambrian). View A and B (B is a detailed view of A): Rhombohedral hydrothermal adularia (grey birefringence) in Cambrian sandy dolostone. Both pictures under crossed nicols.

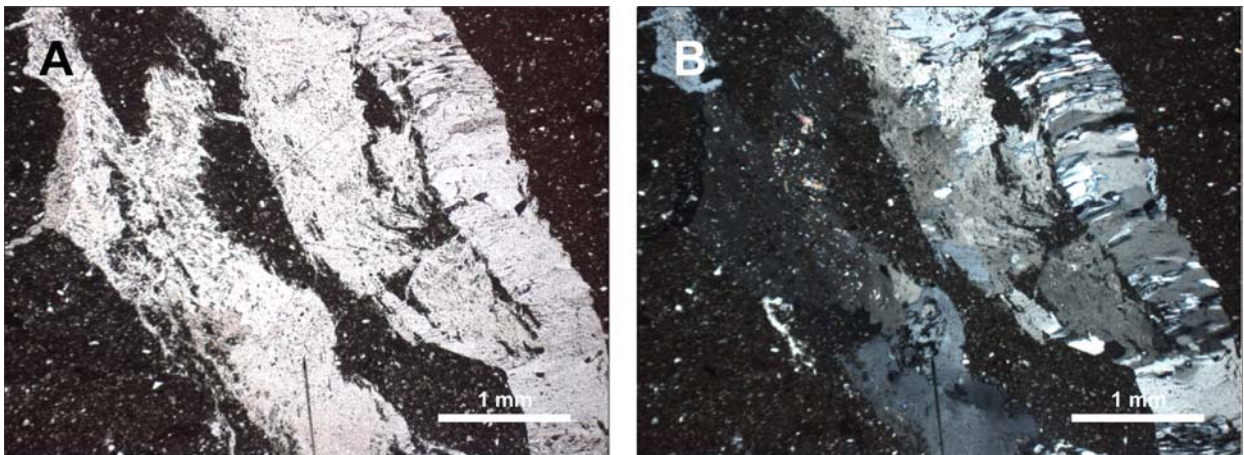


Figure 7: Sample DGR4-189.16 (Salina-F). Grey-blue dolomitic silty shale cut by gypsum veins. Gypsum contains tiny inclusions of anhydrite (higher birefringence order). View A is under parallel and view B is under crossed nicols transmitted light.

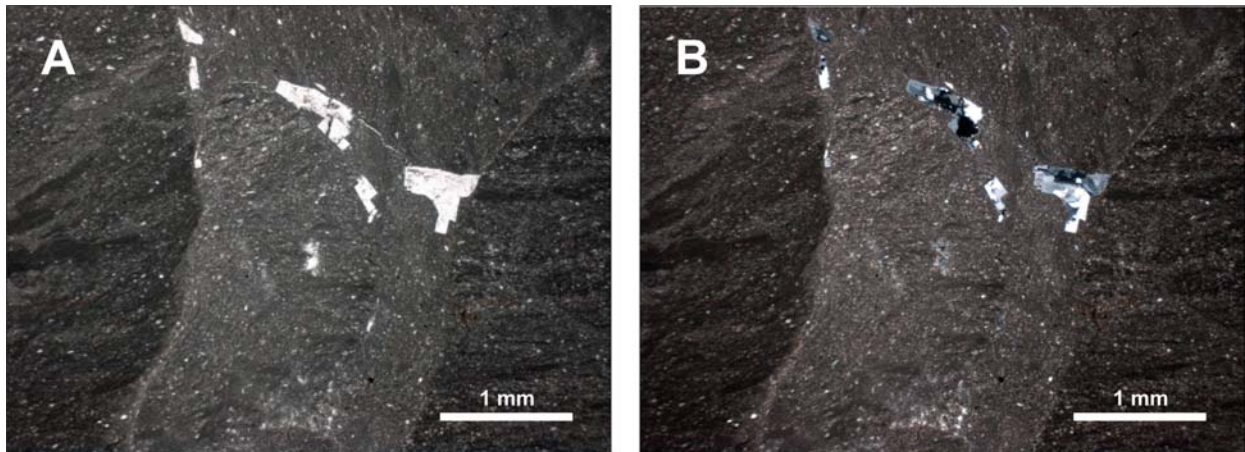


Figure 8: Sample DGR4-229.32 (Salina - E). Silty dolomitic shale cut by veins filled with fluidized rock flour and gypsum crystals (apparently grown in situ). The bedding of the host rock is visible on both sides of the vein structure. View A is under parallel and B under crossed nicols transmitted light.

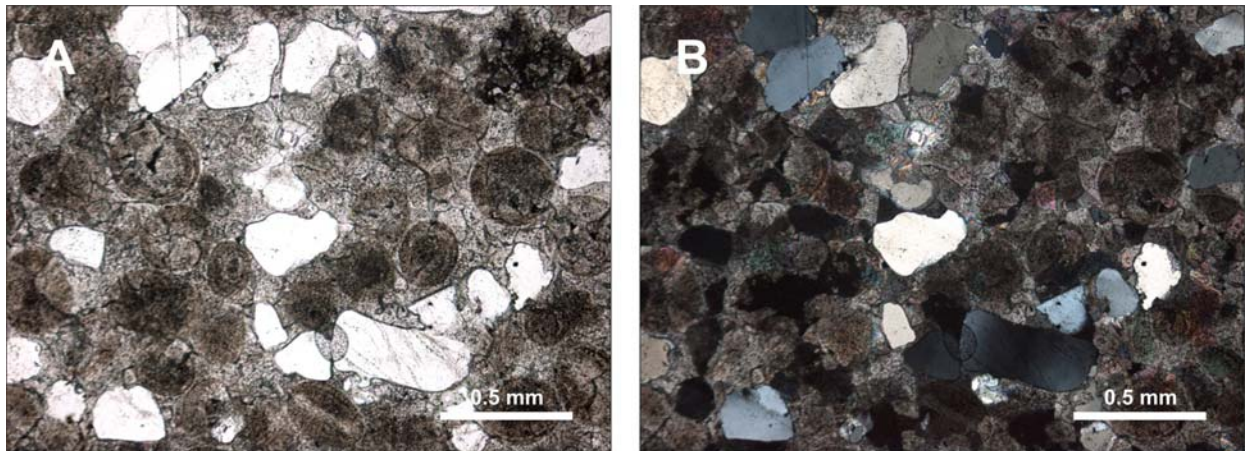


Figure 9: Sample DGR4-847.48 (Cambrian). Sandy medium grained dolostone. The carbonate fraction of the rock is completely recrystallised to dolomite, but the primary oolitic texture is still preserved. View A is under parallel and B under crossed nicols transmitted light. In A, the brightest grains are quartz.

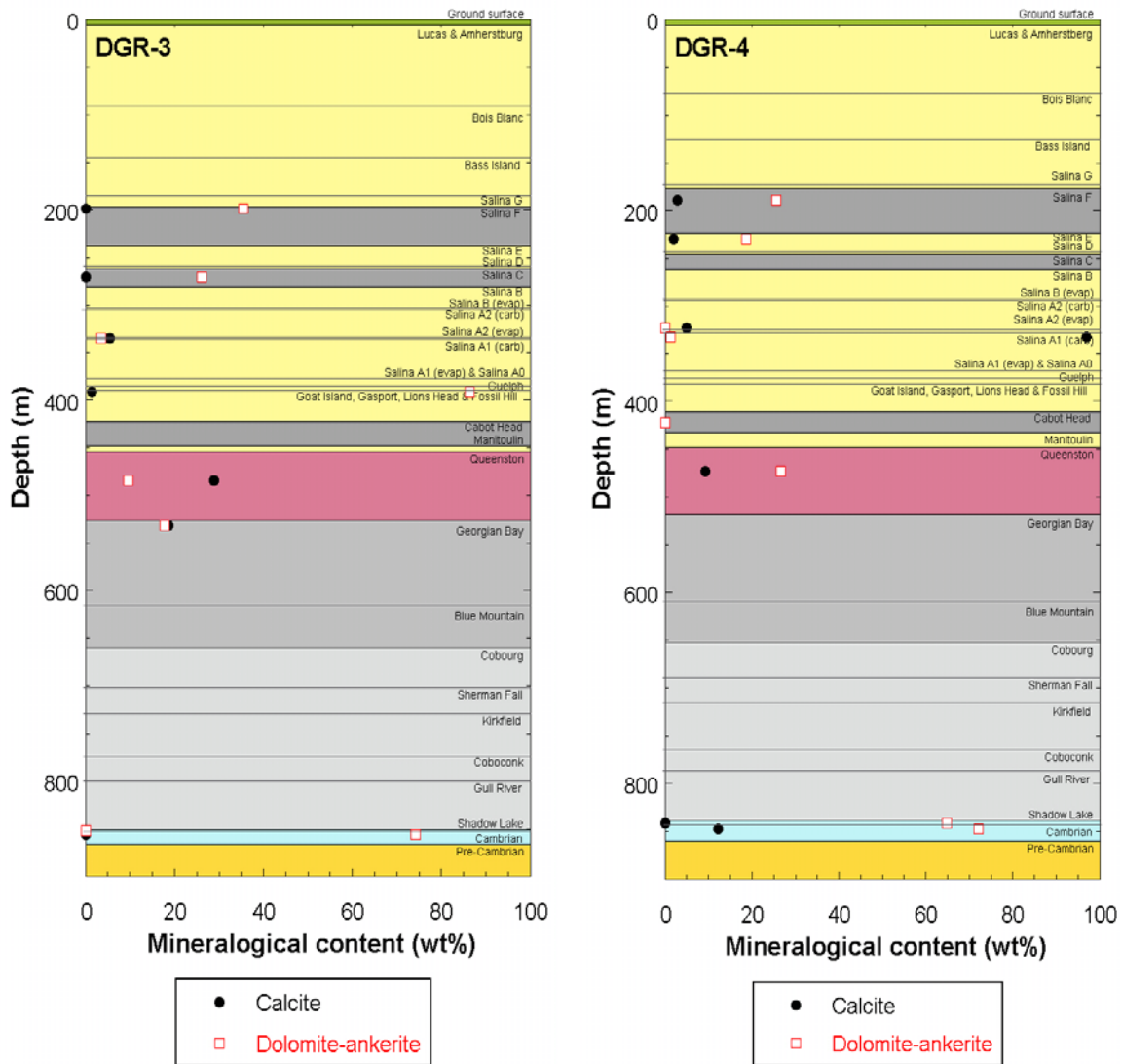


Figure 10: Depth profiles of calcite and dolomite-ankerite contents. Samples that plot at zero are below the detection limit (see Table 3 and Table 4, and Figure 11).

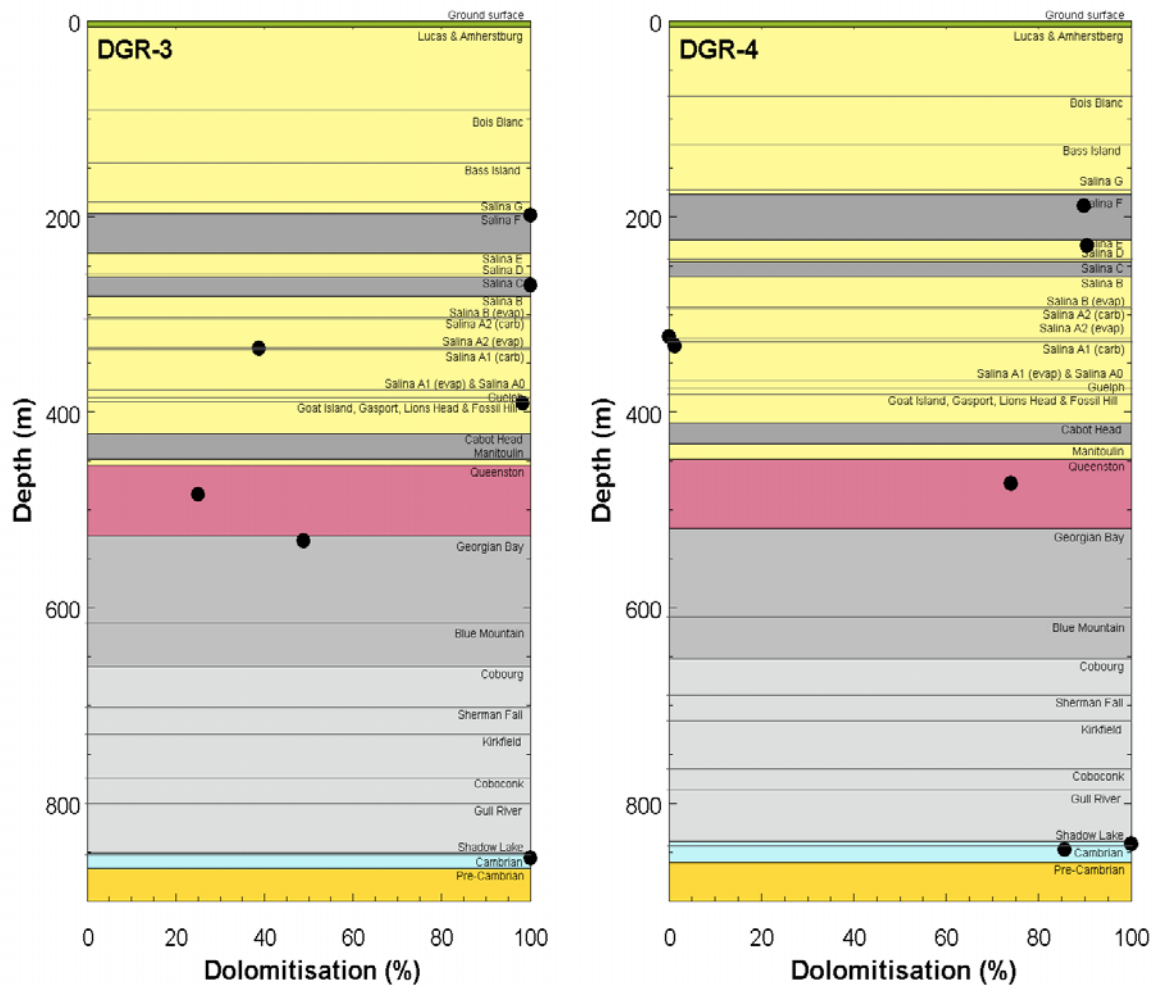


Figure 11: Depth profiles of dolomitisation, expressed as $100 \cdot \text{dolomite} / (\text{dolomite} + \text{calcite})$. In this calculation, the sum of the dolomite and ankerite contents is used as a proxy for dolomite (see Table 3 and Table 4, and Figure 10).

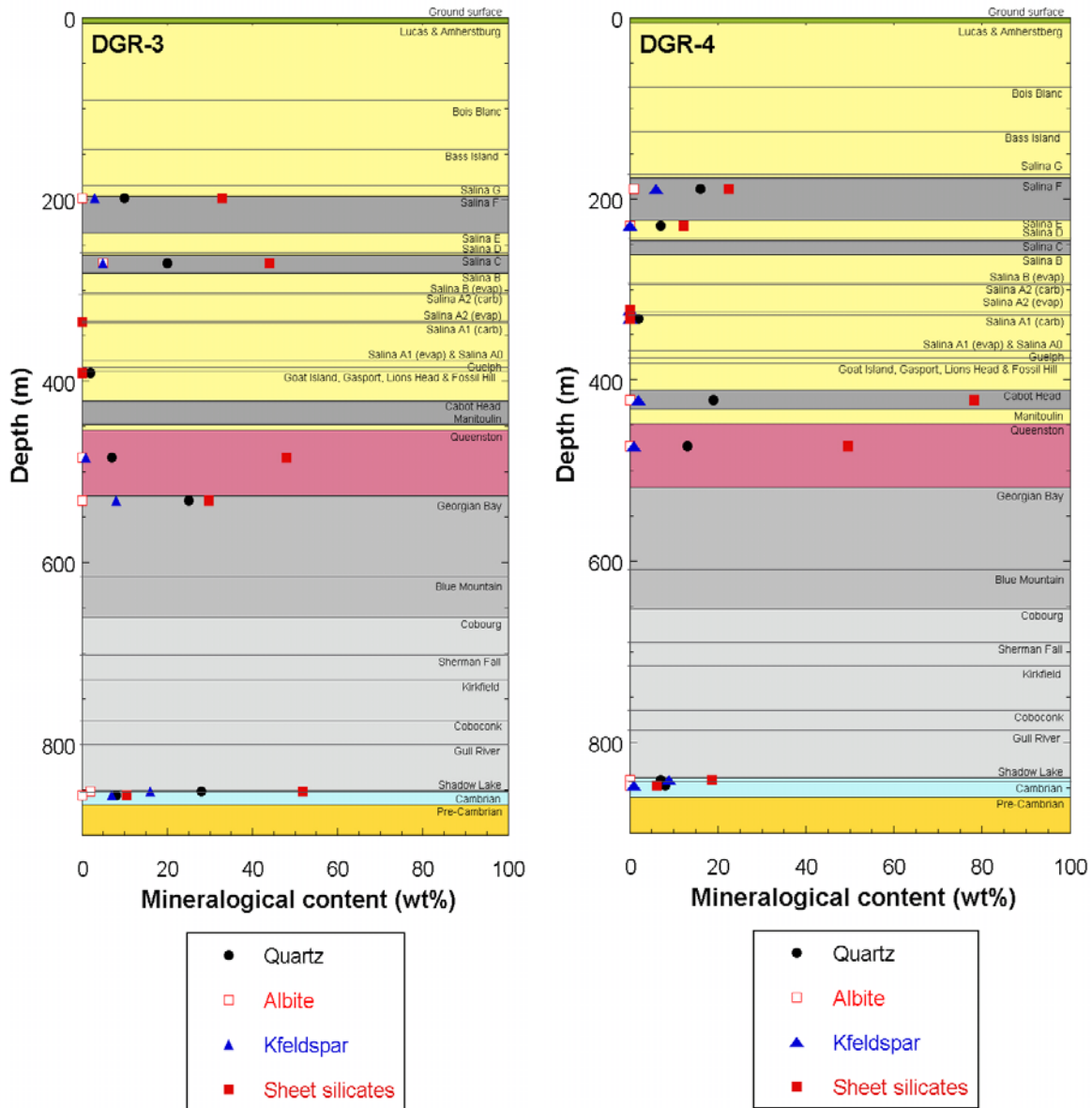


Figure 12: Depth profiles of siliciclastic minerals and total clay content (assumed to correspond closely to the sum of sheet silicates). Samples that plot at zero are below the detection limit (see Table 3 and Table 4).

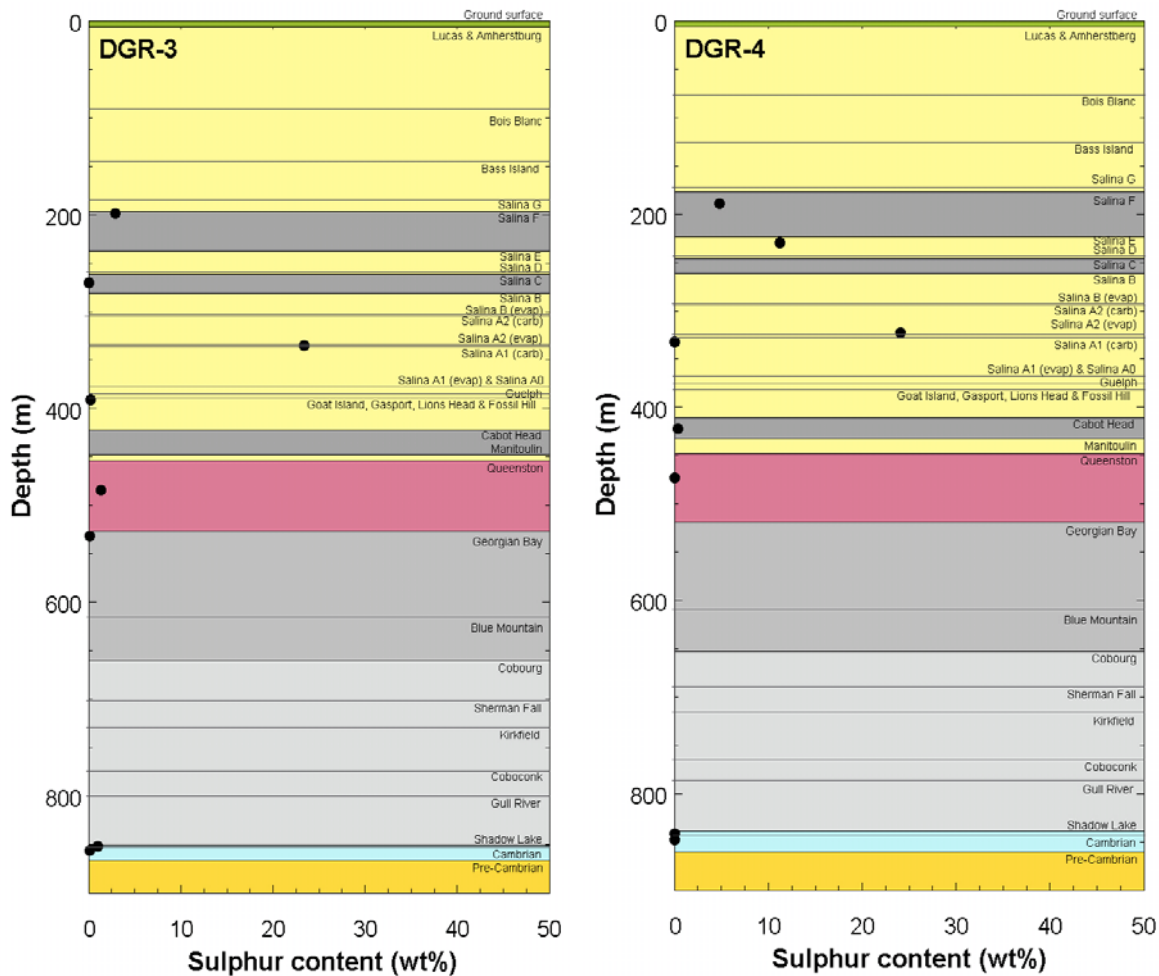


Figure 13: Depth profiles of the total sulphur content as determined by CS-Mat (see Table 3 and Table 4).

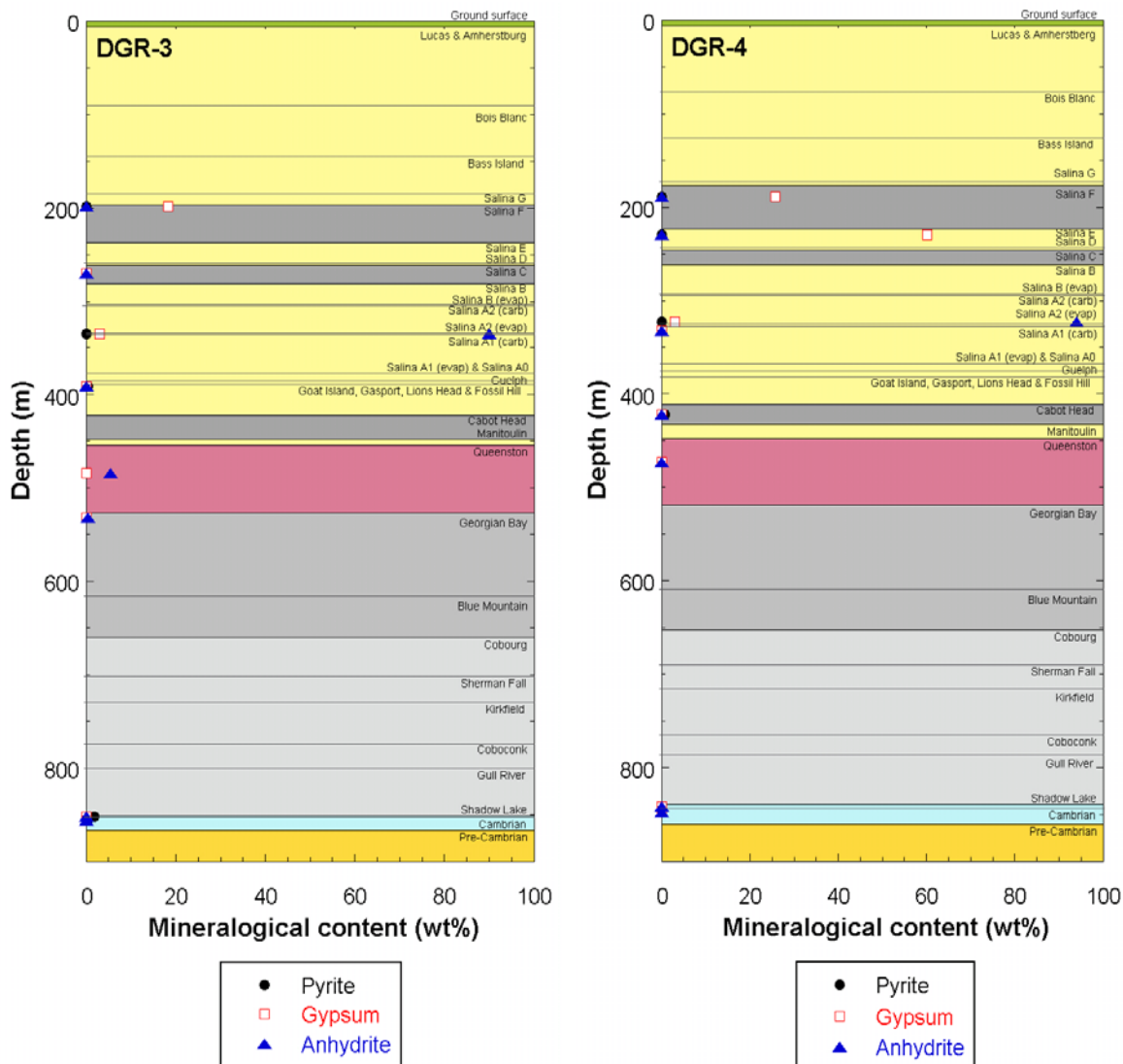


Figure 14: Depth profiles of sulphur-bearing mineral contents. For the Salina-A2 Evaporite samples, these contents were calculated from the total sulphur content measured by CS-Mat and from XRD data (Table 3 and Table 4). In the other samples, all the sulphur was attributed to the main sulphur-bearing phase observed by optical microscopy. In samples for which a sulphur-bearing mineral content of zero is indicated, the mineral was either not detected or was present in negligible amounts (based on microscopic observations).

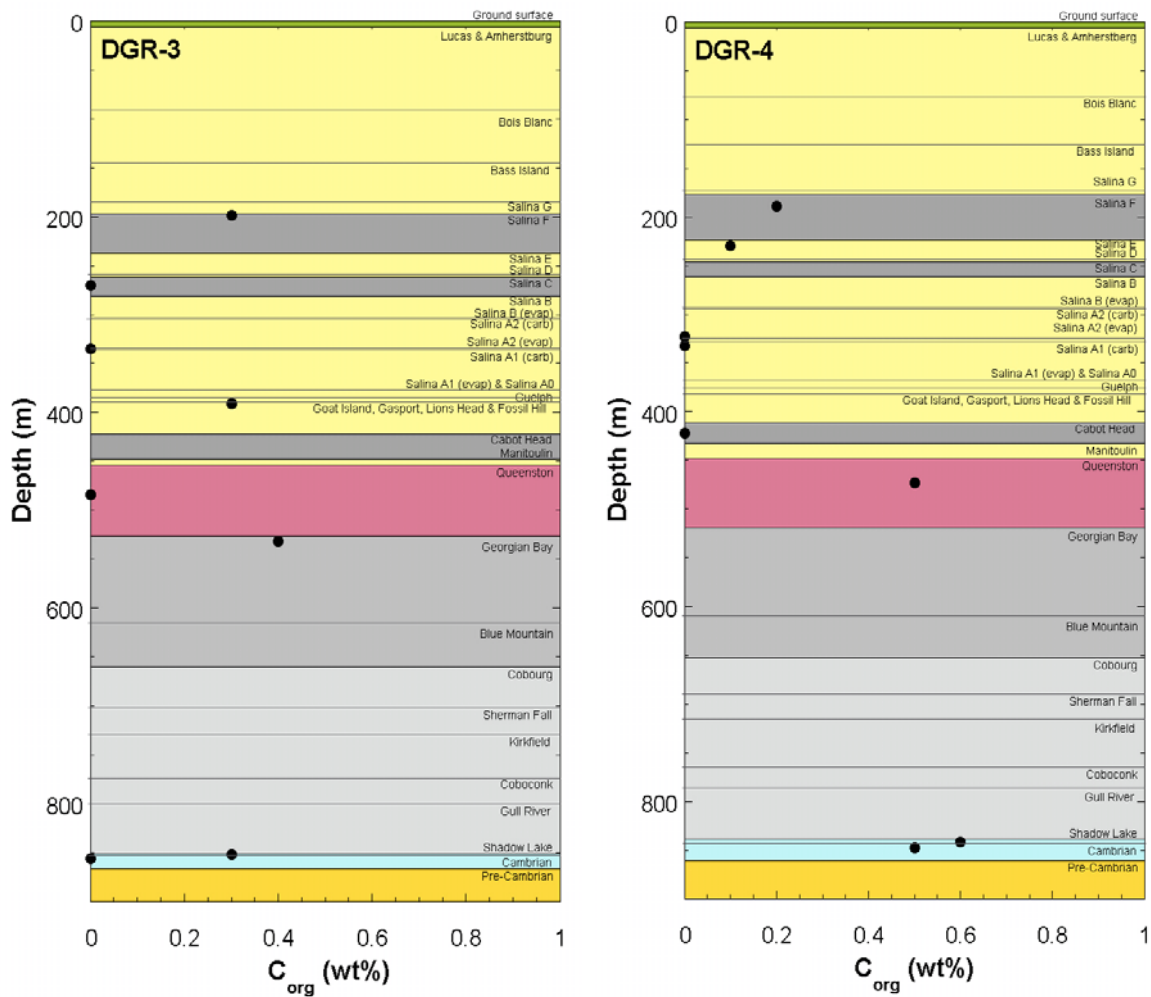


Figure 15: Depth profile of the C_{org} content by CS-Mat (see Table 3 and Table 4).

4 Porewater and petrophysical parameters

In the following sections, water activity measurements and the results of petrophysical testing conducted on samples from boreholes DGR-3 and DGR-4 are presented. Petrophysical testing included measurement of water contents, bulk wet and dry densities and grain densities. Calculated porewater contents and porewater-loss and physical porosities are also presented.

4.1 Water activity

The water activities (a_w) measured for all samples from boreholes DGR-2, -3 and -4 are plotted as a function of depth in Figure 16. The water activities measured for samples from DGR-2 are from Koroleva et al. 2009; values measured for DGR-3 and DGR-4 samples are given in Table 7 and Table 8, respectively. Measured water activities determined from the relative humidity of the core samples range from 1.00 to 0.58, with a measurement accuracy of ± 0.015 activity units. For reference, the activity of pure water is 1.0, the activity of sea water is 0.98, while that of a saturated NaCl solution is 0.75 and that of CaCl₂ solutions can be lower (Koroleva et al., 2009).

In both DGR-3 and -4, samples from the Bass Islands Formation (DGR-4 154.60) and from the Salina F Unit (DGR-3 198.72, DGR-3 208.41; DGR-4 189.16) have measured water activities close to 1.0. Water activities decrease sharply with depth from the F Unit to a value of 0.75 in the B Unit (Figure 16). Higher water activities between 0.84 and 0.92 were measured for rocks of the Salina A2 and A1 carbonate units, with contrasting low water activities of 0.59 to 0.64 measured in the Salina A2 Evaporite located between the two carbonate units and in the underlying Salina A1 Evaporite and Guelph Formation ($a_w \approx 0.74$). However, it is noted that the evaporite beds consist predominantly of anhydrite and because anhydrite readily absorbs water, it is not clear what the measured water activities for these samples represent.

In the Cabot Head Formation and down through the Coboconk Formation, water activities range between 0.56 and 0.72, with an average a_w of 0.67. In DGR-2, the lowest water activity measured was 0.56 for a sample from the Georgian Bay Formation (DGR-2 523.08). In all three boreholes, low a_w values of between 0.58 and 0.62 are measured within the lower member of the Cobourg Formation. From the top of the Gull River Formation, measured water activities increase from 0.66 through the Shadow Lake formation to approximately 0.80 in the Cambrian.

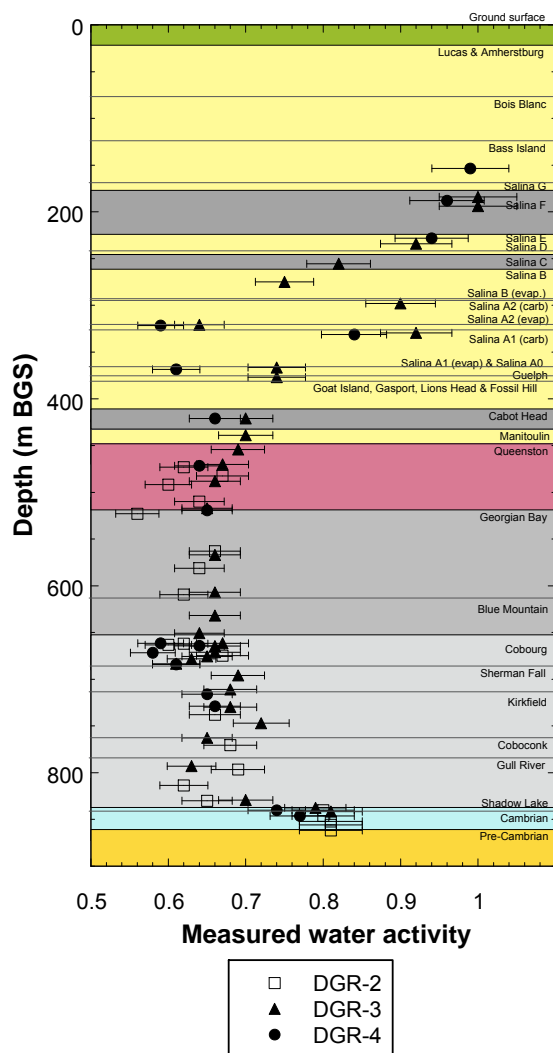


Figure 16: Water activity measured for samples from DGR-2, DGR-3 and DGR-4 as a function of depth (data for DGR-2 samples are from Koroleva et al. 2009). Error bars illustrate the measurement accuracy of the water activities (± 0.015). For samples from DGR-3 and -4, depths have been corrected relative to boreholes DGR-1/-2 (see Table 7 and Table 8).

Table 7: Measured water activities of samples from DGR-3.

Sample ID ¹	Depth relative to DGR-1 & -2 (m BGS)	Formation	Lithology (short)	a _w ²
DGR-3 198.72*	234.3	Salina – F Unit	Dolomitic shale with gypsum	1.00
DGR-3 208.41*	255.6	Salina - F Unit	Dolomitic shale with gypsum	1.00
DGR-3 248.71*	274.9	Salina – E Unit	Dolomitic shale with anhydrite	0.92
DGR-3 270.06*	298.1	Salina - C Unit	Dolomitic shale	0.82
DGR-3 289.36*	320.8	Salina – B Unit	Argillaceous dolostone with anhydrite	0.75
DGR-3 312.53	184.3	Salina - A2 Unit	Dolostone	0.90
DGR-3 335.22*	194.0	Salina A2 Evaporite	Anhydrite	0.64
DGR-3 344.06	329.6	Salina -A1 Unit	Dolostone	0.92
DGR-3 380.88	366.4	Salina A1 Evaporite	Anhydrite	0.74
DGR-3 391.34	376.9	Guelph	Dolostone (veined)	0.74
DGR-3 435.62	421.2	Cabot Head	Dolostone ± shale	0.70
DGR-3 453.41	439.0	Manitoulin	Limestone	0.70
DGR-3 468.76	454.3	Queenston	Shale	0.69
DGR-3 484.58	470.1	Queenston	Shale	0.67
DGR-3 502.55	488.1	Queenston	Shale	0.66
DGR-3 531.65	517.2	Georgian Bay	Shale / sandstone	0.65
DGR-3 581.47	567.0	Georgian Bay	Shale	0.66
DGR-3 621.63	607.2	Blue Mountain	Shale	0.66
DGR-3 646.29	631.8	Blue Mountain	Shale	0.66
DGR-3 665.29	650.8	Cobourg – CM	Argillaceous limestone	0.64
DGR-3 676.21	661.8	Cobourg - LM	Argillaceous limestone	0.67
DGR-3 678.92	664.5	Cobourg - LM	Limestone	0.66
DGR-3 685.52	671.1	Cobourg - LM	Limestone	0.66
DGR-3 690.12	675.7	Cobourg - LM	Limestone	0.65
DGR-3 692.82	678.4	Cobourg - LM	Limestone	0.63
DGR-3 697.94	683.5	Cobourg - LM	Argillaceous limestone	0.61
DGR-3 710.38	695.9	Sherman Fall	Argillaceous limestone	0.69
DGR-3 725.57	711.1	Sherman Fall	Argillaceous limestone	0.68
DGR-3 744.27	729.8	Kirkfield	Argillaceous limestone	0.68
DGR-3 761.56	747.1	Kirkfield	Argillaceous limestone / calcareous shale	0.72
DGR-3 777.33	762.9	Coboconk	Limestone / shale	0.65
DGR-3 807.43	793.0	Gull River	Limestone	0.63
DGR-3 843.92	829.5	Gull River	Limestone	0.70
DGR-3 852.18	837.7	Shadow Lake	Limestone	0.79
DGR-3 856.06	841.6	Cambrian	Sandy limestone	0.81

* Gypsum identified in sample during mineralogical investigations.

¹Actual sample depth in DGR-3 (in mBGS) is given by the second half of the sample ID.

²The measurement accuracy is ± 0.015 a_w

Table 8: Measured water activities of samples from DGR-4.

Sample ID ¹	Depth relative to DGR-1 & -2 (m BGS)	Formation	Lithology (short)	a _w ²
DGR-4 154.60	153.6	Bass Islands	Dolomitic shale with Ca-sulphate	0.99
DGR-4 189.16*	188.1	Salina - F Unit	Dolomitic shale with Ca-sulphate	0.96
DGR-4 229.32*	228.3	Salina - E Unit	Dolomitic shale with Ca-sulphate	0.94
DGR-4 322.68*	321.6	Salina A2 Evaporite	Massive Ca-sulphate	0.59
DGR-4 332.13	331.1	Salina A1 Unit	Argillaceous dolostone with Ca-sulphate	0.84
DGR-4 369.43	368.4	Salina A1 Evaporite	Anhydritic dolostone	0.61
DGR-4 422.21	421.2	Cabot Head	Red-green shale with carbonate and black shale beds	0.66
DGR-4 472.78	471.7	Queenston	Red-green shale with carbonate beds	0.64
DGR-4 520.42	519.4	Georgian Bay	Shale with sandstone/siltstone/limestone beds	0.65
DGR-4 662.83	661.8	Cobourg – LM	Bioclastic limestone and argillaceous limestone	0.59
DGR-4 665.41	664.4	Cobourg – LM	Bioclastic limestone and argillaceous limestone	0.64
DGR-4 672.85	671.8	Cobourg – LM	Bioclastic limestone and argillaceous limestone	0.58
DGR-4 685.14	684.1	Cobourg – LM	Bioclastic limestone and argillaceous limestone	0.61
DGR-4 717.12	716.1	Sherman Fall	Bedded argillaceous limestone and calcareous shale	0.65
DGR-4 730.07	729.0	Kirkfield	Limestone with shale beds	0.66
DGR-4 841.06	840.0	Shadow Lake	Sandy mudstone, siltstone and sandstone	0.74
DGR-4 847.48	846.4	Cambrian	Sandstone/dolostone	0.77

* Gypsum identified in sample during mineralogical investigations.

¹Actual sample depth in DGR-4 (in mBGS) is given by the second half of the sample ID.

²The measurement accuracy is $\pm 0.015 a_w$

4.2 Water and porewater contents

4.2.1 Water content

The water content (pure H₂O only) of each sample was determined using two different methods: i) gravimetrically by oven drying two (40 °C) or four replicate aliquots (105 °C) as described by Koroleva et al. (2009); and ii) using the adapted diffusive isotope exchange technique. Water contents calculated using the measured isotopic compositions of test solutions in the diffusive isotope exchange experiments are given in section 5.2 (Table 22 and Table 26) and a comparison between the water contents determined using these two methods is also presented in that section.

The gravimetric water content $WC_{Grav.wet}$ (expressed as a weight fraction) relative to the wet mass m_{wet} of the rock is calculated from the change in mass upon drying ($m_{wet}-m_{dry}$):

$$WC_{Grav.wet} = \frac{m_{wet} - m_{dry}}{m_{wet}} \quad (4)$$

where m_{wet} = wet mass of the rock and m_{dry} = dry mass of the rock. Water content as a weight fraction relative to the dry mass of rock ($WC_{Grav.dry}$) can be calculated from:

$$WC_{Grav.dry} = \frac{m_{wet} - m_{dry}}{m_{dry}} \quad (5)$$

The gravimetric water contents determined for samples from DGR-3 are given in Table 9 and those for DGR-4 samples are given in Table 10 and Table 11.

For samples from DGR-2 and DGR-3, samples were dried until the change in mass between consecutive measurements was <0.01 grams. For samples from DGR-4, a comprehensive examination of the analytical uncertainty in the water content determinations at both 40 and 105 °C was made by maintaining detailed records of the mass change as a function of time during drying. The analytical uncertainty in the water content measurements was calculated by linear propagation of the measurement uncertainty of all masses through the calculation of water content in weight percent. The analytical uncertainty in the final dry mass of the solid was taken as the difference between the final two recorded masses, or the analytical uncertainty associated with the balance (± 0.002 g), whichever was greater.

The results of the detailed monitoring of DGR-4 samples and example drying curves are provided in Appendix B. The key observations from the experiments conducted at 40 °C are:

- At 40 °C, the mass of the solid decreased steadily during the first few days of drying. However, at longer drying times, mass changes of greater than 0.01 wt. % were observed over a 14-day interval, with the mass of the solid first increasing and then decreasing from one measurement to the next. For these samples, less stringent criteria were used for attainment of stable mass, as documented in Table B-1, Appendix B.

- Several samples showed unusual behaviour during drying. In these cases, selection of the end point of constant mass involved additional interpretation and selection criteria; these cases are documented in Appendix B.

At 105 °C, it was possible to achieve a mass change of less than 0.005 wt. % in the water contents determined for most samples; the exceptions are noted in Table B-2, Appendix B.

Comparing the gravimetric water contents ($WC_{Grav.wet}$) determined at 40 and 105 °C for samples from DGR-4, the largest absolute differences in the water contents (in wt.%) are observed for shale samples from the Salina F and E Units, the Cabot Head and the Queenston formations and for the massive calcium sulphate (anhydrite with some gypsum) beds of the A2 Evaporite. A large difference of >10 wt.% was also observed for the DGR-3 sample from the Salina F Unit shale (DGR-3 208.41). For three additional DGR-4 samples from the Georgian Bay, the Kirkfield and the Shadow Lake formations, the differences between the water contents determined at these two temperatures are lower, but above the standard deviation observed in the 4 replicate measurements made at 105 °C. Similarly, $WC_{Grav.wet}$ results determined at 40 and 105 °C were reported by Koroleva et al. (2009) for select samples from DGR-2. A shale sample from the top of the Queenston Formation (DGR-2 473.19) showed the largest absolute difference (0.7 wt.%) in the water contents determined at these two temperatures.

Gypsum was identified in several samples during mineralogical investigations in both DGR-3 and DGR-4 (see section 3.1, Table 5 and Table 6). Water content values determined at 105 °C are not considered representative for gypsum-bearing samples, because the water lost during drying likely includes waters of dehydration from gypsum, in addition to porewater. The lower drying temperature of 40 °C was originally chosen because it is 2 °C lower than the widely reported temperature of 42 °C (e.g. Deer, Howie & Zussman, 1985) at which gypsum loses its structural water to form anhydrite. If this were the case, then for samples containing gypsum, water contents determined by drying to constant mass at 40 °C could be considered to represent water lost from porewater water only, without contributions from structural water in gypsum. However, it was found that when water contents determined at 40 °C were used to calculate porewater contents and in turn, porewater-loss porosities for samples containing gypsum, the calculated porewater-loss porosities were significantly higher than total physical porosities (see also section 4.4). This observation suggests that the calculated porewater-loss porosities (and therefore also the calculated porewater contents and measured water contents) were overestimated in these samples, even at 40 °C.

At atmospheric pressure, the transition temperature between gypsum and anhydrite has been demonstrated to decrease as solution salinity increases (e.g., Hardie, 1967). With increasing salinity, the vapour pressure of the solution (P_s) decreases relative to the vapour pressure of pure water (P_{H_2O}); where the ratio P_s/P_{H_2O} closely approximates the activity of water (a_{H_2O}). Hardie (1967) conducted a comprehensive study of the gypsum-anhydrite conversion as a function of temperature and water activity, through a series of experiments in which equilibrium was approached from both under- and super-saturation. The results demonstrated that the conversion of gypsum to anhydrite occurs at a temperature of 58 ± 2 °C in solutions with a water activity of 1.0, at 39 ± 2 °C in solutions with a water activity of 0.85 and at temperatures as low as 23 ± 2 °C in solutions with a water activity of 0.77. Gypsum-bearing rock samples examined in DGR-3 and DGR-4 have measured water activities between 0.59 and 1.0; the lower measured water activities for these samples may be due in part, to the presence of saline porewaters (see section 4.2.2 for other factors influencing measured water activities of rock samples). Therefore, the possibility that water contents determined gravimetrically at 40 °C include structural water from gypsum cannot be excluded. For this reason, gravimetric water contents determined for these samples are not used in further calculations or interpretations.

Table 9: Average gravimetric water contents ($WC_{Grav.}$) of DGR-3 samples, determined by drying to constant mass at different temperatures. The water contents are calculated relative to the wet ($WC_{Grav. wet}$) or dry ($WC_{Grav. dry}$) mass of the rock sample.

Sample ID ¹	Depth relative to DGR-1 & -2 (m BGS)	Formation	Lithology (short)	Average $WC_{Grav. wet}$ 40°C ² (n = 2) (wt.%)	Absolute difference (n = 2) (wt.%)	Average $WC_{Grav. wet}$ 105°C ² (n = 4) (wt.%)	STD ($\pm 1\sigma$) (wt.%)	Average $WC_{Grav. dry}$ 105°C ² (n = 4) (wt.%)	STD ($\pm 1\sigma$) (wt.%)
DGR-3 198.72*	234.3	Salina – F Unit	Dolomitic shale with gypsum	1.60*	0.18*	5.82*	2.33*	6.24*	2.63*
DGR-3 208.41*	255.6	Salina - F Unit	Dolomitic shale with gypsum			11.8*	2.39*	13.5*	3.00*
DGR-3 248.71*	274.9	Salina – E Unit	Dolomitic shale with anhydrite			5.36*	0.35*	5.68*	0.38*
DGR-3 270.06*	298.1	Salina - C Unit	Dolomitic shale			6.64*	0.03*	7.11*	0.04*
DGR-3 289.36*	320.8	Salina – B Unit	Argillaceous dolostone with anhydrite			6.65*	0.39*	7.15*	0.44*
DGR-3 312.53	184.3	Salina – A2 Unit	Dolostone			5.33	0.23	5.64	0.26
DGR-3 335.22*	194.0	Salina A2 Evap.	Anhydrite			0.53*	0.07*	0.53*	0.07*
DGR-3 344.06	329.6	Salina - A1 Unit	Dolostone			0.40	0.14	0.40	0.15
DGR-3 380.88	366.4	Salina A1 Evap.	Anhydrite			0.11	0.02	0.11	0.02
DGR-3 391.34	376.9	Guelph	Dolostone (veined)			1.90	0.17	1.95	0.16
DGR-3 435.62	421.2	Cabot Head	Dolostone \pm shale			3.58	0.20	3.75	0.20
DGR-3 453.41	439.0	Manitoulin	Limestone			0.69	0.09	0.70	0.09
DGR-3 468.76	454.3	Queenston	Shale			3.07	0.02	3.19	0.02
DGR-3 484.58	470.1	Queenston	Shale			2.40	0.06	2.47	0.08
DGR-3 502.55	488.1	Queenston	Shale			2.03	0.76	2.09	0.82
DGR-3 531.65	517.2	Georgian Bay	Shale / sandstone			1.81	0.27	1.86	0.30
DGR-3 581.47	567.0	Georgian Bay	Shale			3.20	0.10	3.33	0.13
DGR-3 621.63	607.2	Blue Mountain	Shale			2.96	0.02	3.07	0.04
DGR-3 646.29	631.8	Blue Mountain	Shale			2.74	0.04	2.83	0.05
DGR-3 665.29	650.8	Cobourg – CM	Argillaceous limestone			0.53	0.04	0.54	0.04

*Gypsum identified in samples during mineralogical investigations. Determined values include both water from the pore space and structural water from gypsum and consequently, are not useful.

¹Actual sample depth in DGR-4 (in mBGS) is given by the second half of the sample ID.

² Water content ($WC_{Grav.}$) is defined as the weight proportion of water (H_2O , does not include mass of solutes) in the rock; calculated using equation 4 or 5 (see text).

Table 9 (Cont'd): Average gravimetric water contents (WC_{Grav}) of DGR-3 samples, determined by drying to constant mass at different temperatures. The water contents are calculated relative to the wet ($WC_{Grav.wet}$) or dry ($WC_{Grav.dry}$) mass of the rock sample.

Sample ID ¹	Depth relative to DGR-1 & -2 (m BGS)	Formation	Lithology (short)	Average $WC_{Grav.wet}$ 40°C ¹ (n=2) (wt.%)	Absolute difference (n = 2) (wt.%)	Average $WC_{Grav.wet}$ 105°C ¹ (n=4) (wt.%)	STD ($\pm 1\sigma$) (wt.%)	Average $WC_{Grav.dry}$ 105°C ¹ (n=4) (wt.%)	STD ($\pm 1\sigma$) (wt.%)
DGR-3 676.21	661.8	Cobourg – LM	Argillaceous limestone			0.88	0.19	0.89	0.19
DGR-3 678.92	664.5	Cobourg – LM	Limestone			0.58	0.51	0.59	0.51
DGR-3 685.52	671.1	Cobourg – LM	Limestone			0.63	0.06	0.64	0.06
DGR-3 690.12	675.7	Cobourg – LM	Limestone			0.28	0.12	0.28	0.12
DGR-3 692.82	678.4	Cobourg – LM	Limestone			0.85	0.15	0.86	0.15
DGR-3 697.94	683.5	Cobourg – LM	Argillaceous limestone			0.63	0.06	0.64	0.06
DGR-3 710.38	695.9	Sherman Fall	Argillaceous limestone			0.31	0.10	0.31	0.10
DGR-3 725.57	711.1	Sherman Fall	Argillaceous limestone			0.87	0.10	0.88	0.10
DGR-3 744.27	729.8	Kirkfield	Argillaceous limestone			0.89	0.16	0.90	0.16
DGR-3 761.56	747.1	Kirkfield	Argillaceous limestone / calcareous shale			0.55	0.32	0.55	0.32
DGR-3 777.33	762.9	Coboconk	Limestone / shale			0.46	0.03	0.46	0.03
DGR-3 807.43	793.0	Gull River	Limestone			0.33	0.02	0.33	0.02
DGR-3 843.92	829.5	Gull River	Limestone			0.48	0.21	0.48	0.21
DGR-3 852.18	837.7	Shadow Lake	Limestone			3.06	0.09	3.15	0.10
DGR-3 856.06	841.6	Cambrian	Sandy limestone			0.49	0.12	0.49	0.12

*Gypsum identified in samples during mineralogical investigations. Therefore, determined values likely include both water from the pore space and structural water from gypsum.

¹Actual sample depth in DGR-4 (in mBGS) is given by the second half of the sample ID.

²Water content ($WC_{Grav.}$) is defined as the weight proportion of water (H_2O , does not include mass of solutes) in the rock; calculated using equation 4 or 5 (see text).

Table 10: Average gravimetric water content ($WC_{Grav.wet}$) of DGR-4 samples, calculated relative to the wet mass of the rock sample. Water contents were determined by drying to constant mass at 40 °C or 105 °C.

Sample ID	Depth relative to DGR-1 & -2 (m BGS)	Formation	Lithology (short)	Average $WC_{Grav.wet}$ 40°C ¹ (n=2) (wt.%)	Absolute difference (n=2) (wt. %)	Absolute analytical uncertainty (wt. %)	Average $WC_{Grav.wet}$ 105°C ¹ (n=4) (wt.%)	STD ($\pm 1\sigma$) (wt.%)	Absolute analytical uncertainty (wt.%)
DGR-4 154.60	153.55	Bass Islands	Dolomitic shale with Ca-sulphate	1.56	0.06	<0.01	1.58	0.06	<0.01
DGR-4 189.16*	188.11	Salina - F Unit	Dolomitic shale with Ca-sulphate	3.37* ^A	0.17* ^A	0.02	8.07*	0.59*	<0.01
DGR-4 229.32*	228.27	Salina - E Unit	Dolomitic shale with Ca-sulphate	2.32*	0.43*	<0.01	11.3*	3.36*	0.02
DGR-4 322.68*	321.63	A2 Evaporite	Massive Ca-sulphate	0.04*	0.00*	<0.01	1.27*	0.31*	0.01
DGR-4 332.13	331.08	Salina – A1 Unit	Argillaceous dolostone with Ca-sulphate	0.66	0.07	0.01	0.62	0.10	<0.01
DGR-4 369.43	368.38	A1 Evaporite	Anhydritic dolostone	0.05	0.01	<0.01	0.07	0.01	<0.01
DGR-4 422.21	421.16	Cabot Head	Red-green shale with carbonate/black shale beds	2.76	0.01	0.04	4.05	0.06	<0.01
DGR-4 472.78	471.73	Queenston	Red-green shale with carbonate beds	1.77	0.07	<0.01	2.68	0.04	0.01
DGR-4 520.42	519.37	Georgian Bay	Shale with sandstone/siltstone/ limestone beds	1.37	0.03	0.04	1.61	0.18	<0.01
DGR-4 662.83	661.78	Cobourg	Bioclastic limestone/argillaceous limestone	0.49	0.02	<0.01	0.63	0.12	<0.01
DGR-4 665.41	664.36	Cobourg – LM	Bioclastic limestone/argillaceous limestone	0.53	0.03	0.01	0.57	0.15	<0.01
DGR-4 672.85	671.80	Cobourg – LM	Bioclastic limestone/argillaceous limestone	0.30	0.02	<0.01	0.40	0.07	<0.01
DGR-4 685.14	684.09	Sherman Fall	Bioclastic limestone/argillaceous limestone	0.53	0.14	<0.01	0.73	0.15	<0.01
DGR-4 717.12	716.07	Sherman Fall	Bedded argillaceous limestone/calcareous shale	0.58	0.56	<0.01	1.13	0.46	<0.01
DGR-4 730.07	729.02	Kirkfield	Limestone with shale beds	0.97	0.21	0.03	1.51	0.29	<0.01
DGR-4 841.06	840.01	Shadow Lake	Sandy mudstone, siltstone and sandstone	1.62	0.29	<0.01	2.00	0.13	<0.01
DGR-4 847.48	846.43	Cambrian	Sandstone/dolostone	0.61	0.17	<0.01	0.73	0.08	<0.01

*Gypsum identified in samples during mineralogical investigations. Therefore, determined values likely include both water from the pore space and structural water from gypsum.

^A Value given for average water content is for 4 replicates; Standard deviation of these replicates is given in place of absolute difference.

¹Water content ($WC_{Grav.wet}$) is defined as the weight proportion of water (H_2O , does not include weight of solutes) in the rock; calculated using equation 4 in text. Based on measured values of water loss on drying to constant mass (± 0.005 wt.% for the majority of samples; exceptions are tabulated in Appendix B).

Table 11: Average gravimetric water content ($WC_{Grav.dry}$) of DGR-4 samples, calculated relative to the dry mass of the rock sample. Water contents were determined by drying to constant mass at 40 °C or 105 °C.

Sample ID	Depth relative to DGR-1 & -2 (m BGS)	Formation	Lithology (short)	Average $WC_{Grav.dry}$ 40° C ¹ (n=2) (wt.%)	Absolute difference (wt.%)	Absolute analytical uncertainty (wt.%)	Average $WC_{Grav.dry}$ 105°C ¹ (n=4) (wt.%)	Standard Deviation (n=4) (± wt.%)	Absolute analytical uncertainty (wt.%)
DGR-4 154.60	153.55	Bass Islands	Dolomitic shale with Ca-sulphate	1.58	0.06	<0.01	1.60	0.06	<0.01
DGR-4 189.16*	188.11	Salina - F Unit	Dolomitic shale with Ca-sulphate	3.49* ^A	0.18* ^A	0.02*	8.80*	0.72*	<0.01
DGR-4 229.32*	228.27	Salina - E Unit	Dolomitic shale with Ca-sulphate	2.36*	0.45*	<0.01*	12.76*	4.12*	0.02
DGR-4 322.68*	321.63	Salina - A2 Unit	Massive Ca-sulphate	0.04*	0.00*	<0.01*	1.29*	0.32*	0.01
DGR-4 332.13	331.08	Salina - A1 Unit	Argillaceous dolostone with Ca-sulphate	0.66	0.07	0.01	0.63	0.10	<0.01
DGR-4 369.43	368.38	A1 Evaporite	Anhydritic dolostone	0.05	0.01	<0.01	0.07	0.01	<0.01
DGR-4 422.21	421.16	Cabot Head	Red-green shale with carbonate/black shale beds	2.84	0.01	0.04	4.21	0.07	<0.01
DGR-4 472.78	471.73	Queenston	Red-green shale with carbonate beds	1.80	0.07	<0.01	2.76	0.05	0.01
DGR-4 520.42	519.37	Georgian Bay	Shale with sandstone/siltstone/limestone beds	1.39	0.03	0.04	1.64	0.19	<0.01
DGR-4 662.83	661.78	Cobourg	Bioclastic limestone/argillaceous limestone	0.49	0.02	<0.01	0.63	0.12	<0.01
DGR-4 665.41	664.36	Cobourg - LM	Bioclastic limestone/argillaceous limestone	0.54	0.03	0.01	0.57	0.15	<0.01
DGR-4 672.85	671.80	Cobourg - LM	Bioclastic limestone/argillaceous limestone	0.30	0.02	<0.01	0.40	0.07	<0.01
DGR-4 685.14	684.09	Sherman Fall	Bioclastic limestone/argillaceous limestone	0.53	0.14	<0.01	0.74	0.15	<0.01
DGR-4 717.12	716.07	Sherman Fall	Bedded argillaceous limestone/calcareous shale	0.59	0.57	<0.01	1.15	0.47	<0.01
DGR-4 730.07	729.02	Kirkfield	Limestone with shale beds	0.98	0.22	0.03	1.53	0.29	<0.01
DGR-4 841.06	840.01	Shadow Lake	Sandy mudstone, siltstone and sandstone	1.64	0.30	<0.01	2.04	0.14	<0.01
DGR-4 847.48	846.43	Cambrian	Sandstone/dolostone	0.61	0.17	<0.01	0.73	0.08	<0.01

*Gypsum identified in samples during mineralogical investigations. Therefore, determined values likely include both water from the pore space and structural water from gypsum.

^A Value given for average water content is for 4 replicates; Standard deviation of these replicates is given in place of absolute difference.

¹Water content ($WC_{Grav.dry}$) is defined as the weight proportion of water (H₂O, does not include weight of solutes) in the rock; calculated using equation 5 in text. Based on measured values of water loss on drying to constant mass (± 0.005 wt.% for the majority of samples; exceptions are tabulated in Appendix B).

4.2.2 Porewater contents

When the concentration of solutes in the porewater is low, the porewater content can be taken as equal to the water content (WC) determined gravimetrically. In contrast, in rocks containing highly saline porewaters, the porewater content (PWC) or the weight proportion of brine in the rocks (H₂O plus solutes) will be markedly higher than the water content determined gravimetrically. Blum et al. (1997) proposed the following expression to calculate the mass of porewater (m_{pw}) from the mass of water lost gravimetrically and the salinity:

$$m_{pw} = \frac{(m_{wet} - m_{dry})}{1 - s} \quad (6)$$

where m_{wet} and m_{dry} are the wet and dry masses of the rock material used in the gravimetric water content determinations and s is the salinity of the porewater (expressed as a fraction). Applying this correction to the gravimetric water content, the following equations are derived for pore water contents $PWC_{Grav.wet}$ and $PWC_{Grav.dry}$ (as weight fractions) relative to wet and dry mass of rock:

$$PWC_{Grav.wet} = \frac{(m_{wet} - m_{dry})/(1 - s)}{m_{wet}} \quad (7)$$

$$PWC_{Grav.dry} = \frac{m_{wet} - m_{dry}}{m_{dry} - m_{wet}s} \quad (8)$$

Because the salinity of the porewater is not known, an estimate is required. Based on the water activities measured for the samples, Koroleva et al. (2009) derived two categories for salinity over the DGR-2 profile:

- For the portion of the sedimentary sequence from Queenston Formation through the Cobcoconk Formation ($a_w = 0.56$ to 0.65), a 3.8M CaCl₂, 0.96M NaCl solution with a salinity of 35% and a density of approximately 1.3 g/cm³ was used; and
- For the lower part of the sequence including the Gull River Formation and the Cambrian ($a_w \approx 0.8$), a solution containing 0.9M CaCl₂ and 3.2M NaCl with a salinity of 25% and a density of ca. 1.2 g/cm³ was used.

In the current study, these categories for salinity have been revised to consider the range of water activity measurements from DGR-3 and DGR-4 samples over this same sequence, and expanded to include salinity estimates for porewaters in the upper part of the sedimentary profile from the Bass Islands Formation through the Manitoulin Formation. In addition to dissolved species in the porewater (or osmotic effects), other factors contribute to the measured water activity of a core sample (matrix effects), including i) surface interactions between water and the rock matrix and ii) capillary effects (e.g. Jury et al., 1991; Jarrett et al., 2004).

The measured water activities of the samples were not used as an indicator of porewater salinity for samples from Salina A1 and A2 evaporites (DGR-3 335.22, DGR-3 380.88 and DGR-4 369.43). The evaporite beds consist predominantly of anhydrite and have low water contents (Table 9 and Table 10). Because anhydrite readily absorbs water, it is probable that matrix effects are an important contributor to the measured water activities of these samples. Instead, the solution based on the Cambrian groundwaters with a salinity of 20 wt.% - intermediate with respect to the surrounding formations - was chosen to estimate the porewater salinities for the evaporite formations.

The following procedure was used to develop estimates of porewater salinity over the profile:

1. Four different classes of water activities were defined over the sedimentary sequence, as shown in the first column of Table 12. Measured water activity values for samples from DGR-2, -3 and -4 were considered in the development of these classes (average, measured a_w shown in parenthesis in first column of Table 12).
2. For each water activity class, a chemical composition was derived based on either sampled groundwater composition (where available) or using constraints from porewater studies. The salinity of the solution in weight percent was calculated from the TDS and measured fluid densities of groundwaters for the class with a water activity of 0.84 (Cambrian). For the other three classes, the salinities of the solutions were calculated from the molalities of NaCl or NaCl and CaCl₂. The densities of these solutions at a temperature of 25 °C were approximated from salinity using the following empirical relationship from Maidment (1993):

$$\rho_s(\text{kg}/\text{m}^3) = \rho_0 + AS + BS^{3/2} + CS^2$$

where S is the salinity of the solution in g/kg, ρ_0 is density of pure water at the specified temperature. The parameters A, B, and C are also calculated for this temperature and are defined as follows (Maidment, 1993):

$$A = 8.24493 * 10^{-1} - 4.0899 * 10^{-3} T + 7.6438 * 10^{-4} T^2 - 8.2467 * 10^{-7} T^3 \\ + 5.3675 * 10^{-9} T^4$$

$$B = -5.724 * 10^{-3} + 1.0227 * 10^{-4} T + 1.6546 * 10^{-6} T^2$$

$$C = 4.8314 * 10^{-4}$$

3. For the solutions in water activity classes 0.99, 0.92 and 0.71, the solutions were simulated using PHREEQC and the Pitzer thermodynamic database. An iterative process was used to adjust each of the three solution compositions and the corresponding salinities and densities to the water activity for that class (details are provided in "Basis for Solution Composition" column of Table 12).

The final solution compositions, calculated salinities and estimated or measured densities used for each of the four classes of water activity are shown in Table 12. To enable direct comparison between results from DGR-2, -3 and -4, the salinities and densities of these simulated "porewater" solutions were used to calculate porewater contents for samples from all three boreholes. The calculated porewater contents are given in Table 13 and Table 14 for DGR-3 and -4 samples, respectively; revised values for DGR-2 samples are provided in Appendix E. For samples containing gypsum, porewater contents were not calculated because water content values determined at both 40 and 105 °C are not considered representative (section 4.2.1). Porewater contents calculated for samples from DGR-2, -3 and -4 are plotted as a function of depth in Figure 17.

Porewater content calculated for the Salina A2 Unit (carbonate) is approximately 6 wt.%. From the Salina A1 Evaporite down through the Guelph Formation, porewater contents are lower, ranging between approximately 0.5 and 3 wt. %. In the shales of the Cabot Head Formation through the Blue Mountain Formation, porewater contents of between 1 and 6 wt. % are observed; the underlying limestones of the Cobourg through the Gull River formations have low porewater contents of approximately 0.5 to 2.0 wt. %. In the Shadow Lake Formation through the Cambrian and into the top of the Precambrian, porewater contents increase from values of approximately 1 wt. % to 9 wt. %, with the highest porewater content in this range occurring in the Cambrian.

Table 12: Solutions used as estimates of porewater salinity over the sedimentary sequence (Bass Islands through to the Cambrian).

a_w ¹ class (average, measured a_w)	Formations to which salinity estimate was applied	Basis for Solution Composition	Solution Composition	Salinity (wt. %)	Calculated solution density @ 25 °C ² (g/cm ³)
0.99 (0.99)	Bass Islands	An apparent porewater composition was scaled up from aqueous leaching data using water content (section 6.3.1). The up-scaled solution was equilibrated with dolomite using PHREEQC and the TDS of the solution was used to approximate the salinity.	Mg-HCO ₃ -Cl	3.8 ^A	1.03
0.92 (0.87)	Salina - E Unit, Salina - A2 Unit, Salina - A1 Unit	Groundwaters sampled from the Salina A1 Unit (DGR-3, OGW-8 and DGR-4, OGW-11; from Intera, 2009b). The concentrations of both Na and Cl were increased relative to the groundwater to achieve a simulated water activity of 0.92.	2.25M NaCl	12 ^A	1.09
0.84 (0.80)	Salina - C Unit, Salina - B Unit, Salina A2 Unit, A2 & A1 evaporites, Shadow Lake, Cambrian, Precambrian	Cambrian groundwater (OGW-10, OGW-13) ^A	Cambrian groundwater ^A	20 ^B	1.15 ^B
0.71 (0.65)	Guelph Formation, Cabot Head through Gull River formations	The average Ca/Na molal ratio of 0.67 observed for porewaters in the Cabot Head through Blue Mountain Formations was matched. The salinity of a NaCl/CaCl ₂ solution was then increased to achieve a minimum, predicted water activity without exceeding halite saturation. In the Cobourg through Gull River formations, the average Ca/Na ratio in the porewaters was 0.32. A 4M NaCl, 1.26M CaCl ₂ solution was predicted to be just a saturation with respect to halite with a_w of 0.72 (salinity 27%). Groundwaters from the Guelph formation (OGW-9, OGW-12; Intera, 2009b) give a similar, predicted water activity when equilibrated with both halite and calcite and have a similar, average salinity and solution density.	2.9M NaCl, 1.95 CaCl ₂	28	1.23

¹Simulated water activity of solution using the geochemical modelling code PHREEQC (Pitzer database).

²Calculated using equation from Maidment (1993).

^ASalinity of the solution calculated from the solution components.

^BAverage salinity for the calculated from the TDS values and fluid densities as reported by Intera (2009b).

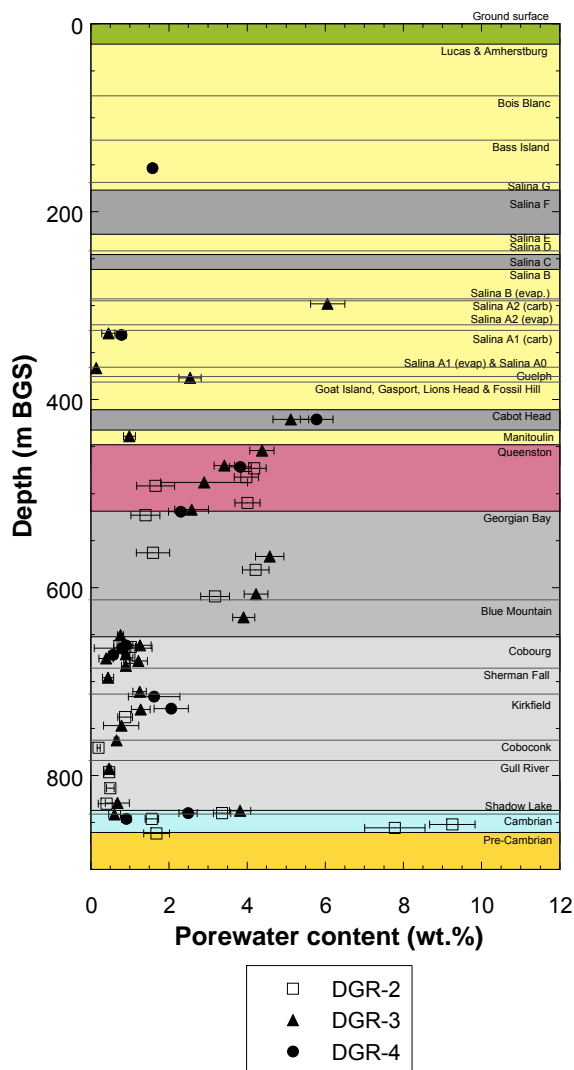


Figure 17: Porewater content ($PWC_{Grav.wet}$) plotted as a function of depth below ground surface in boreholes DGR-2, -3 and -4. Error bars show the uncertainty in the calculated porewater contents. Depths for samples from DGR-3 and -4 are corrected relative to DGR-1/2.

Porewater contents for samples from DGR-3 and DGR-4 were also calculated using porewater salinity and density estimates derived for pore fluids by Intera, 2010a for each formation within the sedimentary sequence. The predicted porewater contents (relative to the wet mass of sample, $PWC_{Grav.wet}$) are compared to those from this study in Table 15 and Table 16 for samples from DGR-3 and DGR-4, respectively (a similar comparison for DGR-2 samples is provided in Appendix E). Considering the uncertainty in $PWC_{Grav.wet}$, the porewater contents predicted using the salinity/density estimates from Intera, 2010a are the same as those calculated in this study.

Table 13: Porewater contents for DGR-3 samples, calculated relative to wet ($PWC_{Grav.wet}$) or dry ($PWC_{Grav.dry}$) mass of rock.

Sample ID	Depth relative to DGR -1 & -2 (m BGS)	Formation	Lithology (short)	Measured a_w	Estimated porewater salinity (%)	$PWC_{Grav.wet}^1$ (wt.%)	Uncertainty ₂ $PWC_{Grav.wet}$ (\pm wt.%)	$PWC_{Grav.dry}^1$ (wt.%)	Uncertainty ₂ $PWC_{Grav.dry}$ (\pm wt. %)
DGR-3 198.72*	234.3	Salina – F Unit	Dolomitic shale with gypsum	1.00	3.2	n.a.	n.a.	n.a.	n.a.
DGR-3 208.41*	255.6	Salina - F Unit	Dolomitic shale with gypsum	1.00	3.2	n.a.	n.a.	n.a.	n.a.
DGR-3 248.71*	274.9	Salina – E Unit	Dolomitic shale with anhydrite	0.92	12	n.a.	n.a.	n.a.	n.a.
DGR-3 270.06*	298.1	Salina - C Unit	Dolomitic shale	0.82	20	n.a.	n.a.	n.a.	n.a.
DGR-3 289.36*	320.8	Salina – B Unit	Argillaceous dolostone with anhydrite	0.75	20	n.a.	n.a.	n.a.	n.a.
DGR-3 312.53	184.3	Salina – A2 Unit	Dolostone	0.90	12	6.06	0.44	6.45	0.47
DGR-3 335.22*	194.0	Salina A2 Evap.	Anhydrite	0.64	20	n.a.	n.a.	n.a.	n.a.
DGR-3 344.06	329.6	Salina - A1 Unit	Dolostone	0.92	12	0.45	0.17	0.45	0.17
DGR-3 380.88	366.4	Salina A1 Evap.	Anhydrite	0.74	20	0.14	0.02	0.14	0.02
DGR-3 391.34	376.9	Guelph	Dolostone (veined)	0.74	28	2.64	0.30	2.71	0.29
DGR-3 435.62	421.2	Cabot Head	Dolostone \pm shale	0.70	28	4.98	0.44	5.24	0.45
DGR-3 453.41	439.0	Manitoulin	Limestone	0.70	28	0.96	0.14	0.97	0.15
DGR-3 468.76	454.3	Queenston	Shale	0.69	28	4.26	0.30	4.45	0.31
DGR-3 484.58	470.1	Queenston	Shale	0.67	28	3.33	0.25	3.44	0.26
DGR-3 502.55	488.1	Queenston	Shale	0.66	28	2.82	1.08	2.91	1.16
DGR-3 531.65	517.2	Georgian Bay	Shale / sandstone	0.65	28	2.51	0.42	2.58	0.45
DGR-3 581.47	567.0	Georgian Bay	Shale	0.66	28	4.45	0.34	4.66	0.37
DGR-3 621.63	607.2	Blue Mountain	Shale	0.66	28	4.11	0.29	4.29	0.30
DGR-3 646.29	631.8	Blue Mountain	Shale	0.66	28	3.80	0.27	3.95	0.28
DGR-3 665.29	650.8	Cobourg – CM	Argillaceous limestone	0.64	28	0.74	0.08	0.74	0.08

*Gypsum identified in samples during mineralogical investigations.

n.a. - indicates that calculation of porewater contents was not applicable to these samples, due to presence of gypsum.

¹Calculated using equation 4 or 5 and average water contents determined at 105 °C.

²Uncertainty determined using Gaussian error propagation (equations 7 and 8).

Table 13 (Cont'd): Porewater contents for DGR-3 samples, calculated relative to wet ($PWC_{Grav.wet}$) or dry ($PWC_{Grav.dry}$) mass of rock.

Sample ID	Depth relative to DGR-1 & -2 (m BGS)	Formation	Lithology (short)	Measured a_w	Estimated porewater salinity (%)	$PWC_{Grav.wet}^1$ (wt.%)	Uncertainty ² $PWC_{Grav.wet}$ (\pm wt.%)	$PWC_{Grav.dry}^1$ (wt.%)	Uncertainty ² $PWC_{Grav.dry}$ (\pm wt.%)
DGR-3 676.21	661.8	Cobourg – LM	Argillaceous limestone	0.67	28	1.22	0.27	1.24	0.27
DGR-3 678.92	664.5	Cobourg – LM	Limestone	0.66	28	0.81	0.72	0.82	0.72
DGR-3 685.52	671.1	Cobourg – LM	Limestone	0.66	28	0.88	0.10	0.88	0.10
DGR-3 690.12	675.7	Cobourg – LM	Limestone	0.65	28	0.38	0.17	0.38	0.17
DGR-3 692.82	678.4	Cobourg – LM	Limestone	0.63	28	1.19	0.22	1.20	0.22
DGR-3 697.94	683.5	Cobourg – LM	Argillaceous limestone	0.61	28	0.88	0.10	0.89	0.10
DGR-3 710.38	695.9	Sherman Fall	Argillaceous limestone	0.69	28	0.42	0.14	0.43	0.14
DGR-3 725.57	711.1	Sherman Fall	Argillaceous limestone	0.68	28	1.21	0.16	1.23	0.16
DGR-3 744.27	729.8	Kirkfield	Argillaceous limestone	0.68	28	1.24	0.24	1.26	0.24
DGR-3 761.56	747.1	Kirkfield	Argillaceous limestone /calcareous shale	0.72	28	0.76	0.44	0.77	0.45
DGR-3 777.33	762.9	Coboconk	Limestone / shale	0.65	28	0.64	0.06	0.64	0.06
DGR-3 807.43	793.0	Gull River	Limestone	0.63	28	0.46	0.04	0.46	0.04
DGR-3 843.92	829.5	Gull River	Limestone	0.70	28	0.66	0.30	0.67	0.30
DGR-3 852.18	837.7	Shadow Lake	Limestone	0.79	20	3.82	0.27	3.98	0.28
DGR-3 856.06	841.6	Cambrian	Sandy limestone	0.81	20	0.61	0.15	0.61	0.15

*Gypsum identified in samples during mineralogical investigations.

n.a. – indicates that calculation of porewater contents was not applicable to these samples, due to presence of gypsum.

¹Calculated using equation 4 or 5 and average water contents determined at 105 °C.

²Uncertainty determined using Gaussian error propagation (equations 7 and 8).

Table 14: Porewater contents for DGR-4 samples, calculated relative to wet ($PWC_{Grav.wet}$) or dry ($PWC_{Grav.dry}$) mass of rock.

Sample ID	Depth relative to DGR-1 & -2 (m BGS)	Formation	Lithology (short)	Measured a_w	Estimated porewater salinity (%)	$PWC_{Grav.wet}^1$ (wt.%)	Uncertainty in $PWC_{Grav.wet}^2$ (\pm wt.%)	$PWC_{Grav.dry}^1$ (wt.%)	Uncertainty in $PWC_{Grav.dry}^2$ (\pm wt.%)
DGR-4 154.60	153.55	Bass Islands	Dolomitic shale with Ca-sulphate	0.99	3.8	1.64	0.11	1.67	0.11
DGR-4 189.16*	188.11	Salina - F Unit	Dolomitic shale with Ca-sulphate	0.96	3.8	n.a.	n.a.	n.a.	n.a.
DGR-4 229.32*	228.27	Salina - E Unit	Dolomitic shale with Ca-sulphate	0.94	12	n.a.	n.a.	n.a.	n.a.
DGR-4 322.68*	321.63	A2 Evaporite	Massive Ca-sulphate	0.59	20	n.a.	n.a.	n.a.	n.a.
DGR-4 332.13	331.08	Salina - A1 Unit	Argillaceous dolostone with Ca-sulphate	0.84	12	0.71	0.12	0.71	0.12
DGR-4 422.21	421.16	Cabot Head	Red-green shale with carbonate/black shale beds	0.66	28	5.62	0.40	5.95	0.42
DGR-4 472.78	471.73	Queenston	Red-green shale with carbonate beds	0.64	28	3.72	0.26	3.87	0.27
DGR-4 520.42	519.37	Georgian Bay	Shale with sandstone/siltstone/limestone beds	0.65	28	2.23	0.30	2.29	0.31
DGR-4 662.83	661.78	Cobourg – LM	Bioclastic limestone/argillaceous limestone	0.59	28	0.87	0.17	0.88	0.17
DGR-4 665.41	664.36	Cobourg - LM	Bioclastic limestone/argillaceous limestone	0.64	28	0.79	0.22	0.80	0.22
DGR-4 672.85	671.80	Cobourg - LM	Bioclastic limestone/argillaceous limestone	0.58	28	0.56	0.10	0.56	0.10
DGR-4 717.12	716.07	Sherman Fall	Bedded argillaceous limestone/calcareous shale	0.65	28	1.57	0.65	1.60	0.66
DGR-4 730.07	729.02	Kirkfield	Limestone with shale beds	0.66	28	2.02	0.42	2.06	0.43
DGR-4 841.06	840.01	Shadow Lake	Sandy mudstone, siltstone and sandstone	0.74	20	2.49	0.23	2.56	0.24
DGR-4 847.48	846.43	Cambrian	Sandstone/dolostone	0.77	20	0.91	0.12	0.92	0.12

*Gypsum identified in samples during mineralogical investigations.

n.a. – indicates that calculation of porewater contents was not applicable to these samples, due to presence of gypsum.

¹Calculated using equation 7 or 8 and average water contents determined at 105 °C.

²Uncertainty determined using Gaussian error propagation (equations 7 and 8).

Table 15: Comparison of porewater contents for DGR-3 samples, calculated relative to wet ($PWC_{Grav.wet}$) mass of rock using estimated porewater salinities and densities from this study and from Intera, 2010a.

Sample ID	Depth relative to DGR -1 & -2 (m BGS)	Formation	This study (Table 12 and Table 13)				From Intera, 2010a		
			Measured a_w -	Porewater Salinity (%)	$PWC_{Grav.wet}$ (wt.%)	Uncertainty $PWC_{Grav.wet}$ (\pm wt.%)	Pore fluid salinity ¹ (%)	Estimated liquid density ¹ (kg/m ³)	$PWC_{Grav.wet}$ ² (wt.%)
DGR-3 198.72*	234.3	Salina – F Unit	1.00	3.8	n.a.	n.a.	n.a.	1004	n.a.
DGR-3 208.41*	255.6	Salina - F Unit	1.00	3.8	n.a.	n.a.	n.a.	1004	n.a.
DGR-3 248.71*	274.9	Salina – E Unit	0.92	12	n.a.	n.a.	n.a.	1029	n.a.
DGR-3 270.06*	298.1	Salina - C Unit	0.82	20	n.a.	n.a.	n.a.	1093	n.a.
DGR-3 289.36*	320.8	Salina – B Unit	0.75	20	n.a.	n.a.	n.a.	1143	n.a.
DGR-3 312.53	184.3	Salina – A2 Unit	0.90	12	6.06	0.44	20.3	1118	6.69
DGR-3 335.22*	194.0	Salina A2 Evap.	0.64	20	n.a.	n.a.	n.a.	1064	n.a.
DGR-3 344.06	329.6	Salina - A1 Unit	0.92	12	0.45	0.17	3.4 ^a	1017 ^a	0.41
DGR-3 380.88	366.4	Salina A1 Evap.	0.74	20	0.14	0.02	11.2	1063	0.12
DGR-3 391.34	376.9	Guelph	0.74	28	2.64	0.30	26.8	1190	2.60
DGR-3 435.62	421.2	Cabot Head	0.70	28	4.98	0.44	27.3	1197	4.93
DGR-3 453.41	439.0	Manitoulin	0.70	28	0.96	0.14	25.9	1179	0.94
DGR-3 468.76	454.3	Queenston	0.69	28	4.26	0.30	28.8	1210	4.31
DGR-3 484.58	470.1	Queenston	0.67	28	3.33	0.25	28.8	1210	3.36
DGR-3 502.55	488.1	Queenston	0.66	28	2.82	1.08	28.8	1210	2.85
DGR-3 531.65	517.2	Georgian Bay	0.65	28	2.51	0.42	25.9	1177	2.44
DGR-3 581.47	567.0	Georgian Bay	0.66	28	4.45	0.34	25.9	1177	4.32
DGR-3 621.63	607.2	Blue Mountain	0.66	28	4.11	0.29	25.7	1179	3.99
DGR-3 646.29	631.8	Blue Mountain	0.66	28	3.80	0.27	25.7	1179	3.68
DGR-3 665.29	650.8	Cobourg – CM	0.64	28	0.74	0.08	25.1	1173	0.71

*Gypsum identified in samples during mineralogical investigations.

n.a. - indicates that calculation of porewater contents was not applicable to these samples, due to presence of gypsum.

^aAverage of values for the Salina A1 Upper and Salina A1 Lower reported in Intera, 2010a.

¹Salinity and density for pore fluids from Table 2 in Intera, 2010a.

²Calculated using equation 4 or 5 and average water contents determined at 105 °C.

Table 15 (Cont'd): Comparison of porewater contents for DGR-3 samples, calculated relative to wet ($PWC_{Grav.wet}$) mass of rock using estimated porewater salinities and densities from this study and from Intera, 2010a.

Sample ID	Depth relative to DGR -1 & -2 (m BGS)	Formation	This study (Table 12 and Table 13)				From Intera, 2010a		
			Measured a_w	Porewater Salinity	$PWC_{Grav.wet}$	Uncertainty $PWC_{Grav.wet}$	Pore fluid salinity ¹	Estimated liquid density ¹	$PWC_{Grav.wet}$ ²
			-	(%)	(wt.%)	(± wt.%)	(%)	(kg/m ³)	(wt.%)
DGR-3 676.21	661.8	Cobourg – LM	0.67	28	1.22	0.27	20.0	1128	1.10
DGR-3 678.92	664.5	Cobourg – LM	0.66	28	0.81	0.72	20.0	1128	0.73
DGR-3 685.52	671.1	Cobourg – LM	0.66	28	0.88	0.10	20.0	1128	0.79
DGR-3 690.12	675.7	Cobourg – LM	0.65	28	0.38	0.17	20.0	1128	0.34
DGR-3 692.82	678.4	Cobourg – LM	0.63	28	1.19	0.22	20.0	1128	1.07
DGR-3 697.94	683.5	Cobourg – LM	0.61	28	0.88	0.10	20.0	1128	0.79
DGR-3 710.38	695.9	Sherman Fall	0.69	28	0.42	0.14	24.5	1168	0.40
DGR-3 725.57	711.1	Sherman Fall	0.68	28	1.21	0.16	24.5	1168	1.16
DGR-3 744.27	729.8	Kirkfield	0.68	28	1.24	0.24	23.3	1157	1.16
DGR-3 761.56	747.1	Kirkfield	0.72	28	0.76	0.44	23.3	1157	0.71
DGR-3 777.33	762.9	Coboconk	0.65	28	0.64	0.06	20.4	1132	0.58
DGR-3 807.43	793.0	Gull River	0.63	28	0.46	0.04	22.3	1148	0.43
DGR-3 843.92	829.5	Gull River	0.70	28	0.66	0.30	22.3	1148	0.61
DGR-3 852.18	837.7	Shadow Lake	0.79	20	3.82	0.27	18.3	1115	3.74
DGR-3 856.06	841.6	Cambrian	0.81	20	0.61	0.15	18.1	1113	0.59

*Gypsum identified in samples during mineralogical investigations.

n.a. - indicates that calculation of porewater contents was not applicable to these samples, due to presence of gypsum.

¹Salinity and density for pore fluids from Table 2 in Intera, 2010a.

²Calculated using equation 4 or 5 and average water contents determined at 105 °C.

Table 16: Comparison of porewater contents for DGR-4 samples, calculated relative to wet ($PWC_{Grav.wet}$) mass of rock using estimated porewater salinities and densities from this study and from Intera, 2010a.

Sample ID	Depth relative to DGR -1 & -2 (m BGS)	Formation	This study (Table 12 and Table 14)				From Intera, 2010a		
			Measured a_w -	Porewater salinity (%)	$PWC_{Grav.wet}$ (wt.%)	Uncertainty $PWC_{Grav.wet}$ (± wt.%)	Pore fluid salinity ¹ (%)	Estimated liquid density ¹ (kg/m ³)	$PWC_{Grav.wet}$ ² (wt.%)
DGR-4 154.60	153.55	Bass Islands	0.99	3.8	1.64	0.11	0.3	993	1.59
DGR-4 189.16*	188.11	Salina – F Unit	0.96	3.8	n.a.	n.a.	1.5	1004	n.a.
DGR-4 229.32*	228.27	Salina – E Unit	0.94	12	n.a.	n.a.	5.9	1029	n.a.
DGR-4 322.68*	321.63	A2 Evaporite	0.59	20	n.a.	n.a.	11.3	1064	n.a.
DGR-4 332.13	331.08	Salina – A1 Unit	0.84	20	0.71	0.12	3.4 ^a	1017	0.64
DGR-4 422.21	421.16	Cabot Head	0.66	28	5.62	0.40	27.3	1197	5.56
DGR-4 472.78	471.73	Queenston	0.64	28	3.72	0.26	28.8	1210	3.77
DGR-4 520.42	519.37	Georgian Bay	0.65	28	2.23	0.30	25.9	1177	2.17
DGR-4 662.83	661.78	Cobourg - LM	0.59	28	0.87	0.17	20.0	1128	0.78
DGR-4 665.41	664.36	Cobourg - LM	0.64	28	0.79	0.22	20.0	1128	0.71
DGR-4 672.85	671.80	Cobourg - LM	0.58	28	0.56	0.10	20.0	1128	0.50
DGR-4 717.12	716.07	Sherman Fall	0.65	28	1.57	0.65	24.5	1168	1.50
DGR-4 730.07	729.02	Kirkfield	0.66	28	2.02	0.42	23.3	1157	1.92
DGR-4 841.06	840.01	Shadow Lake	0.74	20	2.49	0.23	18.3	1115	2.44
DGR-4 847.48	846.43	Cambrian	0.77	20	0.91	0.12	18.1	1113	0.89

*Gypsum identified in samples during mineralogical investigations.

n.a. - indicates that calculation of porewater contents was not applicable to these samples, due to presence of gypsum.

¹Salinity and density for pore fluids from Table 2 in Intera, 2010a.

²Calculated using equation 4 or 5 and average water contents determined at 105 °C.

Samples for which both sheet silicate content (wt.%) and porewater content were determined are plotted in Figure 18. Of the 30 samples examined, approximately three quarters show a positive correlation between the sum of the sheet silicates (i.e., clay content) and porewater content ($PWC_{Grav.wet}$). The exceptions are labelled in Figure 18 and include two samples from the Shadow Lake Formation and three samples from the Cambrian.

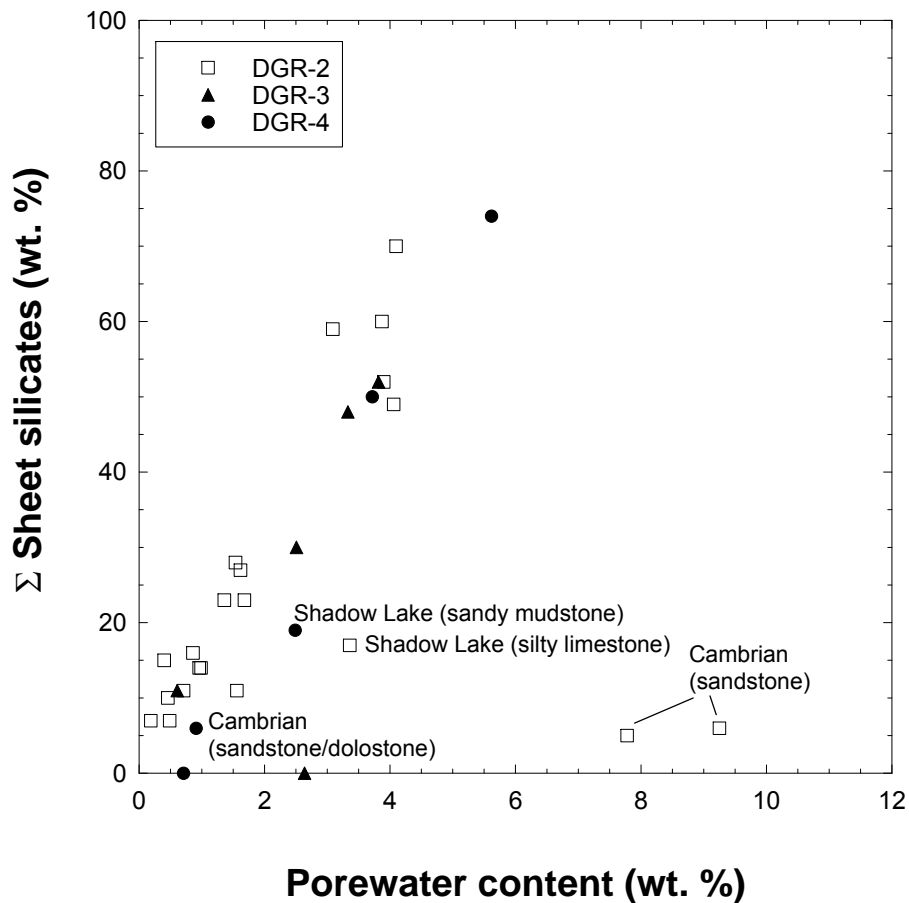


Figure 18: Total sheet silicate content (or clay content) versus calculated porewater content ($PWC_{Grav.wet}$) for select samples for which mineralogy was determined. Samples plotting at zero had a sheet silicate content that was below detection (< 1 wt.%).

4.3 Densities

The bulk wet, bulk dry and grain densities determined for DGR-3 and DGR-4 samples are reported in Table 17 and Table 18, respectively. As for samples from borehole DGR-2, bulk dry densities are calculated using the following expression (Koroleva et al. 2009):

$$\rho_{b,dry} = \frac{\rho_{b,wet}}{1 + PWC_{Grav,dry}} \quad (9)$$

Consequently, bulk dry densities were calculated only for samples for which porewater contents were available; this excludes all gypsum-bearing samples. For DGR-4 samples, bulk dry densities were also measured using the paraffin displacement method described in section 2.1.3. Both the measured and calculated dry bulk densities are reported in Table 18 and compared in Figure 19. The bulk dry density measurements were made on material from the aliquots used to determine water content and, therefore, were dried to constant mass at 105 °C prior to the bulk dry density measurements.

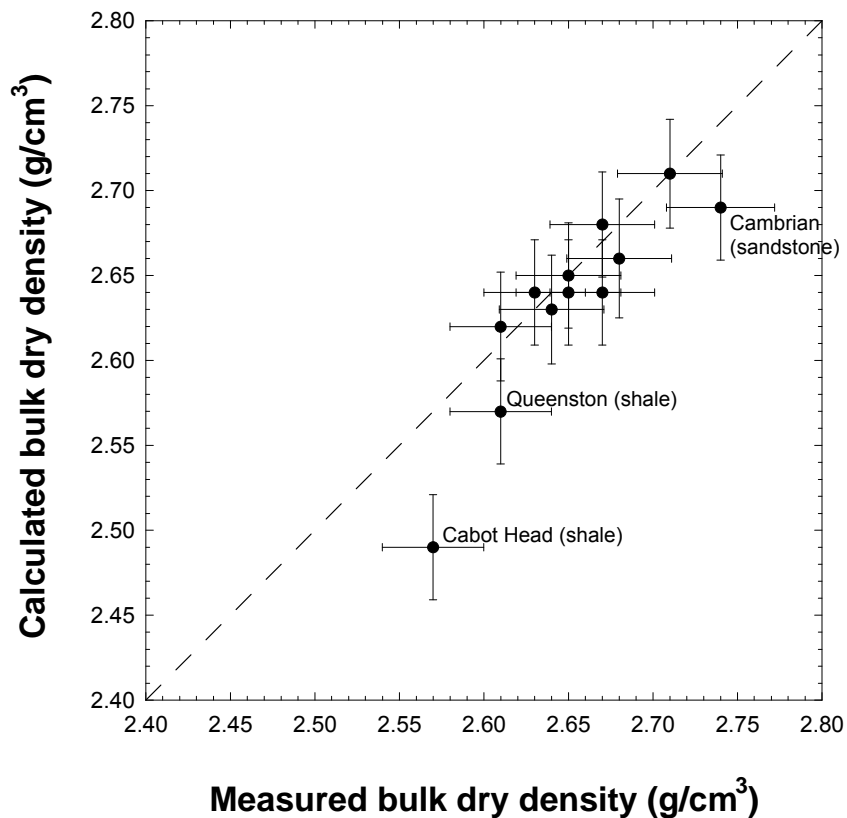


Figure 19: Comparison between calculated and measured bulk densities for DGR-4 samples. Error bars indicate the calculated uncertainty in each parameter.

Three of the samples have measured densities that are higher than the calculated values; of these, the differences are most pronounced for sample DGR-4 422.21 from the Cabot Head Formation and for sample DGR-4 472.78 from the Queenston Formation. For the sample from the Cabot Head Formation, the water content determined at 105 °C was approximately twice that determined at 40 °C. This sample also has the highest sheet silicate content (74%) of all samples examined. The sample from the Queenston Formation also has a relatively high content of sheet silicates (50%). The higher, measured bulk dry densities of these samples could be explained by a decrease in the volume of these clay-rich samples during drying at 105 °C (i.e., due to contraction). A similar comparison between bulk dry densities calculated from porewater contents and values measured on samples dried at 105 °C has been recently made for samples from a clay-rich facies of the Opalinus Clay, where the discrepancy was about 0.1 g/cm³ (Mazurek and Meier, *in prep.*). Measured bulk dry densities were also observed to be higher than those calculated from the bulk wet densities. Taken together, the results of these two studies suggest that some clay-rich rocks are susceptible to decreases in volume during drying at 105 °C. Decreases in volume suggest that interlayer water from the clays is lost during drying. If the measured dry bulk densities of such samples are used in the calculation of physical porosity (section 4.4), the physical porosities will be underestimated.

Grain densities were also measured on subsamples of the rock material dried to constant mass at 105 °C for gravimetric water content determinations. After drying, the rock material includes salts precipitated from the porewater, as well as rock matrix material. A simplified assessment of the potential influence of these salts on the measured grain density was made by considering the proportion of salts in the measured material relative to the mass of rock using the following formulation:

$$\rho_g = (1 - x)\rho_r + x\rho_s \quad (10)$$

where ρ_g is the measured grain density, ρ_s is the density of the salts from the porewater, and ρ_r is the actual density of the rock material without porewater salts; x is the proportion by mass of porewater salts relative to the dry mass of the rock material (rock + porewater salts). Given that the rock material was dried at 105 °C and at atmospheric pressure prior to the measurements, the composition of the salts precipitated from the porewater was estimated as CaCl₂•2H₂O, with a density of 1.84 g/cm³ (ρ_s). This should provide a conservative estimate of the effect of the salts compared to selecting NaCl, which has a higher density (2.17 g/cm³).

When this correction was applied to grain densities measured for samples from DGR-3, the maximum difference between the calculated densities of the rock material without salts (ρ_r) and the measured values was 0.03 g/cm³, which is within the standard deviation determined for measured grain densities (0.01 to 0.04 g/cm³). Based on this finding, and because the porewater compositions and salinities are not known with certainty, application of such corrections to the grain density measurements and use of “salinity-corrected” grain density measurements is not considered to be warranted.

Table 17: Bulk and grain densities determined for DGR-3 samples.

Sample ID	Formation	Grain Density (average, $n=2$) (g/cm ³)	Bulk Wet Density (average, $n=2$) (g/cm ³)	Calculated Bulk Dry Density ¹ (g/cm ³)	Uncertainty in calculated Bulk Dry Density ² (± g/cm ³)
DGR-3 198.72*	Salina – F Unit	2.76*	2.61	n.a.*	n.a.*
DGR-3 208.41*	Salina - F Unit	2.63*	2.42	n.a.*	n.a.*
DGR-3 248.71*	Salina – E Unit	2.69*	2.63	n.a.*	n.a.*
DGR-3 270.06*	Salina - C Unit	2.81*	2.46	n.a.*	n.a.*
DGR-3 289.36*	Salina – B Unit	2.77*	2.54	n.a.*	n.a.*
DGR-3 312.53	Salina - A2 Unit	2.86	2.58	2.42	0.03
DGR-3 335.22*	Salina – A2 Evap.	2.93*	2.88	n.a.*	n.a.*
DGR-3 344.06	Salina -A1 Unit	2.70	2.64	2.63	0.03
DGR-3 380.88	A1 Evaporite	2.95	2.89	2.89	0.05
DGR-3 391.34	Guelph	2.81	2.65	2.58	0.03
DGR-3 435.62	Cabot Head	2.75	2.64	2.51	0.03
DGR-3 453.41	Manitoulin	2.76	2.68	2.65	0.03
DGR-3 468.76	Queenston	2.78	2.65	2.54	0.03
DGR-3 484.58	Queenston	2.78	2.67	2.58	0.08
DGR-3 502.55	Queenston	2.77	2.65	2.58	0.04
DGR-3 531.65	Georgian Bay	2.78	2.65	2.59	0.03
DGR-3 581.47	Georgian Bay	2.77	2.59	2.47	0.06
DGR-3 621.63	Blue Mountain	2.79	2.63	2.52	0.03
DGR-3 646.29	Blue Mountain	2.74	2.64	2.54	0.03
DGR-3 665.29	Cobourg – CM	2.65	2.59	2.57	0.03
DGR-3 676.21	Cobourg – LM	2.74	2.68	2.65	0.03
DGR-3 678.92	Cobourg – LM	2.71	2.68	2.66	0.04
DGR-3 685.52	Cobourg – LM	2.75	2.66	2.63	0.03
DGR-3 690.12	Cobourg – LM	2.75	2.68	2.67	0.03
DGR-3 692.82	Cobourg – LM	2.72	2.66	2.63	0.03
DGR-3 697.94	Cobourg – LM	2.74	2.67	2.65	0.03
DGR-3 710.38	Sherman Fall	2.74	2.66	2.64	0.03
DGR-3 725.57	Sherman Fall	2.70	2.69	2.66	0.03
DGR-3 744.27	Kirkfield	2.70	2.65	2.62	0.03
DGR-3 761.56	Kirkfield	2.71	2.65	2.63	0.03
DGR-3 777.33	Coboconk	2.69	2.67	2.65	0.03
DGR-3 807.43	Gull River	2.68	2.68	2.67	0.03
DGR-3 843.92	Gull River	2.71	2.65	2.63	0.03
DGR-3 852.18	Shadow Lake	2.71	2.53	2.44	0.03
DGR-3 856.06	Cambrian	2.78	2.73	2.72	0.03

*Gypsum identified in sample during mineralogical investigations; measured values are therefore considered suspect.

n.a.- indicates that calculation was not applicable due to presence of gypsum in sample.

¹Bulk dry density was calculated using the average bulk wet density and the average gravimetric porewater content ($PWC_{Grav.dry}$) calculated relative to the dry mass of the rock (equation 9 in text).

²The uncertainty in the calculated bulk dry density was found by Gaussian error propagation, as applied to equation 9.

Table 18: Bulk and grain densities determined for DGR-4 samples.

Sample ID	Lithology (short)	Grain Density (average, n=2) (g/cm ³)	Bulk Wet Density (average, n=2) (g/cm ³)	Measured Bulk Dry Density (average, n=2) (g/cm ³)	Calculated Bulk Dry Density ¹ (g/cm ³)	Uncertainty in Calculated Bulk Dry Density ± (g/cm ³)
DGR-4 154.60	Dolomitic shale with Ca-sulphate	2.84	2.76	2.71	2.71	0.03
DGR-4 189.16*	Dolomitic shale with Ca-sulphate	2.78*	2.46	2.38*	n.a.	n.a.
DGR-4 229.32*	Dolomitic shale with Ca-sulphate	2.61*	2.67	2.48*	n.a.	n.a.
DGR-4 322.68*	Massive Ca-sulphate	2.92*	2.89	2.87*	n.a.	n.a.
DGR-4 332.13	Argillaceous dolostone with Ca-sulphate	2.77	2.66	2.65	2.64	0.03
DGR-4 422.21	Red-green shale with carbonate/black shale beds	2.82	2.64	2.57	2.49	0.03
DGR-4 472.78	Red-green shale with carbonate beds	2.83	2.67	2.61	2.57	0.03
DGR-4 520.42	Shale with sandstone/siltstone/limestone beds	2.79	2.69	2.64	2.63	0.03
DGR-4 662.83	Bioclastic limestone/argillaceous limestone	2.72	2.67	2.65	2.65	0.03
DGR-4 665.41	Bioclastic limestone/argillaceous limestone	2.76	2.66	2.67	2.64	0.03
DGR-4 672.85	Bioclastic limestone/argillaceous limestone	2.69	2.69	2.67	2.68	0.03
DGR-4 717.12	Bedded argillaceous limestone/calcareous shale	2.70	2.70	2.68	2.66	0.04
DGR-4 730.07	Limestone with shale beds	2.76	2.67	2.61	2.62	0.03
DGR-4 841.06	Sandy mudstone, siltstone and sandstone	2.78	2.71	2.63	2.64	0.03
DGR-4 847.48	Sandstone/dolostone	2.85	2.72	2.74	2.69	0.03

*Gypsum identified in sample during mineralogical investigations; measured values are therefore considered suspect.

n.a.- indicates that calculation was not applicable due to presence of gypsum in sample.

¹Bulk dry density was calculated using the average bulk wet density and the average gravimetric porewater content ($PWC_{Grav.dry}$) calculated relative to the dry mass of the rock (equation 9 in text).

²The uncertainty in the calculated bulk dry density was found by Gaussian error propagation, as applied to equation 6. Bulk dry density was calculated according to equation 9 and using values for $PWC_{Grav.dry}$ given in Table 14.

4.4 Physical and porewater-loss porosity

Assuming that the pores of the rock matrix are completely saturated, the porosity can be calculated based on the porewater loss determined gravimetrically. In the case of highly saline porewaters, it is the pure water-loss (H₂O) that is determined gravimetrically; from which the porewater contents were calculated as described in section 4.2.2. The porewater-loss porosity (ϕ_{PWL}) is defined as the ratio of its porewater-filled volume to its total volume (V_{pw}/V_{tot}) and can be calculated using one of the two following relationships:

$$\phi_{PWL} = \frac{PWC_{Grav.wet} \rho_{Bulk.wet}}{\rho_{pw}} \quad (11)$$

or

$$\phi_{PWL} = \frac{PWC_{Grav.wet} \rho_g}{PWC_{Grav.wet} \rho_g + (1 - PWC_{Grav.wet}) \rho_{pw}} \quad (12)$$

where $PWC_{Grav.wet}$ is the gravimetric porewater content calculated relative to the wet mass of rock, ρ_g is the measured grain density and ρ_{pw} is the density of the porewater. Estimation of the porewater density and the calculation of $PWC_{Grav.wet}$ are described in section 4.2.2.

In the experimental work reported here and by Koroleva et al. (2009), grain density measurements were conducted on subsamples used for water content measurements, whereas bulk wet density was measured on separate subsamples. Therefore, the second formulation is implemented to calculate porewater-loss porosities, reducing the potential influence of heterogeneities that could exist between different subsamples.

Total or physical porosity is calculated using the following expression (e.g. Pearson, 1999):

$$\phi_{tot} = 1 - \left(\frac{\rho_{b.dry}}{\rho_g} \right) \quad (13)$$

where $\rho_{b.dry}$ is the bulk dry density calculated for the sample (equation 9) and ρ_g is the measured grain density.

The porewater-loss and physical porosities calculated for DGR-3 and DGR-4 samples are given Table 19 and Table 20, respectively. The uncertainty associated with these values, as determined by Gaussian error propagation, is also given. In calculations of physical porosity values presented in the following tables and figures, calculated bulk dry densities were used for samples from all boreholes. Where the difference between the physical and porewater-loss porosities is greater than the uncertainty in the physical porosity, the corresponding value is shaded in Tables 19 and 20.

Table 19: Calculated porewater-loss (ϕ_{PWL}) and physical porosities (ϕ_{tot}) of DGR-3 samples.

Sample ID	Depth relative to DGR -1 & -2 (m BGS)	Lithology (short)	Porewater-loss Porosity ¹ (vol.%)	Uncertainty Porewater-loss porosity ² (\pm vol. %)	Physical Porosity ¹ (vol.%)	Uncertainty in Physical Porosity ² (\pm vol. %)	Difference between ϕ_{PWL} and ϕ_{tot} (vol.%)
DGR-3 198.72*	234.3	Dolomitic shale with gypsum	n.a.	n.a.	n.a.	n.a.	n.a.
DGR-3 208.41*	255.6	Dolomitic shale with gypsum	n.a.	n.a.	n.a.	n.a.	n.a.
DGR-3 248.71*	274.9	Dolomitic shale with white anhydrite	n.a.	n.a.	n.a.	n.a.	n.a.
DGR-3 270.06*	298.1	Dolomitic shale	n.a.	n.a.	n.a.	n.a.	n.a.
DGR-3 289.36*	320.8	Argillaceous dolostone with anhydrite	n.a.	n.a.	n.a.	n.a.	n.a.
DGR-3 312.53	184.3	Dolostone	14.48	0.73	15.31	1.1	-0.83
DGR-3 335.22*	194.0	Anhydrite	n.a.	n.a.	n.a.	n.a.	n.a.
DGR-3 344.06	329.6	Dolostone	1.11	0.34	2.88	1.2	-1.77
DGR-3 380.88	366.4	Anhydrite	0.35	0.04	2.20	1.6	-1.86
DGR-3 391.34	376.9	Dolostone (veined)	5.83	0.42	8.05	1.1	-2.21
DGR-3 435.62	421.2	Dolostone \pm shale	10.48	0.58	8.76	1.1	1.72
DGR-3 453.41	439.0	Limestone	2.13	0.21	3.80	1.1	-1.66
DGR-3 468.76	454.3	Shale	9.13	0.43	8.67	1.1	0.46
DGR-3 484.58	470.1	Shale	7.22	0.37	7.21	2.9	0.00
DGR-3 502.55	488.1	Shale	6.14	1.41	6.97	1.5	-0.84
DGR-3 531.65	517.2	Shale / sandstone	5.51	0.57	6.95	1.2	-1.44
DGR-3 581.47	567.0	Shale	9.50	0.47	10.89	2.2	-1.39
DGR-3 621.63	607.2	Shale	8.86	0.42	9.65	1.1	-0.79
DGR-3 646.29	631.8	Shale	8.08	0.39	7.31	1.1	0.77
DGR-3 665.29	650.8	Argillaceous limestone	1.58	0.12	3.14	1.1	-1.56

*Gypsum identified in samples during mineralogical investigations.

n.a. – indicates that calculation of porewater contents was not applicable to these samples, due to presence of gypsum.

¹Porewater-loss and physical porosities were calculated using equations 12 and 13, respectively.

²Uncertainty determined using Gaussian error propagation applied to equations 12 or 13.

³Positive value indicates porewater-loss porosity is larger than physical porosity; Shading indicates difference is greater than the uncertainty in the physical porosity.

Table 19 (Cont'd): Calculated porewater-loss (ϕ_{PWL}) and physical porosities (ϕ_{tot}) of DGR-3 samples.

Sample ID	Depth relative to DGR -1 & -2 (m BGS)	Lithology (short)	Porewater-loss Porosity ¹ (vol.%)	Uncertainty Porewater-loss porosity ² (\pm vol. %)	Physical Porosity ¹ (vol.%)	Uncertainty in Physical Porosity ² (\pm vol. %)	Difference between ϕ_{PWL} and ϕ_{tot} (vol.%)
DGR-3 676.21	661.8	Argillaceous limestone	2.68	0.39	3.61	1.2	-0.93
DGR-3 678.92	664.5	Limestone	1.77	1.01	1.90	1.4	-0.13
DGR-3 685.52	671.1	Limestone	1.94	0.15	4.37	1.1	-2.43
DGR-3 690.12	675.7	Limestone	0.85	0.25	2.80	1.2	-1.95
DGR-3 692.82	678.4	Limestone	2.59	0.31	3.36	1.2	-0.78
DGR-3 697.94	683.5	Argillaceous limestone	1.94	0.16	3.47	1.1	-1.53
DGR-3 710.38	695.9	Argillaceous limestone	0.94	0.20	3.51	1.1	-2.57
DGR-3 725.57	711.1	Argillaceous limestone	2.62	0.23	1.55	1.2	1.07
DGR-3 744.27	729.8	Argillaceous limestone	2.69	0.33	3.14	1.2	-0.45
DGR-3 761.56	747.1	Argillaceous limestone / calcareous shale	1.66	0.62	2.95	1.2	-1.29
DGR-3 777.33	762.9	Limestone / shale	1.39	0.10	1.65	1.2	-0.26
DGR-3 807.43	793.0	Limestone	1.00	0.07	0.31	1.2	0.69
DGR-3 843.92	829.5	Limestone	1.44	0.42	2.89	1.2	-1.45
DGR-3 852.18	837.7	Limestone	8.57	0.42	10.08	1.1	-1.51
DGR-3 856.06	841.6	Sandy limestone	1.46	0.27	2.17	1.2	-0.71

*Gypsum identified in samples during mineralogical investigations.

n.a. – indicates that calculation of porewater contents was not applicable to these samples, due to presence of gypsum.

¹Porewater-loss and physical porosities were calculated using equations 12 and 13, respectively.

²Uncertainty determined using Gaussian error propagation applied to equations 12 or 13.

³Positive value indicates porewater-loss porosity is larger than physical porosity; Shading indicates that the difference is greater than the uncertainty in the physical porosity.

Table 20: Calculated porewater-loss (ϕ_{PWL}) and physical porosities (ϕ_{tot}) of DGR-4 samples.

Sample ID	Formation	Lithology (short)	Porewater-loss Porosity ¹ (vol.%)	Uncertainty in porewater-loss porosity ² (± vol. %)	Physical Porosity ¹ (vol.%)	Uncertainty Physical Porosity ² (± vol. %)	Difference between ϕ_{PWL} and ϕ_{tot} ³ (vol.%)
DGR-4 154.60	Bass Islands	Dolomitic shale with Ca-sulphate	4.40	0.26	4.47	1.1	-0.07
DGR-4 189.16*	Salina – F Unit	Dolomitic shale with Ca-sulphate	n.a.	n.a.	n.a.	n.a.	n.a.
DGR-4 229.32*	Salina – E Unit	Dolomitic shale with Ca-sulphate	n.a.	n.a.	n.a.	n.a.	n.a.
DGR-4 322.68*	Salina – A2 Unit	Massive Ca-sulphate	n.a.	n.a.	n.a.	n.a.	n.a.
DGR-4 332.13	Salina – A1 Unit	Argillaceous dolostone with Ca-sulphate	1.69	0.25	4.80	1.1	-3.12
DGR-4 422.21	Cabot Head	Red-green shale with carbonate/black shale beds	12.02	0.54	11.78	1.1	0.24
DGR-4 472.78	Queenston	Red-green shale with carbonate beds	8.17	0.39	9.24	1.1	-1.06
DGR-4 520.42	Georgian Bay	Shale with sandstone/siltstone/limestone beds	4.92	0.42	5.56	1.1	-0.63
DGR-4 662.83	Cobourg	Bioclastic limestone/argillaceous limestone	1.90	0.25	2.45	1.2	-0.54
DGR-4 665.41	Cobourg – LM	Bioclastic limestone/argillaceous limestone	1.76	0.31	4.47	1.1	-2.71
DGR-4 672.85	Cobourg – LM	Bioclastic limestone/argillaceous limestone	1.22	0.15	0.56	1.2	0.65
DGR-4 717.12	Sherman Fall	Bedded argillaceous limestone/calcareous shale	3.39	0.88	1.70	1.3	1.69
DGR-4 730.07	Kirkfield	Limestone with shale beds	4.43	0.58	5.38	1.2	-0.95
DGR-4 841.06	Shadow Lake	Sandy mudstone, siltstone and sandstone	5.83	0.39	5.08	1.1	0.76
DGR-4 847.48	Cambrian	Sandstone/dolostone	2.22	0.21	5.57	1.1	-3.35

*Gypsum identified in samples during mineralogical investigations.

n.a. – indicates that calculation of porewater contents was not applicable to these samples, due to presence of gypsum.

¹Porewater-loss and physical porosities were calculated using equations 12 and 13, respectively.

²Uncertainty determined using Gaussian error propagation applied to equations 12 or 13.

³Positive value indicates porewater-loss porosity is larger than physical porosity. Shading indicates difference is greater than analytical uncertainty in the physical porosity.

The porewater-loss porosities calculated for samples from DGR-2, -3 and -4 are plotted versus physical porosities in Figure 20. For clarity, error bars showing the uncertainty in both porosity values are not shown on this plot, but are included in Figure 21 and Figure 22, in which the data from each borehole are plotted separately.

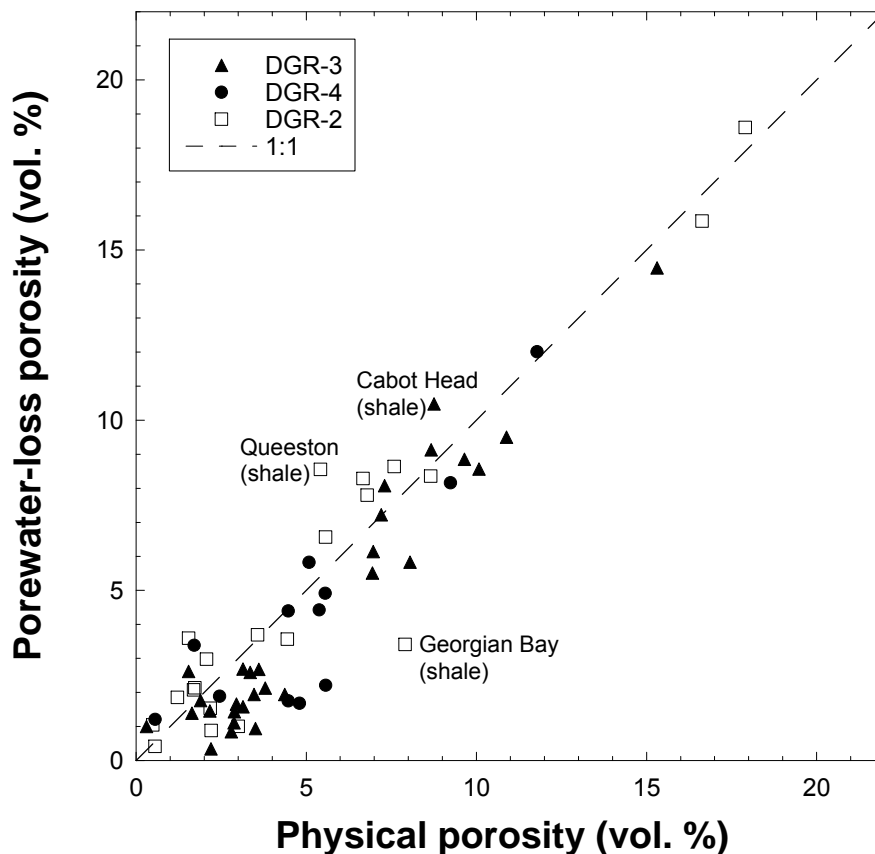


Figure 20: Porewater-loss porosity versus physical (or total) porosity for samples from boreholes DGR-2, -3 and -4. For clarity, the errors associated with both porosities are not shown on this compilation plot, but are included in Figure 21 and Figure 22.

For approximately 55% of samples examined from all three boreholes, the calculated porewater-loss and physical porosities are the same within the uncertainty of the calculated values. This suggests that in these samples, the pore space is completely filled with porewater and interconnected. However, there are several distinct outliers, which are labelled in Figure 20. Several samples have calculated porewater-loss porosities that are higher than their physical porosities, including one sample from the Cabot Head Formation (DGR-3 435.62) and one sample from the Queenston Shale (DGR-2 473.19). As discussed in section 4.3, evidence from comparison of calculated and measured bulk densities for a sample from the Cabot Head Formation and one sample from the Queenston Formation in DGR-4 suggests that these samples may have undergone shrinkage during drying at 105 °C. One shale sample from the Georgian Bay Formation (DGR-2 562.92) has a porewater-loss porosity that is clearly lower than its physical porosity. Considering all samples investigated, approximately 25% have porewater-loss porosities that are lower than their physical porosities - beyond the uncertainty associated with the calculated values.

In Figure 21 and Figure 22, the porewater-loss and physical porosity results are plotted separately for samples from DGR-2 and DGR-3 and -4, respectively. In Figure 21, two additional outliers are observed from DGR-2. The porewater-loss porosity calculated for DGR-2 846.31 from the Cambrian is slightly greater ($\approx 1\%$) than the physical porosity, considering the uncertainty in both parameters. One additional sample from the Gull River Formation (DGR-2 796.54) has a porewater-loss porosity that is lower than its physical porosity by approximately 2%, which is greater than the maximum uncertainty in both parameters (approx. $\pm 1.0\%$)

In DGR-3, there is a group of samples with low physical porosities ($< 5\%$) that also have porewater-loss porosities that are less than their physical porosities by approximately 0.5 to 1.5%, even when the uncertainty in these parameters are taken into account (inside dashed box in Figure 22, top diagram). Samples from the upper portion of the sedimentary sequence included in this group are from the Salina A2 Unit, Salina A1 Unit, Salina A1 Evaporite and from the Manitoulin Formation. From the lower part of the sequence, there are four samples from the Cobourg Formation included in this group and one sample from each of the Sherman Fall, Kirkfield and Gull River formations.

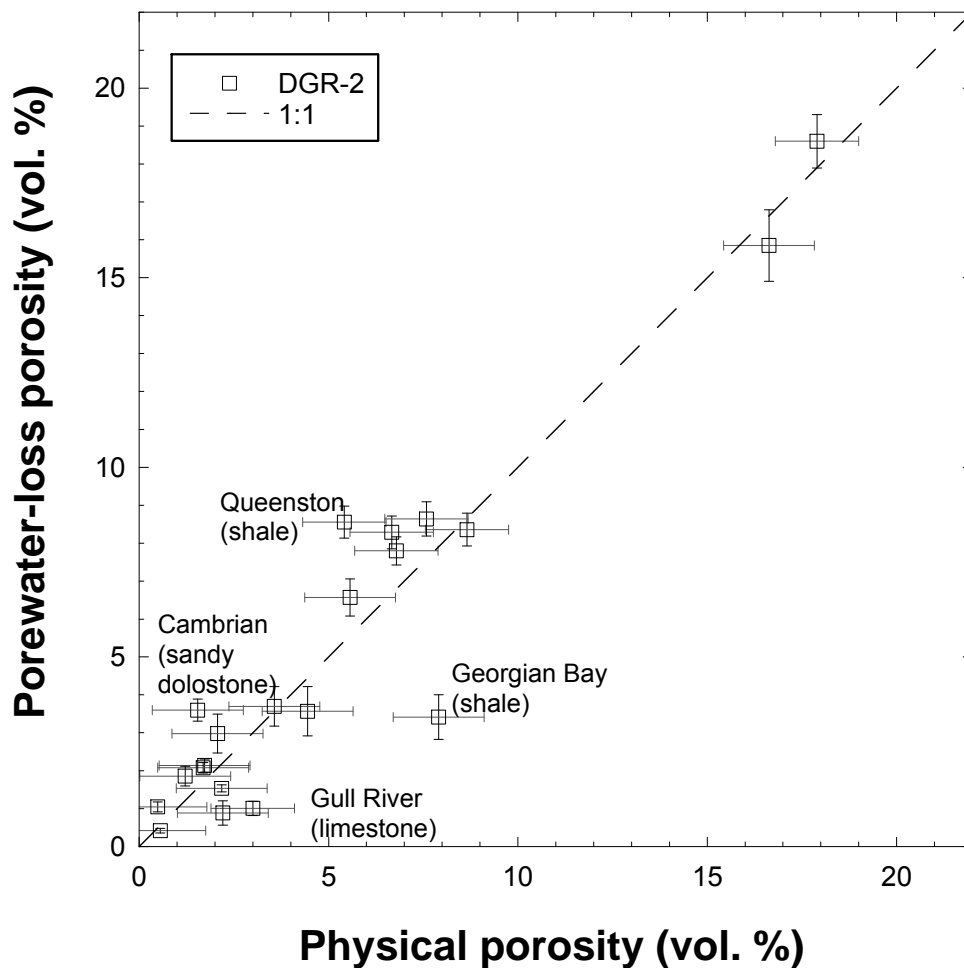


Figure 21: Porewater-loss porosity versus physical porosity for samples from DGR-2. The error bars show the calculated uncertainty in both parameters.

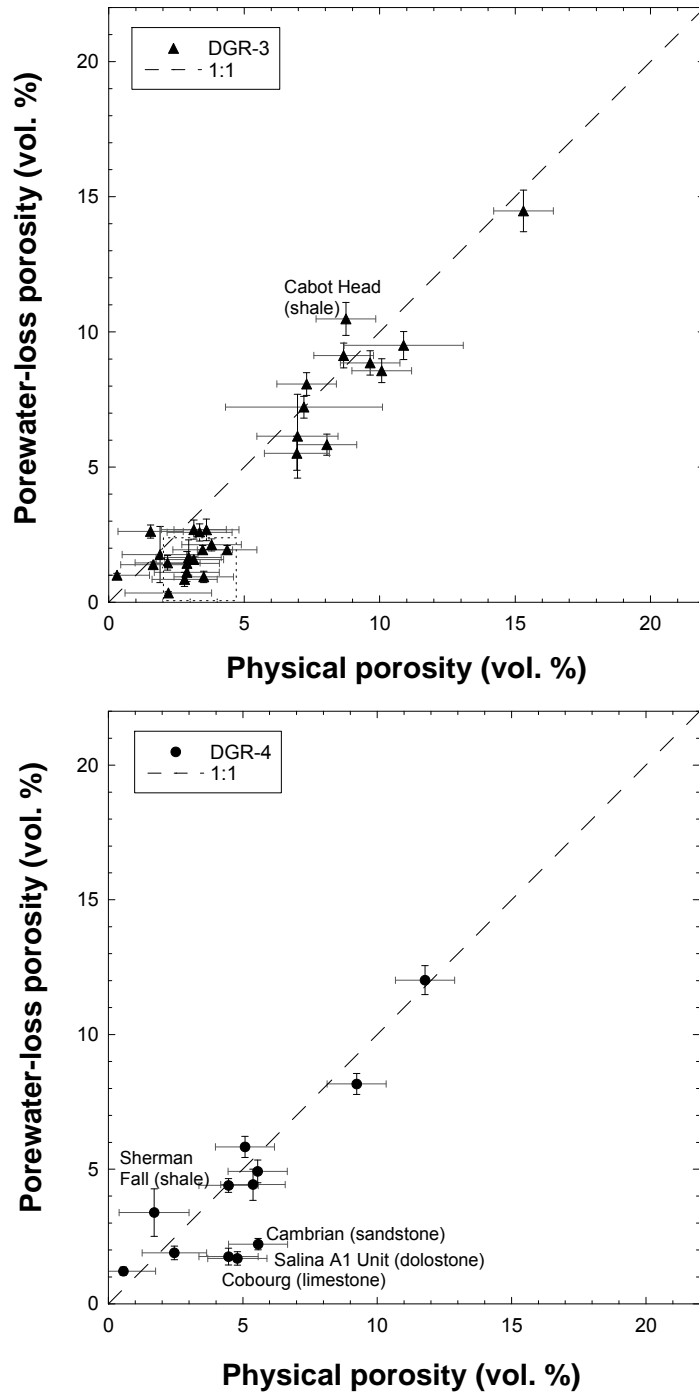


Figure 22: Plots showing porewater-loss porosity versus physical porosity for samples from DGR-3 (upper) and -4 (lower), including error bars showing the uncertainty in both parameters.

In DGR-4, there are three samples with physical porosities below 5% that also have porewater-loss porosities that are lower than their physical porosities. This group includes a sample from the Salina A1 Unit (DGR-4 332.13), one sample from the Cobourg Formation (DGR-4 665.41) and one sample from the Cambrian (DGR-4 847.48). One sample from the Sherman Fall Formation (DGR-4 717.12) has a porewater-loss porosity that is approximately 1.5% higher than its physical porosity, when the uncertainty in both parameters is taken into account.

In the case of dilute porewaters, water-loss porosity (or porewater-loss porosity, when the porewaters are highly saline) is a measure of the connected porosity within the rock (e.g., Pearson, 1999). In a rock that is completely saturated, the porosity value determined using water content measurements (or calculated porewater content for brines) is normally less than or equal to the total porosity (Pearson, 1999), because the water-loss porosity provides a measure of the *connected* porosity within a rock, not its total porosity. In the case where the porewater-loss porosity is equal to the total porosity (within error), this suggests that a) the rock is completely saturated and b) the total porosity within the rock matrix is connected.

In the case presented here, in which specific samples have porewater-loss porosities that are less than the total porosity, there are at least three possible interpretations that could be consistent with these observations:

- i) The rocks are fully saturated, but the entire porosity within the rock is not interconnected. For example, when cementation has occurred during burial diagenesis, some pores may have been sealed and are no longer interconnected to other pores within the rock matrix. Porewater in “cut-off” pores (fluid inclusions) would not be removed during gravimetric water content determinations.
- ii) The porosity of the rock is fully connected, but is not completely saturated with porewater.
- iii) Experimental artefacts affect the measurements. For example, if not all porewater in the sample is removed by heating to 105 °C, the water content (and consequently, the porewater-loss porosity) will be slightly underestimated. Observations of this kind were made for Opalinus Clay in Switzerland. Alternatively, partially unsaturated conditions within the core may have developed during sample handling prior to core preservation (e.g. some evaporation of porewater, prior to sealing of the core, despite the stringent core handling protocols applied).

If there is a separate gas phase present in situ, it is expected that gas would preferentially accumulate in larger pores that occur mainly within carbonate units, whereas pore apertures within shale units are likely too small. Many (but not all) of the samples with porewater-loss porosities lower than their physical porosities are from carbonate units.

5 Stable isotopes of porewater ($\delta^{18}\text{O}$ and $\delta^2\text{H}$)

In this section, an overview of the major improvements made to the adapted diffusive exchange technique and of the screening procedure developed for the data is given (a detailed assessment of the quality of the experimental results is provided in Appendix A). Results from the diffusive exchange experiments that provide information on both water content and on the stable isotopic composition ($\delta^{18}\text{O}$ and $\delta^2\text{H}$) of porewaters are presented, together with an evaluation of the adapted technique as applied to samples from boreholes DGR-3 and -4.

5.1 Methodological improvements and data screening

As described in section 2.4.1, only NaCl solutions were used in diffusive exchange experiments with DGR-3 samples. Consequently, for rock samples with measured water activities (a_w) below 0.75 (NaCl-saturated solution), the activities of the test waters were not closely matched to the rock samples (Figure 23). Prior to testing of the DGR-4 samples, a treatment method was developed to convert CaCl_2 test waters to NaCl waters by addition of sodium fluoride (section 2.4.2 and Appendix A). The treated test waters can then be distilled at 110 °C. This development allowed the test waters used in the DGR-4 experiments to be more closely matched to the water activities measured for rock samples by addition of either NaCl for samples with $a_w > 0.75$ or CaCl_2 to achieve $a_w < 0.75$ (Figure 23). This latest adaptation of the experimental protocol from DGR-3 to DGR-4 is a major step forward, in which the isotope diffusive exchange technique is adapted to the range of water activities found in rocks of DGR boreholes (a_w between 0.6 and 1.0). Additionally, the mass of rock used in the experiments has been increased from 170 ± 40 g (DGR-3) to 300 ± 50 g (DGR-4) to minimize errors, in particular for samples with low water content.

Data from the adapted diffusive exchange technique, which is used to calculate porewater isotope composition and water content, can be affected by several parameters. As part of the DGR-3/4 analytical program, a screening procedure was developed to evaluate the data. A detailed description of the screening criteria is provided in Appendix A and includes an assessment of the main sources of error in the calculated isotopic composition of the porewater and in the calculated water content. In brief, the quality of data obtained using the adapted isotope diffusive exchange technique is assessed using the following criteria:

- I. Total mass of the system (container + rock sample + test water) must remain constant during experiment (< 0.1 g difference between start and end of the experiment);
- II. The water contents calculated from both isotopic systems ($\delta^2\text{H}$ and $\delta^{18}\text{O}$) have to be identical within error;
- III. These calculated water contents should not be lower (within error) than the gravimetric water content $\text{WC}_{\text{Grav.wet}}$ determined at 105°C because this could indicate incomplete equilibration. The exceptions are gypsum-bearing samples, for which gravimetric water contents determined at both $\text{WC}_{\text{Grav.wet}}$ at 40°C and 105°C may contain structural water from gypsum, in addition to water from pore spaces (see section 4.2.1). For the purposes of screening the stable isotope results for

gypsum-bearing samples, calculated water contents were compared to $WC_{\text{Grav.wet}}$ determined at 40°C.

- IV. Mass transfer between the test water and the sample during experiment must be small (currently an upper limit of 10% water-mass change relative to the gravimetric water content is used).

Results that do not meet one or more of these criteria are rejected. The improved matching of the test water and sample water activities in DGR-4 compared to DGR-3 resulted in a higher proportion of accepted samples (Table 21 and Table 22).

Table 21: Summary of data screening procedure for experiments using DGR-3 samples

Sample ID (NWMO)	I: Δ total mass of system < 0.1g	II: $WC_{\delta_{180}} = WC_{\delta_{2H}}$	III: $WC_{D.E.} \geq WC_{\text{Grav.wet}}$	IV: Δ weight test water < 10% of $WC_{\text{Grav.wet}}$	Accepted results
DGR3-198.72	0	0	0	1	0
DGR3-208.41	1	1	0	1	0
DGR3-248.71	1	0	0	1	0
DGR3-270.06	1	1	1	1	1
DGR3-289.36	1	1	0	1	0
DGR3-312.53	1	1	1	1	1
DGR3-335.22	1	1	0	1	0
DGR3-344.06	1	1	1	1	1
DGR3-380.88	1	1	1	0	0
DGR3-391.34	1	1	0	0	0
DGR3-435.62	1	1	0	0	0
DGR3-453.41	1	0	1	0	0
DGR3-468.76	1	1	0	0	0
DGR3-484.58	0	1	0	0	0
DGR3-502.55	1	1	0	0	0
DGR3-531.65	1	1	0	0	0
DGR3-581.47	1	1	0	0	0
DGR3-621.63	1	1	0	0	0
DGR3-646.29	1	1	0	0	0
DGR3-665.29	1	0	0	0	0
DGR3-676.21	1	1	1	0	0
DGR3-678.92	1	0	1	0	0
DGR3-685.52	1	1	0	0	0
DGR3-690.12	0	0	1	0	0
DGR3-692.82	1	1	1	0	0
DGR3-697.94	1	1	0	0	0
DGR3-710.38	0	0	1	0	0
DGR3-725.57	1	1	0	0	0
DGR3-744.27	1	0	1	0	0
DGR3-761.56	1	1	1	0	0
DGR3-777.33	1	1	1	1	1
DGR3-807.43	1	0	1	0	0
DGR3-843.92	1	0	1	1	0
DGR3-852.18	1	0	1	1	0
DGR3-856.06	1	1	1	1	1
Total of accepted samples	31	24	17	12	5

Note: 1 means "true" and 0 means "false". Shading indicates that results failed to pass the screening criterion.

Table 22: Summary of data screening performed for experiments using DGR-4 samples

Sample ID (NWMO)	I: Δ total mass of system < 0.1g	II: $WC_{\delta^{18}O} = WC_{\delta^2H}$	III: $WC_{D.E.} \geq WC_{Grav.wet}$	IV: Δ weight test water < 10% of $WC_{Grav.wet}$	Final result
DGR4-154.60	1	1	1	1	1
DGR4-189.16	1	1	1	1	1
DGR4-229.32	1	1	1	0	0
DGR4-322.68	1	1	1	0	0
DGR4-332.13	1	1	1	1	1
DGR4-369.43	1	0	1	1	0
DGR4-422.21	failed experiment				
DGR4-472.78	1	1	1	1	1
DGR4-520.42	1	1	0	1	0
DGR4-662.83	1	1	1	1	1
DGR4-665.41	1	1	0	1	0
DGR4-672.85	failed experiment				
DGR4-685.14	1	1	1	1	1
DGR4-717.12	1	1	1	1	1
DGR4-730.07	1	1	0	1	0
DGR4-841.06	1	1	1	1	1
DGR4-847.48	1	0	1	0	0
Total of accepted samples	15	13	12	12	8

Note: 1 means "true" and 0 means "false". Shading indicates that results failed to pass the screening criterion.

During DGR-4 sample preparation, care was taken to maximize the rock mass and minimize the volume of the test water, especially in samples suspected of having low water contents. This improved the quality of the DGR-4 results compared to those obtained for samples from the DGR-3 borehole. However, for technical reasons, only samples having a water content > 0.5 wt% could be analysed with acceptable errors (< 2 ‰ for $\delta^{18}O$ and < 10‰ for δ^2H ; see Appendix A). In theory, it would be possible to analyze rocks with lower water contents if the experiments were performed with larger sample masses, but this has not yet been tested. Detailed information on the masses of rock material and the masses and salinities of the test waters used in the isotope diffusive exchange experiments with DGR-3 and DGR-4 samples are given in Appendix A (Tables A-1 and A-3).

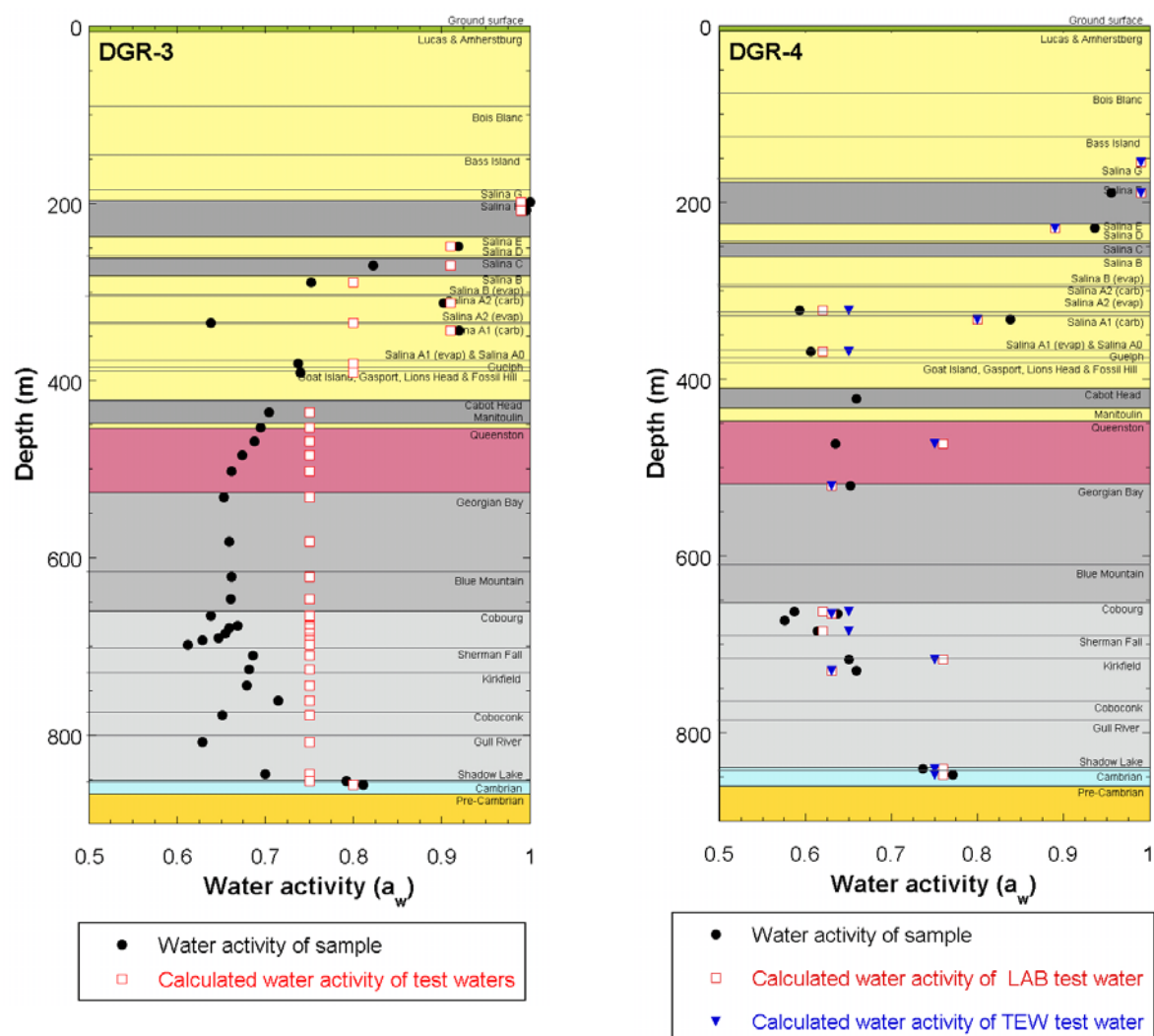


Figure 23: Comparison between sample water activity (a_w) and test water a_w in DGR-3 and DGR-4 samples. In these diagrams, the a_w of each individual test water is calculated from its salinity, based on the recorded amount of salt and standard water added to prepare the test water. For DGR-3, the salinities of the test waters are not known exactly, because the masses of salts and standard waters added were not recorded. The calculated salinities and water activities are, therefore, based on the target concentrations (e.g. 5M NaCl). For two samples from DGR-4 (DGR-4-472.78, Queenston Formation; DGR-4-717.12, Sherman Fall Formation), a 3 molal CaCl_2 was used when a 4 molal solution would have provided a better match to the sample water activity. This resulted in a mismatch in a_w of approximately 0.1 between the rock samples and test solutions.

5.2 Water contents

From the stable isotopic compositions of the two equilibrated test water solutions (LAB and TEW), two water content values can be calculated: one from the measured $\delta^2\text{H}$ values ($WC_{\delta^2\text{H}}$) and one from the $\delta^{18}\text{O}$ values ($WC_{\delta^{18}\text{O}}$). The calculated water contents are given in Table 24 and Table 26; water contents determined gravimetrically ($WC_{\text{Grav.wet}}$) are also shown for comparison. Depth profiles showing the calculated water contents ($WC_{\delta^{18}\text{O}}$ and $WC_{\delta^2\text{H}}$) for DGR-3 and DGR-4 samples are shown in Figure 24. Only data that successfully passed the screening procedure are plotted. For the majority of samples from DGR-4, the agreement between the calculated water contents ($WC_{\delta^{18}\text{O}} = WC_{\delta^2\text{H}}$) is satisfactory, while a significant portion of the results for DGR-3 samples had to be rejected on this basis (Table 21 and Appendix A). For DGR-3, $WC_{\delta^2\text{H}}$ are in general closer to the $WC_{\text{Grav.wet}}$ and have lower errors than $WC_{\delta^{18}\text{O}}$. Theoretically, both $WC_{\delta^2\text{H}}$ and $WC_{\delta^{18}\text{O}}$ should be similar to $WC_{\text{Grav.wet}}$, unless water is expelled from minerals during drying (e.g. gypsum) or if the porewater contains salts that cannot be fully dehydrated at 105°C (e.g., CaCl_2 or MgCl_2).

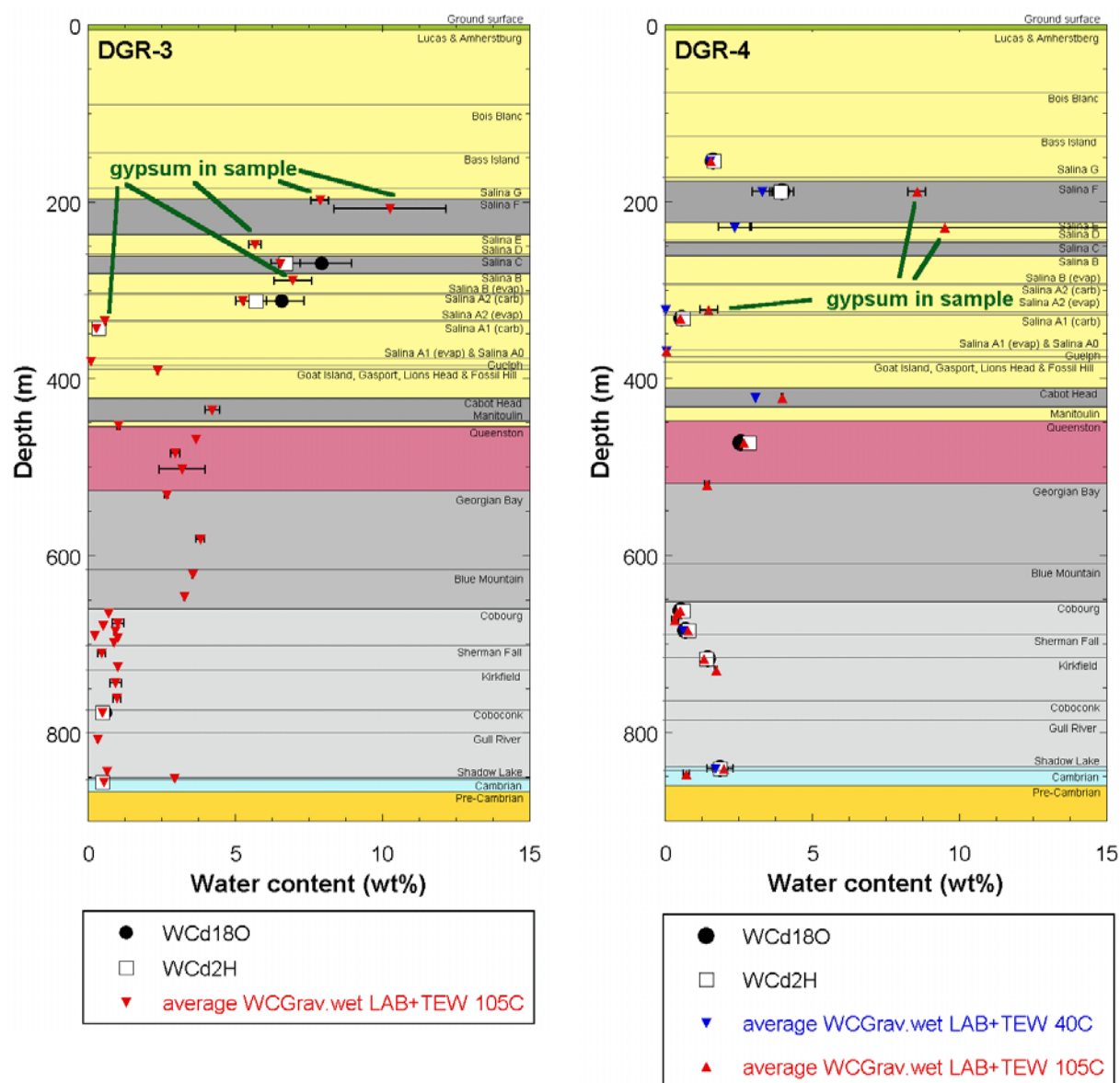


Figure 24: Water content (WC) by isotopic exchange and drying methods. Values of $WC_{\delta 18O}$ and $WC_{\delta 2H}$ are shown only for samples that passed the screening procedure. If not visible, error bars are smaller than the symbol. Gravimetric water contents ($WC_{Grav.wet}$) were measured only at $105^{\circ}C$ in DGR-3 LAB and TEW samples (a correction for mass transfer during experiments was applied, as described in section 2.1.1). Error bars on the gravimetric data correspond to the absolute difference between the values measured on the LAB and TEW subsamples.

5.3 Stable isotopic composition of porewater

The measured isotopic composition of the equilibrated test waters and the calculated isotopic composition of the porewaters for samples from DGR-3 and DGR-4 are given in Table 23 and Table 25, respectively. Data for all samples are shown in these tables; rejected data that failed to meet the screening criteria are highlighted and are not discussed further. The $\delta^{18}\text{O}$ and $\delta^2\text{H}$ values determined for the porewaters in samples from DGR-3 and DGR-4 are plotted as a function of depth in Figure 25 and Figure 26, respectively. The $\delta^{18}\text{O}$ and $\delta^2\text{H}$ signatures of groundwater sampled in both boreholes from formations within the Silurian (Salina A1 and Guelph formations) and from the Cambrian are also shown for comparison (Intera 2009).

Although the number of data points is limited, the $\delta^{18}\text{O}$ and $\delta^2\text{H}$ depth profiles for DGR-3 and for DGR-4 are consistent (Figure 25 and Figure 26). Aside from a local jump toward lower values near the Salina A1 aquifer (Intera, 2009), the porewater $\delta^{18}\text{O}$ values increase from the top of the Salina Formation ($\approx -12\text{‰}$) downward towards the Queenston Formation, where the porewater has a $\delta^{18}\text{O}$ value of $+2\text{‰}$ (Figure 25). Similar to the Queenston Formation, the $\delta^{18}\text{O}$ values measured in porewaters from the Cobourg formation are between 0 and $+2\text{‰}$ (Figure 25). The porewaters $\delta^{18}\text{O}$ values then trend toward lower values with depth, with a value of -3.5‰ in the Shadow Lake Formation in DGR-4. Groundwaters sampled in the underlying Cambrian from both DGR-3 and DGR-4 have $\delta^{18}\text{O}$ signatures of -5‰ (OGW-10 and OGW-13; Intera 2009).

The trends observed for $\delta^2\text{H}$ values as a function of depth are similar to those observed for $\delta^{18}\text{O}$ (Figure 26). Porewater $\delta^2\text{H}$ values increase from the top of the Salina Formation ($\approx -90\text{‰}$) downward to values of approximately -35‰ at the top of the Queenston Formation. As in the $\delta^{18}\text{O}$ profile, an abrupt decrease to more negative $\delta^2\text{H}$ values is observed near the Salina A1 aquifer. However, unlike the behavior of the $\delta^{18}\text{O}$ values, $\delta^2\text{H}$ values in the Queenston Formation, and in the Cobourg, Kirkfield (DGR-4) and Cobocok (DGR-3) formations remain relatively constant at a value of approximately -35‰ , which is similar to the $\delta^2\text{H}$ value measured for groundwaters from the Cambrian from DGR-4 (OGW13, -35.2‰ ; Intera 2009).

The $\delta^2\text{H}$ versus $\delta^{18}\text{O}$ plots are presented in Figure 27 for both DGR-3 and DGR-4. The errors associated with the DGR-4 data are much lower than those associated with DGR-3 data, mainly due to the optimisation of the rock to test water mass ratio used in the experiments (see section 5.1 and Appendix A). In the DGR-4 data, porewaters from the upper section of the sedimentary sequence plot very close to the present day global meteoric water line (GMWL), as do groundwaters from the Salina A1 Formation and from the Cambrian. Porewaters from the Cobourg and Queenston Formations have $\delta^2\text{H}$ values similar to that of the Cambrian groundwater, but have $\delta^{18}\text{O}$ values that are strongly shifted to the right of the global meteoric line. Porewaters in the Sherman Fall and Shadow Lake formations also have similar $\delta^2\text{H}$ values, but have $\delta^{18}\text{O}$ values that are intermediate between those observed Cambrian groundwaters and those of porewaters from the Queenston and Cobourg formations. Groundwaters from within the Guelph Formation have $\delta^{18}\text{O}$ values intermediate in compositions with respect to the Cobourg-Queenston porewaters and the Salina A1 groundwater. The data obtained for DGR-3 are broadly consistent with those from DGR-4, although a more complex behaviour is suggested for samples from the upper part of the section (Salina Formation).

5.4 Evaluation of the adapted diffusive isotope-exchange method applied to DGR samples and comparison with other databases

Using the information currently available, there are two approaches that can be used to assess whether or not calculated porewater compositions and water contents obtained from the diffusive exchange experiments are representative of in situ values. The first approach involves a comparison between the calculated water contents and the gravimetric water contents and forms one part of the screening procedure, as described in section 5.2 and illustrated in (Figure 24). The water content determined gravimetrically ($WC_{Grav.wet}$) is an independent measure of water content against which the water contents determined during the diffusive exchange experiments ($WC_{\delta^{18}O}$ and WC_{δ^2H}) can be assessed. Samples that had not fully equilibrated during the diffusive exchange experiments would have calculated water contents lower than those measured gravimetrically; the screening procedure is designed to remove these results from the sample set. The calculation of water content and porewater isotope composition is linked mathematically, as described in Appendix A. Therefore, agreement of water contents calculated from the stable isotope ratios ($WC_{\delta^{18}O}$ and WC_{δ^2H}) with the water content determined gravimetrically also provides additional confidence in the stable isotope compositions determined for the porewater.

The second approach requires a comparison of the stable isotope ratios ($\delta^{18}O$ and δ^2H) measured in porewaters and groundwaters taken from the same or an immediately adjacent formation. As shown in Figure 25 and Figure 26, two porewater samples (one in DGR-3 and one in DGR-4) were taken close to the Salina A1 aquifer, none were taken close to the Guelph aquifer, and two were taken close to the Cambrian sandstone aquifer (one in DGR-3 and one in DGR-4). The Salina A1 groundwater is off the general trend of the porewaters, but porewaters sampled within or very close to the packer interval used for groundwater sampling also show a shift towards negative values, even though the values are less negative than those of the groundwater. There is a qualitative consistency in that both groundwater and porewater indicate a shift towards negative isotopic values in the Salina A1. Because of the apparently strong local gradient of the $\delta^{18}O$ and δ^2H values in the porewaters near the Salina A1, the groundwater data cannot be used here as a direct benchmark. Of the two porewater samples located close to the Cambrian aquifer, one is within the Cambrian (DGR-3 856.06), while the other (DGR-4 841.06) is in the overlying Shadow Lake Formation. The porewater δ^2H values of these samples are similar within error to those determined for the Cambrian groundwater, but are enriched in ^{18}O by at least 1 ‰ (considering errors). This ^{18}O enrichment could be explained by a compositional gradient in the Shadow Lake sample, but not in the Cambrian sample, which is located within the aquifer and should therefore give a similar value to the groundwater. In conclusion, the diffusive exchange technique gives results that fit with the groundwater value for δ^2H , but a moderate shift to higher values is observed for $\delta^{18}O$.

The profiles obtained from both DGR-3 and DGR-4 using the diffusive exchange method compare well with one another (Figure 28), although the number of data points is limited. The general shape is similar to that of the profile obtained at the University of Ottawa using vacuum distillation at 150°C (Intera, 2008c; Intera, 2009a). Absolute values are similar in both data sets in the upper part of the profile (down to the Salina Formation) and nearly constant values of δ^2H are observed from the Cabot Head down to the Cambrian groundwater in both profiles. However, compared to the vacuum distillation data, more enriched values of both $\delta^{18}O$ and δ^2H are determined using diffusive exchange for samples from the Queenston through the Coboconk formations. The isotopic compositions of porewaters in both datasets converge towards similar values in the Shadow Lake Formation and in the Cambrian at the bottom of the profile and towards the Cambrian groundwater composition. For the diffusive exchange results, this convergence is most clearly seen for the sample from the Shadow Lake from the DGR-4 borehole.

In Figure 29, the data obtained in this study are plotted on a $\delta^2\text{H}$ versus $\delta^{18}\text{O}$ diagram and compared to the data obtained by the University of Ottawa (Intera, 2009a) for DGR-1 through DGR-4 samples. The Salina A1 and the Cambrian groundwaters, as well as the modern meteoric water recharge and glacial meltwater ($\delta^{18}\text{O}$ between -25 and -11 ‰; Husain et al., 2004), plot on the global meteoric water line (GMWL). The Guelph groundwater is shifted by about 5‰ $\delta^{18}\text{O}$ from the GMWL, while our data for the Queenston and Cobourg Formations have a similar $\delta^2\text{H}$ value to the Cambrian groundwater, but are 7 ‰ higher for $\delta^{18}\text{O}$ than the value obtained by vacuum distillation. The main difference between the two datasets is that the Queenston to Cobourg porewaters are close to the Guelph groundwater composition in the dataset of the University of Ottawa (i.e., at lower $\delta^{18}\text{O}$ and $\delta^2\text{H}$ values than the ones obtained in this study). Groundwaters sampled in the Cambrian sandstones and Ordovician limestones of southern Ontario (Hobbs et al., 2008; Figure 30) have $\delta^2\text{H}$ values of approximately -30 ± 10 ‰, similar to the ones we obtained for the Queenston and Cobourg Formations (Figure 29). A portion of the groundwater data for the Ordovician limestones is clustered around a $\delta^{18}\text{O}$ value of about -2 ± 1 ‰ (Figure 30), which is 3 to 4‰ lower than our results (Figure 29). Compared to the Hobbs et al. (2008) dataset, results obtained by the University of Ottawa for the Ordovician shales are similar in terms of $\delta^{18}\text{O}$, but clearly shifted to lower $\delta^2\text{H}$ values.

There is at the moment no definitive explanation for the partially higher values (i.e. isotopically more positive signatures) obtained for the porewaters using the isotope diffusive exchange method compared to those determined using 150°C vacuum distillation. Intera (2010c) reached the conclusion that, if any, the effect of incomplete distillation was below analytical error for DGR samples. As far as the isotope diffusive exchange method is concerned, one open issue is the influence of the differences in the chemical compositions (at the same water activity) between the porewater and the testwater used in the experiments. As described previously, the upper part of the profile was investigated with NaCl test waters, while deeper samples had lower water activities and required the use of CaCl_2 test waters. The simple compositions of these test waters likely do not reflect the complex chemical composition of the porewaters (see section 6). The effect and magnitude of the isotopic fractionation effect due to differences in chemical composition (Horita et al., 1993a and b) is being investigated in an NWMO methodology study (GS85), and a better understanding of the possible advantages and limitations of the adapted isotope diffusive exchange method will be available after its completion.

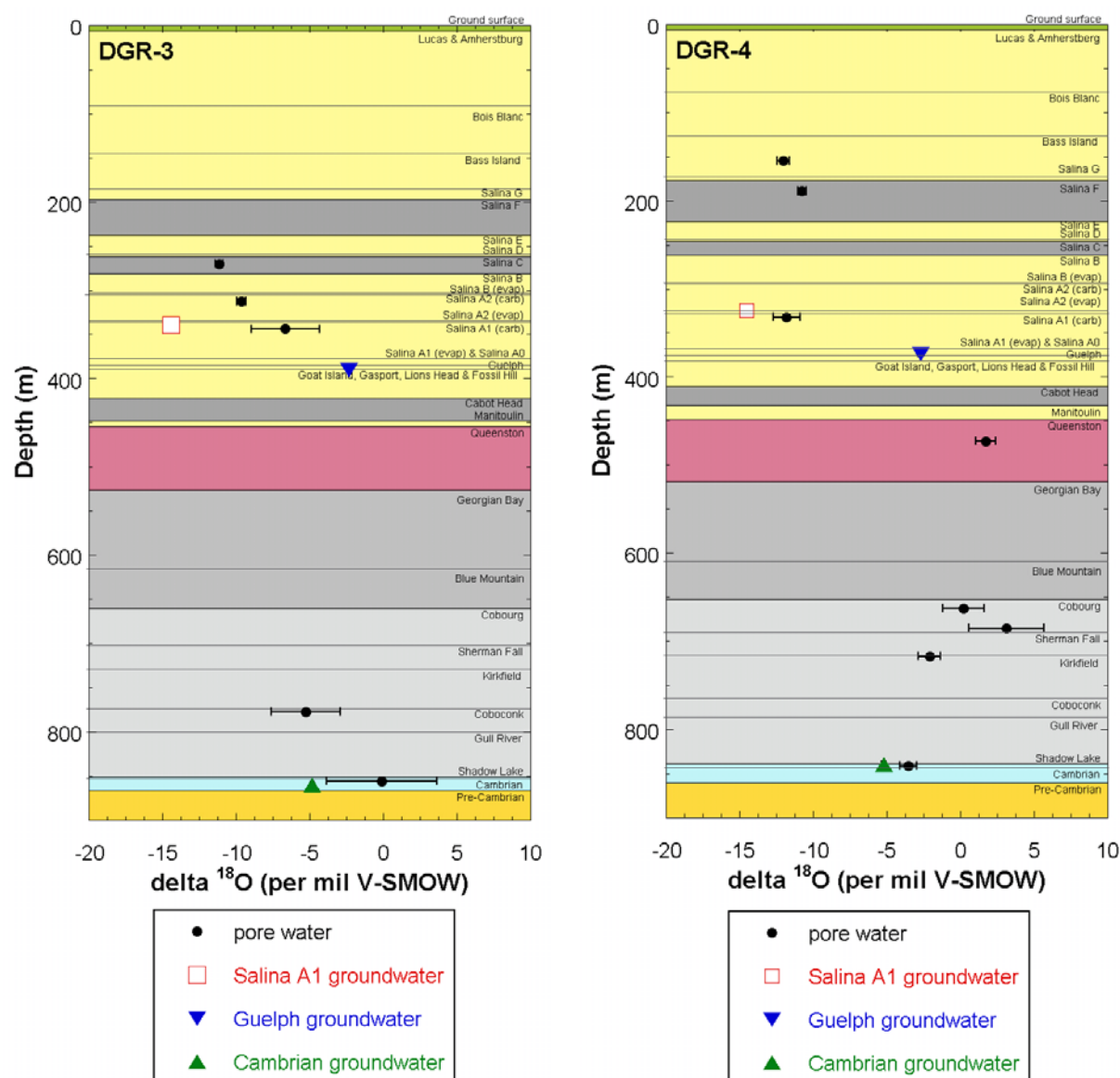


Figure 25: Profiles showing calculated $\delta^{18}\text{O}$ values of porewater and groundwater versus depth along borehole for samples from boreholes DGR-3 and DGR-4 (groundwater values are from Intera 2009). When not visible, error bars are smaller than the symbols.

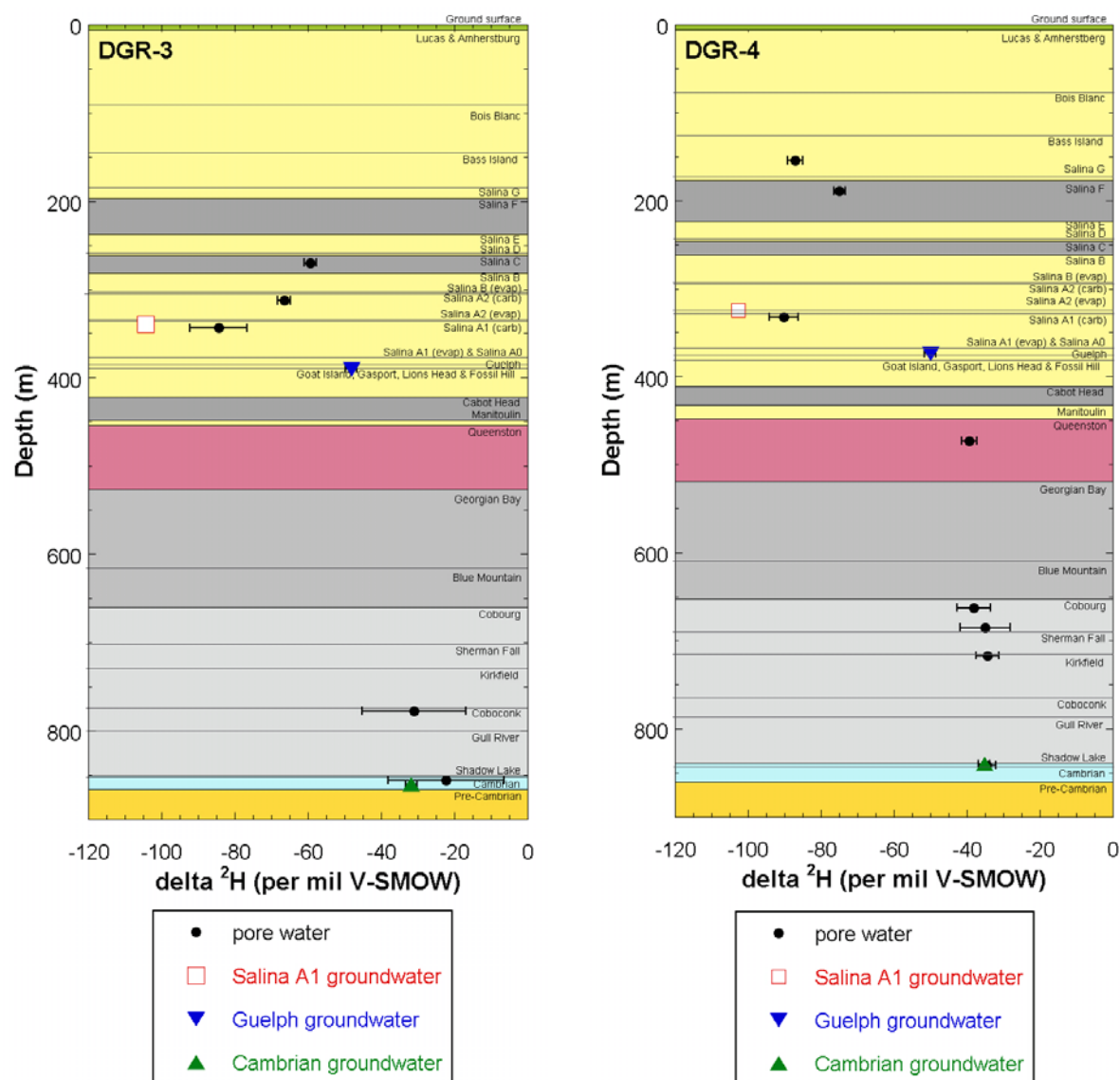


Figure 26: Profiles showing calculated $\delta^2\text{H}$ values of porewater and groundwater versus depth along borehole for samples from boreholes DGR-3 and DGR-4 (groundwater data are from Intera 2009). When not visible, error bars are smaller than the symbols.

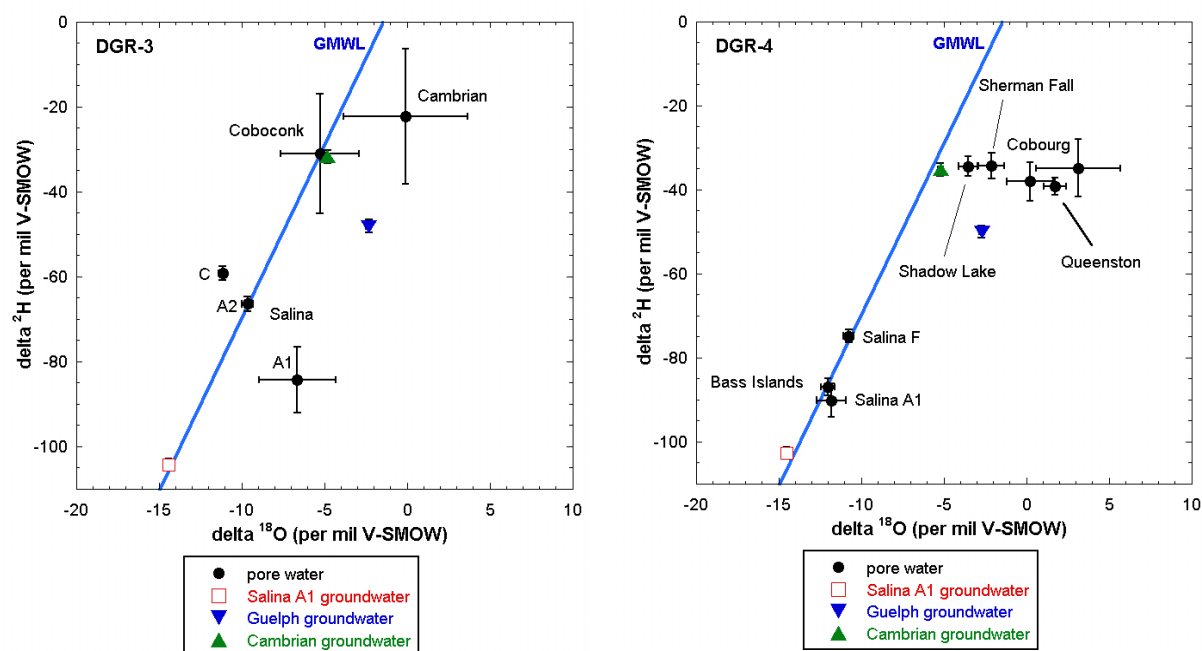


Figure 27: Plot of $\delta^2\text{H}$ versus $\delta^{18}\text{O}$ values of porewaters and groundwaters obtained from samples from DGR-3 and DGR-4 drillholes. The global meteoric water line (GMWL) is also shown.

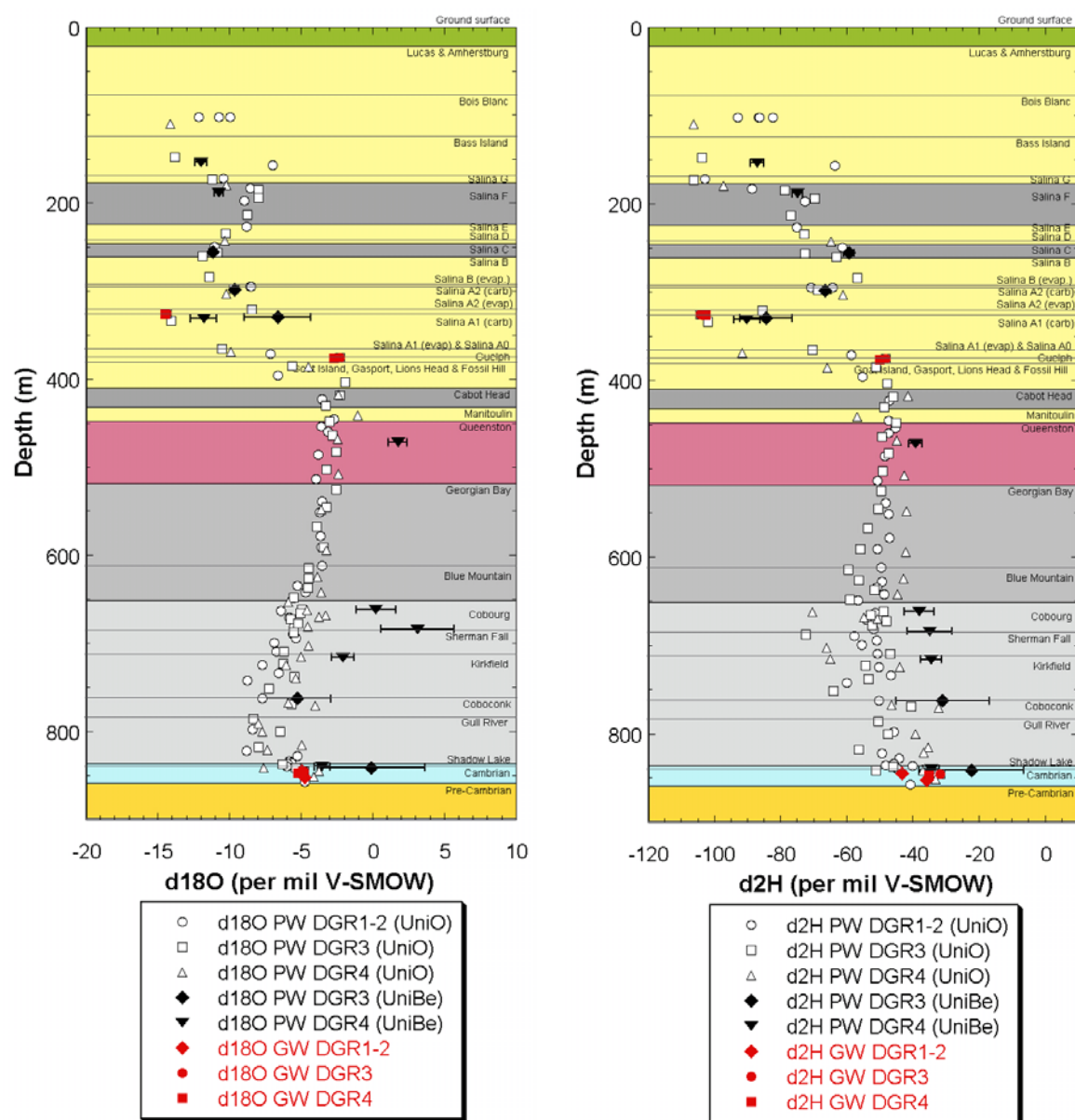


Figure 28: Comparison of the stable isotope compositions of porewaters determined by the University of Bern (UniBe) and University of Ottawa (UniO) versus depth. Values for groundwater samples from DGR-1 to DGR-4 are also shown for comparison. In the legend, PW indicates porewater and GW indicates groundwater. Depths of DGR-3 and DGR-4 samples were corrected relative to the DGR-1/2 borehole (UniBe: DGR-3 sample depths -14.46m; DGR-4 sample depths -1.05m).

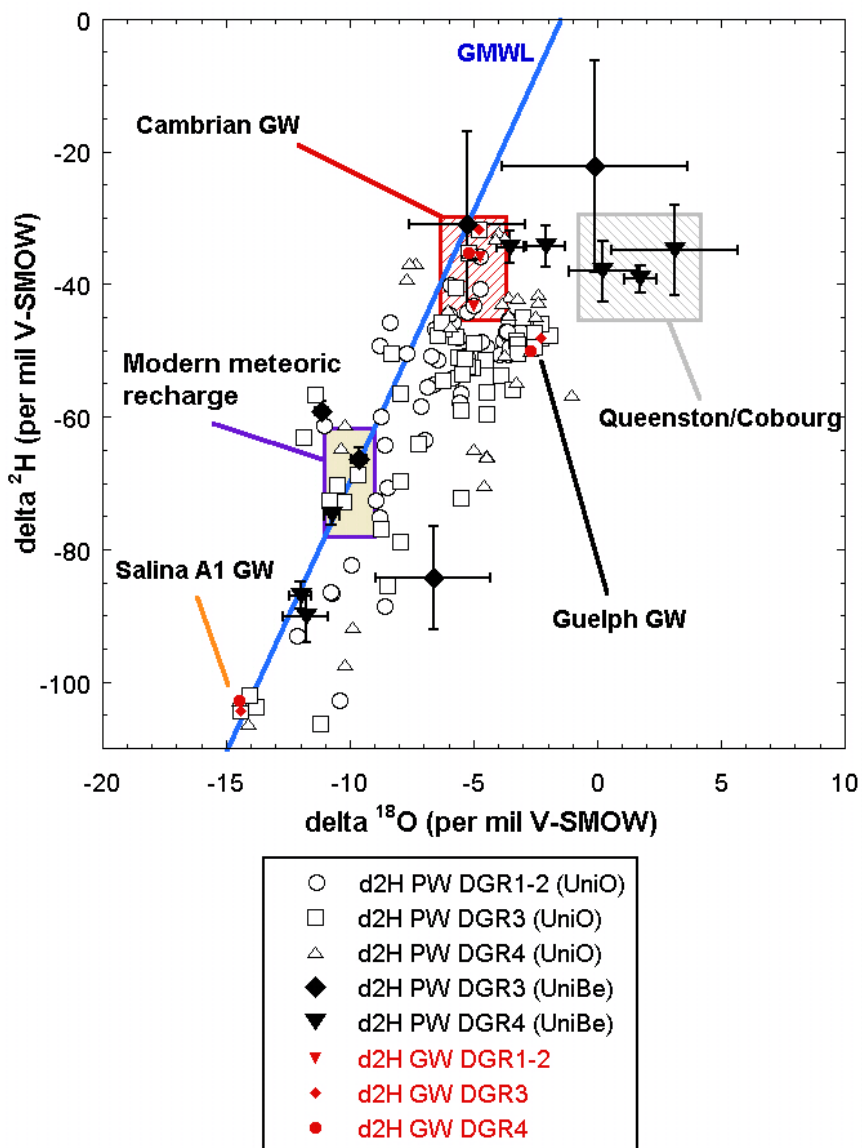


Figure 29: $\delta^2\text{H}$ versus $\delta^{18}\text{O}$ plot of DGR-3 and DGR-4 isotope diffusive exchange results (UniBe) compared to DGR-1 to 4 data by University Ottawa (UniO) and groundwater isotopic compositions from boreholes DGR-1 to 4 (Intera, 2008c; 2009a). GMWL = global meteoric water line. In the legend: PW indicates porewater and GW indicates groundwater. In DGR-3 and DGR-4, groundwaters were sampled in the Salina A1, Guelph and in the Cambrian, whereas in DGR-2, groundwater was sampled in the Cambrian. The lithostratigraphic units to which each UniBern sample belongs are shown in Figure 27.

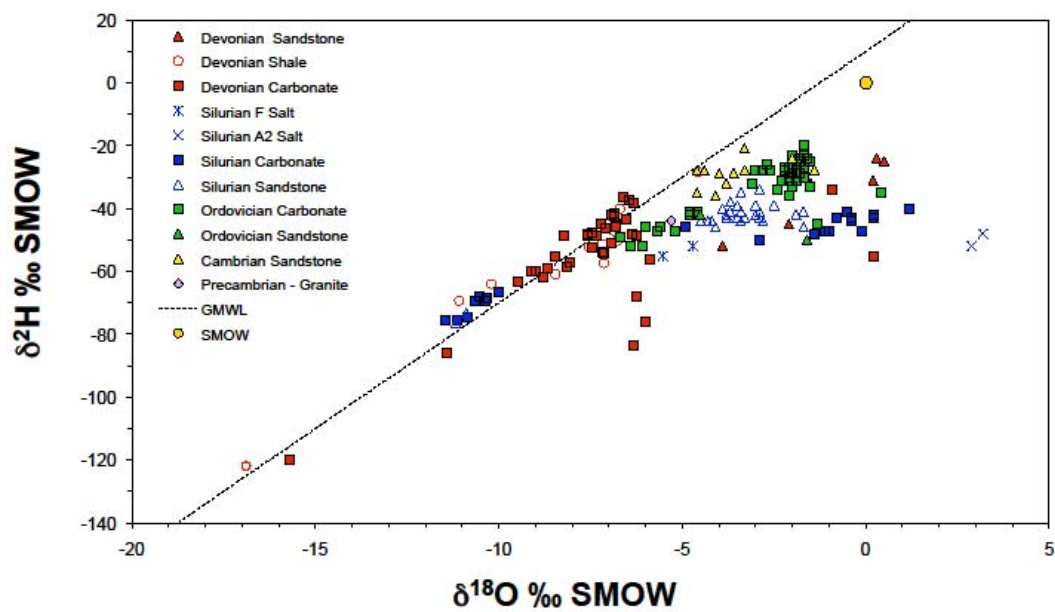


Figure 30: Data for groundwaters from Southern Ontario (Hobbs et al., 2008).

Table 23: Borehole DGR-3. Isotope diffusive exchange experiments: Measured isotopic compositions of the test solutions and calculated porewater compositions.

Sample ID (NWMO) ¹	Formation	Test solution “LAB” (tap water)				Test solution “TEW” (glacial meltwater)				Calculated porewater isotopic composition ⁴			
		Initial $\delta^{18}\text{O}$ of test so- lution ^{2,3}	Final $\delta^{18}\text{O}$ of test so- lution ³	Initial $\delta^2\text{H}$ of test so- lution ^{2,3}	Final $\delta^2\text{H}$ of test so- lution ³	Initial $\delta^{18}\text{O}$ of test so- lution ^{2,3}	Final $\delta^{18}\text{O}$ of test so- lution ³	Initial $\delta^2\text{H}$ of test so- lution ^{2,3}	Final $\delta^2\text{H}$ of test so- lution ³	$\delta^{18}\text{O}$	STD (1 σ)	$\delta^2\text{H}$	STD (1 σ)
		(‰ V- SMOW)	(‰ V- SMOW)	(‰ V- SMOW)	(‰ V- SMOW)	(‰ V- SMOW)	(‰ V- SMOW)	(‰ V- SMOW)	(‰ V- SMOW)	(‰ V- SMOW)	(‰)	(‰ V- SMOW)	(‰)
DGR-3 198.72	Salina – F Unit	-11.1	-9.2	-80.5	-68.7	-24.56	-14.7	-187.94	-106.7	-7.8	0.5	-62.1	2.0
(DGR-3 208.41)	Salina - F Unit	n.m.	n.m.	n.m.	n.m.	n.m.	n.m.	n.m.	n.m.	n.m.	n.m.	n.m.	n.m.
DGR-3 248.71	Salina – E Unit	-11.1	-11.6	-80.5	-73.3	-24.56	-15.8	-187.94	-116.1	-11.8	0.3	-68.3	2.0
DGR-3 270.06	Salina - C Unit	-11.1	-11.1	-80.5	-64.4	-24.56	-14.0	-187.94	-90.4	-11.1	0.3	-59.2	1.7
DGR-3 289.36	Salina – B Unit	-11.1	-11.1	-80.5	-67.5	-24.56	-18.3	-187.94	-125.6	-11.2	0.5	-51.8	3.3
DGR-3 312.53	Salina - A2 Unit	-11.1	-10.0	-80.5	-70.9	-24.56	-13.6	-187.94	-102.6	-9.6	0.3	-66.4	1.8
DGR-3 335.22	Salina – A2 Evap.	-11.1	-10.8	-80.5	-80.7	-24.56	-22.9	-187.94	-180.0	-7.9	3.6	-83.1	18.9
DGR-3 344.06	Salina –A1 Unit	-11.1	-10.4	-80.5	-81.1	-24.56	-21.8	-187.94	-171.3	-6.4	2.4	-84.3	7.8
DGR-3 380.88	A1 Evaporite	-11.1	-10.2	-80.5	-78.1	-24.56	-22.2	-187.94	-176.4	-2.5	4.4	-52.9	20.3
(DGR-3 391.34)	Guelph	n.m.	n.m.	n.m.	n.m.	n.m.	n.m.	n.m.	n.m.	n.m.	n.m.	n.m.	n.m.
(DGR-3 435.62)	Cabot Head	n.m.	n.m.	n.m.	n.m.	n.m.	n.m.	n.m.	n.m.	n.m.	n.m.	n.m.	n.m.
DGR-3 453.41	Manitoulin	-11.1	-8.0	-80.5	-68.6	-24.56	-16.2	-187.94	-150.3	-3.3	1.0	-32.6	7.6
(DGR-3 468.76)	Queenston	n.m.	n.m.	n.m.	n.m.	n.m.	n.m.	n.m.	n.m.	n.m.	n.m.	n.m.	n.m.
(DGR-3 484.58)	Queenston	n.m.	n.m.	n.m.	n.m.	n.m.	n.m.	n.m.	n.m.	n.m.	n.m.	n.m.	n.m.
(DGR-3 502.55)	Queenston	n.m.	n.m.	n.m.	n.m.	n.m.	n.m.	n.m.	n.m.	n.m.	n.m.	n.m.	n.m.
DGR-3 531.65	Georgian Bay	-11.1	-5.8	-80.5	-63.0	-24.56	-15.4	-187.94	-134.8	5.3	1.9	-31.3	5.1
DGR-3 581.47	Georgian Bay	-11.1	-4.6	-80.5	-52.9	-24.56	-10.6	-187.94	-100.6	1.5	0.9	-28.9	3.3
(DGR-3 621.63)	Blue Mountain	n.m.	n.m.	n.m.	n.m.	n.m.	n.m.	n.m.	n.m.	n.m.	n.m.	n.m.	n.m.
(DGR-3 646.29)	Blue Mountain	n.m.	n.m.	n.m.	n.m.	n.m.	n.m.	n.m.	n.m.	n.m.	n.m.	n.m.	n.m.
DGR-3 665.29	Cobourg – Collingwood M.	-11.1	-8.0	-80.5	-71.5	-24.56	-20.6	-187.94	-163.8	38.7	26.2	-16.0	16.2

¹ Depth of sample in meters below ground surface is given by the second half of the NWMO sample ID.

² The isotopic composition of the tap water used to prepare the LAB standard is not constant and may depend on the date of preparation of the standard. Because all LAB waters were prepared in about 10 days (from 20.06.2008 to 1.07.2008), this variation is below the analytical uncertainty (see Table A-2, and Table A-5, Appendix A). The long term averages of the $\delta^{18}\text{O}$ and $\delta^2\text{H}$ values of the TEW glacial meltwater as determined by the Institute of Physics, University of Bern, were used as the initial isotopic composition (Table A-2 and A-5, Appendix A).

³ The estimated errors in the $\delta^{18}\text{O}$ and $\delta^2\text{H}$ values of the initial and final test solutions are <0.2‰ and <1‰, respectively.

⁴ Highlighted, italicized values are considered unreliable; criteria used to assess the data are given in the text (section 5.1).

() Where sample ID is enclosed in brackets, it was not possible to closely match the activity of the test solution to the water activity of these rock samples using NaCl standard solutions. This resulted in a significant (> 1 g) transfer of water from the test solution to the rock. For this reason, the stable water isotopic compositions of these samples were not measured (n.m.).

Table 23 (Cont'd): Borehole DGR-3. Isotope diffusive exchange experiments: Measured isotopic composition of the test solutions and calculated porewater compositions.

Sample ID (NWMO) ¹	Formation	Test solution “LAB” (tap water)				Test solution “TEW” (glacial meltwater)				Calculated porewater isotopic composition ⁵			
		Initial $\delta^{18}\text{O}$ of test so- lution ^{2,3}	Final $\delta^{18}\text{O}$ of test so- lution ³	Initial $\delta^2\text{H}$ of test so- lution ^{2,3}	Final $\delta^2\text{H}$ of test so- lution ³	Initial $\delta^{18}\text{O}$ of test so- lution ^{2,3}	Final $\delta^{18}\text{O}$ of test so- lution ³	Initial $\delta^2\text{H}$ of test so- lution ^{2,3}	Final $\delta^2\text{H}$ of test so- lution ³	$\delta^{18}\text{O}$	STD (1 σ)	$\delta^2\text{H}$	STD (1 σ)
		(‰ V- SMOW)	(‰ V- SMOW)	(‰ V- SMOW)	(‰ V- SMOW)	(‰ V- SMOW)	(‰ V- SMOW)	(‰ V- SMOW)	(‰ V- SMOW)	(‰ V- SMOW)	(‰)	(‰)	(‰ V- SMOW)
DGR-3 676.21	Cobourg – Lower M.	-11.1	-8.5	-80.5	-72.3	-24.56	-19.2	-187.94	-159.4	<i>1.6</i>	<i>2.7</i>	<i>-36.8</i>	<i>10.1</i>
DGR-3 678.92	Cobourg – Lower M.	-11.1	-9.7	-80.5	-75.3	-24.56	-20.3	-187.94	-172.5	<i>-4.9</i>	<i>1.7</i>	<i>-28.0</i>	<i>21.2</i>
DGR-3 685.52	Cobourg – Lower M.	-11.1	-8.9	-80.5	-70.6	-24.56	sample lost ⁴	-187.94	sample lost ⁴	n.m.	n.m.	n.m.	n.m.
DGR-3 690.12	Cobourg – Lower M.	-11.1	-8.1	-80.5	-72.1	-24.56	-19.9	-187.94	-176.4	<i>15.6</i>	<i>8.5</i>	<i>237.9</i>	<i>259.1</i>
DGR-3 692.82	Cobourg – Lower M.	-11.1	-6.2	-80.5	-66.5	-24.56	-15.4	-187.94	-144.0	<i>5.0</i>	<i>2.0</i>	<i>-29.9</i>	<i>6.9</i>
DGR-3 697.94	Cobourg – Lower M.	-11.1	-8.7	-80.5	-71.7	-24.56	-19.9	-187.94	-160.5	<i>1.9</i>	<i>3.0</i>	<i>-34.0</i>	<i>10.1</i>
DGR-3 710.38	Sherman Fall	-11.1	-8.0	-80.5	-70.8	-24.56	n.m.	-187.94	n.m.	<i>-7.0</i>	<i>0.4</i>	<i>-61.0</i>	<i>2.7</i>
DGR-3 725.57	Sherman Fall	-11.1	-8.1	-80.5	-68.4	-24.56	-18.2	-187.94	-145.0	<i>2.0</i>	<i>2.5</i>	<i>-34.5</i>	<i>7.1</i>
DGR-3 744.27	Kirkfield	-11.1	-7.7	-80.5	-63.7	-24.56	-16.6	-187.94	-142.9	<i>-1.3</i>	<i>1.3</i>	<i>-16.3</i>	<i>8.1</i>
DGR-3 761.56	Kirkfield	-11.1	-7.3	-80.5	-66.7	-24.56	-17.4	-187.94	-149.6	<i>2.9</i>	<i>2.1</i>	<i>-22.9</i>	<i>8.5</i>
DGR-3 777.33	Coboconk	-11.1	-10.1	-80.5	-73.4	-24.56	-21.4	-187.94	-165.4	<i>-5.0</i>	<i>2.4</i>	<i>-31.0</i>	<i>14.1</i>
DGR-3 807.43	Gull River	-11.1	-9.1	-80.5	-74.6	-24.56	-22.1	-187.94	-171.6	<i>77.6</i>	<i>120.1</i>	<i>-14.9</i>	<i>25.8</i>
DGR-3 843.92	Gull River	-11.1	-9.3	-80.5	-70.5	-24.56	-16.9	-187.94	-153.9	<i>-6.9</i>	<i>0.7</i>	<i>-37.7</i>	<i>7.9</i>
DGR-3 852.18	Shadow Lake	-11.1	-5.1	-80.5	-56.3	-24.56	-13.8	-187.94	-108.1	<i>6.5</i>	<i>1.9</i>	<i>-33.2</i>	<i>3.3</i>
DGR-3 856.06	Cambrian	-11.1	-9.5	-80.5	-72.6	-24.56	-21.2	-187.94	-166.0	<i>0.2</i>	<i>3.9</i>	<i>-22.2</i>	<i>15.9</i>

¹ Depth of sample in meters below ground surface is given by the second half of the NWMO sample ID.

² The isotopic composition of the tap water used to prepare the LAB standard is not constant and may depend on the date of preparation of the standard. Because all LAB waters were prepared in about 10 days (from 20.06.2008 to 1.07.2008), this variation is below the analytical uncertainty (see Table A-2 and Table A-5, Appendix A). The long term averages of the $\delta^{18}\text{O}$ and $\delta^2\text{H}$ values of the TEW glacial meltwater as determined by the Institute of Physics, University of Bern, were used as the initial isotopic composition (Table A-2 and A-5 Appendix A).

³ The estimated errors in the $\delta^{18}\text{O}$ and $\delta^2\text{H}$ values of the initial and final test solutions are <0.2‰ and <1‰, respectively.

⁴ Sample lost during distillation due to a crack in the glass vial.

⁵ **Highlighted**, italicized values are considered unreliable; criteria used to assess the data are given in the text (section 5.1).

() Where sample ID is enclosed in brackets, it was not possible to closely match the activity of the test solution to the water activity of these rock samples using NaCl standard solutions. This resulted in a significant (> 1 g) transfer of water from the test solution to the rock. For this reason, the stable water isotopic compositions of these samples were not measured (n.m.).

Table 24: Borehole DGR-3. Water contents calculated from isotope diffusive exchange data and measured by oven-drying.

Sample ID (NWMO) ¹	Formation	WC _{δ18O} ²	STD (1σ)	WC _{δ2H} ²	STD (1σ)	WC _{Grav. wet} 40°C ³	STD (1σ)	WC _{Grav. wet} 105°C ³	STD (1σ)
		(wt%)	(wt%)	(wt%)	(wt%)	(n=2)	(wt%)	(n=4)	(wt%)
DGR-3 198.72*	Salina – F Unit	2.6	0.2	3.4	0.2	n.m.	n.m.	5.82*	2.33*
(DGR-3 208.41)*	Salina - F Unit	n.m.	n.m.	n.m.	n.m.	1.60	0.13	11.8*	2.39*
DGR-3 248.71	Salina – E Unit	4.2	0.4	2.9	0.2	n.m.	n.m.	5.36	0.35
DGR-3 270.06	Salina - C Unit	7.9	1.0	6.7	0.5	n.m.	n.m.	6.64	0.03
DGR-3 289.36	Salina – B Unit	2.7	0.3	2.6	0.2	n.m.	n.m.	6.65	0.39
DGR-3 312.53	Salina - A2 Unit	6.6	0.7	5.7	0.4	n.m.	n.m.	5.33	0.23
DGR-3 335.22*	Salina – A2 Evap.	0.2	0.1	0.1	0.0	n.m.	n.m.	0.53*	0.07*
DGR-3 344.06	Salina -A1 Unit	0.4	0.1	0.4	0.0	n.m.	n.m.	0.40	0.14
DGR-3 380.88	A1 Evaporite	0.2	0.1	0.2	0.0	n.m.	n.m.	0.11	0.02
(DGR-3 391.34)	Guelph	n.m.	n.m.	n.m.	n.m.	n.m.	n.m.	1.90	0.17
(DGR-3 435.62)	Cabot Head	n.m.	n.m.	n.m.	n.m.	n.m.	n.m.	3.58	0.20
DGR-3 453.41	Manitoulin	1.7	0.2	0.8	0.1	n.m.	n.m.	0.69	0.09
(DGR-3 468.76)	Queenston	n.m.	n.m.	n.m.	n.m.	n.m.	n.m.	3.07	0.02
(DGR-3 484.58)	Queenston	n.m.	n.m.	n.m.	n.m.	n.m.	n.m.	2.40	0.06
(DGR-3 502.55)	Queenston	n.m.	n.m.	n.m.	n.m.	n.m.	n.m.	2.03	0.76
DGR-3 531.65	Georgian Bay	1.8	0.2	2.1	0.1	n.m.	n.m.	1.81	0.27
DGR-3 581.47	Georgian Bay	2.9	0.3	3.0	0.2	n.m.	n.m.	3.20	0.10
(DGR-3 621.63)	Blue Mountain	n.m.	n.m.	n.m.	n.m.	n.m.	n.m.	2.96	0.02

¹ Depth of sample in meters below ground surface is given by the second half of the NWMO sample ID.

² **Highlighted** italicized values are considered unreliable; criteria used to assess the data are given in the text (section 5.1).

³ Water content is defined as the weight proportion of water (H₂O, does not include weight of solutes) in the rock; calculated as reported by Koroleva et al. 2009.

*Gypsum identified in samples during mineralogical investigations. Therefore, values determined at both 40°C and 105 °C may include structural water from gypsum, in addition to water from the pore space (section 4.2.1).

() Where sample ID is enclosed in brackets, it was not possible to closely match the activity of the test solution to the water activity of these rock samples using NaCl standard solutions. This resulted in a significant (> 1 g) transfer of water from the test solution to the rock. For this reason, the stable water isotopic compositions of these samples were not measured (n.m.) and therefore, water contents could not be derived.

Table 24 (Cont'd.): Borehole DGR-3. Water contents calculated from isotope diffusive exchange data and measured gravimetrically.

Sample ID (NWMO) ¹	Formation	WC _{δ18O} ²	STD (1σ)	WC _{δ2H} ²	STD (1σ)	WC _{Grav. wet} 40°C ³	STD (1σ)	WC _{Grav. wet} 105°C ³	STD (1σ)
		(wt.%)	(wt.%)	(wt.%)	(wt.%)	(n=2)	(wt.%)	(n=4)	(wt.%)
(DGR-3 646.29)	Blue Mountain	n.m.	n.m.	n.m.	n.m.	n.m.	n.m.	2.74	0.04
DGR-3 665.29	Cobourg – Collingwood M.	<i>0.2</i>	<i>0.1</i>	<i>0.5</i>	<i>0.1</i>	n.m.	n.m.	0.53	0.04
DGR-3 676.21	Cobourg – Lower M.	<i>1.0</i>	<i>0.2</i>	<i>0.9</i>	<i>0.1</i>	n.m.	n.m.	0.88	0.19
DGR-3 678.92	Cobourg – Lower M.	<i>1.2</i>	<i>0.2</i>	<i>0.4</i>	<i>0.1</i>	n.m.	n.m.	0.58	0.51
DGR-3 685.52	Cobourg – Lower M.	n.m.	n.m.	n.m.	n.m.	n.m.	n.m.	0.63	0.06
DGR-3 690.12	Cobourg – Lower M.	<i>0.4</i>	<i>0.1</i>	<i>0.1</i>	<i>0.1</i>	n.m.	n.m.	0.28	0.12
DGR-3 692.82	Cobourg – Lower M.	<i>0.9</i>	<i>0.1</i>	<i>0.8</i>	<i>0.1</i>	n.m.	n.m.	0.85	0.15
DGR-3 697.94	Cobourg – Lower M.	<i>0.7</i>	<i>0.1</i>	<i>0.7</i>	<i>0.1</i>	n.m.	n.m.	0.63	0.06
DGR-3 710.38	Sherman Fall	<i>6.6</i>	<i>0.8</i>	<i>1.9</i>	<i>0.1</i>	n.m.	n.m.	0.31	0.10
DGR-3 725.57	Sherman Fall	<i>0.7</i>	<i>0.1</i>	<i>0.9</i>	<i>0.1</i>	n.m.	n.m.	0.87	0.10
DGR-3 744.27	Kirkfield	<i>1.0</i>	<i>0.1</i>	<i>0.7</i>	<i>0.1</i>	n.m.	n.m.	0.89	0.16
DGR-3 761.56	Kirkfield	<i>0.9</i>	<i>0.1</i>	<i>0.8</i>	<i>0.1</i>	n.m.	n.m.	0.55	0.32
DGR-3 777.33	Coboconk	0.6	0.1	0.5	0.1	n.m.	n.m.	0.46	0.03
DGR-3 807.43	Gull River	<i>0.1</i>	<i>0.1</i>	<i>0.3</i>	<i>0.1</i>	n.m.	n.m.	0.33	0.02
DGR-3 843.92	Gull River	<i>2.2</i>	<i>0.2</i>	<i>0.8</i>	<i>0.1</i>	n.m.	n.m.	0.48	0.21
DGR-3 852.18	Shadow Lake	<i>1.6</i>	<i>0.2</i>	<i>3.2</i>	<i>0.2</i>	n.m.	n.m.	3.06	0.09
DGR-3 856.06	Cambrian	0.5	0.1	0.5	0.1	n.m.	n.m.	0.49	0.12

¹ Depth of sample in meters below ground surface is given by the second half of the NWMO sample ID. Using NaCl standard solutions, it was not possible to closely match the activity of the test solution to the water activity of these rock samples which label is in (). This resulted in a significant (>1 g) transfer of water from the test solution to the rock. For this reason, the test waters of these samples were not measured (n.m.) and the water content was not calculated.

² **Highlighted**, italicized values are considered unreliable; criteria used to assess the data are given in the text (section 5.1).

³ Water content is defined as the weight proportion of water (H₂O, does not include weight of solutes) in the rock; calculated as described in section 4.2.1.

Table 25: Borehole DGR-4. Isotope diffusive exchange experiments: Measured isotopic composition of the test solutions and calculated porewater compositions.

Sample ID (NWMO) ¹	Formation	Test solution “LAB” (tap water)				Test solution “TEW” (glacial meltwater)				Calculated porewater isotopic composition ³			
		Initial $\delta^{18}\text{O}$ of test solu- tion ²	Final $\delta^{18}\text{O}$ of test solu- tion ²	Initial $\delta^2\text{H}$ of test solu- tion ²	Final $\delta^2\text{H}$ of test solution ²	Initial $\delta^{18}\text{O}$ of test solu- tion ²	Final $\delta^{18}\text{O}$ of test solu- tion ²	Initial $\delta^2\text{H}$ of test solu- tion ²	Final $\delta^2\text{H}$ of test solution ²	$\delta^{18}\text{O}$	STD (1 σ)	$\delta^2\text{H}$	STD (1 σ)
		(‰ V- SMOW)	(‰ V- SMOW)	(‰ V- SMOW)	(‰ V- SMOW)	(‰ V- SMOW)	(‰ V- SMOW)	(‰ V- SMOW)	(‰ V- SMOW)	(‰ V- SMOW)	(‰)	(‰ V- SMOW)	(‰)
DGR-4 154.60	Bass Islands	-10.9	-11.4	-76.1	-81.6	-24.56	-18.4	-187.94	-138	-12.0	0.4	-87.0	2.0
DGR-4 189.16	Salina – F	-10.9	-10.8	-76.1	-75.2	-24.56	-15.0	-187.94	-110.5	-10.7	0.3	-74.8	1.5
DGR-4 229.32	Salina – E	-10.9	-10.7	-76.1	-73.3	-24.56	-16.2	-187.94	-117.6	<i>-10.6</i>	<i>0.4</i>	<i>-71.0</i>	<i>2.1</i>
DGR-4 322.68	A2 Evaporite	-10.9	-10.6	-76.1	-74.5	-24.56	-23.5	-187.94	-178.0	<i>-5.6</i>	<i>6.6</i>	<i>-55.2</i>	<i>21.4</i>
DGR-4 332.13	Salina - A1	-10.9	-11.1	-76.1	-80.0	-24.56	-21.3	-187.94	-160.8	-11.8	0.9	-90.1	3.9
DGR-4 369.43	A1 Evaporite	-10.9	-10.4	-76.1	-72.9	-24.56	-23.7	-187.94	-174.6	<i>40.2</i>	<i>150.4</i>	<i>-31.6</i>	<i>27.3</i>
DGR-4 422.21	Cabot Head		Failed experiment					Failed experiment					
DGR-4 472.78	Queenston	-10.9	-2.3	-76.1	-50.2	-24.56	-6.6	-187.94	-83.2	1.7	0.7	-39.3	2.0
DGR-4 520.42	Georgian Bay	-10.9	-3.10	-76.1	-50.4	-24.56	-10.5	-187.94	-108.9	<i>4.4</i>	<i>1.0</i>	<i>-26.0</i>	<i>3.2</i>
DGR-4 662.83	Cobourg - Lower M.	-10.9	-7.2	-76.1	-62.6	-24.56	-17.7	-187.94	-143.3	0.2	1.4	-38.0	4.6
DGR-4 665.41	Cobourg - Lower M.	-10.9	-7.7	-76.1	-64.4	-24.56	-19.7	-187.94	-161.5	<i>16.3</i>	<i>8.0</i>	<i>14.4</i>	<i>20.3</i>
DGR-4 672.85	Cobourg - Lower M.		Failed experiment					Failed experiment					
DGR-4 685.14	Cobourg - Lower M.	-10.9	-7.7	-76.1	-65.4	-24.56	-17.9	-187.94	-145.9	3.1	2.6	-34.9	6.8
DGR-4 717.12	Sherman Fall	-10.9	-6.3	-76.1	-54.6	-24.56	-12.2	-187.94	-104.9	-2.1	0.8	-34.3	3.1
DGR-4 730.07	Kirkfield	-10.9	-6.8	-76.1	-58.1	-24.56	-14.7	-187.94	-120.5	<i>-1.4</i>	<i>1.0</i>	<i>-35.3</i>	<i>3.7</i>
DGR-4 841.06	Shadow Lake	-10.9	-6.4	-76.1	-50.4	-24.56	-11.8	-187.94	-95.0	-3.5	0.6	-34.4	2.4
DGR-4 847.48	Cambrian	-10.9	-8.6	-76.1	-63.6	-24.56	-19.2	-187.94	-144.8	<i>-3.6</i>	<i>1.2</i>	<i>-41.2</i>	<i>4.4</i>

¹ Depth of sample in meters below ground surface is given by the second half of the NWMO sample ID.

² The $\delta^{18}\text{O}$ and $\delta^2\text{H}$ values of the LAB water correspond to the average of 3 analyses of the 23.03.2009 Uni-Bern lab tap water (See Table A-5). The long-term averages of the $\delta^{18}\text{O}$ and $\delta^2\text{H}$ values of the TEW glacial melt water as determined by the Institute of Physics, University of Bern, were used as the initial isotopic composition (Table A-5). The estimated errors in the $\delta^{18}\text{O}$ and $\delta^2\text{H}$ values of the initial and final test solutions are <0.2‰ and <1‰, respectively.

³ **Highlighted**, italicized values are considered unreliable; criteria used to assess the data are given in the text (section 5.1).

Table 26: Borehole DGR-4. Water contents calculated from isotope diffusive exchange data and determined by oven-drying.

Sample ID (NWMO) ¹	Formation	WC _{δ18O} ²	STD (1σ)	WC _{δ2H} ²	STD (1σ)	WC _{Grav, wet} 40°C ³	STD (1σ)	WC _{Grav, wet} 105°C ³	STD (1σ)
		(wt%)	(wt%)	(wt%)	(wt%)	(n=2 to 4)	(wt%)	(n=4)	(wt%)
DGR-4 154.60	Bass Islands	1.66	0.15	1.68	0.09	1.56	0.04	1.58	0.06
DGR-4 189.16*	Salina - F	3.99	0.40	3.93	0.24	3.38*	0.17*	8.07*	0.59*
DGR-4 229.32*	Salina - E	<i>3.10</i>	<i>0.30</i>	<i>3.16</i>	<i>0.19</i>	2.37*	0.37*	11.3*	3.36*
DGR-4 322.68*	A2 Evaporite	<i>0.13</i>	<i>0.06</i>	<i>0.17</i>	<i>0.04</i>	0.66*	0.05*	1.27*	0.31*
DGR-4 332.13	Salina - A1	0.57	0.08	0.62	0.05	0.04	0.00	0.62	0.10
DGR-4 369.43	A1 Evaporite	<i>0.03</i>	<i>0.07</i>	<i>0.19</i>	<i>0.05</i>	0.06	0.01	0.07	0.01
DGR-4 422.21	Cabot Head	Failed experiment				3.09	0.01	4.05	0.06
DGR-4 472.78	Queenston	2.60	0.27	2.87	0.18	1.77	0.05	2.68	0.04
DGR-4 520.42	Georgian Bay	<i>1.01</i>	<i>0.09</i>	<i>1.02</i>	<i>0.05</i>	1.37	0.02	1.61	0.18
DGR-4 662.83	Cobourg - Lower M.	0.56	0.06	0.62	0.04	0.49	0.01	0.63	0.12
DGR-4 665.41	Cobourg - Lower M.	<i>0.17</i>	<i>0.04</i>	<i>0.18</i>	<i>0.03</i>	0.53	0.02	0.57	0.15
DGR-4 672.85	Cobourg - Lower M.	Failed experiment				0.30	0.02	0.40	0.07
DGR-4 685.14	Cobourg - Lower M.	0.70	0.10	0.83	0.07	0.64	0.07	0.73	0.15
DGR-4 717.12	Sherman Fall	1.47	0.14	1.42	0.08	0.58	0.40	1.13	0.46
DGR-4 730.07	Kirkfield	<i>1.34</i>	<i>0.13</i>	<i>1.42</i>	<i>0.08</i>	0.97	0.15	1.51	0.29
DGR-4 841.06	Shadow Lake	1.88	0.17	1.88	0.10	1.73	0.21	2.00	0.13
DGR-4 847.48	Cambrian	<i>0.84</i>	<i>0.10</i>	<i>1.02</i>	<i>0.07</i>	0.61	0.12	0.73	0.08

¹ Depth of sample in meters below ground surface is given by the second half of the NWMO sample ID.

² **Highlighted**, italicized values are considered unreliable; criteria used to assess the data are given in the text (section 5.1).

³ Water content is defined as the weight proportion of water (H₂O, does not include weight of solutes) in the rock; calculated as reported in section 4.2.1.

*Gypsum identified in samples during mineralogical investigations. Therefore, values determined at both 40°C and 105 °C may include structural water from gypsum, in addition to water from the pore space (section 4.2.1).

6 Aqueous extractions

The ion concentrations measured in the aqueous extracts may be representative of pore fluids compositions within the rock matrix if i) the ions can be considered non-reactive during aqueous leaching and not subject to changes due to reaction processes such as ion exchange or oxidation (e.g. of sulphide minerals); and ii) if there are no additional sources of dissolved ions contributing to the extract solutions from mineral dissolution (e.g. salts, carbonates, sulphates) or released from fluid inclusions during milling. In argillaceous sedimentary rocks, the volume of fluid inclusions is commonly low compared to the connected pore space and therefore, contributions to aqueous extractions are usually considered to be negligible. The elements most likely to behave conservatively (i.e. to be non-reactive) during aqueous leaching and are potential tracers for pore fluid concentrations are chloride and bromide. Sulphate may also be a useful tracer of pore fluid if there are no readily soluble sulphate minerals, and if precautions are taken during sample preservation and laboratory handling to minimize oxidation of any sulphide minerals. In the following sections, the possible impact of mineral dissolution and ion exchange process on the major ion compositions of the extract solutions is evaluated along with supporting mineralogical information and mineral saturation indices calculated for the aqueous extract solutions.

The results of the aqueous extractions conducted on core from DGR-3 and DGR-4 are given in Table 27 and Table 28, respectively. The values reported are the average of two replicates. In Table 30 and Table 31, concentrations of ions are expressed in milliequivalents per kilogram of dry rock material. The two criteria used to evaluate the quality of the aqueous extract data are the charge balance and the reproducibility of the pH values, major ion concentrations and alkalinities for duplicate extractions. Charge balance in percent is defined as:

$$\frac{[(\text{cation charge}) - (\text{anion charge})]}{[(\text{cation charge}) + (\text{anion charge})]} \cdot 100 \quad (14)$$

The quality of the analysis of the aqueous extractions is good with respect the reproducibility of i) major concentrations ions measured for duplicate extractions and analyses, which are within the analytical error of 5% for concentrations <100 mg/l and within 10% for higher concentrations, ii) measured pH values, which differ by a maximum of ± 0.3 pH units for duplicate extractions and iii) measured alkalinities, which differ by a maximum of 0.06 meq/L for duplicate extractions (See Appendix C for dataset including results for duplicate extractions). Although the reproducibility of pH values for duplicate extractions can be used an indicator of the quality of the solution data, it must be emphasised that aqueous extract pH values do not represent porewater pH values. The pH values of the aqueous extract solutions are a result of the original pH of the distilled water added to extract ions originally present in the porewater of the rock, plus any reactions with minerals that occurred during the extractions.

The quality of the aqueous extraction data is also excellent with respect to charge balance. The majority of aqueous extract solutions from both DGR-3 and DGR-4 have charge balances within $\pm 4\%$. The exceptions in DGR-3 are one sample from each of the Salina F and A2 units, one sample from the Guelph Formation and two from the Queenston Formation with charge balances in the range of -4.4 to -7.6% (Table 27). In DGR-4 (Table 28), two samples from the Cobourg and one sample from each of the Sherman Fall Formation and from the Cambrian have charge balances ranging from +5.2 to 6.0%. Considering the large differences in element concentrations and the multiple dilutions and measurements required for some elements, these charge balances which are within $\pm 8\%$ are considered to be very good.

As an additional check on the quality of the Br⁻ analyses, in samples where Br⁻ concentrations were close to or below detection in the aqueous extract solutions in the IC analyses (<1 mg/L or <2 mg/L), the solutions were also analyzed using ICP-MS at the British Geological Survey. Bromide concentrations determined using both methods are compared in Table 29. In cases where Br⁻ concentrations were close to but still above detection using IC analysis, the agreement with the ICP-MS values is excellent (<5%); in extract solutions where Br⁻ concentrations were right at the detection limit using IC analysis, the difference is larger (10 to 20%), as expected. For these samples, the average Br⁻ concentration determined in the aqueous extract solutions using ICP-MS is reported in Table 27 and Table 28.

Consistent with observations for DGR-2 samples, the concentrations of F⁻ in DGR-3 and DGR-4 aqueous extracts are below the detection limit of 1 to 2 mg/L (depending on the dilution factor) for most samples. Koroleva et al. (2009) described the possible presence of low-molecular weight organic acids in the ion chromatograms for several DGR-2 samples containing measurable F⁻. Similar interference was observed in the aqueous extract solutions from DGR-3 and DGR-4 samples. Due to the overlap between these peaks in the ion chromatograms, F⁻ concentrations determined using this method are considered unreliable and therefore, these results are not used. Nitrate concentrations in the aqueous extracts from DGR-3 and -4 were at or below the detection limit of 1 to 2 mg/L and are therefore not discussed.

The aqueous extract composition determined for each duplicate sample (see Appendix C) was speciated with PHREEQC (Parkhurst and Appelo, 1999; v. 2.15.0, 2008) using the PHREEQC thermodynamic database to calculate saturation indices and the partial pressure of carbon dioxide. For consistency, the pH measured at the time of alkalinity titration was used and the titrated alkalinity was taken as the total carbonate alkalinity. Other species that may contribute to the total alkalinity but which were not measured include Si and B. All modelling was carried out at 20 °C. The calculated saturation indices (SI) for diagnostic minerals in the aqueous extractions from DGR-3 and DGR-4 are given in Table 32 and Table 33, respectively. In the interpretation of the saturation indices for the aqueous extracts, a solution is considered to be at saturation when the SI is equal to 0.0 ± 0.15 SI units for minerals with a simple stoichiometry.

In the following sections, the compositions of the aqueous extracts, calculated mineral saturation indices and mineralogy (section 3) are examined together for evidence suggesting mineral dissolution during extraction, with an emphasis on soluble phases. This evidence is then summarized and the dataset is sorted on this basis.

Table 27: Borehole DGR-3: Chemical composition of aqueous extract solutions from experiments conducted at a solid:liquid ratio of 1:1. Reported values are the average of two replicates.

Sample ID ¹ (NWMO)	Formation	pH	Na ⁺	K ⁺	Mg ²⁺	Ca ²⁺	Sr ²⁺	¹ F ⁻	Cl ⁻	Br ⁻	SO ₄ ²⁻	NO ₃ ⁻	Total Alkalinity	Charge Balance	Br/Cl
			(mg/l)	(mg/l)	(mg/l)	(mg/l)	(mg/l)	(mg/l)	(mg/l)	(mg/l)	(mg/l)	(mg/l)	(mg/l)	(meq/l)	(%)
DGR-3 198.72*	Salina – F Unit	8.18	581	160	54.6	599	5.2	5.8	714	2.3	2170	<1.0	0.83	-1.94%	1.42E-03
DGR-3 208.41*	Salina - F Unit	8.33	781	115	38.2	620	3.9	4.7	1250	2.7	2040	<1.0	0.67	-5.07%	9.61E-04
DGR-3 248.71*	Salina – E Unit	8.50	1500	129	44.2	719	5.1	5.7	2030	2.6	2400	<1.0	0.90	-0.14%	5.78E-04
DGR-3 270.06*	Salina - C Unit	8.36	6450	210	46.7	1140	13.1	3.6	10400	10.1	2920	4.3	0.42	-1.25%	4.30E-04
DGR-3 289.36*	Salina – B Unit	8.43	3850	132	75.8	1060	6.4	5.8	6430	10.7	2740	3.7	0.76	-1.99%	7.41E-04
DGR-3 312.53	Salina - A2 Unit	8.34	2400	110	131	349	26.7	5.8	4160	5.5	1440	4.0	0.81	-4.38%	5.83E-04
DGR-3 335.22*	Salina – A2 Evaporite	8.74	51.8	11.7	5.2	795	17.2	<1.0	102	0.37	1890	1.6	0.35	0.42%	3.19E-03
DGR-3 344.06	Salina -A1 Unit	8.98	182	27.6	3.3	16.9	<0.5	3.0	230	1.1	111	<1.0	0.93	-0.93%	2.11E-03
DGR-3 380.88*	A1 Evaporite	8.66	62.1	15.0	3.5	1090	<0.5	<1.0	187	1.2	2510	<1.0	0.43	-0.39%	0.00E+00
DGR-3 391.34*	Guelph	8.70	10600	120	112	1270	4.2	<1.0	19900	48.3	2090	20.6	0.73	-6.05%	1.08E-03
DGR-3 435.62	Cabot Head	7.92	1640	718	274	2140	53.4	2.2	8060	97.4	12.1	12.1	0.49	-2.03%	5.36E-03
DGR-3 453.41	Manitoulin	8.07	478	131	127	591	14.4	<1.0	2230	33.5	17.3	2.5	0.35	0.32%	6.68E-03
DGR-3 468.76	Queenston	7.93	1240	618	206	1640	34.6	1.9	6930	85.3	19.5	7.9	0.39	-7.61%	5.46E-03
DGR-3 484.58*	Queenston	8.05	1030	488	155	1670	29.8	1.7	5170	64.5	1160	6.5	0.43	-5.35%	5.53E-03
DGR-3 502.55	Queenston	8.12	525	291	72.4	644	14.6	1.0	2060	25.4	439	1.3	0.48	0.45%	5.48E-03
DGR-3 531.65*	Georgian Bay	8.11	844	279	96.6	782	16.7	<1.0	2850	32.2	327	1.5	0.50	1.76%	5.01E-03
DGR-3 581.47	Georgian Bay	7.92	1630	637	111	1480	40.4	1.3	6260	72.7	9.4	6.0	0.41	-2.06%	5.15E-03
DGR-3 621.63	Blue Mountain	7.87	1600	634	117	1530	42.0	1.2	6300	74.0	19.3	6.1	0.42	-1.94%	5.21E-03
DGR-3 646.29	Blue Mountain	7.98	1410	472	91.9	1280	33.0	1.2	5190	62.5	28.8	4.7	0.42	-1.02%	5.34E-03
DGR-3 665.29	Cobourg –C M	8.61	221	133	22.3	93.3	4.0	1.1	677	6.8	54.9	<1.0	0.77	-3.78%	4.46E-03

¹Data for F⁻ are considered semi-quantitative due to overlap with peaks for organic acids in the ion chromatograms.

Shading of Br⁻ value indicates that it is the average of measurements made on the two replicate extraction solutions using ICP-MS at the British Geological Survey.

Table 27 (Cont'd): Borehole DGR-3: Chemical composition of aqueous extract solutions for experiments conducted at a solid:liquid ratio of 1:1. Reported values are the average of two replicates.

Sample ID ¹ (NWMO)	Formation	pH	Na ⁺	K ⁺	Mg ²⁺	Ca ²⁺	Sr ²⁺	¹ F ⁻	Cl ⁻	Br ⁻	SO ₄ ²⁻	NO ₃ ⁻	Total Alkalinity	Charge Balance	Br/Cl
			(mg/l)	(mg/l)	(mg/l)	(mg/l)	(mg/l)	(mg/l)	(mg/l)	(mg/l)	(mg/l)	(mg/l)	(mg/l)	(meq/l)	(%)
DGR-3 676.21	Cobourg – LM	8.25	721	321	85.3	446	14.5	<1.0	2530	25.3	26.4	<1.0	0.51	-2.50%	4.43E-03
DGR-3 678.92	Cobourg – LM	8.40	220	113	25.5	134	3.9	<1.0	761	7.6	41.4	<1.0	0.58	-3.83%	4.42E-03
DGR-3 685.52	Cobourg – LM	8.32	299	136	33.2	184	5.0	<1.0	1030	11.3	35.8	<1.0	0.57	-3.38%	4.87E-03
DGR-3 690.12	Cobourg – LM	8.51	231	88.8	26.1	144	4.7	<1.0	774	7.4	32.4	<1.0	0.46	-3.00%	4.21E-03
DGR-3 692.82	Cobourg – LM	8.42	456	166	43.5	247	8.5	<1.0	1490	15.3	28.5	<1.0	0.46	-3.82%	4.54E-03
DGR-3 697.94	Cobourg – LM	8.35	350	150	36.9	205	5.4	<1.0	1160	12.3	27.4	<1.0	0.47	-2.29%	4.72E-03
DGR-3 710.38	Sherman Fall	8.63	141	43.7	18.6	107	3.3	<1.0	464	4.4	18.7	<1.0	0.37	0.87%	4.22E-03
DGR-3 725.57	Sherman Fall	8.41	629	271	51.5	284	7.4	1.4	1810	20.6	29.3	<1.0	0.51	0.46%	5.07E-03
DGR-3 744.27	Kirkfield	8.25	593	262	36.8	244	6.1	1.4	1600	15.6	27.9	<1.0	0.55	1.39%	4.33E-03
DGR-3 761.56*	Kirkfield	8.79	62.4	19.2	9.1	72.4	<1.0	<1.0	178	1.5	91.1	<1.0	0.35	1.70%	3.66E-03
DGR-3 777.33	Coboconk	8.65	226	94.3	13.1	69.1	1.8	1.3	507	4.5	54.5	1.3	0.63	1.84%	3.97E-03
DGR-3 807.43	Gull River	8.75	164	51.6	15.3	80.2	1.9	<1.0	435	3.8	47.1	1.3	0.43	-0.20%	3.86E-03
DGR-3 843.92	Gull River	8.59	232	78.9	14.9	75.7	1.9	1.7	534	4.7	54.6	1.4	0.63	0.47%	3.87E-03
DGR-3 852.18	Shadow Lake	7.98	1270	305	114	745	10.0	3.5	3910	42.7	64.2	2.7	0.40	-1.25%	4.85E-03
DGR-3 856.06	Cambrian	9.03	314	70.3	120	137	4.2	<1.0	1130	10.1	16.8	<1.0	0.60	-1.07%	3.96E-03

*Soluble sulphates and/or halite were identified in the sample during mineralogical investigations.

¹Data for F⁻ are considered semi-quantitative due to overlap with peaks for organic acids in the ion chromatograms.

Shading of Br⁻ value indicates that it is the average of measurements made on the two replicate extraction solutions using ICP-MS at the British Geological Survey.

Table 28: Borehole DGR-4: Chemical composition of aqueous extract solutions from experiments conducted at a solid:liquid ratio of 1:1. Reported values are the average of two replicates.

Sample ID ¹ (NWMO)	Formation	pH	Na ⁺	K ⁺	Mg ²⁺	Ca ²⁺	Sr ²⁺	¹ F ⁻	Cl ⁻	Br ⁻	SO ₄ ²⁻	NO ₃ ⁻	Total Alkalinity	Charge Balance	Br/Cl
			(mg/l)	(mg/l)	(mg/l)	(mg/l)	(mg/l)	(mg/l)	(mg/l)	(mg/l)	(mg/l)	(mg/l)	(meq/l)	(%)	(mol/mol)
DGR-4 154.60	Bass Islands	9.48	23.2	15.2	111	14.3	<1	<2	210	3.46	41.2	<1	3.75	3.11%	7.32E-03
DGR-4 189.16*	Salina - F Unit	8.72	292	94.6	34.3	640	4.09	5.15	440	1.40	1880	<2	0.76	-2.09%	1.41E-03
DGR-4 229.32*	Salina - E Unit	8.66	292	105	43.1	644	4.35	5.63	255	1.01	1950	<1	0.69	2.36%	1.75E-03
DGR-4 322.68*	A2 Evaporite	8.53	57.4	7.0	2.41	850	16.6	<2	108	0.32	1870	<1	0.32	3.73%	
DGR-4 332.13	Salina A1 Unit	9.09	294	45.2	3.88	19.7	<1	2.71	417	1.39	128	<2	1.12	-0.48%	1.48E-03
DGR-4 422.21	Cabot Head	7.91	2010	873	426	2680	71.1	3.18	9430	118	52.4	<1	0.33	1.99%	5.53E-03
DGR-4 472.78*	Queenston	7.97	1270	583	212	1990	32.0	2.64	5550	71.3	954	<1	0.51	2.59%	5.70E-03
DGR-4 520.42	Georgian Bay	8.10	706	297	99.1	791	11.1	<2	2880	32.8	400	<2	0.53	-2.48%	5.04E-03
DGR-4 662.83	Cobourg – LM	8.40	407	176	41.6	245	6.79	<2	1150	12.5	39.2	<1	0.54	5.62%	4.80E-03
DGR-4 665.41	Cobourg – LM	8.32	364	158	51.5	231	6.52	<2	1360	15.3	35.1	<2	0.48	-5.15%	4.99E-03
DGR-4 672.85	Cobourg – LM	8.49	222	105	28.7	143	4.37	<2	698	7.30	34.5	<1	0.59	1.92%	4.64E-03
DGR-4 717.12	Sherman Fall	8.54	482	199	30.9	206	4.34	<2	1180	12.0	23.9	<1	0.45	6.02%	4.49E-03
DGR-4 730.07	Kirkfield	8.58	642	249	38.3	287	6.85	<2	1830	18.1	34.7	<2	0.43	-0.93%	4.39E-03
DGR-4 841.06	Shadow Lake	8.44	1020	167	181	695	10.8	2.74	3170	31.8	36.2	<1	0.72	3.65%	4.45E-03
DGR-4 847.48*	Cambrian	8.76	421	27.9	170	213	5.81	<2	1340	14.0	17.0	<1	0.48	6.01%	4.65E-03

*Soluble sulphates and/or halite were identified in the sample during mineralogical investigations.

¹Data for F⁻ are considered semi-quantitative due to overlap with peaks for organic acids in the ion chromatograms.

Shading of Br⁻ value indicates that it is the average of measurements made on the two replicate extraction solutions using ICP-MS at the British Geological Survey.

Table 29: Comparison of Br⁻ concentrations determined in aqueous extract solutions for samples from boreholes DGR-3 and DGR-4 using IC and ICP-MS analyses.

Sample ID ¹ (NWMO)	Formation	Replicate Extraction	IC Analysis (UniBern) Br ⁻ (mg/l)	ICP-MS (BGS) ¹ Br ⁻ (mg/l) ²	Difference (%)
DGR-3 335.22	Salina – A2 Evaporite	A	1.0	0.36	62
DGR-3 335.22	Salina – A2 Evaporite	B	<1.0	0.37	n.a.
DGR-3 344.06	Salina -A1 Unit	A	1.0	1.16	-15
DGR-3 344.06	Salina -A1 Unit	B	1.2	1.15	2.5
DGR-3 380.88	A1 Evaporite	A	<1.0	1.24	n.a.
DGR-3 380.88	A1 Evaporite	B	<1.0	1.20	n.a.
DGR-3 761.56	Kirkfield	A	1.5	1.45	2.8
DGR-3 761.56	Kirkfield	B	1.4	1.48	-2.5
DGR-4 189.16	Salina - F Unit	A	<2	1.40	n.a.
DGR-4 189.16	Salina - F Unit	B	<2	1.40	n.a.
DGR-4 229.32	A2 Evaporite	A	1.0	0.87	10
DGR-4 229.32	A2 Evaporite	B	1.0	0.82	22
DGR-4 322.68	Salina A1 Unit	A	0.3	0.32	n.a.
DGR-4 322.68	Salina A1 Unit	B	0.3	0.31	n.a.
DGR-4 332.13	Salina A1 Unit	A	<2	1.36	n.a.
DGR-4 332.13	Salina A1 Unit	B	<2	1.43	n.a.

¹British Geological Survey

²Detection limit for Br⁻ reported for the ICP-MS analysis is 0.091 mg/L (91 ug/L)

Table 30: Borehole DGR-3: Concentration of ions in meq/kg_{rock} calculated from the chemical compositions of aqueous extract solutions. Reported values are the average of two replicates.

Sample ID ¹ (NWMO)	Formation	Na ⁺	K ⁺	Mg ²⁺	Ca ²⁺	Sr ²⁺	F ⁻	Cl ⁻	Br ⁻	SO ₄ ²⁻	NO ₃ ⁻
		(meq/kg _r)	(meq/kg _r)	(meq/kg _r)	(meq/kg _r)	(meq/kg _r)	(meq/kg _r)	(meq/kg _r)	(meq/kg _r)	(meq/kg _r)	(meq/kg _r)
DGR-3 198.72*	Salina – F Unit	25.3	4.10	4.50	29.9	0.12	0.31	20.1	0.03	45.2	b.d.
DGR-3 208.41*	Salina - F Unit	34.0	2.94	3.14	30.9	0.09	0.25	35.3	0.03	42.5	b.d.
DGR-3 248.71*	Salina – E Unit	65.3	3.30	3.63	35.9	0.12	0.30	57.3	0.03	59.0	b.d.
DGR-3 270.06*	Salina - C Unit	281	5.38	3.84	56.9	0.30	0.19	293	0.13	60.8	0.07
DGR-3 289.36*	Salina – B Unit	168	3.39	6.24	52.9	0.15	0.30	181	0.13	57.1	0.06
DGR-3 312.53	Salina - A2 Unit	104	2.82	10.8	17.4	0.61	0.31	117	0.07	30.0	0.06
DGR-3 335.22*	Salina – A2 Evaporite	2.25	0.30	0.43	39.7	0.39	b.d.	2.89	0.01	39.4	0.03
DGR-3 344.06	Salina -A1 Unit	7.90	0.71	0.27	0.84	b.d.	0.16	6.48	0.014	2.32	b.d.
DGR-3 380.88*	A1 Evaporite	2.70	0.38	0.29	54.4	b.d.	b.d.	5.27	1.22	52.3	b.d.
DGR-3 391.34*	Guelph	461	3.06	9.23	63.4	0.10	b.d.	561	0.61	43.5	0.33
DGR-3 435.62	Cabot Head	71.3	18.4	22.6	106.8	1.22	0.18	227	1.22	0.25	0.20
DGR-3 453.41	Manitoulin	20.8	3.35	10.5	29.5	0.33	b.d.	62.9	0.42	0.36	0.04
DGR-3 468.76	Queenston	53.9	15.8	17.0	81.8	0.79	0.10	195	1.07	0.41	0.13
DGR-3 484.58*	Queenston	44.8	12.5	12.8	83.3	0.68	0.09	146	0.81	24.2	0.11
DGR-3 502.55	Queenston	22.8	7.44	5.96	32.1	0.33	0.05	58.1	0.32	9.15	0.02
DGR-3 531.65*	Georgian Bay	36.7	7.15	7.95	39.0	0.38	b.d.	80.4	0.40	6.80	0.02
DGR-3 581.47	Georgian Bay	70.9	16.3	9.17	73.9	0.92	0.07	177	0.91	0.20	0.10
DGR-3 621.63	Blue Mountain	69.6	16.2	9.60	76.3	0.96	0.07	178	0.93	0.40	0.10
DGR-3 646.29	Blue Mountain	61.3	12.1	7.57	63.9	0.75	0.06	146	0.78	0.60	0.08
DGR-3 665.29	Cobourg –C M	9.62	3.41	1.83	4.66	0.09	0.06	19.1	0.09	1.14	b.d.

*Indicates that a soluble salt was identified in the sample during mineralogical investigations (see section 3.2, Table 5).

b.d indicates concentration of ion was below detection in aqueous extract solution.

Table 30 (Cont'd.). Borehole DGR-3: Concentration of ions in meq/kg rock calculated from the chemical compositions of aqueous extract solutions. Reported values are the average of two replicates.

Sample ID ¹ (NWMO)	Formation	Na ⁺	K ⁺	Mg ²⁺	Ca ²⁺	Sr ²⁺	F ⁻	Cl ⁻	Br ⁻	SO ₄ ²⁻	NO ₃ ⁻
		(meq/kg _r)	(meq/kg _r)	(meq/kg _r)	(meq/kg _r)	(meq/kg _r)	(meq/kg _r)	(meq/kg _r)	(meq/kg _r)	(meq/kg _r)	(meq/kg _r)
DGR-3 676.21	Cobourg – LM	31.4	8.21	7.02	22.2	0.33	b.d.	71.4	0.32	0.55	b.d.
DGR-3 678.92	Cobourg – LM	9.58	2.89	2.10	6.67	0.09	b.d.	21.5	0.10	0.86	b.d.
DGR-3 685.52	Cobourg – LM	13.0	3.49	2.73	9.20	0.11	b.d.	29.1	0.14	0.74	b.d.
DGR-3 690.12	Cobourg – LM	10.1	2.27	2.15	7.17	0.11	b.d.	21.8	0.09	0.67	b.d.
DGR-3 692.82	Cobourg – LM	19.9	4.25	3.58	12.3	0.19	b.d.	42.0	0.19	0.59	b.d.
DGR-3 697.94	Cobourg – LM	15.2	3.85	3.03	10.3	0.12	b.d.	32.7	0.16	0.57	b.d.
DGR-3 710.38	Sherman Fall	6.12	1.12	1.53	5.32	0.07	b.d.	13.1	0.06	0.39	b.d.
DGR-3 725.57	Sherman Fall	27.4	6.94	4.24	14.2	0.17	0.07	51.1	0.26	0.61	b.d.
DGR-3 744.27	Kirkfield	25.8	6.70	3.03	12.2	0.14	0.07	45.1	0.20	0.58	b.d.
DGR-3 761.56*	Kirkfield	2.72	0.49	0.75	3.61	b.d.	b.d.	5.02	0.02	1.90	b.d.
DGR-3 777.33	Coboconk	9.85	2.41	1.08	3.45	0.04	0.07	14.3	0.06	1.13	0.02
DGR-3 807.43	Gull River	7.12	1.32	1.26	4.00	0.04	b.d.	12.3	0.05	0.98	0.02
DGR-3 843.92	Gull River	10.1	2.02	1.23	3.78	0.04	0.09	15.1	0.06	1.14	0.02
DGR-3 852.18	Shadow Lake	55.2	7.81	9.41	37.2	0.23	0.18	110	0.53	1.34	0.04
DGR-3 856.06	Cambrian	13.7	1.80	9.85	6.84	0.10	b.d.	31.9	0.13	0.35	b.d.

*Indicates that a soluble salt was identified in the sample during mineralogical investigations (see section 3.2, Table 5).
b.d indicates concentration of ion was below detection in aqueous extract solution.

Table 31: Borehole DGR-4: Concentration of ions in meq/kg_{rock} calculated from the chemical compositions of aqueous extract solutions. Reported values are the average of two replicates.

Sample ID ¹ (NWMO)	Formation	Na ⁺	K ⁺	Mg ²⁺	Ca ²⁺	Sr ²⁺	F ⁻	Cl ⁻	Br ⁻	SO ₄ ²⁻	NO ₃ ⁻
		(meq/kg _r)	(meq/kg _r)	(meq/kg _r)	(meq/kg _r)	(meq/kg _r)	(meq/kg _r)	(meq/kg _r)	(meq/kg _r)	(meq/kg _r)	(meq/kg _r)
DGR-4 154.60	Bass Islands	1.01	0.39	9.17	0.71	b.d.	b.d.	5.91	0.04	0.86	b.d.
DGR-4 189.16*	Salina - F Unit	12.7	2.42	2.82	31.9	0.09	0.27	12.4	0.02	39.1	b.d.
DGR-4 229.32*	Salina - E Unit	12.7	2.69	3.55	32.1	0.10	0.30	7.19	0.01	40.6	b.d.
DGR-4 322.68*	A2 Evaporite	2.50	0.17	0.20	42.4	0.38	0.02	3.04	0.004	38.9	b.d.
DGR-4 332.13	Salina A1 Unit	12.8	1.16	0.32	0.98	b.d.	0.14	11.8	0.02	2.67	b.d.
DGR-4 422.21	Cabot Head	87.4	22.3	35.1	134	1.62	0.17	266	1.47	1.09	b.d.
DGR-4 472.78*	Queenston	55.2	14.9	17.4	99.3	0.73	0.14	157	0.89	19.9	b.d.
DGR-4 520.42	Georgian Bay	30.7	7.61	8.16	39.5	0.25	b.d.	81.2	0.41	8.33	b.d.
DGR-4 662.83	Cobourg – LM	17.7	4.50	3.43	12.2	0.16	b.d.	32.4	0.16	0.82	b.d.
DGR-4 665.41	Cobourg – LM	15.8	4.05	4.24	11.5	0.15	b.d.	38.4	0.19	0.73	b.d.
DGR-4 672.85	Cobourg – LM	9.65	2.67	2.37	7.11	0.10	b.d.	19.7	0.09	0.72	b.d.
DGR-4 717.12[^]	Sherman Fall	21.0	5.09	2.54	10.3	0.10	b.d.	33.3	0.15	0.50	b.d.
DGR-4 730.07	Kirkfield	27.9	6.38	3.15	14.3	0.16	b.d.	51.6	0.23	0.72	b.d.
DGR-4 841.06	Shadow Lake	44.4	4.28	14.9	34.7	0.25	0.14	89.4	0.40	0.75	b.d.
DGR-4 847.48*	Cambrian	18.3	0.71	14.0	10.6	0.13	b.d.	37.8	0.18	0.35	b.d.

*Indicates that a soluble salt was identified in the sample during mineralogical investigations (see section 3.2, Table 6).

b.d indicates concentration of ion was below detection in aqueous extract solution.

[^]Average of three replicates.

Table 32: Borehole DGR-3: Saturation indices (SI) calculated for aqueous extraction solutions. Shading indicates SI values ≈ 0.0 .

Sample ID	Formation	Anhydrite	Aragonite	Calcite	Celestite	CO ₂ (g)	Dolomite	Gypsum	Halite	Strontianite
DGR-3 198.72a	Salina – F Unit	-0.23	0.67	0.82	-0.32	-3.66	0.87	0.01	-5.08	-0.74
DGR-3 198.72b	Salina – F Unit	-0.23	0.71	0.86	-0.36	-3.73	0.95	0.00	-5.08	-0.73
DGR-3 208.41a	Salina - F Unit	-0.27	0.69	0.84	-0.53	-3.92	0.75	-0.03	-4.74	-0.88
DGR-3 208.41b	Salina - F Unit	-0.24	0.72	0.87	-0.47	-3.92	0.82	0.00	-4.69	-0.83
DGR-3 248.71a	Salina – E Unit	-0.21	1.00	1.15	-0.42	-4.05	1.38	0.03	-4.24	-0.53
DGR-3 248.71b	Salina – E Unit	-0.20	1.04	1.19	-0.40	-4.07	1.44	0.03	-4.25	-0.47
DGR-3 270.06a	Salina - C Unit	-0.19	0.49	0.63	-0.18	-4.09	0.19	0.04	-2.97	-0.82
DGR-3 270.06b	Salina - C Unit	-0.19	0.52	0.67	-0.18	-4.16	0.26	0.04	-2.96	-0.79
DGR-3 289.36a	Salina – B Unit	-0.15	0.82	0.97	-0.42	-3.88	1.07	0.08	-3.38	-0.77
DGR-3 289.36b	Salina – B Unit	-0.17	0.85	1.00	-0.44	-3.94	1.16	0.07	-3.39	-0.75
DGR-3 312.53a	Salina - A2 Unit	-0.74	-0.65	-0.51	0.10	-2.56	-1.14	-0.50	-3.71	-1.13
DGR-3 312.53b	Salina - A2 Unit	-0.72	0.28	0.43	0.10	-3.52	0.72	-0.48	-3.77	-0.22
DGR-3 335.22a	Salina – A2 Evaporite	-0.11	0.85	1.00	0.21	-4.66	0.11	0.13	-6.92	-0.15
DGR-3 335.22b	Salina – A2 Evaporite	-0.11	0.91	1.06	0.14	-4.79	0.20	0.13	-6.97	-0.15
DGR-3 344.06a	Salina -A1 Unit	-2.38	-0.91	-0.76	-	-2.95	-2.03	-2.14	-5.96	-
DGR-3 344.06b	Salina -A1 Unit	-2.44	0.14	0.29	-	-4.13	0.22	-2.20	-5.96	-
DGR-3 380.88a	A1 Evaporite	0.08	0.94	1.09	-	-4.42	-0.08	0.32	-6.63	-
DGR-3 380.88b	A1 Evaporite	0.03	1.01	1.16	-	-4.73	0.12	0.26	-6.62	-
DGR-3 391.34a	Guelph	-0.37	0.00	0.15	-0.92	-3.02	-0.43	-0.15	-2.48	-1.87
DGR-3 391.34b	Guelph	-0.38	1.05	1.20	-0.91	-4.39	1.68	-0.16	-2.49	-0.80
DGR-3 435.62a	Cabot Head	-2.25	0.55	0.70	-1.91	-3.65	0.83	-2.02	-3.65	-0.43
DGR-3 435.62b	Cabot Head	-2.32	0.45	0.60	-1.95	-3.60	0.66	-2.09	-3.68	-0.49
DGR-3 453.41a	Manitoulin	-2.23	0.31	0.46	-1.91	-3.93	0.56	-2.00	-4.64	-0.68
DGR-3 453.41b	Manitoulin	-2.25	0.23	0.38	-1.92	-3.83	0.39	-2.02	-4.68	-0.75
DGR-3 468.76a	Queenston	-2.05	0.18	0.33	-1.83	-3.45	0.04	-1.82	-3.80	-0.91
DGR-3 468.76b	Queenston	-2.09	0.16	0.31	-1.79	-3.48	0.06	-1.86	-3.86	-0.85
DGR-3 484.58a	Queenston	-0.28	0.39	0.53	-0.11	-3.60	0.32	-0.05	-4.01	-0.76
DGR-3 484.58b	Queenston	-0.29	0.36	0.50	-0.08	-3.61	0.30	-0.06	-4.05	-0.74
DGR-3 502.55a	Queenston	-0.81	0.39	0.54	-0.50	-3.70	0.42	-0.58	-4.65	-0.61
DGR-3 502.55b	Queenston	-0.82	0.44	0.59	-0.54	-3.78	0.52	-0.59	-4.66	-0.60
DGR-3 531.65a	Georgian Bay	-0.93	0.31	0.46	-0.65	-3.54	0.31	-0.70	-4.33	-0.72
DGR-3 531.65b	Georgian Bay	-0.94	0.35	0.50	-0.68	-3.58	0.39	-0.70	-4.32	-0.70
DGR-3 581.47a	Georgian Bay	-2.39	0.20	0.35	-2.03	-3.46	-0.11	-2.16	-3.74	-0.75
DGR-3 581.47b	Georgian Bay	-2.40	0.24	0.39	-2.01	-3.54	-0.02	-2.17	-3.75	-0.68

Shading indicates aqueous extract solutions that are predicated to be just at saturation with respect to the mineral phase (within ± 0.15 SI units). Solutions with $SI \geq +0.15$ are considered as supersaturated with respect to the mineral phase and those with $SI \leq -0.15$ are considered as undersaturated.

Table 32 (Cont'd.): Borehole DGR-3: Saturation indices (SI) calculated for aqueous extraction solutions. Shading indicates SI values ≈ 0.0 .

Sample ID	Formation	Anhydrite	Aragonite	Calcite	Celestite	CO ₂ (g)	Dolomite	Gypsum	Halite	Strontianite
DGR-3 621.63a	Blue Mountain	-2.08	0.24	0.38	-1.71	-3.47	-0.04	-1.85	-3.75	-0.71
DGR-3 621.63b	Blue Mountain	-2.07	0.30	0.45	-1.68	-3.54	0.09	-1.84	-3.75	-0.63
DGR-3 646.29a	Blue Mountain	-1.92	0.20	0.35	-1.57	-3.46	-0.13	-1.69	-3.88	-0.77
DGR-3 646.29b	Blue Mountain	-1.92	0.17	0.32	-1.56	-3.44	-0.21	-1.68	-3.87	-0.79
DGR-3 665.29a	Cobourg – CM	-2.14	0.27	0.41	-1.58	-3.74	0.49	-1.90	-5.43	-0.50
DGR-3 665.29b	Cobourg – CM	-2.13	0.28	0.43	-1.54	-3.69	0.53	-1.90	-5.44	-0.44
DGR-3 676.21a	Cobourg – LM	-2.14	0.25	0.39	-1.69	-3.61	0.37	-1.90	-4.43	-0.62
DGR-3 676.21b	Cobourg – LM	-2.16	0.13	0.28	-1.70	-3.49	0.13	-1.93	-4.43	-0.72
DGR-3 678.92a	Cobourg – LM	-2.13	0.03	0.18	-1.71	-3.55	-0.07	-1.90	-5.39	-0.86
DGR-3 678.92b	Cobourg – LM	-2.14	0.06	0.21	-1.75	-3.59	-0.01	-1.90	-5.39	-0.86
DGR-3 685.52a	Cobourg – LM	-2.12	0.13	0.27	-1.75	-3.58	0.10	-1.88	-5.15	-0.82
DGR-3 685.52b	Cobourg – LM	-2.15	0.17	0.32	-1.77	-3.64	0.18	-1.92	-5.14	-0.76
DGR-3 690.12a	Cobourg – LM	-2.20	0.04	0.18	-1.71	-3.74	-0.09	-1.97	-5.35	-0.82
DGR-3 690.12b	Cobourg – LM	-2.24	0.05	0.20	-1.78	-3.78	-0.05	-2.00	-5.38	-0.80
DGR-3 692.82a	Cobourg – LM	-2.22	0.19	0.33	-1.74	-3.80	0.20	-1.99	-4.85	-0.64
DGR-3 692.82b	Cobourg – LM	-2.18	0.22	0.37	-1.70	-3.81	0.28	-1.94	-4.79	-0.62
DGR-3 697.94a	Cobourg – LM	-2.27	0.12	0.27	-1.90	-3.72	0.08	-2.03	-5.04	-0.83
DGR-3 697.94b	Cobourg – LM	-2.21	0.14	0.28	-1.84	-3.74	0.11	-1.97	-5.02	-0.82
DGR-3 710.38a	Sherman Fall	-2.49	0.02	0.17	-2.08	-3.96	-0.15	-2.25	-5.77	-0.89
DGR-3 710.38b	Sherman Fall	-2.49	-0.03	0.12	-2.04	-3.95	-0.22	-2.25	-5.79	-0.90
DGR-3 725.57a	Sherman Fall	-2.18	0.23	0.38	-1.82	-3.71	0.32	-1.95	-4.61	-0.72
DGR-3 725.57b	Sherman Fall	-2.19	0.23	0.37	-1.84	-3.71	0.29	-1.95	-4.62	-0.74
DGR-3 744.27a	Kirkfield	-2.23	0.19	0.34	-1.88	-3.64	0.15	-1.99	-4.68	-0.78
DGR-3 744.27b	Kirkfield	-2.23	0.16	0.31	-1.90	-3.62	0.10	-1.99	-4.68	-0.82
DGR-3 761.56a	Kirkfield	-1.87	-0.29	-0.15	-	-3.82	-0.91	-1.63	-6.53	-
DGR-3 761.56b	Kirkfield	-1.88	-0.19	-0.04	-	-3.91	-0.69	-1.64	-6.52	-
DGR-3 777.33a	Coboconk	-2.22	0.21	0.36	-1.92	-3.95	0.29	-1.98	-5.55	-0.81
DGR-3 777.33b	Coboconk	-2.21	0.12	0.27	-1.82	-3.83	0.10	-1.97	-5.53	-0.80
DGR-3 807.43a	Gull River	-2.21	-0.14	0.01	-1.91	-3.80	-0.43	-1.98	-5.57	-1.15
DGR-3 807.43b	Gull River	-2.17	-0.09	0.06	-1.82	-3.86	-0.32	-1.93	-5.71	-1.06
DGR-3 843.92a	Gull River	-2.17	-0.15	0.00	-1.81	-3.44	-0.43	-1.94	-5.51	-1.10
DGR-3 843.92b	Gull River	-2.19	-0.01	0.13	-1.87	-3.70	-0.14	-1.95	-5.51	-1.01
DGR-3 852.18a	Shadow Lake	-1.69	-0.22	-0.07	-1.62	-3.21	-0.65	-1.46	-4.02	-1.46
DGR-3 852.18b	Shadow Lake	-1.69	-0.17	-0.02	-1.62	-3.27	-0.56	-1.45	-4.03	-1.42
DGR-3 856.06a	Cambrian	-2.61	0.63	0.77	-2.17	-4.40	1.79	-2.37	-5.09	-0.26
DGR-3 856.06b	Cambrian	-2.71	0.62	0.77	-2.29	-4.39	1.77	-2.47	-5.09	-0.27

Shading indicates aqueous extract solutions that are predicated to be just at saturation with respect to the mineral phase (within ± 0.15 SI units). Solutions with $SI \geq +0.15$ are considered as supersaturated with respect to the mineral phase and those with $SI \leq -0.15$ are considered as undersaturated.

Table 33: Borehole DGR-4. Saturation indices (SI) calculated for aqueous extraction solutions. Shading indicates SI values ≈ 0.0 .

Sample ID	Formation	Anhydrite	Aragonite	Calcite	Celestite	CO ₂ (g)	Dolomite	Gypsum	Halite	Strontianite
DGR-4 154.60a	Bass Islands	-3.18	1.03	1.18	-	-4.41	3.52	-2.94	-6.90	-
DGR-4 154.60b	Bass Islands	-3.08	0.89	1.04	-	-4.32	3.35	-2.85	-6.90	-
DGR-4 189.16a	Salina F Unit	-0.21	0.93	1.08	-0.49	-4.03	1.16	0.03	-5.58	-0.67
DGR-4 189.16b	Salina F Unit	-0.21	0.97	1.11	-0.43	-4.07	1.23	0.02	-5.57	-0.56
DGR-4 229.32a	Salina – E Unit	-0.20	0.99	1.14	-0.41	-4.21	1.37	0.04	-5.78	-0.53
DGR-4 229.32b	Salina – E Unit	-0.20	0.93	1.07	-0.44	-4.15	1.26	0.04	-5.83	-0.63
DGR-4 322.68a	A2 Evaporite	-0.09	0.67	0.82	0.14	-4.41	-0.60	0.15	-6.89	-0.41
DGR-4 322.68b	A2 Evaporite	-0.09	0.61	0.75	0.15	-4.35	-0.78	0.14	-6.87	-0.46
DGR-4 332.13a	Salina A1 Unit	-2.37	0.18	0.33	-	-3.99	0.23	-2.13	-5.50	-
DGR-4 332.13b	Salina A1 Unit	-2.35	0.17	0.32	-	-3.93	0.23	-2.11	-5.51	-
DGR-4 422.21a	Cabot Head	-1.57	0.44	0.59	-1.22	-3.84	0.69	-1.34	-3.50	-0.53
DGR-4 422.21b	Cabot Head	1.63	0.36	0.51	-1.25	-3.83	0.54	-1.40	-3.52	-0.58
DGR-4 472.78a	Queenston	-0.35	0.62	0.77	-0.21	-3.70	0.85	-0.11	-3.92	-0.56
DGR-4 472.78b	Queenston	-0.34	0.54	0.69	-0.19	-3.60	0.73	-0.11	-3.91	-0.62
DGR-4 520.42a	Georgian Bay	-0.86	0.37	0.52	-0.78	-3.54	0.45	-0.63	-4.39	-0.87
DGR-4 520.42b	Georgian Bay	-0.82	0.38	0.53	-0.72	-3.58	0.44	-0.59	-4.41	-0.83
DGR-4 662.83a	Cobourg – LM	-2.04	0.49	0.64	-1.67	-3.98	0.80	-1.80	-4.98	-0.45
DGR-4 662.83b	Cobourg – LM	-2.04	0.42	0.57	-1.64	-3.91	0.67	-1.80	-4.97	-0.49
DGR-4 665.41a	Cobourg – LM	-2.09	0.22	0.36	-1.68	-3.77	0.37	-1.86	-4.96	-0.68
DGR-4 665.41b	Cobourg – LM	-2.15	0.22	0.37	-1.78	-3.80	0.38	-1.91	-4.95	-0.72
DGR-4 672.85a	Cobourg – LM	-2.19	0.44	0.59	-1.75	-3.98	0.77	-1.96	-5.43	-0.43
DGR-4 672.85b	Cobourg – LM	-2.19	0.43	0.57	-1.78	-3.96	0.75	-1.95	-5.42	-0.48
DGR-4 717.12a	Sherman Fall	-2.31	0.48	0.63	-2.03	-4.12	0.70	-2.08	-4.92	-0.55
DGR-4 717.12b	Sherman Fall	-2.31	0.50	0.65	-2.05	-4.13	0.79	-2.07	-4.86	-0.56
DGR-4 730.07a	Kirkfield	-2.08	0.43	0.58	-1.76	-4.14	0.57	-1.85	-4.59	-0.56
DGR-4 730.07b	Kirkfield	-2.11	0.43	0.58	-1.79	-4.09	0.58	-1.88	-4.60	-0.57
DGR-4 841.06a	Shadow Lake	-1.95	0.85	1.00	-1.87	-3.93	1.70	-1.71	-4.20	-0.39
DGR-4 841.06b	Shadow Lake	-1.96	0.87	1.02	-1.77	-3.99	1.77	-1.73	-4.21	-0.26
DGR-4 847.48a	Cambrian	-2.56	0.59	0.73	-2.17	-4.43	1.66	-2.32	-4.90	-0.34
DGR-4 847.48b	Cambrian	-2.55	0.60	0.75	-2.18	-4.47	1.69	-2.31	-4.91	-0.35

Shading indicates aqueous extract solutions that are predicated to be just at saturation with respect to the mineral phase (within ± 0.15 SI units). Solutions with $SI \geq +0.15$ are considered as supersaturated with respect to the mineral phase and those with $SI \leq -0.15$ are considered as undersaturated.

6.1 Evidence for mineral dissolution

6.1.1 Halite

The possible influence of halite dissolution in the aqueous extracts is first evaluated by examining the concentrations of Na^+ and Cl^- in $\text{meq/kg}_{\text{rock}}$ in Figure 31. If the primary source of these ions was halite dissolution, a 1:1 ratio is expected for Na:Cl. However, it is noted that on the basis of this ratio alone, it is not possible to distinguish whether halite dissolution occurred during aqueous extraction or whether it reflects the in situ evolution of the porewaters.

In several samples from both boreholes, the concentrations of Na^+ and Cl^- are very close to a 1:1 ratio. These samples are from the F, E, C, B, A1 and A2 units of the Salina Formation. Mineralogical investigations were conducted on samples from the Salina C Unit and the Guelph Formation in DGR-3, which have the highest Cl^- concentrations. Halite was identified in both samples by XRD and SEM-EDS analyses (DGR-3 270.06 and DGR-3 391.34, Table 1, section 3.1), although it is notable that sample DGR-3 391.34 has higher Cl^- concentrations relative to Na^+ than expected if halite dissolution was the only source of these ions. In addition, there could be contributions of Cl^- from the porewater, balanced by Ca^{2+} , consistent with the observed extracted Ca^{2+} concentration of 63 $\text{meq/kg}_{\text{rock}}$ in this sample. Halite was not observed in mineralogical analyses conducted on samples from the Salina F, E and B units. However, to produce the Cl^- concentrations observed in these samples, less than 1.0 wt.% halite would be required, which is below the detection limits of the XRD technique and may also be difficult to detect using SEM-EDS (e.g., if it occurs as discreet veinlets with a heterogeneous distribution throughout the rock mass and not present in the particular sample(s) examined). All aqueous extract solutions from both DGR-3 and DGR-4 are undersaturated with respect to halite, notably even in those from sample DGR-3 391.34 (Guelph Formation), in which halite was identified in veins. This suggests that the quantity of halite present in the aliquot used in the extraction was insufficient to reach equilibrium conditions. This is not surprising considering that for rocks with between 1 and 10% porosity, the dilution factors in a 1:1 solid:liquid extraction are 100 and 10, respectively. Therefore, it is not expected that halite saturation will be reached when only small quantities of this mineral are present.

For the remainder of samples, there also appears to be a relatively linear relationship between Na^+ and Cl^- at a lower Na/Cl ratio (Figure 31). This trend is also seen in Figure 32, where the Na/Cl ratio (on a molar basis) is plotted as a function of depth for all samples from DGR-2, DGR-3 and DGR-4. In the upper portion of the sedimentary sequence from the Salina F Unit to the Cabot Head Formation, the Na/Cl ratios of the samples range between 0.6 to a high of 1.8 in the Salina E Unit. Several samples within the units of the Salina Formation have a Na/Cl ratio close to 1.0, as discussed above. From the Cabot Head Formation down through the Sherman Fall Formation, the Na/Cl ratio observed in the aqueous extracts is relatively constant at a ratio between 0.4 and 0.5. The exceptions are two samples from DGR-2 (DGR-2 523.08 and DGR-3 562.92). Halite was positively identified in sample DGR-2 523.08 (Georgian Bay Formation) by SEM analysis, whereas an additional source of Na^+ , possibly a sodium sulphate mineral was proposed for DGR-2 562.92 (Koroleva et al. 2009). From the Kirkfield Formation, there is an apparent increase in the Na/Cl ratio with values between approximately 0.5 and 0.7 that persists through the Shadow Lake Formation. Within the Cambrian and Precambrian, the Na/Cl ratio is between 0.4 and 0.5.

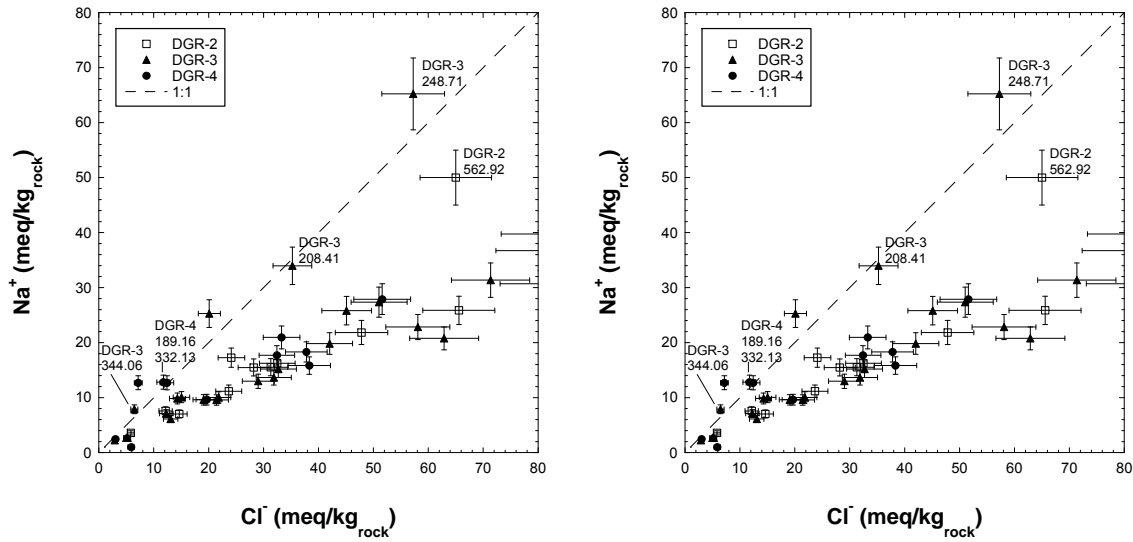


Figure 31: Concentrations in milliequivalents of Na⁺ and Cl⁻ extracted per kilogram of dry rock at a S:L ratio of 1:1. Error bars indicate analytical uncertainty in concentrations measured in aqueous extract solutions (max. ±10%). In several samples, the Na:Cl ratio is 1:1, within the analytical uncertainty, suggesting halite dissolution (in situ or during the extraction) could be the source of these ions.

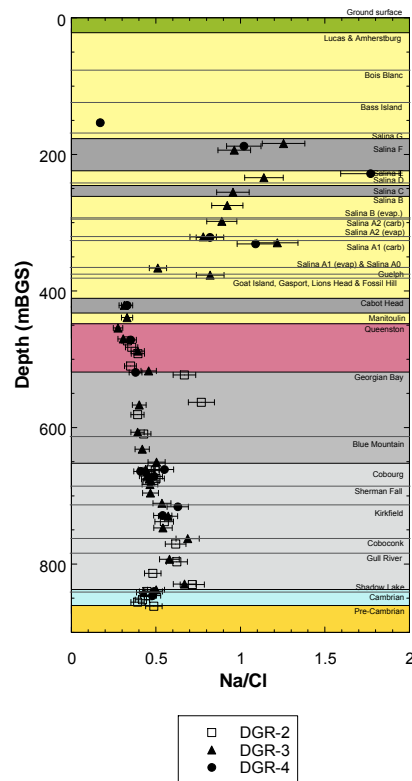


Figure 32: Na/Cl ratio (mol/mol) for samples from boreholes DGR-2, DGR-3 and DGR-4 plotted versus depth in meters (relative to DGR-1/2). Error bars indicate the maximum analytical uncertainty in the measured ion concentrations in the aqueous extracts (±10%).

The possibility of Cl^- addition from dissolution of Cl^- -bearing salts can also be investigated by comparing the Cl^- and Br^- concentrations. In saline groundwaters, Br^- is generally considered to be a conservative tracer of the evolution of waters (e.g. Kharaka and Hanor, 2005). The concentration of Br^- in $\text{meq/kg}_{\text{rock}}$ is plotted versus Cl^- in for all aqueous extract solutions from DGR-2, -3 and -4 in Figure 33. For the majority of samples, there is a strong linear relationship between the concentrations of these ions. The exceptions include samples from the units of the Salina Formation which have Na/Cl ratios close to 1.0, suggesting that dissolution of halite may be the primary source of Cl^- in these samples, as discussed above. Two additional samples, including one from the Georgian Bay Formation (DGR-2 581.32) and one from the Cambrian (DGR-2 852.39) also show Cl^- concentrations that are slightly elevated, relative to Br^- . The agreement between the Br^- contents determined for sample DGR-2 581.32 based on extractions 4 different solid:liquid ratios was poor (Koroleva et al., 2009). This suggests that the analytical uncertainty in the Br^- concentrations determined for these samples may be higher than $\pm 10\%$.

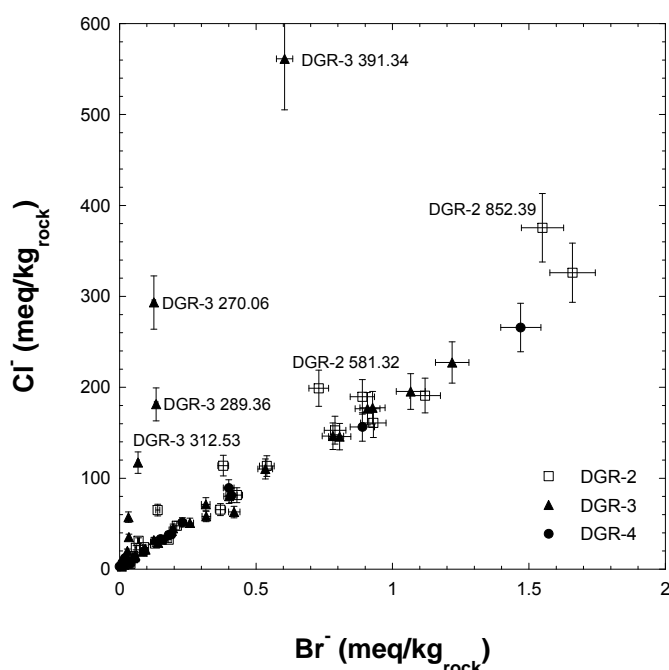


Figure 33: Concentrations in $\text{meq/kg}_{\text{rock}}$ of Br^- and Cl^- in aqueous extracts at a S:L ratio of 1:1. Data for DGR-2 samples is from Koroleva et al. (2009). Error bars indicate analytical uncertainty in Br^- and Cl^- concentrations (max. $\pm 10\%$) measured in aqueous extract solution.

The trends observed for Br^- and Cl^- can also be seen in Figure 34, where the Br/Cl ratio is plotted as function of depth for samples from the 3 boreholes. The highest Br/Cl ratio is observed in the Bass Island Formation (DGR-4 154.60) where the concentrations of both ions are low in the aqueous extract solution. The Br/Cl molar ratios are lowest in the upper part of the Salina Formation (F Unit) down through the A1 Evaporite and are close to or below the Br/Cl ratio of seawater ($\text{Br}/\text{Cl} = 1.54 \times 10^{-3}$). The Br/Cl ratio is relatively constant at $\approx 5.2 \times 10^{-3}$ through the Queenston, Georgian Bay and Blue Mountain formations. The Br/Cl ratio then decreases to 4.2×10^{-3} at the top of the Cobourg formation down through to the bottom of the Gull River Formation, below which the ratio increases again to values similar to those determined in the overlying shales. The scatter in the Br/Cl

ratio for samples from the Queenston, Georgian Bay and Blue Mountain formations in DGR-2 is much larger than that observed samples from the other two boreholes. The majority of samples from these formations in DGR-2 have lower Br/Cl ratios than observed in the other two boreholes. For sample DGR-2 523.08, the lower Br/Cl ratio is consistent with the identification of halite using SEM analysis (Koroleva et al. 2009). In the extractions conducted on DGR-2 samples, a reaction time of 48 hours was employed to establish equilibrium with respect to calcite, whereas for DGR-3 and -4 samples the extraction time was reduced to 10 minutes in an effort to reduce mineral-water reactions. Only one sample from DGR-2 (DGR-2 770.60, Coboconk Formation) has a higher Br/Cl ratio than observed in DGR-3 and DGR-4 samples within these same formations. One sample from the Manitoulin Formation in borehole DGR-3 (DGR-3 453.41) also has a similarly high Br/Cl ratio.

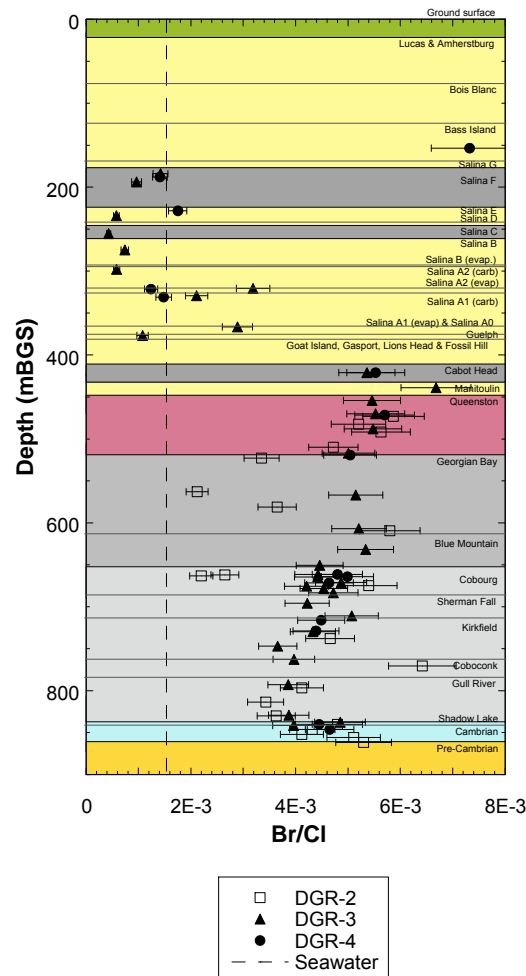


Figure 34: Br/Cl ratio (mol/mol) for samples from boreholes DGR-2, DGR-3 and DGR-4 plotted versus depth in meters. Error bars indicate analytical uncertainty in Cl⁻ concentrations of ±10%. Depths for samples from DGR-3 and DGR-4 are corrected relative to DGR-1/2. The Br/Cl ratio of seawater is also shown (dashed line).

In summary, based on Na/Cl ratios close to 1.0 in the aqueous extract solutions, dissolution of halite could be the predominant source of these two ions in DGR-3 and DGR-4 samples from within several units of the Salina Formation (Salina F, E, C, B, A2 and A1 Units). The presence of halite was

confirmed in both the Salina C Unit and the Guelph Formation during mineralogical investigations. Halite was positively identified in one sample from each of the Georgian Bay and Gull River formations in borehole DGR-2 by Herwegh and Mazurek (2008).

6.1.2 Sulphate minerals

In Figure 35, the concentrations of sulphate in $\text{meq/kg}_{\text{rock}}$ determined for samples from boreholes DGR-2, -3 and -4 are plotted versus depth. From a low sulphate concentration of $< 1 \text{ meq/kg}_{\text{rock}}$ in the Bass Islands Formation, much higher concentrations between 30 and 60 $\text{meq/kg}_{\text{rock}}$ are observed through the units of the Salina Formation and in the Guelph Formation. The exceptions are two samples from the Salina A1 carbonate unit with low sulphate (max. 2 $\text{meq/kg}_{\text{rock}}$). In the lower part of the sedimentary sequence from the Cabot Head through the Cambrian, sulphate concentrations are between 1 and 3 $\text{meq/kg}_{\text{rock}}$, with the exception of several samples within the Queenston Formation and the top of the Georgian Bay Formation with sulphate concentrations between approximately 6 and 25 $\text{meq/kg}_{\text{rock}}$. Two samples from DGR-2 (DGR-2 523.08 and DGR-2 562.92) have even higher sulphate concentrations of 37 and 52 $\text{meq/kg}_{\text{rock}}$, respectively.

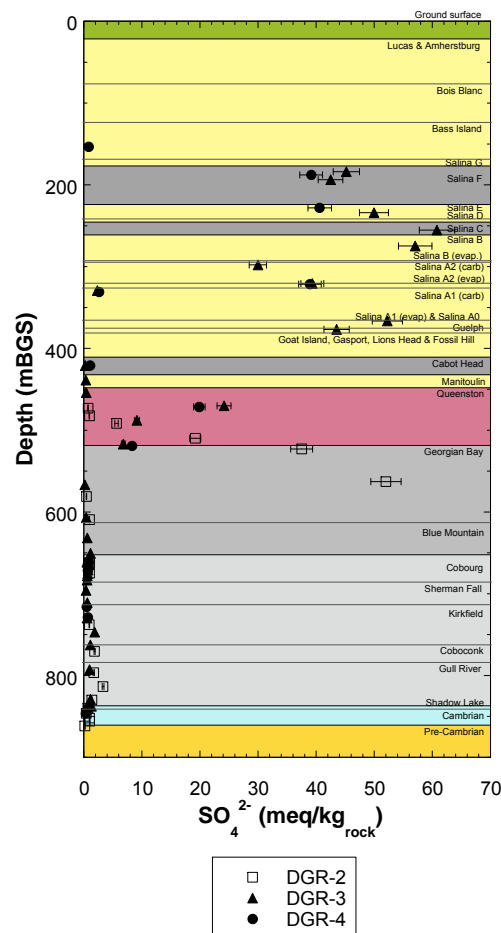


Figure 35: Sulphate concentration in $\text{meq/kg}_{\text{rock}}$ plotted as a function of depth as determined for samples from DGR-3, DGR-4 (solid symbols) and DGR-2 (open squares) by aqueous extraction at a S:L ratio of 1:1. Data for DGR-2 samples is from Koroleva et al. (2009).

The concentrations of sulphate in $\text{meq/kg}_{\text{rock}}$ are plotted versus Ca^{2+} in Figure 36. The molar ratio $\text{Ca}:\text{SO}_4$ of 1:1 expected if these ions are primarily from the dissolution of anhydrite or gypsum is also plotted (dashed line). Samples from both DGR-3 and DGR-4 that plot on or close to this line are from within the units of the Salina Formation. This is consistent with the identification of gypsum or anhydrite in all samples from within these units for which mineralogical investigations were conducted (see Table 5 and Table 6, section 3.1). The one sample from DGR-2 which has a $\text{Ca}:\text{SO}_4$ ratio near 1 is DGR-2 562.92 from the Georgian Bay Formation (Figure 36). Based on the results of aqueous extractions conducted at different solid:liquid ratios, Koroleva et al. (2009) concluded that the leached sulphate in this sample must be highly disturbed by mineral dissolution and/or sulphide oxidation prior to laboratory treatment. The $\text{Ca}:\text{SO}_4$ ratio near one observed in Figure 36 further supports the interpretation that dissolution of anhydrite or gypsum is likely the source of the high sulphate and calcium concentrations in this sample. As discussed by Koroleva et al. (2009), the fact that sulphate minerals were not identified in this sample by XRD and microscopic techniques likely reflects the small quantity (0.2 wt.%) of calcium sulphate that would need to be dissolved to reach gypsum saturation, which is well below the detection limit of these techniques.

The other two samples specifically labelled in Figure 36 are from the Guelph (DGR-3 391.34) and the Georgian Bay (DGR-2 523.08) formations. Although the SO_4^{2-} concentrations of these samples are high ($\approx 40 \text{ meq/kg}_{\text{rock}}$) and similar to those determined for samples the Salina Formation, the calcium concentrations determined for these two samples are higher relative to sulphate than expected from gypsum or anhydrite dissolution alone. This could suggest Ca^{2+} contributions from both porewater and calcium-sulphate mineral dissolution. The presence of halite was confirmed in both samples using XRD and/or SEM/EDS analyses; neither anhydrite nor gypsum was observed.

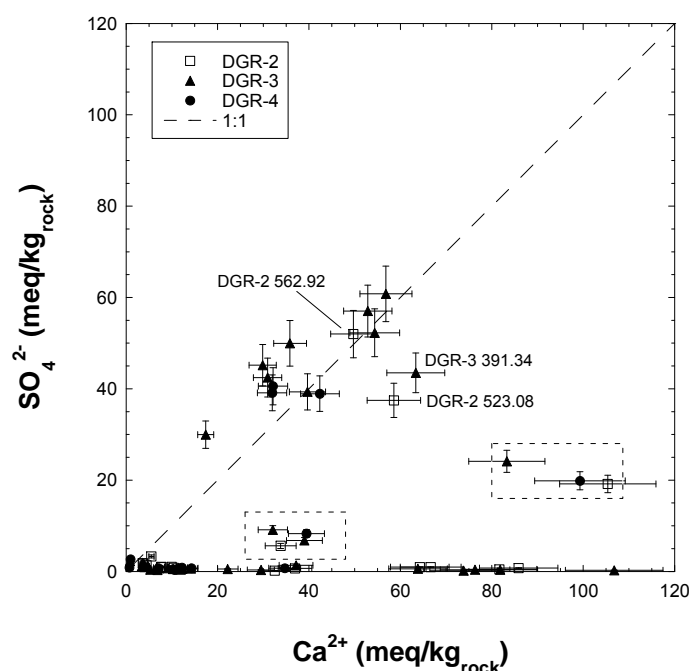


Figure 36: Concentration of SO_4^{2-} versus Ca^{2+} in $\text{meq/kg}_{\text{rock}}$ determined by aqueous extraction at a S:L ratio of 1:1. Data for DGR-2 samples is from Koroleva et al. (2009). Error bars indicate analytical uncertainty (max. $\pm 10\%$).

Samples from both the Queenston and Georgian Bay formations that show elevated sulphate (5 to 37 meq/kg_{rock}) in the depth profile (Figure 35) fall into two groups on the sulphate versus calcium plot (Figure 36); these are indicated in the dashed rectangles. Of these, the group with higher concentrations of both ions includes three samples from the Queenston Formation (DGR-2 510.12, DGR-3 484.58 and DGR-4 472.78). In all three samples, anhydrite was identified during mineralogical investigations (in sample DGR-2 510.12, anhydrite cement was identified by Koroleva et al. 2009). The second group with lower sulphate concentrations includes two samples from the Queenston Formation and two from the Georgian Bay Formation. Anhydrite was identified in one of these samples within the Georgian Bay Formation (DGR-3 531.65). In samples from both groups, it is likely that the calcium and sulphate concentrations measured in the aqueous extract solutions include contributions from the dissolution of sulphate minerals, in addition to porewater.

Extract solutions for all samples from the Salina Formation, from the F Unit down through the A1 Evaporite in DGR-3 and DGR-4 are all calculated to be at or slightly above saturation with respect to gypsum, with the exception of those from samples of the Salina A2 and A1 carbonate units, which are predicted to be undersaturated with respect to gypsum. This is consistent with the identification of gypsum in the F, E, C and B units of the Salina Formation and anhydrite in Salina A1 Evaporite, and both gypsum and anhydrite in the Salina A2 Evaporite. Aqueous extracts for two samples from the Queenston Formation (DGR-3 484.58 and DGR-4 472.78) are also predicted to be at saturation with respect to gypsum. This is consistent with the identification of anhydrite-celestite nodules in DGR-3 484.58 and anhydrite in sample DGR-4 472.78. For samples from the Salina A1 and A2 evaporites that consisting of primarily of massive anhydrite, aqueous extract solutions from both boreholes are predicted to be at saturation with respect to anhydrite and slightly supersaturated with respect to gypsum.

Several extract solutions are predicted to at or very close to saturation with respect to celestite, including one sample from the Salina A2 Unit (DGR-3 312.53), two samples from the Salina A2 Evaporite (DGR-3 335.22 and DGR-4 322.68) (Salina A2 Evaporite) and two samples from the Queenston Formation (DGR-3 484.58 and DGR-4 472.78). Celestite was observed to occur in nodules together with anhydrite in sample DGR-3 484.58.

In summary, the ratio close to 1.0 observed for Ca:SO₄ (expressed in meq/kg_{rock}) in samples from several units within the Salina Formation (Salina F, E, C, B, A1 Evaporite and A2 Evaporite units) suggests that these ions are predominantly from dissolution of gypsum or anhydrite. Gypsum was predicted to be at or above saturation in the aqueous extract solutions of samples from these formations, and gypsum or gypsum and anhydrite were identified in these units during mineralogical investigations. Elevated sulphate concentrations measured in the aqueous extracts of samples from the Queenston and Georgian Bay formations are also consistent with the identification of anhydrite and celestite in the Queenston Formation and anhydrite in the samples from the Georgian Bay Formation. With the exception of samples from these two formations, the extracted SO₄²⁻ concentrations are very low (< 3 meq/kg_{rock}) from the Cabot Head Formation down through to the Precambrian basement.

6.1.3 Carbonate minerals

In the previous section, specific samples were identified in which the concentration of Ca²⁺ and SO₄²⁻ are likely primarily from the dissolution of gypsum and anhydrite. Other minerals that may contribute to the dissolved concentrations of calcium and magnesium include calcite and dolomite. In Figure 37, the concentrations of magnesium are plotted versus calcium in units of meq/kg_{rock}. The activity Ca/Mg ratio at equilibrium with calcite and dolomite (approx. 1.34) is also shown as a dashed line (in this plot, it assumed that in the relatively dilute extract solutions, activities ≈ concentrations). Koroleva et al. (2009) observed that for samples from DGR-2, the ratio of Ca/Mg ob-

served is close to that expected at calcite-dolomite equilibrium at calcium concentrations below 10 mmol/kg_{rock} (or 20 meq/kg_{rock}). This suggests that for these samples, the Ca²⁺ and Mg²⁺ measured in the aqueous extract solutions are primarily from calcite-dolomite dissolution. A reaction time of 48 hours was used in the aqueous extractions conducted on DGR-2 samples in order to attain equilibrium with respect to calcite. Much longer reaction times of 7 days have been suggested for attainment of dolomite equilibrium (Bradbury and Baeyens, 1998).

A different approach was used for aqueous extractions on DGR-3 and DGR-4 samples; in an attempt to minimize dissolution of mineral phases, a short extraction time of 10 minutes was applied to samples from DGR-3 and DGR-4. In the aqueous extracts for samples from both these boreholes, the Ca/Mg activity ratio is lower than that expected at calcite-dolomite equilibrium, even at low calcium concentrations. This likely reflects the fact that the shorter reaction time of 10 minutes used for these extractions is insufficient to reach either calcite or dolomite equilibrium. In experiments conducted on DGR-2 samples by Koroleva et al. (2009) at multiple solid:liquid ratios, all extract solutions showed a linear trend in Mg²⁺ concentrations, passing through the origin. This suggests that contributions of Mg²⁺ to the aqueous extract solutions by cation exchange processes were negligible for these samples.

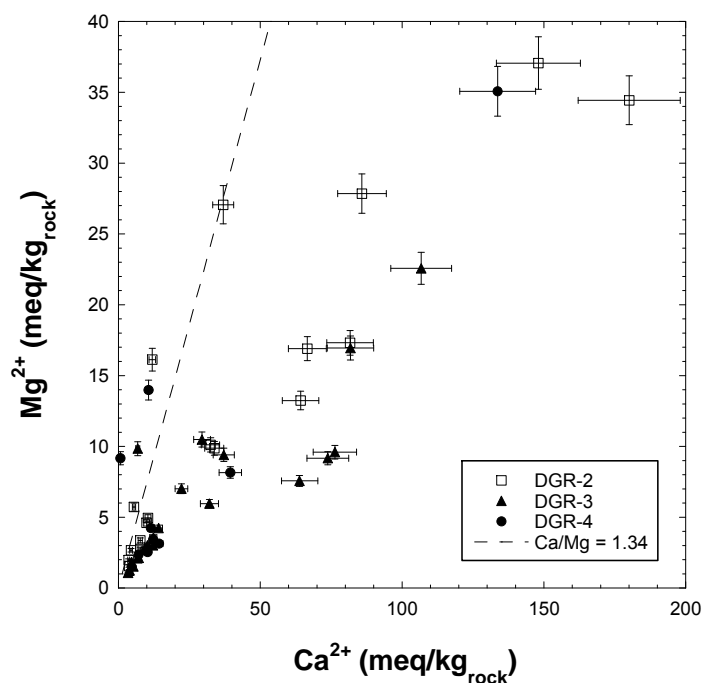


Figure 37: Concentrations of Mg²⁺ versus Ca²⁺ in extract solutions per kg rock for experiments conducted at a S:L ratio of 1:1. The dashed line represents the Ca/Mg activity ratio at equilibrium with both calcite and dolomite (1.34).

The majority of the extract solutions are predicted to be above saturation with respect to calcite. The exceptions are one replicate from each of the Salina A2 and A1 units (DGR-3 312.53a, DGR-3 344.06a), which are predicted to be below saturation with respect to calcite and several samples from DGR-3 that are just at saturation with respect to calcite (includes two samples from the Gull River and one sample from each of Sherman Fall, Kirkfield and Shadow Lake formations). The

majority of aqueous extract solutions from DGR-3 are also predicted to be at or above saturation with respect to dolomite. Exceptions are one sample from each of the Kirkfield, Gull River and Shadow Lake formations. In DGR-4, all aqueous extract solutions are predicted to be oversaturated with respect to dolomite, with the exception of one sample from the A2 Evaporite (DGR-4 322.68).

The oversaturation with respect to calcite predicted in the aqueous extract solutions from both DGR-3 and DGR-4 was also observed in DGR-2 samples. For the DGR-2 samples, it was hypothesised that out-gassing of CO₂ during pH measurement and alkalinity titration under the N₂ atmosphere in the glovebox may have resulted in measured pH values that were higher than the actual solution pH values, and assuming calcite did not precipitate from solution prior to analysis, to the apparent oversaturation with respect to calcite (Koroleva et al., 2009). In aqueous extractions conducted on DGR-3 and DGR-4 samples, measurements of both pH and alkalinity were conducted outside of the glovebox (i.e., under atmospheric conditions). The fact that the apparent oversaturation with respect to calcite is again observed in the extract solutions indicates that the analytical data for the DGR-3 and DGR-4 aqueous extract solutions do not form a consistent set; some process(es) altered the pH, PCO₂ or alkalinity during pH measurement or during the alkalinity titration. The pH values measured for DGR-3 and DGR-4 aqueous extract solutions at the time the alkalinity titrations were performed are, on average, 0.2 pH units lower than those measured immediately after extraction. This suggests that in-gassing of CO₂ to these extract solutions may have occurred before the alkalinity measurements were conducted. However, if the initial, higher pH values measured immediately after extraction are used together with the measured alkalinity values in the speciation modelling, a higher degree of supersaturation with respect to calcite is predicted. Therefore, the observed decrease in pH prior to the alkalinity measurements cannot explain the predicted oversaturation with respect to calcite in the extract solutions.

An alternative explanation for the predicted oversaturation of calcite in the aqueous extraction solutions could be related to the alkalinity values used in the geochemical modelling, where the total, measured alkalinity was taken to be equal to the carbonate alkalinity. Low-molecular-weight organic acids were present in most extract solutions (as observed in anion chromatograms) and may also contribute to the measured alkalinity values. Consequently, the carbonate alkalinity may have been overestimated in the speciation modelling, resulting in the predicted supersaturation with respect to calcite and/or dolomite (see section 6 above). It is currently not possible to assess the relative contribution of these acids to the measured alkalinity values, because the organic acids present in the aqueous extracts could not be quantified using the analytical procedures employed.

6.2 Data screening for soluble salts

Samples from boreholes DGR-3 and DGR-4 for which there is evidence for the presence of soluble salts are listed in **Table 34**; evidence from both the aqueous extractions and supporting evidence from mineralogical investigations is summarized. For completeness, mineralogical and/or evidence from aqueous extractions given by Koroleva et al. (2009) for the presence of soluble salts in DGR-2 samples is included in this summary table. In these samples, porewater is not the sole source of Na⁺ and Cl⁻, Ca²⁺ and SO₄²⁻, Ca²⁺, Mg²⁺ and CO₃²⁻ or Sr²⁺ and SO₄²⁻ ions determined in the aqueous extracts; their concentrations have been perturbed by the dissolution of halite, gypsum/anhydrite, calcite/dolomite or celestite, respectively.

The next steps in the evaluation process consider only those samples in which there is no immediate evidence for the presence of soluble salts. A list of the samples from DGR-3 and -4 that meet this criterion is given in Table 35. For DGR-2, the only samples not considered in the dataset are those

listed in Table 34 (i.e. samples in which there is evidence for soluble salts). In Table 35, the chemical compositions of the aqueous extract solutions for DGR-3 and DGR-4 are classified into solution-types based on concentrations of major cations and anions, expressed in meq/L. For samples from the Cabot Head Formation through the Manitoulin Island, Queenston, Georgian Bay and Blue Mountain formations, the extract solutions are all Ca-Na-Cl type. Within the Cobourg Formation and lower in the sedimentary sequence, the extract solutions are Na-Ca-Cl type with only one exception: sample DGR-4 847.48 from the Cambrian, in which magnesium is the second most abundant cation (Na-Mg-Ca-Cl type solution).

The Cl⁻ concentrations determined by aqueous extraction are plotted against the porewater content ($PWC_{Grav.wet}$) for samples from all three boreholes in Figure 38A (includes only samples listed in Table 35). There is a strong, linear correlation between these parameters, suggesting that the differences in the extracted Cl⁻ concentrations between the samples are due to differences in the quantity of porewater present in the different lithologies. There are, however, two samples from DGR-3 and three samples from DGR-4 that have higher porewater contents relative to Cl⁻ than would be predicted based on the observed trend, although two of these samples could be considered to be on the trend, within analytical uncertainty. These samples are from a variety of lithologies including shales (one sample from each of the Bass Islands and Queenston formations), limestone (one sample each from the Sherman Fall, Kirkfield formations) and sandy mudstone (a sample from the Shadow Lake Formation). Furthermore, it is reasonable that the sample from the Bass Island Formation does not fall on this trend because Cl⁻ is not the dominant anion in the aqueous extract solution. Calculation of porewater content ($PWC_{Grav.wet}$) from the water content determined gravimetrically involves a salinity correction (see section 4.2.2). For comparison, Cl⁻ concentration is also plotted against the water content of the samples (i.e. pure H₂O) in Figure 38B; the same five samples are also seen to deviate from the linear trend between Cl⁻ and water content ($WC_{Grav.wet}$). This indicates that that deviation observed in the Cl⁻ of these samples as a function of porewater content is not simply an artefact of the salinity correction applied.

Table 34: Evidence suggesting the presence of soluble salts in samples from DGR-3 and DGR-4; Evidence for DGR-2 samples is primarily from Koroleva et al. (2009).

Sample ID (NWMO)	Formation	Mineralogical Investigations ¹	Ion ratios in aqueous extract solutions		Predicted saturation indices in aqueous extract solutions ²	
			Na/Cl \approx 1.0	Ca/SO ₄ \approx 1.0	SI Gypsum \geq 0	Celestite \geq 0
DGR-3 198.72	Salina – F Unit	Gypsum	√	√	√	
DGR-3 208.41	Salina - F Unit	Gypsum	√	√	√	
DGR-3 248.71	Salina – E Unit	Gypsum	√	√	√	
DGR-3 270.06	Salina - C Unit	Halite, gypsum, anhydrite	√	√	√	
DGR-3 289.36	Salina – B Unit	Gypsum	√	√	√	
DGR-3 312.53	Salina – A2 Unit		√			√
DGR-3 335.22	Salina – A2 Evaporite	Anhydrite, gypsum		√	√	√
DGR-3 344.06	Salina -A1 Unit		√			
DGR-3 380.88	A1 Evaporite	Anhydrite		√	√	
DGR-3 391.34	Guelph	Halite				
DGR-3 484.58	Queenston	Anhydrite, celestite			√	√
DGR-3 531.65	Georgian Bay	Anhydrite				
DGR-3 761.56	Kirkfield	Anhydrite				
DGR-4 189.16	Salina - F Unit	Gypsum, anhydrite	√	√	√	
DGR-4 229.32	Salina - E Unit	Gypsum	√	√	√	
DGR-4 322.68	Salina – A2 Evaporite	Anhydrite, gypsum	√	√	√	√
DGR-4 332.13	Salina – A1 Unit		√			
DGR-4 472.78	Queenston	Anhydrite				
DGR-4 847.48^A	Cambrian	Halite (from evaporation of porewater?)				
DGR-2 473.19	Queenston	Anhydrite, celestite				
DGR-2 510.12	Queenston	Anhydrite (matrix cement)			√	
DGR-2 523.08	Georgian Bay	Halite (SEM/EDS)			√	
DGR-2 562.92	Georgian Bay			√	√	
DGR-2 830.05	Gull River	Halite (SEM/EDS)				

¹ From Tables 1, 2, 5 and 6, section 3. Note that only selected samples were investigated in thin section and/or by SEM/EDS; in some cases, minerals were identifiable in hand specimen.

² Aqueous extraction solutions were modelled using PHREEQC (section 6).

Table 35: Dataset of DGR-3 and DGR-4 samples for further evaluation showing dominant ions in solution.

Sample ID (NWMO)	Formation	Extract solution type ¹	Sample ID (NWMO)	Formation	Extract solution type ¹
DGR-3 435.62	Cabot Head	Ca-Na-Cl	DGR-4 154.60 DGR-4 422.21	Bass Islands	Mg-Cl-HCO ₃
DGR-3 453.41	Manitoulin	Ca-Na-Cl		Cabot Head	Ca-Na-Cl
DGR-3 468.76	Queenston	Ca-Na-Cl	DGR-4 520.42	Georgian Bay	Ca-Na-Cl
DGR-3 502.55	Queenston	Ca-Na-Cl			
DGR-3 581.47	Georgian Bay	Ca-Na-Cl			
DGR-3 621.63	Blue Mountain	Ca-Na-Cl			
DGR-3 646.29	Blue Mountain	Ca-Na-Cl			
DGR-3 665.29	Cobourg –C M	Na-Ca-Cl			
DGR-3 676.21	Cobourg – LM	Na-Ca-Cl			
DGR-3 678.92	Cobourg – LM	Na-Ca-Cl			
DGR-3 685.52	Cobourg – LM	Na-Ca-Cl	Sherman Fall	Na-Ca-Cl	
DGR-3 690.12	Cobourg – LM	Na-Ca-Cl			
DGR-3 692.82	Cobourg – LM	Na-Ca-Cl	Kirkfield	Na-Ca-Cl	
DGR-3 697.94	Cobourg – LM	Na-Ca-Cl			
DGR-3 710.38	Sherman Fall	Na-Ca-Cl	Kirkfield	Na-Ca-Cl	
DGR-3 725.57	Sherman Fall	Na-Ca-Cl			
DGR-3 744.27	Kirkfield	Na-Ca-Cl	Shadow Lake	Na-Ca-Cl	
DGR-3 777.33	Coboconk	Na-Ca-Cl			
DGR-3 807.43	Gull River	Na-Ca-Cl	Cambrian	Na-Mg-Ca-Cl	
DGR-3 843.92	Gull River	Na-Ca-Cl			
DGR-3 852.18	Shadow Lake	Na-Ca-Cl			
DGR-3 856.06	Cambrian	Na-Ca-Cl	DGR-4 841.06 DGR-4 847.48 **		

¹ Based on concentrations of ions in aqueous extract solutions, expressed in meq/L.

** This sample is included for further evaluations, because it was not certain from mineralogical investigations if halite was present in situ in the rock matrix or formed by evaporation of porewater.

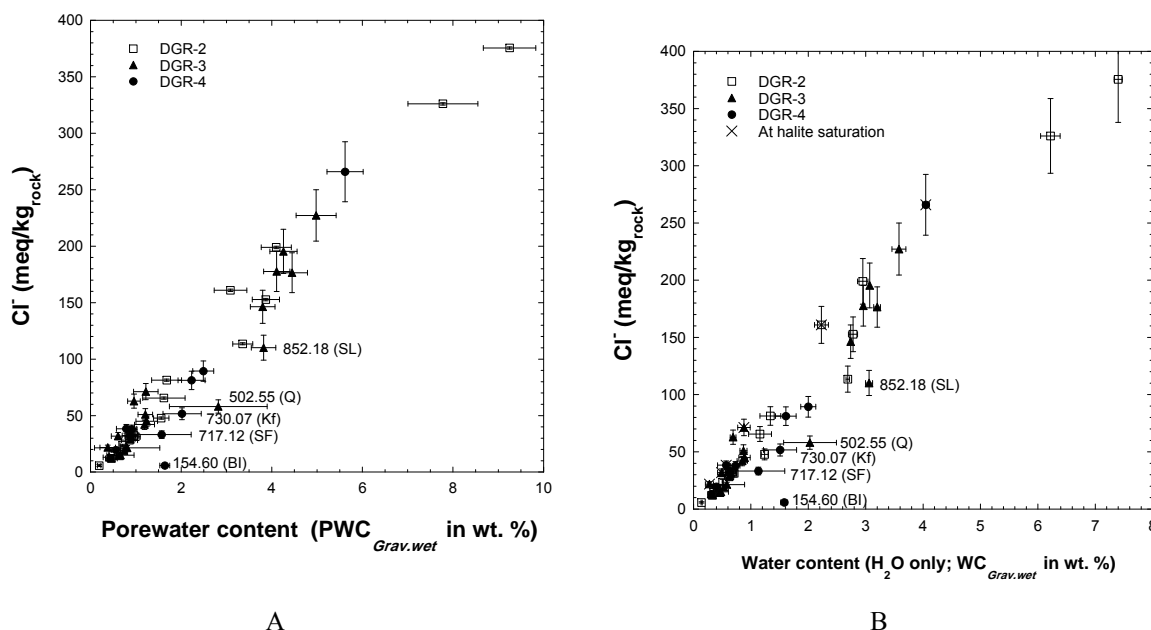


Figure 38: Cl^- concentration determined using aqueous extraction plotted versus A) porewater content ($\text{PWC}_{\text{Grav.wet}}$), and B) water content ($\text{WC}_{\text{Grav.wet}}$) for samples in which soluble salts were not identified (see Table 35). BI = Bass Islands, Q = Queenston, Kf = Kirkfield, SF = Sherman Fall. Error bars show the analytical uncertainty in Cl^- of $\pm 10\%$, the standard deviation observed in the water content determinations and the calculated uncertainty in the porewater contents (see section 4.2 for details). When the extracted ion concentrations are scaled to porewater content (section 6.3.2), several samples are predicted to be close to saturation with respect to halite (SI of approximately ± 0.3), as indicated in B).

As mentioned previously, although Br^- is not a major component of the aqueous extract solutions, it is considered to be conservative tracer in subsurface brines and may provide insight into their evolution (e.g. Kharaka and Hanor, 2005). In Figure 39A, a similar, linear trend is observed between Br^- and porewater content. More scatter is observed than for Cl^- , possibly due to the low Br^- concentrations measured in the aqueous extracts and the higher uncertainties in the measured concentrations when close to detection. In addition to the five samples which had lower Cl^- relative to their porewater contents than would be predicted based on the linear trend observed between these parameters, there is one sample from the Georgian Bay Formation shale (DGR-2 581.32) and one from the Cambrian (DGR-2 852.39) which have lower Br^- concentrations than would be predicted based on this trend and their porewater contents. The Br^- concentrations determined by aqueous extraction are plotted in Figure 39B. There is a strong, linear correlation ($r^2=0.97$) between these two ions, with the exception of the samples noted above from the Georgian Bay Formation and the Cambrian (note that these outliers were included in the dataset for calculation of the linear correlation coefficient). Although the Cl^- and Br^- concentrations correlate well using a single linear trend, there are actually two separate linear trends within the data, reflecting the fact that the Br/Cl ratio is not constant throughout Ordovician-aged formations and into the Cambrian (Figure 34).

The strong linear relationships observed between the Cl^- and Br^- concentrations and the porewater contents suggest that the differences in the concentrations of these ions determined during the aqueous extractions reflects different amounts of porewater extracted. The direct implication is that the ions extracted by this technique are from the porewater, rather than from other sources, such as mineral dissolution. Applying this as a tool, the concentrations of other ions determined using aqueous extraction are examined as a function of porewater content to give some indication of whether or not porewater may be the dominant source of these ions.

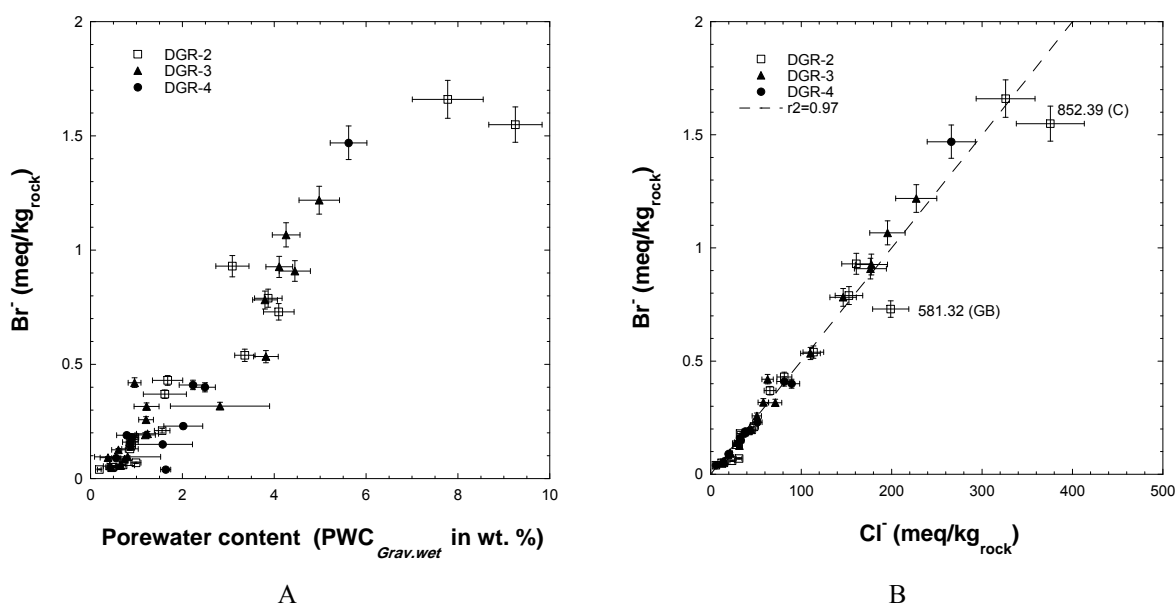


Figure 39: Br^- concentration determined by aqueous extraction plotted against A) porewater content in wt.% (PWC_{Grav.wet}) and B) Cl^- concentration, for samples in which soluble salts were not identified (see Table 35). C = Cambrian, GB = Georgian Bay formations. The dashed line shows the linear correlation coefficient, $r^2=0.97$, calculated for all plotted data points (i.e. including labelled samples).

The trends in the concentrations of the two dominant cations in the aqueous extractions, Na^+ and Ca^{2+} , are shown as a function of porewater content in Figure 40 and Figure 41, respectively. The trends observed between Na^+ or Ca^{2+} and porewater content are also linear, suggesting that these ions are predominantly from the porewater. The Na^+ and Cl^- concentrations also correlate well ($r^2=0.96$) with the exception of four shale-rich samples: two from the Queenston Formation (DGR-2 482.69 and DGR-3 468.76) and two from the Cabot Head Formation (DGR-3 435.62 and DGR-4 422.21). In these shale samples, the Na^+ concentrations are lower relative to Cl^- than observed for the majority of the samples, which may indicate impact by cation exchange reactions during extraction. The Ca^{2+} concentrations also show a strong correlation with Cl^- concentrations ($r^2=0.98$).

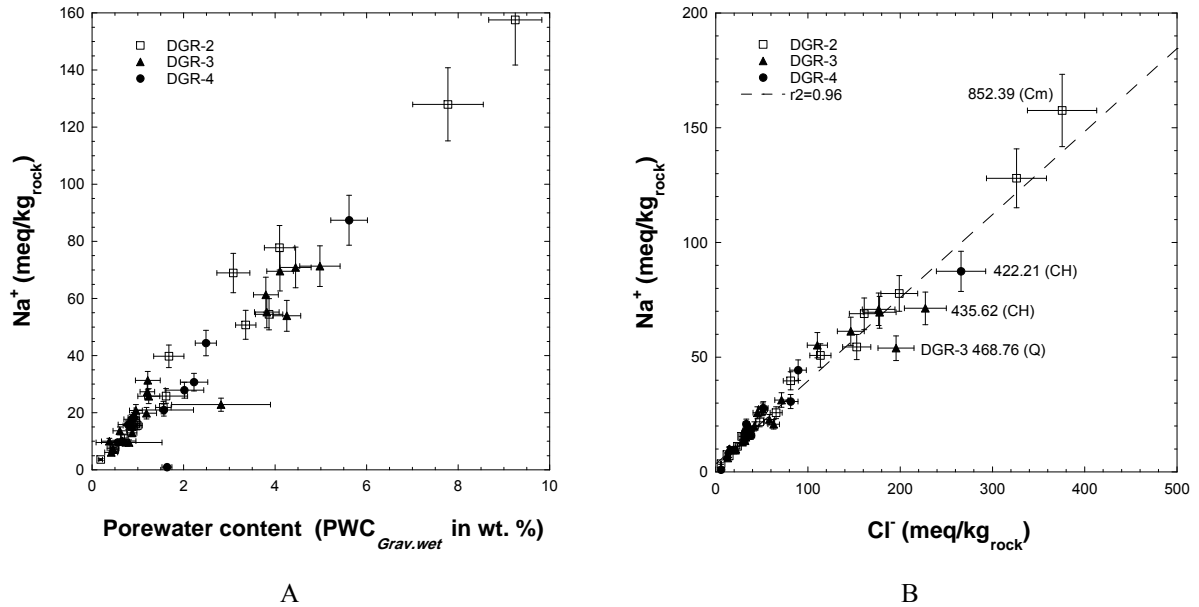


Figure 40: Na⁺ concentration determined by aqueous extraction plotted against A) porewater content in wt.% (PWC_{Grav.wet}) and B) Cl⁻ concentration, for samples in which soluble salts were not identified (see Table 35). CH = Cabot Head, Q = Queenston, Cm = Cambrian. The dashed line shows the linear correlation coefficient $r^2=0.96$ calculated for all plotted data points (i.e. including labelled samples).

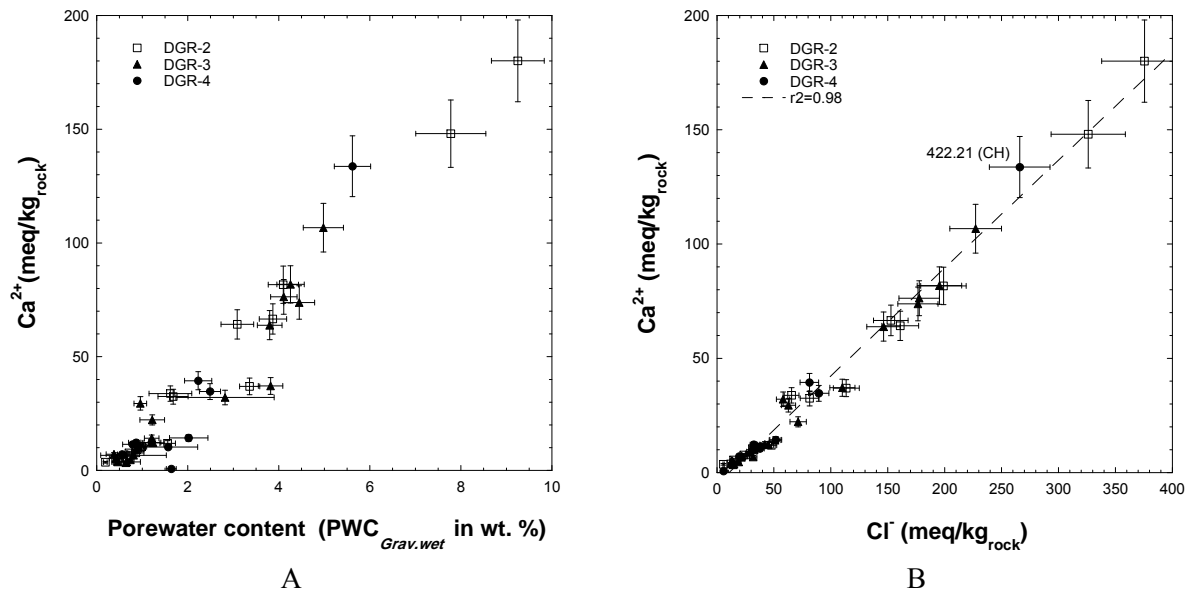


Figure 41: Ca²⁺ concentration determined by aqueous extraction plotted against A) porewater content in wt.% (PWC_{Grav.wet}) and B) Cl⁻ concentration, for samples in which soluble salts were not identified (see Table 35). CH = Cabot Head Formation. The dashed line shows the linear correlation ($r^2=0.98$) calculated for all plotted data points (i.e. including labelled samples).

In terms of concentrations expressed in $\text{meq/kg}_{\text{rock}}$, the next most important ion is magnesium, although Mg^{2+} may be influenced by cation exchange or mineral dissolution/precipitation reactions during the extractions. The highest Mg^{2+} concentrations determined in the aqueous extracts are a factor of 4 lower than Na^+ or Ca^{2+} (Figure 42). For magnesium, there is no clear linear trend with porewater content, as expected. Nevertheless, it might be argued that in general, higher Mg^{2+} concentrations are associated with higher porewater contents. Only a small number of samples appear to show an almost linear relationship between the extracted Mg^{2+} and Cl^- concentrations. Koroleva et al. (2009) noted a similarity between the trend in Mg^{2+} concentrations extracted from DGR-2 samples with the degree of dolomitisation in the formations, suggesting that Mg^{2+} concentrations are at equilibrium with dolomite. Figure 44 is a plot showing the Mg^{2+} concentrations as a function of depth for samples from all three boreholes. Only limited information on the degree of dolomitisation is available for samples from DGR-3 and DGR-4 (section 3.2, Figure 11). However, considered together with the degree of dolomitisation observed in samples from DGR-2 (Koroleva et al., 2009), higher Mg^{2+} concentrations are observed the Queenston, Georgian Bay, Shadow Lake and Cambrian, where the degree of dolomitisation is also high (Figure 4-6, Koroleva et al., 2009). Lower concentrations of Mg^{2+} are observed from the top of the Cobourg Formation down through to the top of the Gull River Formation, where a low degree ($< 20\%$) of dolomitisation was observed.

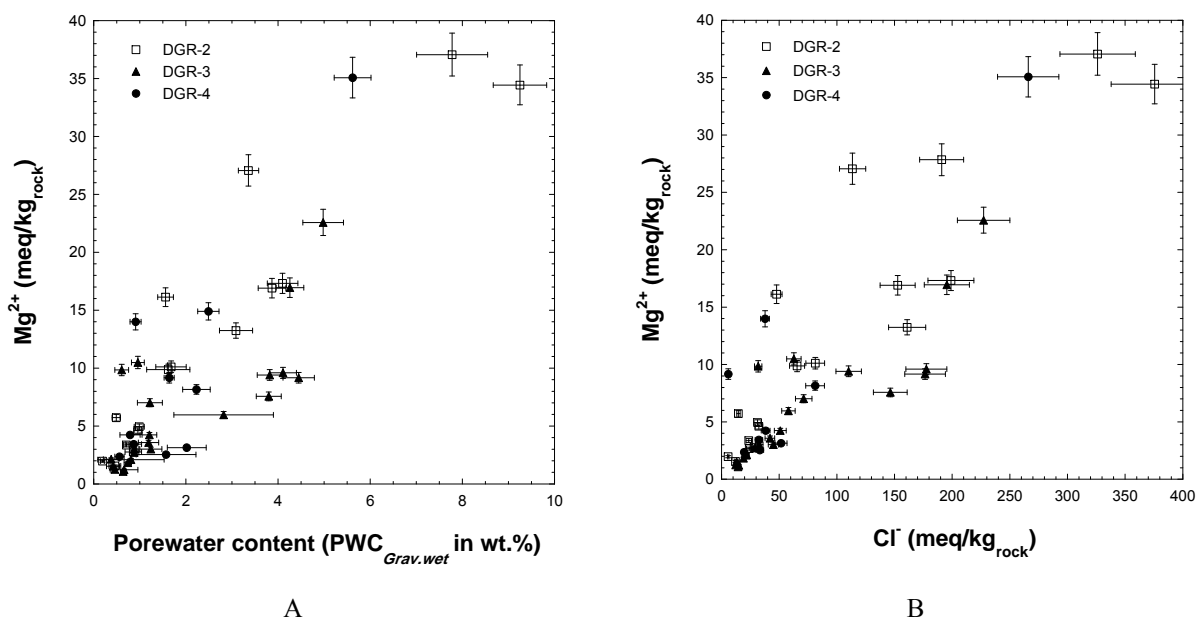


Figure 42: Mg^{2+} concentration determined by aqueous extraction plotted against A) porewater content in wt.% ($\text{PWC}_{\text{Grav.wet}}$) and B) Cl^- concentration, for samples in which soluble salts were not identified (see Table 35).

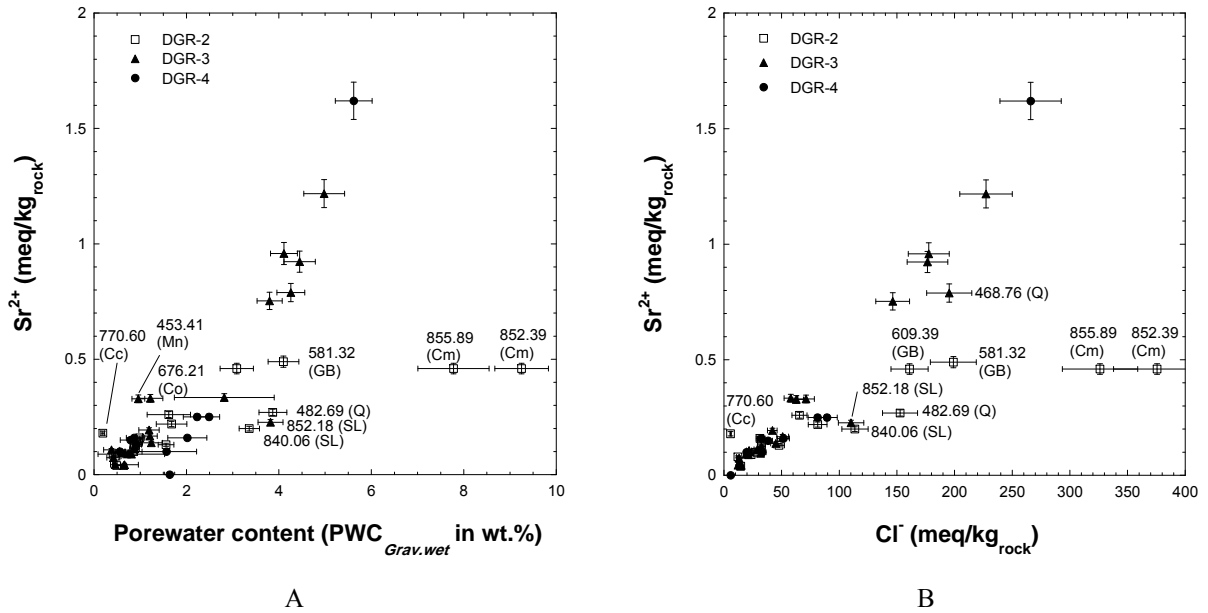


Figure 43: Sr^{2+} concentration determined by aqueous extraction plotted against A) porewater content in wt.% ($\text{PWC}_{\text{Grav.wet}}$) and B) Cl^- concentration, for samples in which soluble salts were not identified (see Table 35). Q = Queenston, GB = Georgian Bay, Cc = Coboconk, SL = Shadow Lake, Cm = Cambrian.

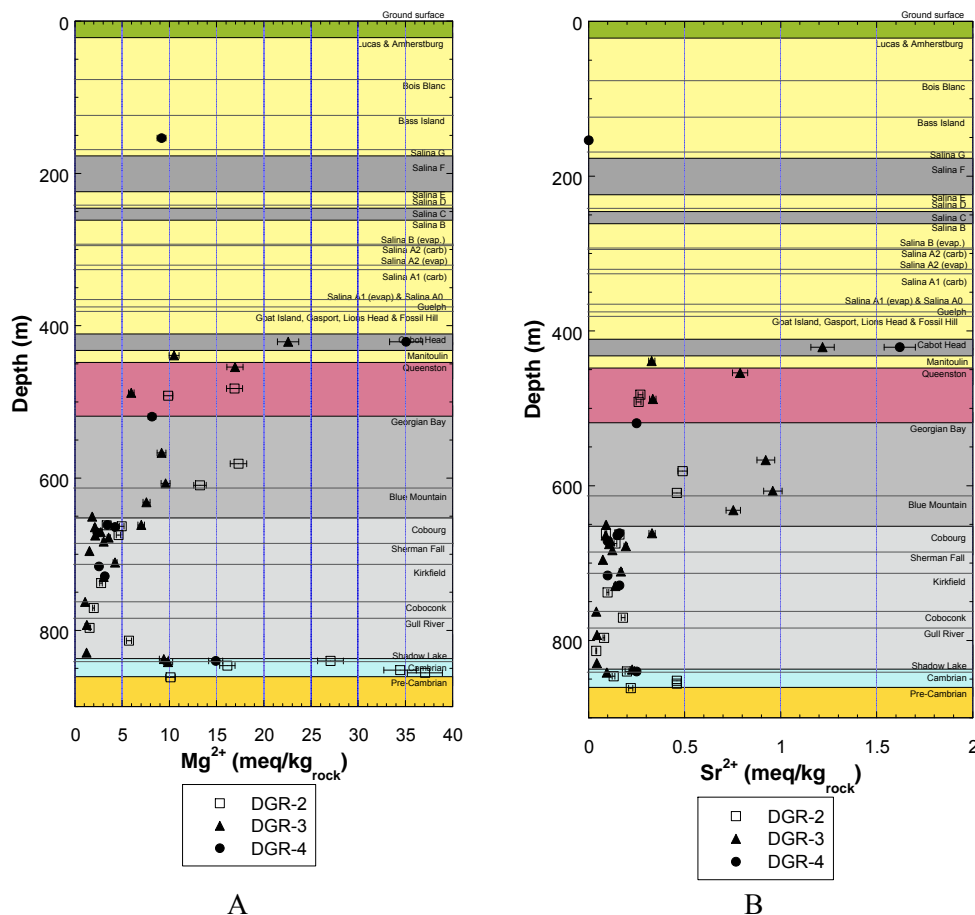


Figure 44: Concentration of A) Mg^{2+} and B) Sr^{2+} extracted from samples from DGR-2, -3 and -4 plotted as a function of depth. Depths of DGR-3 and DGR-4 samples are plotted as a function of depth relative to boreholes DGR-1/2. Data for DGR-2 samples are from Koroleva et al. (2009).

In terms of extracted Sr^{2+} concentrations, there does appear to be a trend of increasing Sr^{2+} concentrations with increasing porewater content (Figure 43A) and with extracted Cl^- concentration (Figure 43B). The trends are most pronounced in aqueous extractions for DGR-3 and DGR-4 samples, although some DGR-2 samples fall within the general trend. Several samples from DGR-2 and -3 have Sr^{2+} concentrations that are below the observed trends with respect to both porewater content and Cl^- concentration. These samples are labelled in Figure 43 and include two samples from each of the Queenston, Georgian Bay, Shadow Lake and Cambrian. The majority of these samples are from the DGR-2 borehole and have extracted Sr^{2+} concentrations of 0.5 meq/kg_{rock} or less. One sample from each of the Manitoulin, Cobourg and Coboconk formations have higher Sr^{2+} concentrations than would be predicted based on the observed trends in porewater content and Cl^- concentration.

In the aqueous extractions conducted on DGR-2 samples, a much longer extraction time of 48 hours was used, whereas for samples from both DGR-3 and DGR-4, the extraction time was reduced to 10 minutes. The shorter extraction time may have reduced the impact of mineral dissolution and/or ion

exchange. At the lower ionic strength of the aqueous extraction solution compared to the original porewater, Sr^{2+} would be favoured on the exchange sites of clay minerals compared to monovalent ions, resulting in lower Sr^{2+} concentrations in the aqueous extract solutions, as observed. This explanation seems reasonable for samples from the Queenston, Georgian Bay and Shadow Lake formations, where clay contents range from 20 to 50 wt.%. However, it does not appear to explain the results for the two DGR-2 samples from the Cambrian, which have clay contents between 5 and 6 wt.% (Koroleva et al., 2009).

In Figure 44B, the Sr^{2+} concentrations determined for samples from all three boreholes is plotted as a function of depth. Similar to the trend observed for Mg^{2+} , the highest concentrations of Sr^{2+} are observed in formations where the degree of dolomitisation is high (Queenston, Georgian Bay and Cambrian). High concentrations are also observed in the Cabot Head and Manitoulin formations. Celestite was identified (together with anhydrite) in two samples from the Queenston Formation, one in borehole DGR-2 and one from DGR-3.

The concentrations of K^+ are plotted versus porewater content and Cl^- concentration in Figure 45A and B, respectively. A linear trend is observed between the concentrations of K^+ and both the porewater content and extracted Cl^- concentration, suggesting that in many of the samples, K^+ measured by aqueous extraction may be predominantly from the porewater. However, there are also 9 samples that have lower K^+ concentrations than would be predicted based on their porewater contents and the observed linear trend between these two parameters. These samples are from the Shadow Lake, Cambrian and Precambrian in DGR-2, one sample from the Queenston Formation in DGR-3 and one sample from each of the Bass Islands, Shadow Lake and Cambrian in DGR-4. These lower concentrations may reflect a mineral solubility control on the K^+ concentrations during the aqueous extraction. Data from aqueous extractions performed at multiple solid:liquid ratios would be needed for these specific samples in order to evaluate this potential control. Although a suite of samples were examined at multiple solid:liquid ratios in DGR-2 by Koroleva et al., (2009), samples from the Shadow Lake, Cambrian and Precambrian were not included.

One sample in particular, from the Cobourg Formation (DGR-3 676.21), has a higher K^+ concentration than would be predicted based on its porewater content (or Cl^- concentration) alone. As discussed by Koroleva et al. (2009), in theory, it is expected that K^+ will be sensitive to cation-exchange processes even when the CEC is quite low. The dilution caused by the addition of water in the aqueous extraction procedure leads to lower ionic strengths, at which the divalent cations (Ca^{2+} , Mg^{2+} and Sr^{2+}) will be preferred on the exchange sites. This exchange would result in addition of K^+ (and Na^+) to the aqueous extract solution from the exchange sites. In this case, the K^+ concentrations would include contributions from both the porewater and the exchange sites. In samples examined at multiple solid:liquid ratios in DGR-2, linear trends in K^+ concentrations were observed with increasing solid:liquid ratios (Koroleva et al., 2009), suggesting that the impact of ion exchange was minimal.

In the majority of samples, the extracted SO_4^{2-} concentrations are low (approximately 1 meq/kg_{rock}), regardless of the porewater content or extracted Cl^- concentration (Figure 46). There are several exceptions labelled in Figure 46. These include shale samples from the Queenston (2 samples) and Georgian Bay (1 sample) formations, two samples from the Gull River Formation and one from the Coboconk Formation. In aqueous extractions conducted with DGR-2 samples at multiple solid:liquid ratios, the majority of samples (6 out of 8) showed a non-linear trend in sulphate concentrations, which could indicate contributions of sulphate from mineral dissolution or generated by oxidation of sulphide minerals (Koroleva et al., 2009). In future campaigns, immediate preservation of fresh core in liquid nitrogen might be used for select samples as an alternative approach to

minimize sulphide oxidation, as a further step towards better constraining sources of sulphate in aqueous extraction solutions (e.g. Gaucher et al., 2009).

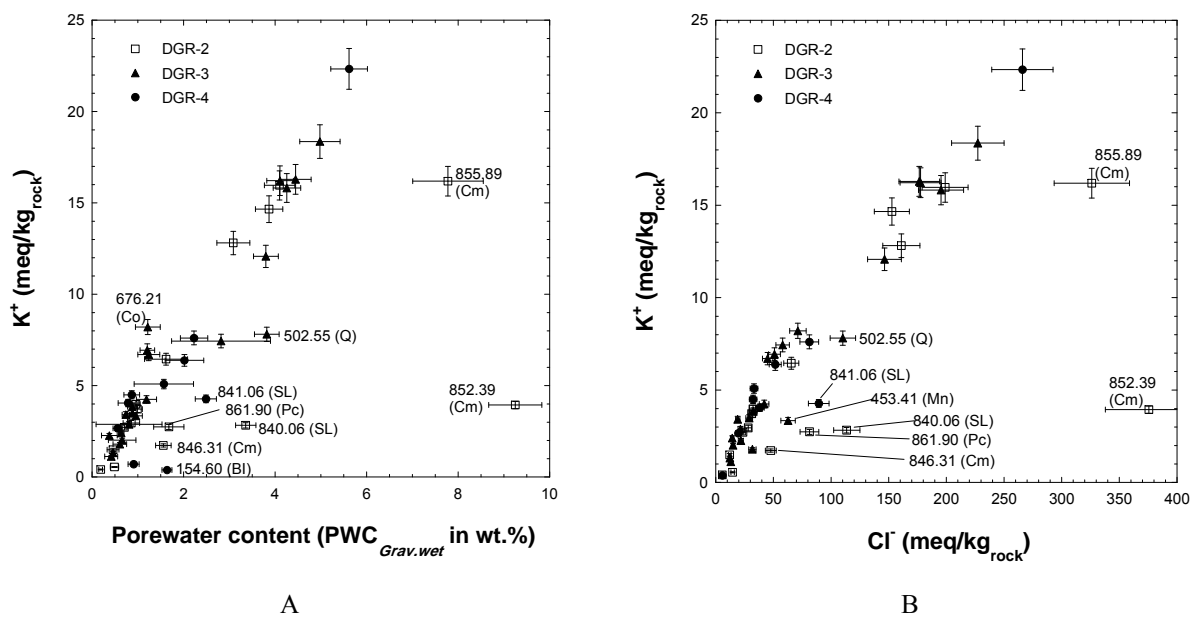


Figure 45: K^+ concentration determined by aqueous extraction plotted against A) porewater content in wt.% ($PWC_{Grav.wet}$) and B) Cl^- concentration, for samples in which soluble salts were not identified (see Table 35). BI = Bass Islands, Mn= Manitoulin, Q = Queenston, SL = Shadow Lake, Cm = Cambrian, Pc = Precambrian.

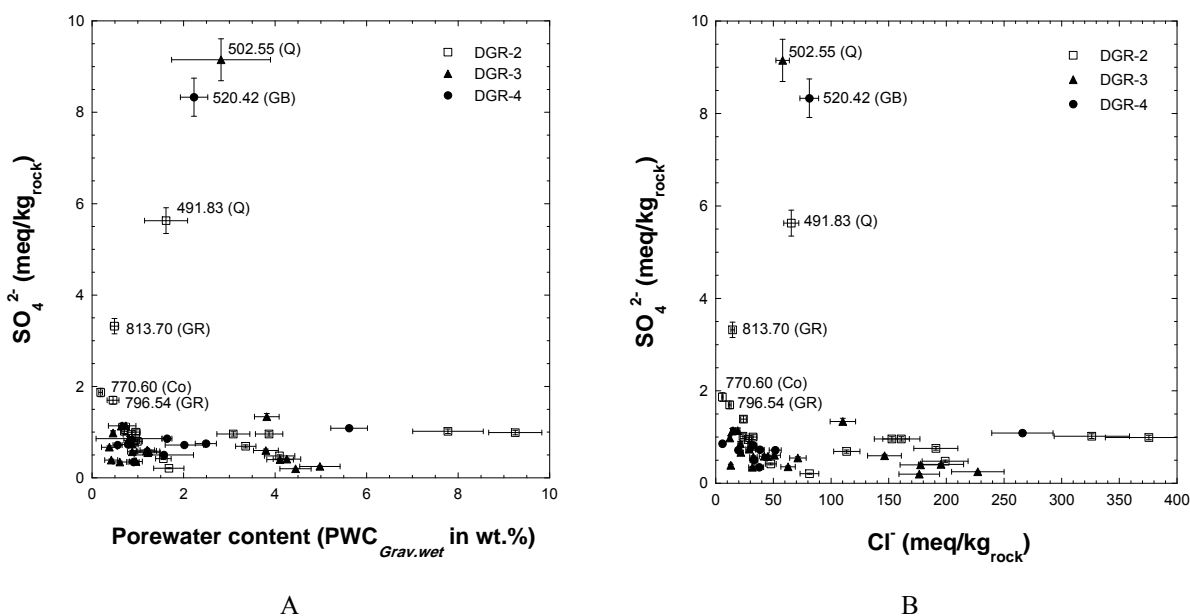


Figure 46: SO_4^{2-} concentration determined by aqueous extraction plotted against A) porewater content in wt.% ($PWC_{Grav.wet}$) and B) Cl^- concentration, for samples in which soluble salts were not identified (see Table 35). Q = Queenston, GB = Georgian Bay, Co = Cobourg, GR = Gull River.

In summary, for the dominant ions observed in the extract solutions, Na^+ , Ca^{2+} and Cl^- , the strong linear correlations with porewater contents suggest that these ions are predominantly from the porewater, with minimal contributions from mineral dissolution. One exception for Ca^{2+} is sample DGR-4 422.21 from the Cabot Head Formation; for DGR-2 samples, the longer extraction time (48 hours) likely resulted in some contributions of Ca^{2+} from calcite and/or dolomite dissolution. Similarly, Br^- shows a strong, linear correlation to porewater content, suggesting that porewater is the dominant source of this ion. In the many samples, the concentration of K^+ determined by aqueous extraction also shows a general, linear trend with porewater contents, although there are several exceptions, notably from the Shadow Lake, Cambrian and Precambrian, where the extracted K^+ concentrations are lower than would be predicted based on their porewater contents. Mg^{2+} and Sr^{2+} concentrations appear to be related to the degree of dolomitisation, with the highest concentrations observed in the Cabot Head, Manitoulin, Queenston, Georgian Bay and Cambrian. The majority of samples have low ($1 \text{ meq/kg}_{\text{rock}}$) SO_4^{2-} concentrations that do not vary systematically with porewater content.

6.3 Additional screening from scaling to water content

The scaling of ion concentrations determined by aqueous extraction is used here as another tool to investigate the possible impact of soluble phases in samples where there was no immediate evidence from extract solution compositions for the presence of soluble salts (see Table 35). The purpose of scaling the extracted ion concentrations to water content is to investigate the saturation indices of calcium sulphate minerals and simple chloride salts (halite and sylvite) using geochemical equilibrium modelling. As emphasized by Koroleva et al. (2009) and discussed in section 10 of this report, the upscaled aqueous extracts cannot be considered representative of porewater compositions; they are simply scaled to water content for the purposes of investigating the predicted mineral saturation indices of the soluble salts.

6.3.1 Scaling to water content

In the scaling procedure, the average composition of the aqueous extract solutions is used (reported in Table 30 and Table 31 for DGR-3 and DGR-4 samples, respectively). Only aqueous extract solutions for those samples without evidence for soluble salts (see Table 35) were considered. To scale the concentrations of ions measured in the aqueous extractions (at a solid:liquid ratio of 1:1), the quantity of ions extracted per kilogram of dry rock (expressed in $\text{mmol/kg}_{\text{rock}}$) is divided by water content of the sample, reported relative to the dry mass of rock ($\text{WC}_{\text{Grav.dry}}$) and expressed as a weight fraction ($\text{kg}_{\text{H}_2\text{O}}/\text{kg}_{\text{rock}}$). The mass of dry rock material (kg_{rock}) in both measurements is comparable, in that it includes the mass of rock plus the mass of salts precipitated from the porewater during drying. The upscaled concentration of a given ion has units of $\text{mmol/kg}_{\text{H}_2\text{O}}$. For the purposes of scaling, it is assumed that the ions extracted were originally in present in the water that was removed gravimetrically by drying at 105°C .

The concentrations in the scaled extraction solutions (expressed in millimolality) are given in Table 36 and Table 37, for samples from DGR-3 and DGR-4, respectively. For DGR-2 samples, a scaling factor was calculated according to the following equation (Koroleva et al., 2009):

$$\Xi = \frac{m_{\text{H}_2\text{O},\text{aq.ex.}}}{\text{WC}_{\text{Grav.dry}} m_{\text{rock},\text{aq.ex.}}} \approx \left[\frac{1}{\text{WC}} \right]_{S:L=1:1} \quad (15)$$

In this case, the concentrations of ions measured in the aqueous extracts (reported in $\text{g}/\text{kg}_{\text{rock}}$ or $\text{mol}/\text{kg}_{\text{rock}}$) are multiplied by this scaling factor ($1/\text{WC}_{\text{Grav.dry}}$). Both formulations yield identical values for the upscaled aqueous extract concentrations.

Table 36: Millimolalties of ions for aqueous extract solutions from DGR-3 scaled to water content ($WC_{Grav.dry}$).

Sample ID	$WC_{Grav.dry}$	Relative uncertainty in WC	Na^+	K^+	Mg^{2+}	Ca^{2+}	Sr^{2+}	Cl^-	Br^-	SO_4^{2-}
	Wt. %	%	mmol/ kg_{H_2O}	mmol/ kg_{H_2O}	mmol/ kg_{H_2O}	mmol/ kg_{H_2O}	mmol/ kg_{H_2O}	mmol/ kg_{H_2O}	mmol/ kg_{H_2O}	mmol/ kg_{H_2O}
DGR-3 435.62	3.75	3.1	1900	490	301	1430	16	6070	33	3
DGR-3 453.41	0.70	7.9	2970	478	748	2100	24	8980	60	26
DGR-3 468.76	3.19	0.4	1690	496	266	1280	12	6130	33	6
DGR-3 502.55	2.09	24	1090	355	142	767	8	2780	15	218
DGR-3 581.47	3.33	2.3	2130	489	138	1110	14	5300	27	3
DGR-3 621.63	3.07	0.8	2270	528	156	1240	16	5780	30	7
DGR-3 646.29	2.83	1.0	2170	427	134	1130	13	5170	28	11
DGR-3 665.29	0.54	4.9	1800	637	171	434	8	3560	16	107
DGR-3 676.21	0.89	13	3530	922	394	1250	19	8020	36	31
DGR-3 678.92	0.59	53	1640	493	179	570	8	3660	16	74
DGR-3 685.52	0.64	5.7	2040	548	215	723	9	4570	22	59
DGR-3 690.12	0.28	27	3640	823	390	1300	20	7910	33	122
DGR-3 692.82	0.86	10	2300	492	207	712	11	4860	22	34
DGR-3 697.94	0.64	5.7	2380	602	237	802	10	5120	24	45
DGR-3 710.38	0.31	19	1990	364	249	867	12	4260	18	63
DGR-3 725.57	0.88	6.6	3100	785	240	802	10	5780	29	35
DGR-3 744.27	0.90	11	2860	742	168	675	8	4500	22	32
DGR-3 777.33	0.46	4.1	2140	523	117	374	4	3100	12	123
DGR-3 807.43	0.33	3.9	2140	396	188	600	7	3680	14	147
DGR-3 843.92	0.48	27	2110	422	128	395	5	3150	12	119
DGR-3 852.18	3.15	1.9	1750	248	149	590	4	3500	17	21
DGR-3 856.06	0.49	15	2790	367	1007	699	10	6520	26	36

Table 37: Millimolalties of ions for aqueous extract solutions for samples from DGR-4 scaled to water content ($WC_{Grav.dry}$).

Sample ID (NWMO)	$WC_{Grav.dry}$ Wt. %	Relative uncertainty in WC %	Na⁺ mmol/ kg_{H2O}	K⁺ mmol/ kg_{H2O}	Mg²⁺ mmol/ kg_{H2O}	Ca²⁺ mmol/ kg_{H2O}	Sr²⁺ mmol/ kg_{H2O}	Cl⁻ mmol/ kg_{H2O}	Br⁻ mmol/ kg_{H2O}	SO₄²⁻ mmol/ kg_{H2O}
DGR-4 154.60	1.60	3.9	63	24	286	22	b.d	369	3	27
DGR-4 422.21	4.21	1.7	2080	530	416	1590	19	6310	35	13
DGR-4 520.42	1.64	12	1880	465	249	1210	8	4970	25	255
DGR-4 662.83	0.63	19	2810	713	271	969	12	5140	25	65
DGR-4 665.41	0.57	27	2760	707	370	1000	13	6690	33	64
DGR-4 672.85	0.40	17	2390	662	293	881	12	4870	23	89
DGR-4 717.12	1.15	41	1830	444	111	448	4	2900	13	22
DGR-4 730.07	1.53	19	1830	417	103	468	5	3380	15	24
DGR-4 841.06	2.04	6.9	2180	210	367	852	6	4390	20	19
DGR-4 847.48	0.73	11	2510	98	958	726	9	5170	24	24

6.3.2 Speciation modelling to predict saturation indices

The geochemical modelling code PHREEQC, was used in conjunction with the *pitzer.dat* thermodynamic database to speciate the scaled aqueous extract solutions and provide predications of saturation indices of soluble salts. The simplified modelling approach used by Koroleva et al. (2009) for DGR-2 samples was also applied to DGR-3 and DGR-4 samples (samples listed in Table 36 and Table 37). As discussed by Koroleva et al. (2009), the pH values of the aqueous extracts do not reflect those of the original brine; therefore, a nominal pH value of 7.5 is used. The redox conditions were stipulated using a *pe* value of 4.0. The alkalinities determined for the aqueous extracts are likely impacted by calcite/dolomite dissolution during the extraction and cannot be scaled. In addition, because a short extraction time of 10 minutes was used for samples from both DGR-3 and DGR-4, the extract solutions cannot be assumed to be at equilibrium with respect to calcite or dolomite. Therefore, the carbonate system is not included in this exploratory modelling.

Selected results from the speciation modelling are presented in Table 38 and Table 39 for scaled extract solutions from DGR-3 and DGR-4, respectively. Shading in these tables indicates that the scaled extract solution is predicted to be at or above saturation with respect to the mineral phase, within ± 0.2 units. The charge balance (percent error) calculated by PHREEQC is also included and is within $\pm 10\%$ for all samples except for sample DGR-4 154.60 from the Bass Islands Formation, where the charge balance is +24.5%, suggesting a large surplus of cations in solution relative to anions. This reflects the fact that carbonates were not included in the speciation calculations and that carbonate was identified as a dominant anion in the aqueous extract solution for this sample (section 6.2, Table 35). Consequently, the modelling results for this sample are not meaningful and are not considered in the following discussion.

All scaled aqueous extract solutions are predicted to be oversaturated with respect to anhydrite, gypsum and celestite. To date, celestite has been identified only in the Queenston Formation in one sample from DGR-3 (section 3.2, Table 5) and one sample in DGR-2 (Koroleva et al., 2009). Of the samples considered, mineralogical investigations were conducted on one sample each from the Gull River, Shadow Lake and Cambrian in DGR-3 (section 3.1, Table 1). For DGR-4 samples, detailed mineralogical investigations (including SEM/EDS) were conducted on one sample from each of the Cabot Head, Shadow Lake and the Cambrian. No sulphate-bearing mineral phases were identified in these samples, although sulphide minerals (pyrite, sphalerite) were observed in all but the sample from the Cabot Head Formation, which is a red, oxidized shale. The detailed mineralogical observations available do not support the ubiquitous presence of calcium sulphate minerals through the sedimentary sequence from the Cabot Head Formation to the Cambrian, as predicted using the simplified geochemical modelling approach. However, even with such detailed mineralogical studies, the presence of trace amounts of finely disseminated calcium sulphate minerals in the rock matrix cannot be completely ruled out. Where present in the rock material, gypsum/anhydrite will be more soluble in the more dilute geochemical conditions in the aqueous extract solutions than at porewater concentrations (Koroleva et al., 2009).

Alternatively, the inconsistency between the mineralogical observations and the predicted saturation indices may indicate that predictions made using this simplified approach are not realistic. Other factors that could contribute to the apparent oversaturation with respect to the calcium sulphate phases include:

- Extracted sulphate concentrations are elevated relative to actual in situ porewater concentrations due to sulphide oxidation during the extractions. As discussed in section 6.2, Koroleva et al. (2009) presented evidence to suggest that in select samples, the sulphate concentrations in the

aqueous extract solutions may have been impacted by sulphide oxidation or sulphate mineral dissolution, although it was not possible to distinguish between these processes based on the available data.

- The extracted Ca^{2+} concentrations are elevated relative to actual, in situ porewater concentrations as a result of dissolution of calcite or dolomite during the aqueous extractions. Although equilibrium with respect to calcite and/or dolomite is expected in situ, these phases were not included in the simplified modelling approach, as discussed above. If the extraction time were sufficiently long to justify an equilibrium assumption in the aqueous extract solutions (≈ 48 hours for calcite, ≈ 7 days for dolomite) and if inorganic carbon in the system could be constrained (e.g. by specifying PCO_2), equilibrium with respect to calcite and dolomite equilibrium could be stipulated in the modelling. This would also allow correction of Ca^{2+} dissolved from these minerals during the extraction experiments. Based on the good correlation between Ca^{2+} concentrations and porewater contents (section 6.2), it appears that the contributions of calcium to the extraction solutions due to mineral dissolution during the extraction are relatively minor, compared to the total Ca^{2+} inventory in the porewater. However, if present, excess extracted calcium above and beyond what is actually present in situ could contribute to the observed oversaturation with respect to the soluble calcium sulphate mineral phases.

Based on the available information, the saturation indices predicted for sulphate-bearing phases in the scaled extract solutions are currently considered at best, weak evidence for the presence of sulphate-bearing phases through the profile from the Cabot Head Formation to the Cambrian. Therefore, these results are not used to further infer the presence (or absence) of these mineral phases in the rock matrix.

For the purposes of exploring the potential presence of soluble salts in the rock samples, only the saturation indices for the simple Cl-bearing salts, halite and sylvite are considered. The saturation indices for halite calculated in the scaled aqueous extract solutions are plotted versus depth in Figure 47. In DGR-3, all scaled aqueous extract solutions are undersaturated with respect to halite, with the exception of those for three samples from DGR-3; one shale from the Manitoulin Formation (DGR-3 453.41) and two limestones from the Cobourg Formation (DGR-3 676.21, DGR-3 690.12). Sylvite is also predicted to be close to saturation in sample DGR-3 676.21. No mineralogical data are available for these three samples to confirm or refute these predictions. Similarly, the scaled extraction solution for a limestone sample from the Cobourg Formation (DGR-4 665.41) is at or above saturation with respect to halite (within ± 0.2 SI units). A shale sample from the Cabot Head Formation (DGR-4 422.21) is predicted to be close to saturation with respect to halite. The calculated oversaturation with respect to halite may indicate the presence of primary halite (i.e., in situ in the rock matrix) in these few samples, but this would need to be confirmed with follow-up, detailed mineralogical investigations (e.g. SEM/EDS). It must be noted, however, that for the three limestone samples from the Cobourg, the error associated with the water content measurements is high (up to 30%; Table 36 and Table 37). If the water contents have been underestimated, then the saturation indices calculated for halite will be overestimated.

The saturation indices calculated for scaled aqueous extraction solutions for DGR-2 samples (without evidence for the presence of soluble salts) are also shown in Figure 47. Only one additional sample from the Georgian Bay Formation is predicted to be close to saturation with respect to halite (DGR-2 609.32) in the scaled solutions. Halite was not identified in this sample using basic mineralogical investigations (thin section, XRD analysis). In DGR-2, halite was identified in one sample from each of the Georgian Bay and Gull River formations (DGR-2 523.08 and DGR-2 830.05, respectively) using SEM/EDS (Herwegh and Mazurek, 2008). In one sample from the Cambrian in borehole DGR-4 (DGR-4 847.48), halite was identified in thin section, but could not be confirmed to be primary (section 3.1, Table 2). The scaled

aqueous extract solution for this sample is undersaturated with respect to halite, which supports the interpretation that the halite observed is most likely secondary (i.e., formed as a result of porewater evaporation during sample handling and/or preparation).

Table 38: DGR-3 - Saturation indices for selected minerals, calculated using the scaled aqueous extract solutions and PHREEQC with pitzer thermodynamic database.

Sample ID	Depth Relative to DGR1/-2	Calculated water activity	Charge balance (% Error)	Anhydrite	Gypsum	Celestite	Halite	Sylvite
DGR-3 435.62	421.16	0.76	-1.90	0.10	0.08	0.30	-0.38	-0.66
DGR-3 453.41	438.95	0.58	0.58	1.70	1.45	1.87	0.48	-0.29
DGR-3 468.76	454.30	0.77	-7.54	0.39	0.39	0.51	-0.47	-0.69
DGR-3 502.55	488.09	0.90	0.81	1.32	1.45	1.55	-1.33	-1.30
DGR-3 581.47	567.01	0.80	-1.86	-0.10	-0.07	0.16	-0.52	-0.78
DGR-3 621.63	607.17	0.78	-1.81	0.37	0.37	0.63	-0.39	-0.68
DGR-3 646.29	631.83	0.80	-0.74	0.45	0.48	0.67	-0.52	-0.85
DGR-3 665.29	650.83	0.87	-1.80	0.91	1.01	1.37	-0.99	-0.95
DGR-3 676.21	661.75	0.66	-2.18	1.37	1.23	1.69	0.19	-0.19
DGR-3 678.92	664.46	0.87	-2.45	0.87	0.97	1.21	-1.00	-1.03
DGR-3 685.52	671.06	0.83	-2.42	0.95	1.01	1.22	-0.71	-0.85
DGR-3 690.12	675.66	0.66	-1.93	1.96	1.82	2.29	0.21	-0.24
DGR-3 692.82	678.36	0.82	-3.17	0.76	0.81	1.11	-0.60	-0.86
DGR-3 697.94	683.48	0.81	-1.48	0.94	0.97	1.20	-0.53	-0.72
DGR-3 710.38	695.92	0.84	2.34	1.00	1.06	1.31	-0.72	-1.03
DGR-3 725.57	711.11	0.77	0.93	0.91	0.90	1.16	-0.28	-0.52
DGR-3 744.27	729.81	0.81	2.10	0.70	0.73	0.94	-0.48	-0.65
DGR-3 777.33	762.87	0.88	4.09	0.86	0.97	1.08	-1.00	-1.10
DGR-3 807.43	792.97	0.86	1.63	1.16	1.25	1.42	-0.85	-1.11
DGR-3 843.92	829.46	0.88	2.69	0.88	0.99	1.18	-1.00	-1.18
DGR-3 852.18	837.72	0.88	-0.99	0.34	0.45	0.36	-0.98	-1.34
DGR-3 856.06	841.60	0.72	-0.18	1.06	1.00	1.37	-0.08	-0.70

Shading indicates that upscaled aqueous extract solution is at or above saturation with respect to the mineral phase (± 0.2 units).

Table 39: DGR-4 - Saturation indices for selected minerals, calculated using the scaled aqueous extract solutions and PHREEQC with the pitzer thermodynamic database.

Sample ID	Depth Relative to DGR1/-2	Calculated water activity	Charge balance (% Error)	Anhydrite	Gypsum	Celestite	Halite	Sylvite
DGR4-154.60	153.55	0.99	24.5	-0.76	-0.55	n.a.	-3.53	-3.32
DGR4-422.21	421.16	0.73	2.11	0.81	0.76	1.03	-0.23	-0.55
DGR4-520.42	519.37	0.80	-2.14	1.79	1.82	1.79	-0.60	-0.83
DGR4-662.83	661.78	0.79	6.42	1.13	1.14	1.39	-0.38	-0.60
DGR4-665.41	664.36	0.74	-4.65	1.41	1.36	1.67	-0.17	-0.47
DGR4-672.85	671.80	0.81	3.32	1.21	1.24	1.52	-0.53	-0.69
DGR4-717.12	716.07	0.89	6.89	0.19	0.31	0.33	-1.10	-1.19
DGR4-730.07	729.02	0.88	-0.66	0.30	0.41	0.52	-1.02	-1.15
DGR4-841.06	840.01	0.83	4.19	0.50	0.56	0.52	-0.63	-1.23
DGR4-847.48	846.43	0.77	6.63	0.69	0.69	0.94	-0.32	-1.39

n.a. Not applicable because Sr^{2+} was below detection in the aqueous extract solutions

Shading indicates that scaled aqueous extract solution is at or above saturation with respect to the mineral phase (± 0.2 SI units).

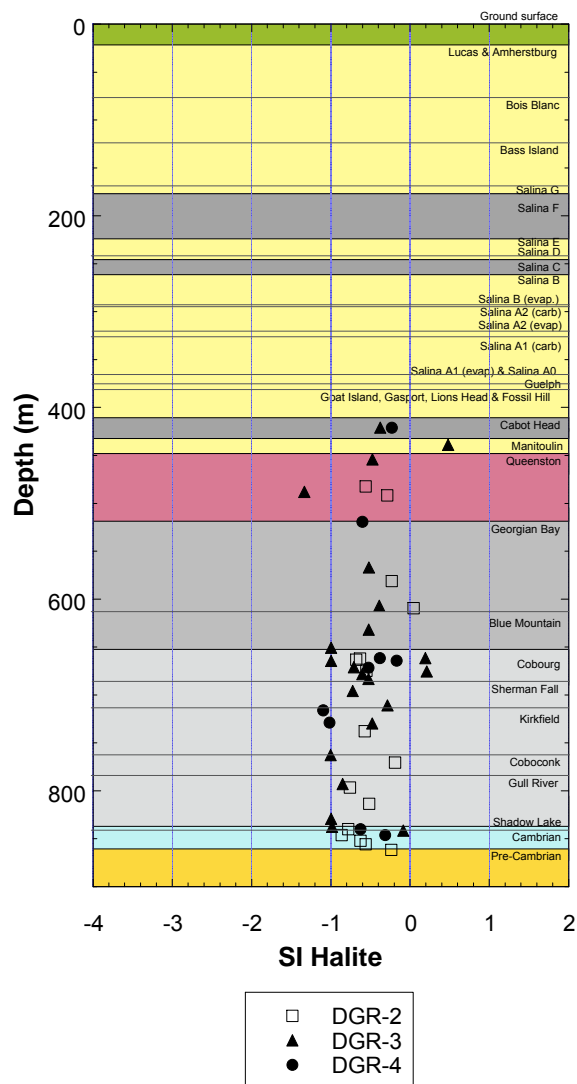


Figure 47: Saturation indices of halite calculated for scaled aqueous extract solutions from DGR-3 and DGR-4 samples. Data are plotted as a function of depth relative to boreholes DGR-1/2. Data for DGR-2 samples are from Koroleva et al. (2009).

7 Ethanol-water extractions

The ethanol-water extraction technique has been investigated as a potential method to improve estimations of ion concentrations in porewater by reducing, or if possible, eliminating contributions of ions due to the dissolution of highly soluble mineral phases present in the rock matrix (e.g. gypsum, anhydrite, halite) during aqueous extractions. In the following sections, the current understanding of the behaviour of ions in ethanol-water mixtures is first reviewed. The results of initial testing and application of ethanol-water extractions to soluble minerals (gypsum, celestite and halite) and to samples from DGR-3 are then reported and evaluated.

7.1 Behaviour of ethanol-water mixtures

Alcohols do not act as purely neutral liquids when added to a system containing pure water and salts and determining the effect of the alcohol on the activity of ions in solution is quite complex (Kan et al., 2003 and references therein). In aqueous solutions, non-ideal behaviour due to the presence of salts can be predicted using the concept of activity effects (e.g., Pitzer theory of specific ion interactions). The concentration of a single ion (m_i) in an aqueous solution is:

$$m_i = \frac{a_i}{\gamma_i} \quad (16)$$

where a_i is the activity of the ion in the aqueous solution and γ_i is its activity coefficient. Kan et al. (2002) conducted studies on the solubility of calcite and of sulphates (BaSO_4 , celestite and gypsum) and halite (Kan et al., 2003) in solutions containing varying percentages of water and methanol or ethylene glycol. To describe the solubility behaviour of these mineral phases in mixed ethylene glycol- or methanol-water solutions, the authors assume that the overall activity coefficient for each ion in a mixed alcohol-water system is:

$$\gamma_{overall} = \gamma^s * \gamma^N \quad (17)$$

where γ^s is the activity effect due to ion-ion interactions in water (or the “salt-effect”) and γ^N accounts for interactions with the alcohol (or the “alcohol-effect”). The ion-ion activity coefficient (γ^s) is calculated using conventional methods (e.g., Pitzer theory), whereas the alcohol activity coefficient (γ^N) is a curve-fitted parameter obtained using an equation similar to the Born equation (Kan et al., 2002). Applying the approach of Kan et al. (2003) to a single ion in a mixed ethanol-water solution, its concentration will be given by:

$$m_i = \frac{a_i}{\gamma_i^s \gamma_i^N} \quad (18)$$

where the concentration of the ion in the mixed ethanol-water solution, m_i , is expressed in units of “aqueous molality” (i.e. mol/kg_{H2O}). Comparison with equation (16) demonstrates that the concentration of a given ion in a mixed ethanol-water solution will not be the same as in an aqueous solution, unless γ^N is equal to unity. In halite solubility studies, Kan et al. (2003) determined that the mean alcohol activity coefficient for Na^+ and Cl^- (γ_{NaCl}^N) increased from 1.00 to 2.62 as the quantity of methanol in solution in-

creased from 0 to 59.5 wt.% but decreased and then increased again with continued increases in methanol to 90 wt.%.

Theoretically, the ion concentrations measured in the ethanol-water extracts could be corrected to a concentration in the original aqueous phase, if the alcohol interaction coefficient (γ^N) could be predicted. For example for Br^- , the concentration in the aqueous phase, m_{aqBr} would be:

$$m_{\text{aqBr}} = \frac{a_{\text{Br}}}{\gamma_{\text{Br}}^S} = m_{\text{Breth}} * \gamma_{\text{Br}}^N \quad (19)$$

Unlike the situation for aqueous solutions where it is possible to predict activity coefficients (γ^S) for ion-ion interactions, for mixed alcohol/water/salt systems, there is currently no similar method for predicting γ^N (Kan et al., 2002). Using the semi-empirical approach of Kan et al. (2003, 2002), it is currently only possible to predict alcohol activity coefficients (γ^N) for a limited number of salt/water mineral systems and over a limited range of methanol-water or ethylene glycol-water compositions (see also Kan et al., 2003). Ethanol activity coefficients (γ^N) for specific salt/water mineral systems over a range of ethanol-water compositions could likely be predicted using a similar, semi-empirical approach, if experiments were conducted to obtain the required supporting data.

7.2 Extractions with minerals

As a first step in developing and testing an ethanol-water extraction methodology, extractions were conducted on minerals, including celestite, gypsum and halite. For extractions conducted on both celestite and gypsum, the concentrations of Sr^{2+} and SO_4^{2-} or Ca^{2+} and SO_4^{2-} , respectively, were below or near the detection limits at both ethanol-water ratios of 99.3:0.7 and 90:10 for reaction times of 2 and 60 minutes. The detection limits for Sr^{2+} , Ca^{2+} , and SO_4^{2-} in the analysed solutions are 0.5, 0.5 and 1 mg/L, respectively (IC analysis). All other major ions were also below detection in the analysed solutions. The corresponding detection limits per kilogram of solid (in this case, mineral) are Sr^{2+} , $\text{Ca}^{2+} < 2.5 \text{ mg/kg}_{\text{mineral}}$ and $\text{SO}_4^{2-} < 5.0 \text{ mg/kg}_{\text{mineral}}$.

The results for the extractions conducted on halite are given in Table 40 in units of mg/kg of halite. The analytical uncertainty associated with the results is estimated at $\pm 10\%$ based on the analytical uncertainty in measuring ion concentrations greater than 100 mg/L using ion chromatography. In extractions conducted at the same ethanol:water ratio with different reaction times of 2 or 60 minutes (Table 40), the extracted Na^+ and Cl^- concentrations are the same within $\pm 8\%$, within the analytical uncertainty. With an increase in the volume percent of ethanol from 90 to 99.3%, the concentrations of Na^+ and Cl^- decrease by approximately 75%.

Table 40: Amount of Na⁺ and Cl⁻ dissolved in ethanol-water solutions during extraction experiments with halite for two different reaction times (units are mg per kg of halite).

Ethanol in solution (volume %)	Mass of halite (g)	Reaction time (minutes)	Na ⁺ (mg/kg _{NaCl})	Difference between replicates (%)	Cl ⁻ (mg/kg _{NaCl})	Difference between replicates (%)
99.3	6	2	1010		1670	
99.3	6	60	933	8.3	1560	7.1
90	2	2	3580		5850	
90	2	60	3770	5.3	6260	7.0

7.3 Extractions with DGR-3 samples

Based on the limited dissolution of celestite and gypsum and the significant decrease in the solubility of halite in ethanol-water mixtures observed in the extractions conducted on these minerals, a series of trial experiments were conducted on DGR-3 samples. The results of extractions conducted on select samples using different volume percentages of ethanol in solution are presented in Table 41.

During experiments with samples DGR-3 335.22 and DGR-3 380.88 from the Salina A2 and A1 Evaporites, respectively, a white precipitate was observed in the filtered solution immediately after the ethanol-water extraction, prior to drying of the filtrate. Both evaporites consist primarily of anhydrite; sample DGR-3 335.22 consists of 90% anhydrite by weight (Table 3, section 3.2). The precipitates in the filtered solution were also identified as anhydrite using XRD analysis. Consequently, the calcium and sulphate concentrations determined for these two samples cannot be used (shaded values in Table 41).

Five replicate extractions were conducted at an ethanol-water ratio of 99.3:0.7 on sample DGR-3 531.65 from the Georgian Bay Formation (Table 41). The identical experimental procedure was applied to all five samples. The standard deviation in the concentration determined for each ion and the maximum and average difference between the measured ion concentrations (in percent) are also shown. The maximum difference observed between the Na⁺ and Cl⁻ concentrations in the five replicates are 11 and 19%, respectively. This is significantly higher deviation than observed for the two experiments conducted on halite (with different reaction times) of 2 and 60 minutes, where a maximum difference of ±8% or less was observed in the concentrations of both these ions. For Mg²⁺ and Ca²⁺, the maximum difference measured in their concentrations in the five replicate analyses is 20% or less, whereas higher values are calculated for Br⁻ (23%) and K⁺ (42%). Using the maximum difference observed between the measured concentration of ion in the five replicate extractions (in mg/kg_{rock}) and its average concentration in the five replicates, the average percent difference between the five replicates was calculated (% Diff. – Aver. in Table 41). On the basis of the 14% difference observed in the concentration of K⁺, an estimated uncertainty of ±15% is assigned to the results of the ethanol-water extractions in the following discussion and in all figures.

In mineralogical investigations, halite was identified in samples DGR-3 270.06 (Salina C-Unit) and DGR-3 391.34 (Guelph Formation). The quantities of Na⁺ and Cl⁻ extracted in these two samples in solutions containing 90% ethanol can be compared to those determined for pure halite in 90% ethanol solutions (Table 40). Both the Na⁺ and Cl⁻ concentrations measured in the extracts of these two samples are within

$\pm 15\%$ of those measured for pure halite. This observation suggests that Na^+ and Cl^- in these extractions are predominantly from halite dissolution and that their concentrations are likely controlled by the solubility of halite in a 90% ethanol solution.

Comparing the results for the ethanol-water and aqueous extractions in Table 41, in most cases, ion concentrations determined in the ethanol-water extractions are lower than in the aqueous extractions. The effect of varying the percentage of ethanol in solution from 0 to 99.9% on the extracted ion concentrations is illustrated in Figure 48 for the two samples in which halite was identified based on aqueous leaching and mineralogical studies. The quantities of both Na^+ and Cl^- extracted from the two samples decreased as the volume percent ethanol in solution was increased from 0 to 70% and decreased further as the proportion of ethanol in the solution was increased. A similar behaviour is observed for K^+ , although the decrease between 0 and 70% ethanol is within the analytical uncertainty. Extracted Ca^{2+} concentrations decreased sharply in the 70% ethanol solution in both samples and then decreased further in one sample with increasing ethanol in solution, but increased in the other sample. The change observed in the extracted concentrations of both Mg^{2+} and Br^- as a function of the volume % ethanol is not systematic for these two samples.

In Figure 49, the quantities of major ions extracted are plotted as a function of the volume of ethanol in solution for four samples in which no halite was identified (in terms of the Ca^{2+} concentrations, note that anhydrite was identified in sample DGR-3 531.65). In all four samples examined, the extracted K^+ concentrations decrease with increasing volume percent ethanol from 0 to over 99%. In three of the four samples (DGR-3 646.29 is the exception), the concentrations of Na^+ , Ca^{2+} , Mg^{2+} , Cl^- and Br^- appear to be relatively constant (within the approximate analytical uncertainty of $\pm 15\%$) with increasing ethanol in solution from 0 up to 80% and decrease in 90 vol.% ethanol solutions, with the lowest values measured in the solutions containing ≈ 98 to 99% ethanol.

The extracted concentrations of Na^+ and Cl^- decrease from the aqueous (0% ethanol) to the 70 vol.% ethanol-water extraction in sample DGR-3 646.29 (Blue Mountain Formation). Although the extracted concentrations of Na^+ , Ca^{2+} , Mg^{2+} and Br^- decrease with an increase from 0 to 80 vol.% ethanol in solution, an apparent increase is observed in the 90 vol.% ethanol solution and then a decrease in the 98-99 vol.% solution; these changes are within the estimated analytical uncertainty. Taken together, the results of ethanol-water extractions conducted at multiple ethanol-water ratios on samples with no evidence for the presence of soluble salts, suggest that the extracted concentrations vary significantly from the aqueous extractions when the volume percent ethanol is 90% or higher. If these differences simply reflected the accuracy with which the small quantities of water can be added, then we would expect to see the same behaviour for all ions as a function of the volume percent ethanol in solution.

The results of extractions conducted on all samples at an ethanol-water ratio designed to match the quantity of water originally in the sample are given in Table 42. As described in section 2.3, all samples were dried and powdered prior to the ethanol-water extractions. During the drying process, water is removed from the samples, but solutes originally present in the porewater remain in the powdered rock material. The solutions containing the highest volume percentages of ethanol were designed to replace the amount of water (as H_2O) removed from the rock material by drying at 105°C ($\text{WC}_{\text{Grav.dry}}$). This ratio was selected on the premise that only salts precipitated from the porewater during drying would be redissolved during the extractions and because the amount of water added back in was equal to the quantity originally present in the rock material, the ion concentrations in the extract solutions would be equal to those originally present in the porewater. One issue is the high uncertainties that will be induced by “adding back in” the amount of water originally in the rock material, particularly when the water content of the sample is low. In addition, as described in section 7.1 above, the activities of the ions in the water-salt solution of

the porewater should be equal to their activities in a mixed ethanol-water-salt solution. However, due to ion-alcohol interactions, the concentration of an ion in the mixed ethanol-water-salt solution formed during the extraction procedure will not be directly equivalent to the concentration that would have been present in the water-salt solution of the original porewater.

In order to evaluate the results given in Table 42, it is assumed that Br^- behaves conservatively during the extractions, in that any Br^- extracted is from the porewater and is not influenced by mineral dissolution/precipitation reactions or by ion exchange processes. The concentrations of Br^- and Cl^- determined in the aqueous and ethanol-water extractions in which the amount of water was matched to the amount of water (as H_2O) originally in the sample are compared in Table 4. Out of the 35 samples examined, 9 samples have Br^- concentrations that are the same as those determined in the aqueous extractions, within the approximate analytical uncertainty of $\pm 15\%$. For the remainder of the samples, the Br^- concentrations determined using the ethanol-water extractions matched to the water content of the sample are between 20 and 40% lower than those determined using aqueous leaching.

If there are no Cl-bearing salts present in the samples, then Cl^- may also be used a conservative tracer of porewater concentrations. Considering only DGR-3 samples in which no evidence of soluble salts was found (based on mineralogical and/or saturation indices of soluble mineral phases in the aqueous extract solutions, Table 35, section 6.2), chloride concentrations in the ethanol extracts are between 27 and 65% lower than those determined in the aqueous extracts (Table 40). For ethanol extractions conducted at 70% (8 samples in Table 41), the difference in Br^- and Cl^- concentrations compared to the aqueous extractions is lower. Br^- concentrations determined are between 17 and 31% lower and Cl^- concentrations are 18 to 29% lower than in the aqueous solutions. These large differences may be the result of i) incomplete dissolution of salts originally present in the porewater, if the amount of water and/or contact time is too short to completely redissolve all the salts; ii) increased importance of ion-alcohol interaction coefficients at very high ethanol-water ratios, or a combination of both these factors. Consequently, these results are not considered further in the interpretation of porewater compositions.

It was noted above that the difference between the Cl^- concentrations measured in the aqueous and ethanol extractions was much smaller in solution with the lowest volume percent ethanol (70%) examined in this study. If the ethanol-water extraction method is to be further tested, it may be worthwhile to investigate ethanol-water extractions in solutions containing much lower volumes of alcohol. Kan et al. (2003) also noted that halite was much less soluble in methanol than in ethylene glycol, suggesting that the use of different alcohols in the extractions could also be explored. Finally, further testing of the method should include replicate extractions conducted on multiple samples to establish more firmly the analytical uncertainty associated with the extractions, as well as implementing any modifications to the experimental technique that could reduce the analytical uncertainty.

Table 41: Results of ethanol-water extractions conducted at multiple ethanol:water ratios (mg/kg of dry rock). Concentrations determined in the aqueous extractions (0% ethanol) are also shown for comparison.

Sample ID ¹ (NWMO)	Formation	Soluble minerals ²	Ethanol in solution (Vol. %)	Na ⁺	K ⁺	Mg ²⁺	Ca ²⁺	Sr ²⁺	Cl ⁻	Br ⁻	SO ₄ ²⁻
				(mg/kg _{rock})	(mg/kg _{rock})	(mg/kg _{rock})	(mg/kg _{rock})	(mg/kg _{rock})	(mg/kg _{rock})	(mg/kg _{rock})	(mg/kg _{rock})
DGR-3 270.06	Salina - C Unit	Halite, gypsum, anhydrite	0.00	6450	210	46.7	1140	13.1	10400	10.1	2920
			70.00	5620	55.5	39.5	b.d.	7759	b.d.	39.9	
			90.00	4230	24.2	18.2	b.d.	5820	19.7	b.d.	
			97.13	1330	b.d.	b.d.	47.6	b.d.	2018	b.d.	b.d.
DGR-3 335.22	Salina – A2 Evaporite	Anhydrite, gypsum	0.00	51.8	11.7	5.2	795	17.2	102	b.d.	1890
			70.00	44.5	b.d.	2.95	47.7	b.d.	83.9	b.d.	99.5
			90.00	33.7	b.d.	2.07	309	3.41	64.7	b.d.	776
			99.80	13.4	b.d.	b.d.	369	9.06	23.3	b.d.	984
DGR-3 380.88	A1 Evaporite	Anhydrite	0.00	62.1	15.0	3.5	1090	b.d.	187	b.d.	2510
			70.00	74.3	6.39	17.3	194	b.d.	151	b.d.	429
			90.00	53.5	2.68	11.1	53.8	b.d.	136	1.99	93.5
			99.93	66.0	b.d.	14.2	612	b.d.	89.4	b.d.	1850
DGR-3 391.34	Guelph	Halite	0.00	10600	120	112	1270	4.2	19900	48.3	2090
			70.00	11300	102	278	270	b.d.	16300	72.6	46.0
			90.00	3680	54.8	263	272	b.d.	6410	36.9	37.2
			99.13	974	71.2	272	380	b.d.	2910	39.2	b.d.
DGR-3 502.55	Queenston		0.00	525	291	72.4	644	14.6	2060	25.4	439
			70.00	477	155	68.5	456	b.d.	1830	21.2	9.93
			80.00	467	130	62.0	462	b.d.	1790	20.8	b.d.
			90.00	469	81.6	57.5	505	b.d.	1760	21.5	b.d.
			95.00	419	54.4	48.4	455	b.d.	1570	19.2	b.d.
			99.43	368	48.3	18.2	327	1.88	1330	19.1	b.d.

¹ Depth of sample in meters below ground surface is given by the second half of the NWMO sample ID.

² Identified during mineralogical investigations using XRD analysis and/or SEM-EDS.

b.d. indicates that the ion concentration was below detection in the extraction solution and corresponds to concentrations of K⁺ < 0.9, Mg²⁺ < 0.9, Sr²⁺ < 0.9, Br⁻ < 1.7 and SO₄²⁻ < 1.0 mg/kg_{rock}.

All extractions were conducted using a mass of solid to volume of liquid (ethanol + water) ratio of 1:2.5.

Shaded values are suspected due to anhydrite precipitation in filtrate.

Table 41 (Cont'd): Results of ethanol-water extractions conducted at multiple ethanol:water ratios (mg/kg of dry rock).

Sample ID ¹ (NWMO)	Formation	Soluble min- erals ²	Ethanol in solution (Vol. %)	Na ⁺	K ⁺	Mg ²⁺	Ca ²⁺	Sr ²⁺	Cl ⁻	Br ⁻	SO ₄ ²⁻
				(mg/kg _{rock})	(mg/kg _{rock})	(mg/kg _{rock})	(mg/kg _{rock})	(mg/kg _{rock})	(mg/kg _{rock})	(mg/kg _{rock})	(mg/kg _{rock})
DGR-3 531.65	Georgian Bay	Anhydrite	0.00	844	279	96.6	782	16.7	2850	32.2	327
			70.00	862	163	103	717	b.d.	2840	31.4	7.91
			80.00	847	144	97.3	710	b.d.	2800	32.2	b.d.
			90.00	802	84.0	91.8	727	b.d.	2720	30.5	b.d.
			95.00	653	63.8	72.6	648	b.d.	2290	25.9	b.d.
			99.34	540	32.9	44.7	518	b.d.	1750	21.9	b.d.
			99.34	578	46.9	51.8	474	b.d.	2090	26.5	b.d.
			99.34	520	39.9	50.0	503	b.d.	1880	25.3	b.d.
			99.34	532	40.6	51.2	488	b.d.	1980	26.4	b.d.
			99.34	570	44.9	51.1	503	3.96	2010	27.0	2.13
			STD	25	5	3	17	n.a.	130	2	n.a.
			% Diff. - Max.	11	42	16	9	n.a.	19	23	n.a.
% Diff. - Aver.	5	14	4	4	n.a.	8	6	n.a.			
DGR-3 646.29	Blue Mountain		0.00	1410	472	91.9	1280	33.0	5190	62.5	28.8
			70.00	970	80.9	58.3	933	b.d.	4210	50.5	16.3
			90.00	1020	39.6	67.1	1060	b.d.	3980	56.4	b.d.
			98.87	820	61.3	53.6	1020	b.d.	2430	52.2	b.d.
DGR-3 676.21	Cobourg – LM		0.00	721	321	85.3	446	14.5	2530	25.3	26.4
			70.00	744	113	71.6	406	b.d.	1820	18.5	11.7
			90.00	617	51.7	62.8	445	b.d.	1930	31.9	b.d.
			99.60	541	48.7	38.2	390	b.d.	1520	32.7	b.d.

¹ Depth of sample in meters below ground surface is given by second half of the NWMO sample ID.

² Identified during targeted mineralogical investigations using XRD analysis and/or SEM-EDS.

b.d. indicates that the ion concentration was below detection in the extraction solution and corresponds to concentrations of K⁺ < 0.9, Mg²⁺ < 0.9, Sr²⁺ < 0.9, Br⁻ < 1.7 and SO₄²⁻ < 1.0 mg/kg_{rock}.

All extractions were conducted using a mass of solid to volume of liquid (ethanol + water) ratio of 1:2.5.

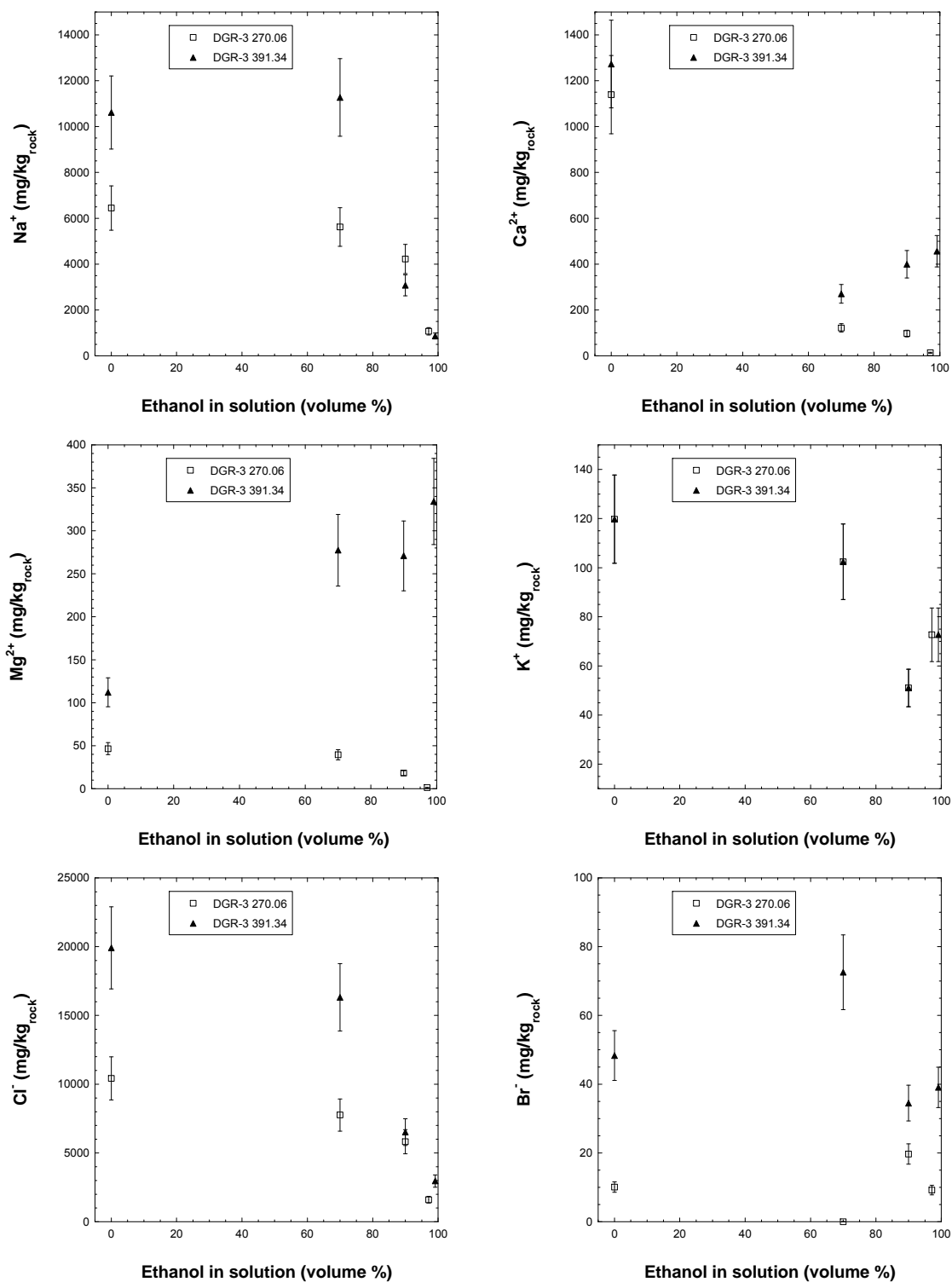


Figure 48: Extracted major ion concentrations in mg/kg_{rock} with increasing ethanol in solution from 0 to over 99 vol.%. Results are shown for two samples in which halite was identified. Error bars show the approximate analytical uncertainty of $\pm 15\%$ in the concentrations determined using ethanol-water extractions.

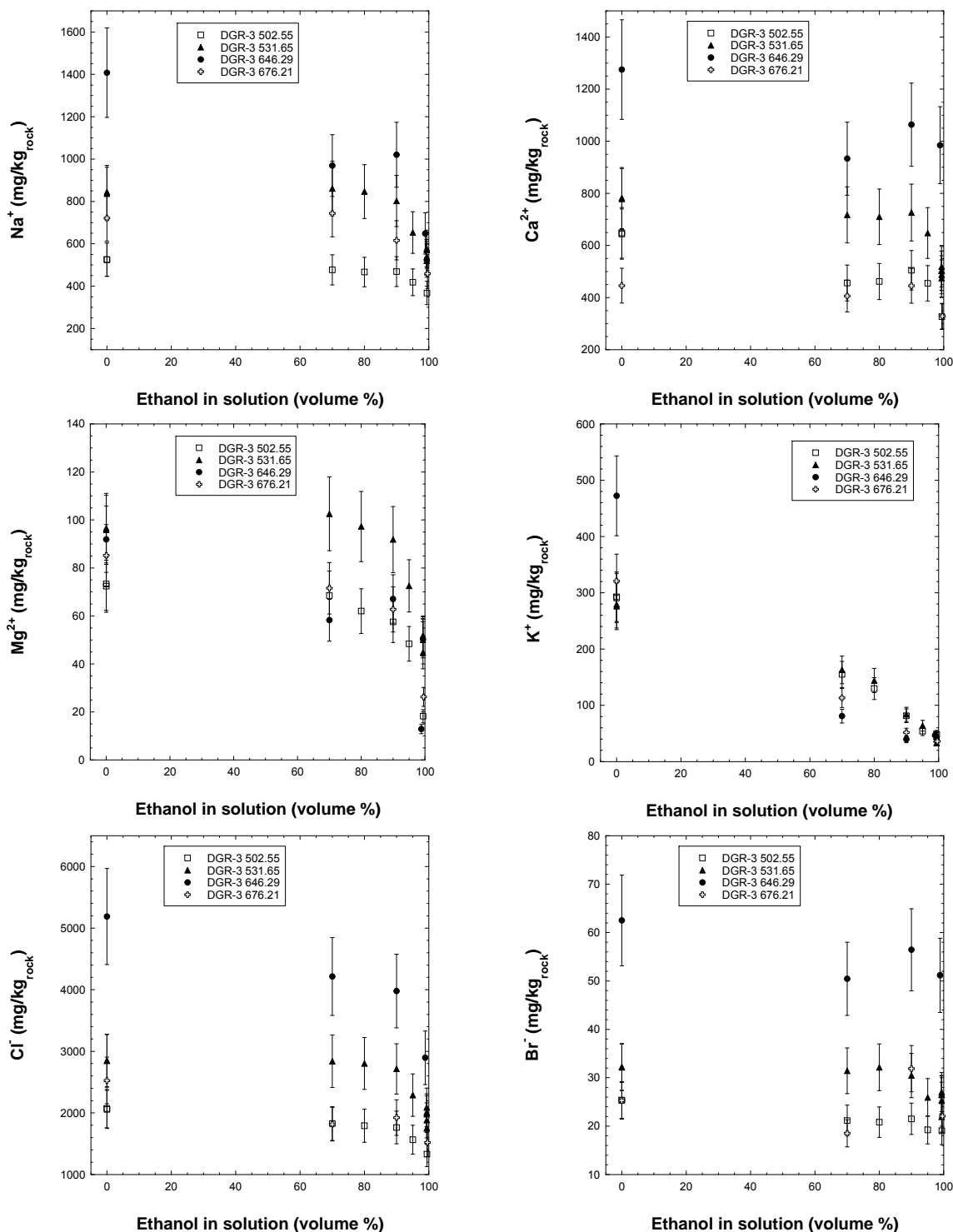


Figure 49: Extracted major ion concentrations in mg/kg_{rock} with increasing ethanol in solution from 0 to over 99 vol.%. Results are shown for selected samples where no evidence for halite was found (anhydrite was identified in DGR-3 531.65). Error bars show the estimated analytical uncertainty of $\pm 15\%$ in the concentrations determined using ethanol-water extraction

Table 42: Results of ethanol-water extractions conducted at one ethanol:water ratio chosen to replicate the original water content of the rock. Results are reported in mg/kg of dry rock.

Sample ID ¹ (NWMO)	Formation	Soluble minerals ²	Ethanol in solution (Vol. %)	Na ⁺	K ⁺	Mg ²⁺	Ca ²⁺	Sr ²⁺	Cl ⁻	Br ⁻	SO ₄ ²⁻
				(mg/kg _{rock})	(mg/kg _{rock})	(mg/kg _{rock})	(mg/kg _{rock})	(mg/kg _{rock})	(mg/kg _{rock})	(mg/kg _{rock})	(mg/kg _{rock})
DGR-3 198.72	Salina – F Unit	Gypsum	98.35	294	1.43	b.d.	2.78	b.d.	447	b.d.	2.62
DGR-3 208.41	Salina - F Unit	Gypsum	93.39	550	2.77	2.29	16.7	b.d.	912	2.61	2.74
DGR-3 248.71	Salina – E Unit	Gypsum	97.89	795	2.33	b.d.	5.63	b.d.	1280	2.81	4.58
DGR-3 270.06	Salina - C Unit	Halite, gypsum, anhydrite	97.13	1330	b.d.	b.d.	47.6	b.d.	2020	b.d.	b.d.
DGR-3 289.36	Salina – B Unit	Gypsum	96.98	1030	5.74	6.34	24.0	b.d.	1680	6.28	15.4
DGR-3 312.53	Salina - A2 Unit		97.61	928	2.77	11.3	3.41	b.d.	1510	3.84	8.13
DGR-3 335.22	Salina – A2 Evap.	Anhydrite, gypsum	99.80	13.4	b.d.	b.d.	369	9.06	23.3	b.d.	984
DGR-3 344.06	Salina -A1 Unit		99.85	63.5	b.d.	b.d.	3.55	b.d.	98.3	b.d.	1.62
DGR-3 380.88	A1 Evaporite	Anhydrite	99.93	66.0	b.d.	14.2	612	b.d.	89.4	b.d.	1850
DGR-3 391.34	Guelph	Halite	99.13	974	71.2	272	380	b.d.	2910	39.2	b.d.
DGR-3 435.62	Cabot Head		98.54	666	81.3	193	1790	13.3	5060	85.0	2.31
DGR-3 453.41	Manitoulin		99.77	321	35.9	73.8	463	1.72	1590	24.5	2.04
DGR-3 468.76	Queenston		98.73	602	65.9	126	1530	7.66	4320	71.8	1.75
DGR-3 484.58	Queenston	Anhydrite, celestite	99.01	617	56.4	85.5	869	4.69	3360	54.5	7.04
DGR-3 502.55	Queenston		99.43	368	48.3	18.2	327	1.88	1330	19.1	b.d.
DGR-3 531.65	Georgian Bay	Anhydrite	99.34	548 ^a	41.1 ^a	49.8 ^a	497 ^a	b.d.	1940 ^a	25.4 ^a	1.19 ^a
DGR-3 581.47	Georgian Bay		98.71	477	60.4	40.0	1255	11.8	3560	64.2	1.93
DGR-3 621.63	Blue Mountain		98.79	683	63.6	47.5	1300	9.87	3790	66.8	3.20
DGR-3 646.29	Blue Mountain		98.87	820	61.3	53.6	1016	b.d.	2430	52.2	b.d.
DGR-3 665.29	Cobourg – CM		99.80	161	17.6	b.d.	24.9	b.d.	310	5.27	1.81

¹ Depth of sample in meters below ground surface is given by the second half of the NWMO sample ID.

² Identified during targeted mineralogical investigations using XRD analysis and/or SEM-EDS.

^a Average value calculated from 5 replicate analyses; standard deviations for each ion are given in Table 41.

b.d. indicates that the ion concentration was below detection in the extraction solution and corresponds to concentrations of K⁺ < 0.9, Mg²⁺ < 0.9, Sr²⁺ < 0.9, Br⁻ < 1.7 and SO₄²⁻ < 1.0 mg/kg_{rock}.

All extractions were conducted using a mass of solid to volume of liquid (ethanol + water) ratio of 1:2.5.

Table 42 (Cont'd): Results of ethanol-water extractions conducted at one ethanol:water ratio chosen to replicate the original water content of the rock. Results are reported in units of mg/kg of dry rock.

Sample ID ¹ (NWMO)	Formation	Soluble Minerals ²	Ethanol in solution (Vol. %)	Na ⁺	K ⁺	Mg ²⁺	Ca ²⁺	Sr ²⁺	Cl ⁻	Br ⁻	SO ₄ ²⁻
				(mg/kg _{rock})	(mg/kg _{rock})	(mg/kg _{rock})	(mg/kg _{rock})	(mg/kg _{rock})	(mg/kg _{rock})	(mg/kg _{rock})	(mg/kg _{rock})
DGR-3 676.21	Cobourg – LM		99.60	541	48.7	38.2	390	b.d.	1520	32.7	b.d.
DGR-3 678.92	Cobourg – LM		99.87	159	10.4	1.09	26.2	b.d.	302	5.05	2.69
DGR-3 685.52	Cobourg – LM		99.76	245	16.0	5.37	75.7	b.d.	564	8.49	2.11
DGR-3 690.12	Cobourg – LM		99.84	185	10.6	3.29	58.9	b.d.	423	5.80	1.28
DGR-3 692.82	Cobourg – LM		99.69	386	24.0	12.7	186	b.d.	1090	14.0	1.42
DGR-3 697.94	Cobourg – LM		99.71	261	14.6	5.84	100	b.d.	673	9.39	1.62
DGR-3 710.38	Sherman Fall		99.92	95.3	5.16	1.38	28.5	b.d.	213	3.07	1.92
DGR-3 725.57	Sherman Fall		99.60	424	22.4	8.25	180	1.07	1140	15.1	2.30
DGR-3 744.27	Kirkfield		99.56	427	19.4	6.28	139	b.d.	1034	13.8	1.83
DGR-3 761.56	Kirkfield		99.89	33.0	0.94	b.d.	7.08	b.d.	57.7	b.d.	2.73
DGR-3 777.33	Coboconk		99.83	103	2.00	b.d.	9.00	b.d.	177	3.00	5.00
DGR-3 807.43	Gull River		99.86	111	2.95	b.d.	13.5	b.d.	201	2.64	2.26
DGR-3 843.92	Gull River		99.88	135	2.14	b.d.	10.5	b.d.	232	3.47	1.74
DGR-3 852.18	Shadow Lake		98.75	580	13.6	46.3	581	2.28	2110	28.8	1.31
DGR-3 856.06	Cambrian		99.81	262	20.8	62.6	65.7	b.d.	730	8.94	3.37

¹ Depth of sample in meters below ground surface is given by the second half of the NWMO sample ID.

² Identified during targeted mineralogical investigations using XRD analysis and/or SEM-EDS.

b.d. indicates that the ion concentration was below detection in the extraction solution and corresponds to concentrations of K⁺ < 0.9, Mg²⁺ < 0.9, Sr²⁺ < 0.9 and Br⁻ < 1.7 and SO₄²⁻ < 1.0 mg/kg_{rock}.

All extractions were conducted using a mass of solid to volume of liquid (ethanol + water) ratio of 1:2.5.

Table 43: Comparison between the quantity of Br⁻ and Cl⁻ determined using aqueous extraction and an ethanol-water extraction in which the quantity of water added was matched to the original water content of the sample.

Sample ID ¹ (NWMO)	Formation	Aqueous Extraction		Ethanol Extraction			Difference (Ethanol – aqueous)	
		Br (mg/kg _{rock})	Cl (mg/kg _{rock})	Ethanol in solution (vol. %)	Br (mg/kg _{rock})	Cl (mg/kg _{rock})	Br (%)	Cl (%)
DGR-3 198.72*	Salina – F Unit	2.3	n.a.	98.35	b.d.	n.a.	-	n.a.
DGR-3 208.41*	Salina - F Unit	2.7	n.a.	93.39	2.61	n.a.	-4	n.a.
DGR-3 248.71*	Salina – E Unit	2.6	n.a.	97.89	2.81	n.a.	6	n.a.
DGR-3 270.06*	Salina - C Unit	10.1	n.a.	97.13	9.21	n.a.	-9	n.a.
DGR-3 289.36*	Salina – B Unit	10.7	n.a.	96.98	8.00	n.a.	-25	n.a.
DGR-3 312.53	Salina - A2 Unit	5.5	n.a.	97.61	3.84	n.a.	-30	n.a.
DGR-3 335.22*	Salina – A2 Evaporite	b.d.	n.a.	99.80	b.d.	n.a.	-	n.a.
DGR-3 344.06	Salina -A1 Unit	b.d.	n.a.	99.85	b.d.	n.a.	-	n.a.
DGR-3 380.88*	A1 Evaporite	b.d.	n.a.	99.93	b.d.	n.a.	-	n.a.
DGR-3 391.34*	Guelph	48.3	n.a.	99.13	39.2	n.a.	-19	n.a.
DGR-3 435.62	Cabot Head	97.4	8060	98.54	85.0	5060	-13	-37
DGR-3 453.41	Manitoulin	33.5	2230	99.77	24.5	1590	-27	-29
DGR-3 468.76	Queenston	85.3	6930	98.73	71.8	4320	-16	-38
DGR-3 484.58*	Queenston	64.5	n.a.	99.01	54.5	n.a.	-16	n.a.
DGR-3 502.55	Queenston	25.4	2060	99.43	19.1	1330	-25	-35
DGR-3 531.65*	Georgian Bay	32.2	n.a.	99.34	25.4	n.a.	-21	n.a.
DGR-3 581.47	Georgian Bay	72.7	6260	98.71	64.2	3560	-12	-43
DGR-3 621.63	Blue Mountain	74.0	6300	98.79	66.8	3790	-10	-40
DGR-3 646.29	Blue Mountain	62.5	5190	98.87	51.2	2900	-18	-44
DGR-3 665.29	Cobourg – CM	6.8	677	99.80	5.27	310	-23	-54

b.d. below detection limit for Br of <1.7 mg/kg_{rock}.

n.a. not applicable. It is assumed that chloride cannot be used as a tracer for these samples due to presence of soluble mineral phases.

- not calculated because Br concentration was below detection in ethanol-water extracts.

Table 43 (Cont'd): Comparison between the quantity of Br⁻ and Cl⁻ determined using aqueous extraction and an ethanol-water extraction in which the quantity of water added was matched to the original water content of the sample.

Sample ID ¹ (NWMO)	Formation	Aqueous Extraction		Ethanol Extraction			Difference (Ethanol – aqueous)	
		Br (mg/kg _{rock})	Cl (mg/kg _{rock})	Ethanol in solution (vol. %)	Br (mg/kg _{rock})	Cl (mg/kg _{rock})	Br (%)	Cl (%)
DGR-3 676.21	Cobourg – LM	25.3	2530	99.60	22.1	1520	-13	-40
DGR-3 678.92	Cobourg – LM	7.6	761	99.87	5.05	302	-33	-60
DGR-3 685.52	Cobourg – LM	11.3	1030	99.76	8.49	564	-25	-45
DGR-3 690.12	Cobourg – LM	7.4	774	99.84	5.80	423	-21	-45
DGR-3 692.82	Cobourg – LM	15.3	1490	99.69	14.0	1090	-8	-27
DGR-3 697.94	Cobourg – LM	12.3	1160	99.71	9.97	673	-19	-42
DGR-3 710.38	Sherman Fall	4.4	464	99.92	3.07	213	-30	-54
DGR-3 725.57	Sherman Fall	20.6	1810	99.60	15.1	1140	-27	-37
DGR-3 744.27	Kirkfield	15.6	1600	99.56	13.8	1034	-12	-35
DGR-3 761.56*	Kirkfield	1.5	n.a.	99.89	b.d.	n.a.	n.a.	n.a.
DGR-3 777.33	Coboconk	4.5	507	99.83	3.00	177	-34	-65
DGR-3 807.43	Gull River	3.8	435	99.86	2.64	201	-30	-54
DGR-3 843.92	Gull River	4.7	534	99.88	3.47	232	-26	-57
DGR-3 852.18	Shadow Lake	42.7	3910	98.75	26.6	1980	-38	-49
DGR-3 856.06	Cambrian	10.1	1130	99.81	8.94	730	-11	-35

b.d. below detection limit for Br of <1.7 mg/kg_{rock}.

n.a. not applicable. It is assumed that chloride cannot be used as a tracer for these samples due to presence of soluble mineral phases.

- not calculated because Br concentration was below detection in ethanol-water extracts.

8 Out-diffusion Experiments

A detailed description of the methodology for the out-diffusion experiments is given in Koroleva et al. (2009). In brief, the central part of a fresh core sample is immersed in an experimental solution of known chemical and isotopic ($\delta^{13}\text{C}$) composition and sealed in a container. The container is placed in a water bath at 45 °C, which also provides slow, continuous mixing. As shown in Table 44, out-diffusion experiments were conducted on four samples from borehole DGR-4, including a dolomitic shale from the Salina F Unit (DGR-4 189.16), a shale from the Georgian Bay Formation (DGR-4 520.42), an argillaceous limestone from the Cobourg Formation (DGR-4 665.41) and a limestone from the Kirkfield Formation (DGR-4 730.07). The water:solid ratio ranged from 1.4 to 2.6.

Table 44: DGR-4 samples and experimental parameters used in the out-diffusion experiments.

Sample / Parameter	Unit	DGR-4 189.16	DGR-4 520.42	DGR-4 665.41	DGR-4 730.07
Formation		Salina F Unit	Georgian Bay	Cobourg	Kirkfield
Experimental temperature <i>Before out-diffusion experiment</i>	°C				
Initial mass experimental solution	g	178.55	148.90	180.07	150.60
Initial mass rock	g	328.732	233.810	244.311	389.144
Solid / Liquid ratio		1.84	1.57	1.36	2.58

Possible alterations to the rock samples that may occur during out-diffusion experiments include i) mineral dissolution reactions, which will modify the composition of the test solution and may also lead to an increase in the porosity of the rock core and ii) sulphide mineral oxidation, which will effect the sulphate concentrations and pH values of the test solution. To minimize dissolution of calcite and dolomite during the experiments, the initial test solution was prepared by adding synthetic CaCO_3 and MgCO_3 to saturation with these phases at room temperature ($20 \pm 2^\circ\text{C}$) and equilibration with atmospheric pressure (PCO_2 of $10^{-3.5}$). The measured chemical and $\delta^{13}\text{C}$ composition of the initial test solution is given in Table 45. This initial solution has a relatively high concentration of Mg^{2+} (161 mg/L) and alkalinity (12.3 meq/L). The measurable potassium in the initial test solution suggests that K^+ occurs as an impurity in the synthetic carbonates used to prepare the solution. The test solution is predicted to be supersaturated with respect to both calcite and dolomite and to be at a PCO_2 of $10^{-2.79}$ when modelled using PHREEQC v.2.15.0 and the PHREEQC thermodynamic database (phreeqC.dat). The predicted, supersaturation may reflect higher solubility of synthetic calcium and magnesium carbonates, compared to the solubility of the calcite and dolomite mineral phases included in the thermodynamic database of the geochemical modelling code. The negative $\delta^{13}\text{C}$ value of the test solution reflects the isotopic carbon composition of the synthetic calcium and magnesium carbonates used to prepare the solution.

Table 45: Chemical and isotopic composition of initial test solution used in the out-diffusion experiments.

Parameter	Test solution
pH	8.63
pH initial (alk. Titration)	8.60
K ⁺	1.7 mg/L
Ca ²⁺	6.5 mg/L
Mg ²⁺	161 mg/L
Alkalinity	12.3 meq/L
Mineral saturation indices	
Calcite	+0.64
Dolomite	+2.99
δ ¹³ C	-17.4 ‰
PCO ₂	10 ^{-2.79}

The approach of the system to steady-state is monitored by withdrawing small (0.5 ml) subsamples of the experimental solution at intervals and measuring the concentration of chemically conservative anions (e.g., Cl⁻, Br⁻ and in some cases, SO₄²⁻). After attainment of steady-state conditions (i.e., when the Cl⁻ concentration in the reservoir was constant, within the analytical uncertainty of ±5%), the experiment is terminated, the final chemical and isotopic (δ¹³C) composition of experimental solution is measured and the water content of the core is determined gravimetrically after being dried for a few days at 40 °C and then at 105 °C.

8.1 Time-series Cl⁻ concentrations

The chloride concentrations determined in the time-series subsamples and the final solutions are corrected for both the mass of solution removed from the cells and the mass of an ion (*i*) removed using the following expression:

$$C_{S_x,cor} = \frac{C_S * (m_{ExSi} - \sum m_S) - m_{ExSi} * C_{ExSi} + \sum m_S * C_S}{m_{ExSi}}$$

Where $C_{S_x,cor}$ is the corrected concentration of ion *i* in a subsample or final solution, C_S is the concentration of ion *i* in solution, m_S is the mass of the subsample, m_{ExSi} is the initial mass of the experimental solution and C_{ExSi} is the initial concentration of ion in the experimental solution.

The corrected Cl⁻ concentrations in the subsamples and final solution are plotted as a function of reaction time for the four samples examined in Figure 50. In the experiments conducted with shale from the Salina F Unit and limestones from the Cobourg and Kirkfield formations, the chloride concentrations increased within the first few days of reaction, reaching plateaus at chloride concentrations of between 560 and 3800 mg/L after approximately 20 days. To ensure steady-state conditions had been achieved, the experiments were run over 110 days. In the experiment with the Salina F Unit shale (DGR-4 189.16), the attainment of steady-state conditions is less clear, with an apparent trend towards lower Cl⁻ concentrations in the final three samples, although these values are within the analytical uncertainty of ±10%.

In the experiment with the shale from the Georgian Bay Formation, chloride concentrations are observed to increase sharply at the beginning of the experiment to a high of ca. 8500 mg/L after 4 days of reaction and then decrease to a steady-state value of 6100 mg/L by 21 days. This behaviour could be explained by the immediate dissolution of a soluble, Cl-bearing phase(s) such as halite present in the rock matrix as a primary phase, or formed at the rim of the core by evaporation of porewater during sample preparation, prior to the start of the experiments. In this case, the decrease in Cl⁻ concentrations observed at later times would be a result of increased equilibration (i.e., mixing) with porewater having lower Cl⁻ concentrations. When the experiment was terminated, it was found that the core had split in half during the experiment, apparently along a bedding plane, possibly as a result of stress-release. After several days of drying at 40 °C, a reaction rim was visible on both halves of the bedding plane, along the outer rim (Figure 51A). In contrast, reaction rims were not observed on the top or bottom of the core. An example of a bedding plane observed in the sample after the experiment, along which the sample did not split, is shown in Figure 51B. No supporting mineralogical information is available for this sample. In principle, dissolution of soluble salts along such a plane upon submersion in the experimental solution is one possible explanation for the high concentration of Cl⁻ observed at early times during the out-diffusion experiment.

8.2 Final solutions

8.2.1 Chemical compositions

The final compositions of test solutions are given in Table 44. The composition of the final solutions reflect the original Mg²⁺, Ca²⁺ and DIC in the initial experimental solution, dissolved ions from the porewater, as well as changes in ion concentrations as a result of mineral dissolution/precipitation reactions and/or ion exchange reactions that occurred during the experiments. In all four samples examined, Ca²⁺, Mg²⁺ and alkalinity may have been influenced by reactions with carbonates (calcite, dolomite) present in the rock matrix. In the out-diffusion experiment with the sample from the Salina F Unit (DGR-4 189.16), gypsum present in the vein in this sample is expected to dissolve until saturation with respect to gypsum is reached. This is consistent with the composition determined for the final experimental solution, which is predicted to be at equilibrium with respect to gypsum (see results under “Modelled using measured pH and alkalinity” in Table 47).

The final solutions are predicted to be at partial CO₂ pressures above atmospheric and supersaturated with respect to calcite (Table 47). Based on the kinetics of calcite precipitation/dissolution reactions, it can be assumed that equilibrium with calcite was attained when the experiments were terminated (i.e. after 110 days). When the final solutions are modelled using PHREEQC and stipulating equilibrium with calcite (Table 47; for the Salina F Unit saturation with respect to gypsum was also stipulated), a lower pH and higher partial pressure of CO_{2(g)} are predicted. This may suggest that CO_{2(g)} was lost from the system over the course of the experiments, during subsampling and/or during sampling of the final solution. Therefore, in the final solutions, the pH values measured are higher and the dissolved inorganic carbon concentrations are lower than the actual values that would have been present in solution under closed system conditions.

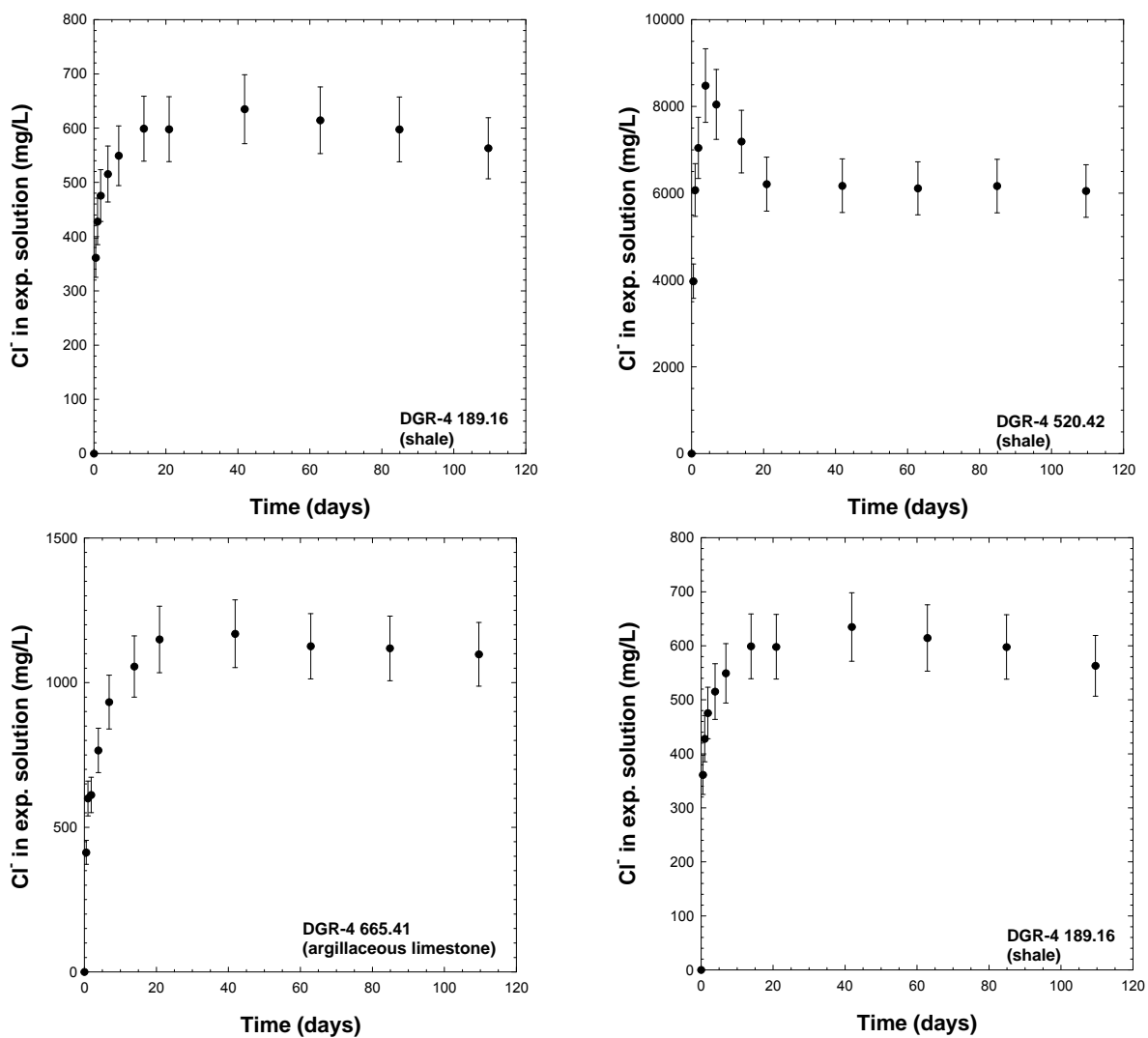


Figure 50: Cl^- concentrations in the experimental solutions as a function of time in the out-diffusion experiments; conducted on DGR-4 core samples from the Salina F Unit (DGR-4 189.16), Georgian Bay (DGR-4 520.42), Cobourg (DGR-4 665.41) and Kirkfield formations (DGR-4 730.07).

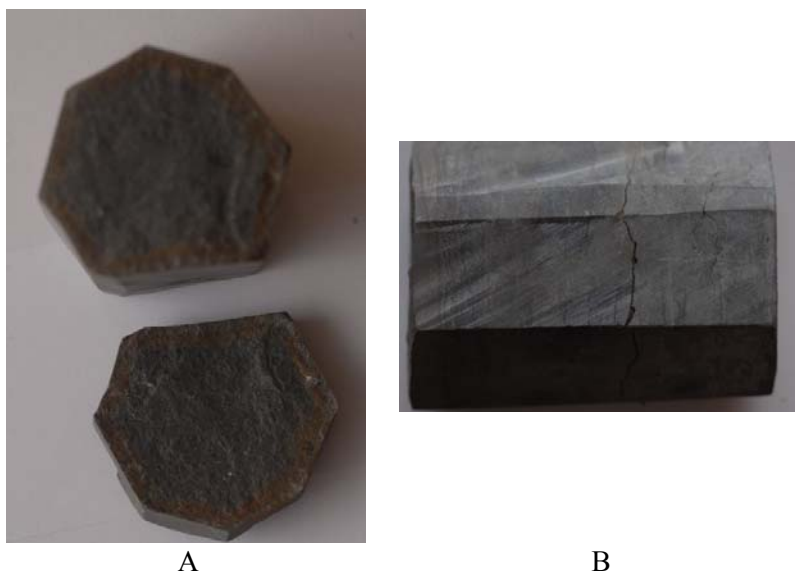


Figure 51: Photographs of the sample of the Georgian Bay Formation (DGR-4 520.42) taken after termination of the out-diffusion experiment and water content determinations (105 °C). A) Both sides of the parting along which the sample split during the out-diffusion experiments are shown. Alteration products (iron oxyhydroxides) were visible on the outside rims after several days of drying at 40°C. B) Parting in larger, intact piece of core after the out-diffusion experiments.

Table 46: Chemical and isotopic data for the final experimental solutions from out-diffusion experiments conducted on samples from borehole DGR-4.

Sample		DGR-4 189.16	DGR-4 520.42	DGR-4 665.41	DGR-4 730.07
Formation		Salina F Unit	Georgian Bay	Cobourg	Kirkfield
Chemical Type		<u>Na-Ca-Mg*-SO₄</u>	<u>Ca-Na-Mg*-Cl</u>	<u>Na-Mg*-Ca-Cl</u>	<u>Na-Ca-Mg*-Cl</u>
Miscellaneous Parameters					
pH (lab)	-log(H ⁺)	7.25	6.83	7.55	7.10
Sample Temperature	°C	20	20	20	20
Dissolved Constituents					
Cations					
Sodium (Na ⁺)	mg/L	440	1390	298	1220
Potassium (K ⁺)	mg/L	26.7	192	60.8	17
Magnesium (Mg ⁺²)	mg/L	135	247	139	195
Calcium (Ca ⁺²)	mg/L	583	1540	149	664
Strontium (Sr ⁺²)	mg/L	<10	27.3	<10	17.1
Anions					
Fluoride (F ⁻)	mg/L	2.4	1.3	1.1	1.3
Chloride (Cl ⁻)	mg/L	564	6030	1110	3850
Bromide (Br ⁻)	mg/L	1.6	71.7	10.2	33.7
Sulfate (SO ₄ ⁻²)	mg/L	2060	347	73.5	189
Nitrate (NO ₃ ⁻)	mg/L	<0.5	<0.5	<0.5	<0.5
Bicarb. (HCO ₃ ⁻), calc.	mg/L	222	167	233	175
Total Alkalinity	meq/L	3.63	2.73	3.82	2.87
Neutral Species (at measured pH)					
Silica (Si _{tot})	mg/L	5.50	2.24	1.46	2.86
Aluminium (Al _{tot})	mg/L	<5	<5	<5	<5
Parameters Calculated from Analytical Data					
Total Dissolved Solids	mg/L	4040	10000	2070	6520
Charge balance error	%	-2.10%	-5.19%	-4.70%	-4.09%
Br/Cl	mol/mol	5.28E-03	4.09E-03	1.29E-03	3.88E-03
Na/Cl	mol/mol	0.36	0.42	1.20	0.49
SO ₄ /Cl	mol/mol	0.02	0.03	1.35	0.02
Na/K	mol/mol	12.3	8.35	28.1	12.0
Ca/Mg	mol/mol	3.77	0.65	2.61	2.07
Ca/SO ₄	mol/mol	10.63	4.85	0.68	8.43
Isotopes					
δ ¹³ C _{DIC}	‰ V-PDB	-16.6	-10.1	-12.5	-7.9

Table 47: Modelled parameters for the final experiment solutions from out-diffusion experiments conducted on samples from borehole DGR-4.

Sample	DGR-4 189.16	DGR-4 520.42	DGR-4 665.41	DGR-4 730.07
Formation	Salina F Unit	Georgian Bay	Cobourg	Kirkfield
Solid:Liquid Ratio	1.84	1.57	1.36	2.58
Carbonate System				
<i>Measured values</i>				
Sample Temp. °C	20	20	20	20
pH (prior to alk. Titration) -log(H ⁺)	7.29	6.86	7.59	7.16
Total Alkalinity meq/l	3.63	2.73	3.82	2.87
Modelled using measured pH and alkalinity				
Total dissolved CO ₂ mol/l				
SI calcite	0.50	0.32	0.47	0.38
Log pCO ₂	-1.98	-1.75	-2.24	-1.99
SI gypsum	-0.03	-0.61	-1.78	-1.05
Modelled by equilibration with calcite (& gypsum in Salina F Unit)				
pH -log(H ⁺)	6.87	6.62	7.21	6.86
Total dissolved CO ₂ mol/l	4.36E-03	3.71E-03	4.56E-03	3.61E-03
Log pCO ₂ °C	-1.66	-1.60	-1.91	-1.76
Mineral Saturation indices (log(IAP/KT))				
Anhydrite	-0.24	-0.85	-2.04	-1.29
Aragonite	-0.15	-0.15	-0.15	-0.15
Calcite	0	0	0	0
Celestite	-	-0.65	-	-0.93
Chalcedony	-0.42	-0.79	-1.00	-0.69
Dolomite	-0.37	-0.48	0.30	-0.22
Fluorite	0.18	-0.12	-0.92	-0.35
Gypsum	0	-0.60	-1.80	-1.06
Halite	-5.30	-3.83	-5.13	-4.05
Quartz	0.03	-0.34	-0.55	-0.25
SiO ₂ (a)	-1.27	-1.64	-1.86	-1.55
Strontianite	-	-1.27	-	-1.10

- Not calculated; Sr²⁺ was below detection limit of 10 mg/L in final solution

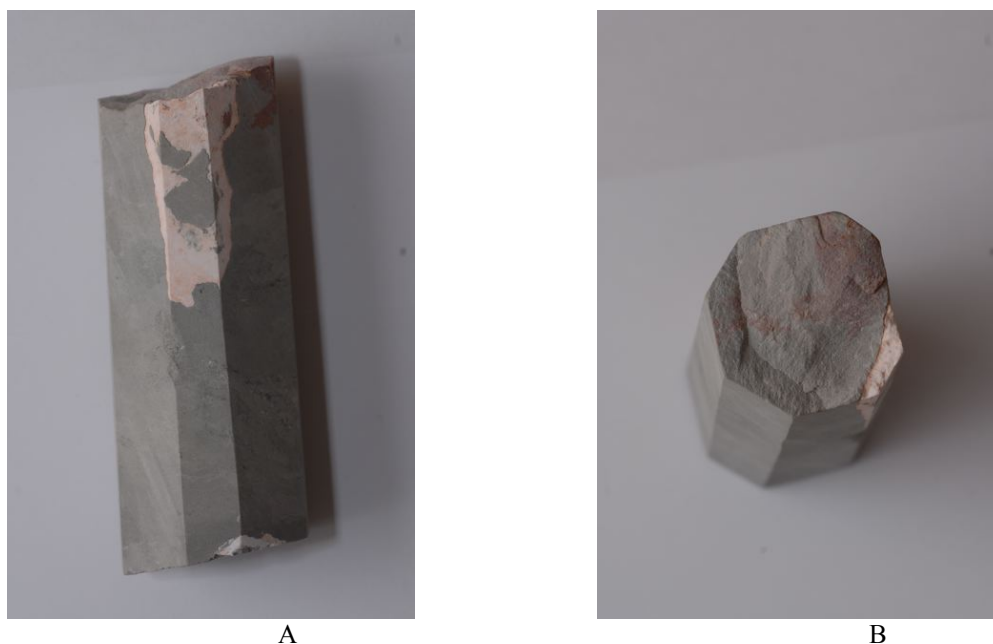


Figure 52: Sample from the Salina F Unit (DGR-4 189.16) used in the out-diffusion experiment showing gypsum vein (length of core sample is 11 cm). Photographs were taken after 110 days of submersion in the out-diffusion experiment and drying to constant mass at 105 °C.

The concentration of the ions measured in the final solutions, uncorrected for change in concentration due to removal of subsamples (Table 46), were normalized to a solid:liquid ratio of 1:1 and compared to the ion concentrations determined by aqueous extraction (Table 28) of aliquots of the same core (S:L = 1:1) in Figure 53. For the time-series samples, the full suite of ions was not measured and therefore, it is not possible to correct the final solutions for the quantities removed in the subsamples. However, based on the calculated difference between the corrected and uncorrected Cl^- concentrations, the final concentrations of the other ions in the final solution are estimated to be a maximum of 1% lower than the actual concentrations, well within the analytical uncertainty ($\pm 5\%$ for ions at concentrations < 100 mg/L and $\pm 10\%$ for concentrations > 100 mg/L).

For samples from the Georgian Bay (DGR-4 520.42) and Kirkfield (DGR-4 730.07) formations, the concentrations of Na^+ , Ca^{2+} , Sr^{2+} , Cl^- and Br^- determined in the aqueous extracts (Table 28) and the normalized concentrations from the final out-diffusion experiments agree fairly well. The concentrations of Na^+ , Cl^- and Br^- determined using both methods are similar for the sample from the Salina F Unit (DGR-4 189.16) and Sr^{2+} was below detection in the final out-diffusion solution of this sample. The Ca^{2+} and SO_4^{2-} concentrations are slightly higher in the aqueous extractions; this reflects control of these ions by gypsum. At the lower solid:liquid ratio used in the aqueous extractions, the mass of gypsum dissolved to reach saturation with respect to this phase would be higher. In the sample from the Cobourg Formation (DGR-4 665.41), the concentrations of Na^+ , Ca^{2+} , Cl^- and Br^- are all higher in the aqueous extract solutions than in the final out-diffusion solution.

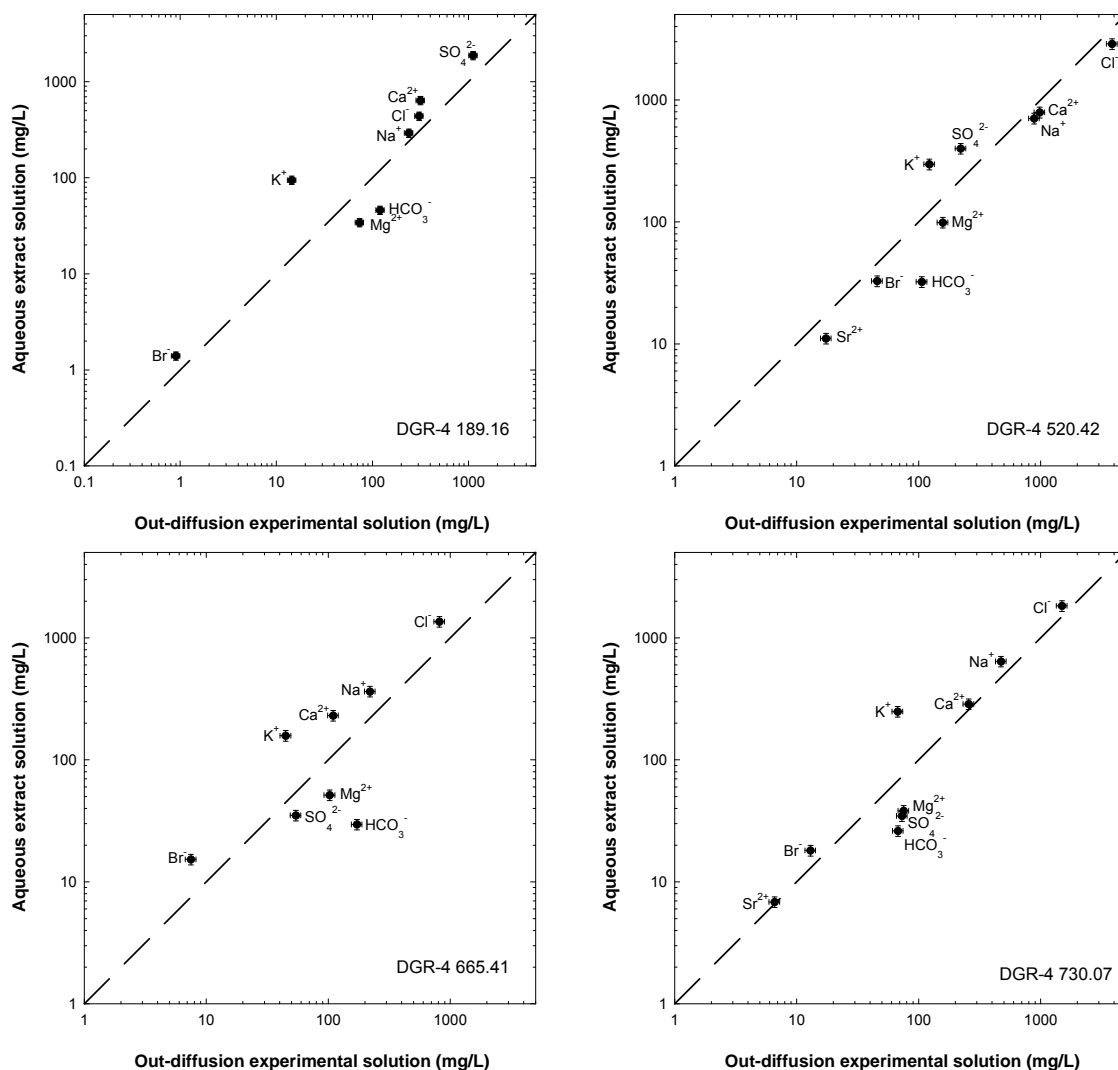


Figure 53: Comparison of ion concentrations in the aqueous extract solutions (solid:liquid = 1:1; values are average of 2 replicates) with the final concentrations determined in the final solutions from the out-diffusion experiments, normalized to a solid:liquid ratio of 1:1. Error bars show the maximum analytical uncertainty of $\pm 10\%$ in the measured ion concentrations.

In all four samples examined, the concentrations of Mg^{2+} and HCO_3^- calculated from the measured alkalinities are higher in the final solutions from the out-diffusion experiment than those determined using aqueous leaching. This likely reflects the higher Mg^{2+} and alkalinity of the initial experimental solution used in the out-diffusion experiments. The K^+ concentrations in the aqueous leachates are consistently higher in the aqueous extract solutions than in the normalized out-diffusion samples. This suggests that cation exchange may have influenced the K^+ concentrations more strongly in the aqueous extractions, where the solid to liquid ratio was lower than in the out-diffusion experiments. A lower solid:liquid ratio results in more dilute extraction solutions, in which the divalent cations are preferred on the exchange sites compared to the monovalent cations. In the out-diffusion experiments with samples from the Cobourg and Kirkfield forma-

tions, the normalized concentrations of SO_4^{2-} are also higher than in the aqueous extract solutions. No detailed mineralogical information is available for these samples. However, it is noted that sulphide minerals (pyrite, marcasite) were identified in sample from both formations in DGR-2 (Table 10.2 in Koroleva et al. 2009). Assuming sulphide phase(s) are also present in the DGR-4 samples, the higher concentration of SO_4^{2-} in the final out-diffusion solution may reflect oxidation of these phases during the course of the out-diffusion experiment. Sulphide oxidation is expected to be much more limited in the aqueous extractions, which were conducted in an N_2 -atmosphere.

8.2.2 Carbon isotopic compositions

The carbon isotopic composition measured for carbonates in the rock matrix of DGR-4 samples used in the out-diffusion experiments are given in Table 48.

Table 48: Isotope composition ($\delta^{13}\text{C}$ and $\delta^{18}\text{O}$) of matrix carbonate (calcite and/or dolomite) in DGR-4 samples used in out-diffusion experiments.

Sample ID	Formation	$\delta^{13}\text{C}$	$\delta^{18}\text{O}$
		‰ V-PDB	‰ V-SMOW
DGR4 520.42	Georgian Bay	+2.17	-3.41
DGR4 665.41	Cobourg	-0.32	-5.76
DGR4 189.16	Salina F Unit	-0.77	-5.55
DGR4 730.07	Kirkfield	+0.14	-5.03

The initial experimental solution has a strongly negative carbon isotopic signature (-17.4‰), distinct from the range of $\delta^{13}\text{C}$ signatures measured for the carbonates the rock matrix (-0.77 to +2.17‰). The carbon isotopic signatures of the final experimental solutions are intermediate between the initial experimental solution and the matrix carbonates, with $\delta^{13}\text{C}$ signatures ranging from -7.9 to -16.6‰. This suggests that some dissolution of the rock matrix carbonates occurred, shifting the isotopic composition to less negative $\delta^{13}\text{C}$ values in the final experimental solutions. If the experimental system was closed (in terms of carbon mass transfer), the following mass balance expression could be used to estimate the amount of carbon dissolved from the rock matrix:

$$C_{solid} = \frac{C_{ExSf} * \delta^{13}C_{ExSf} - C_{ExSi} * \delta^{13}C_{ExSi}}{\delta^{13}C_{solid}}$$

where C_{solid} is the amount of carbon contributed to the solution from the rock matrix, $\delta^{13}C_{solid}$ is the carbon isotopic signature of the carbonates within the rock matrix, C_{ExSf} and $\delta^{13}C_{ExSf}$ are the amount of dissolved inorganic carbon and the carbon isotopic signature of the final experimental solution, respectively, C_{ExSi} is the amount of dissolved inorganic carbon (1.42E-02 mol/kg_{H2O}) and $\delta^{13}C_{ExSi}$ is the carbon isotopic signature of the initial experimental solution (-17.4‰). However, as noted in section 8.2.1, the out-diffusion experiments may not represent a closed system, as evidenced by an apparent loss of $\text{CO}_{2(g)}$ and therefore, dissolved inorganic carbon may also be lost from the system during sampling (i.e. the out-diffusion experiments represent a partially-open system). In this case, the dissolved carbonate concentrations measured in the final experiments solutions (C_{ExSf}), do not include all carbon released to solution during attainment of steady-state conditions. It is therefore not possible to calculate the amount of carbonate dissolution using

mass balance considerations. It should be noted, however, that the low mass change observed for all four samples from the beginning to the end of the out-diffusion experiments (see section 8.3) suggests that carbonate dissolution/precipitation is minor.

8.3 Porosity

After completion of the out-diffusion experiments, the bulk wet densities of the samples were determined by recording the mass of the sample in air and when suspended in water, according to Archimedes' Principle. Bulk wet densities determined for samples from the Georgian Bay and the Kirkfield formations after the out-diffusion experiment are the same as those determined for small aliquots (≈ 15 g) of fresh core from the same formations (Table 18; section 4.3). Bulk wet densities determined for out-diffusion samples from Salina F Unit and the Cobourg formation are approximately 4.5 and 1.5% higher, respectively, than the bulk wet densities determined for fresh aliquots. This difference may reflect the larger core masses (230 to 390 g) used in the out-diffusion experiments, better capturing heterogeneities within the rock.

Changes in the mass of the core sample may occur from the beginning to the end of the out-diffusion experiment due to uptake of water by the core during the experiment (e.g. if partial drying of the outer rims occurred during sample preparation), due to mineral precipitation within the core (mass gain), or dissolution of mineral phases (mass loss). The final masses of the DGR-4 core samples were essentially the same as their initial masses, with only slight increases of between 0.1 and 1.2 wt.% observed (Table 47).

After attainment of steady-state conditions and at the end of the out-diffusion experiments, the TDS of the final solutions and the porewaters within the core are more dilute than in the original samples (equal to or less than 10,000 mg/L). Therefore, the impact of the porewater density at the end of the experiment on the calculated water content is also likely to be lower. As a first approximation, a density of 1.0 g/cm^3 is assumed for the porewater in the core at the end of the experiment and the porewater content is assumed to be equal to the water content ($WC_{\text{Grav.wet}}$, equation 4, section 4.2.1). Similarly, the volume of the pores occupied by porewater (porewater-loss porosity) can be calculated directly from the calculated porewater content and measured grain density, assuming a density of 1.0 g/cm^3 for the porewater (equation 12, section 4.4). The water contents determined gravimetrically for each sample after completion of the experiments are given in Table 47. For the sample from the Salina F Unit, water contents calculated at both 40 and 105 °C are not considered to be representative of porewater content, because both may include structural water released from gypsum during drying (see also section 4.2.1).

For comparison, the gravimetric porewater contents determined on separate aliquots of fresh (i.e. "as received") core are also given (see also section 4.2.2). The water-loss porosity calculated for the out-diffusion sample from the Georgian Bay Formation is higher by 2 vol.% than the porewater-loss porosity determined for fresh aliquots from the same core. This likely reflects the increase in porosity of the core during the out-diffusion experiment due to dissolution and/or expansion of the core, consistent with the observation of partings in this sample (Figure 51). For samples from the Cobourg and Kirkfield formations, the water-loss porosities determined for the out-diffusion samples are lower than porewater-loss porosities determined for fresh aliquots by 0.5 and 0.8 vol.%, respectively. This is larger than the analytical uncertainty in the porewater-loss porosities of 0.28 and 0.54 vol.%, respectively, as calculated by Gaussian error propagation (section 4.2.2). This can be, in part, attributed to the assumed porewater density of 1.0 g/cm^3

used to calculate water-loss porosities at the end of the out-diffusion experiments. Higher densities of the actual porewaters would result in higher calculated porewater-loss porosities.

Table 49: Water content and water-loss porosity of samples used for out-diffusion experiments from boreholes DGR-1 and DGR-2. The data are not corrected for mineral dissolution effects during the experiment.

Sample / Parameter	Unit	DGR-4 189.16	DGR-4 520.42	DGR-4 665.41	DGR-4 730.07
Formation		Salina F Unit	Georgian Bay	Cobourg	Kirkfield
<i>Before out-diffusion experiment</i>					
Initial mass experimental solution	g	178.55	148.90	180.07	150.60
Initial mass rock	g	328.732	233.810	244.311	389.144
Solid / Liquid ratio		1.84	1.57	1.36	2.58
<i>After out-diffusion experiment</i>					
Volume test water removed (time series) ¹	ml	0.5	0.5	0.5	0.5
Final mass rock	g	328.970	236.580	244.790	390.680
Relative change of mass during expt.	%	0.07	1.18	0.20	0.39
Final water loss (40°C)	g	8.45	5.271	0.998	4.623
Final water loss (105°C)	g	17.238	5.557	1.099	5.055
Final water content (WC _{Grav.wet} , 40°C)	wt.%	2.58*	2.26	0.41	1.19
Final water content (WC _{Grav.wet} , 105°C)	wt.%	5.27*	2.38	0.45	1.30
Final bulk wet density	g/cm ³	2.57	2.69	2.70	2.67
Final water-loss porosity (WL at 105°C)	vol.%	n.a.	6.36	1.23	3.51
<i>Average density and porosity of aliquots, corrected for salinity¹</i>					
Bulk wet density	g/cm ³	2.46	2.69	2.66	2.67
Grain density	g/cm ³	2.78	2.79	2.76	2.76
Porewater content (PWC _{Grav.wet} , 105°C)	wt.%	n.a.	2.30	0.81	2.06
Porewater-loss porosity (105°C)	vol.%	n.a.	4.83	1.73	4.32

¹Original presentation of these values is given in section 4.2.

²The volume of each subsample was 0.5 ml. The mass of each subsample was estimated from the measured decrease in mass of the entire container plus contents at the start and end of an experiment (between 6 and 7 grams) and dividing by the number of subsamples taken.

n.a. not applicable due to presence of gypsum in sample.

*value determined may include structural water from gypsum, in addition to water from the pore spaces.

8.4 Constraints on Cl⁻ concentration of porewaters

For ions that behave conservatively during the out-diffusion experiments, the concentration in the final experimental solution (corrected for mass of ion and solution removed during time-series sampling) can be converted to apparent porewater concentrations, if the geochemical porosity of

the ions is known. As a first approximation for Cl^- , it is assumed that its geochemical porosity is equal to the water-loss porosity. This approach to calculating porewater concentrations is not applicable to i) the sample from the Salina F Unit, where water content and water-loss porosity could not be accurately determined due to the presence of gypsum; and ii) the sample from the Georgian Bay Formation, where the presence of halite was indicated (although it is not known if the halite was originally present in the rock matrix or whether it a tertiary precipitate formed by evaporation during sample preparation).

The calculated apparent porewater Cl^- concentrations are given in Table 50. Values estimated by upscaling the aqueous extraction results for the same samples are also given, as well as the apparent porewater concentrations for Cl^- determined in the same formations from DGR-2. The uncertainty in the apparent porewater concentrations is estimated at $\pm 15\%$ (additive assuming an uncertainty of 10% in the water-content and water-loss porosities and 5% analytical uncertainty in ion concentrations measured in the final solution by Ion Chromotography).

Table 50: Apparent concentrations of Cl^- in the porewater calculated based on corrected Cl^- concentrations in final experimental solution (out-diffusion), the mass of test solution added and the water content ($\text{WC}_{\text{Grav.wet}}$) of the samples determined at the end of the experiment.

Borehole		DGR-4		DGR-2	
Method		Out-Diffusion	Upscaling of aqueous extracts	Out-Diffusion	Upscaling of aqueous extracts
Formation	Lithology	Apparent porewater Cl^- (mmol/kg H_2O)	¹ Apparent porewater Cl^- (mmol/kg H_2O)	² Apparent porewater Cl^- (mmol/kg H_2O)	² Apparent porewater Cl^- (mmol/kg H_2O)
Cobourg	Limestone	5100 (± 760)	4960 (± 730)	4060 (± 620)	4770(± 400)
Kirkfield	Limestone	3330 (± 510)	3390 (± 510)	-	-

¹For details on calculations, see section 6.3.1.

²From Koroleva et al. (2009), Table 10-4.

Uncertainty in apparent porewater concentrations is estimated at $\pm 15\%$ (see text).

For DGR-4 samples from the Cobourg and Kirkfield formation limestones, the apparent porewater concentrations determined using both aqueous extraction and out-diffusion experiments are the same within the analytical uncertainty of the out-diffusion results ($\pm 15\%$).

8.5 Estimation of Cl^- pore diffusion coefficient (D_p)

For the Salina F Unit shale and limestones from the Cobourg and Kirkfield formations examined using out-diffusion experiments, the general shape of the Cl^- concentration versus reaction time suggests that transport could be described by diffusion (Figure 50). An estimate for the pore diffusion coefficient of Cl^- in each sample can be obtained by fitting the observed values with values calculated assuming radial diffusion from the core sample and assuming a homogeneous porosity distribution. As described in section 8.1, the Cl^- versus time profile for the out-diffusion experiment conducted with the shale from the Georgian Bay Formation does not represent a simple diffusion profile. Another process, likely dissolution of a Cl^- -bearing soluble salt, controls the Cl^-

concentrations at early times. The Cl⁻ profile for this sample cannot be used to estimate the Cl⁻ pore diffusion coefficient and, therefore, is not considered here.

The fit of the radial diffusion model for the estimated pore diffusion coefficients for Cl⁻ to the time series data is shown in Figure 54. In Figure 54, the complete profile for each sample shown in the left-hand diagram and the fit to the early time data is emphasized in the right-hand diagram. The best fit of the modelled diffusion profile to experimental data was achieved for the limestone sample from the Kirkfield Formation (DGR-4 730.07); variations in the measured parameters are captured by a range in the uncertainty ± 1.4 (square root of 2), corresponding to a factor of 2 in the diffusion time. For the limestone sample from the Cobourg Formation (DGR-4 655.41) and for the Salina F Unit shale (DGR-4 189.16), the fit of the modelled and measured profiles is not as good as that obtained for the results from Kirkfield formations, in particular at early times (see right hand diagrams in Figure 54). An improved fit might be obtained by considering a heterogeneous porosity distribution in these samples, with a disturbed zone around the perimeter of the core (e.g., damage during dry sawing of the samples to remove outer rims of core), and a lower porosity, undisturbed zone in the interior.

The estimated pore diffusion coefficients for Cl⁻ in the Salina F Unit, the Cobourg and the Kirkfield formations are provided in Table 51. The core samples examined in the out-diffusion experiments have most certainly undergone stress release during drilling and removal to the surface. Disturbances due to stress release can be minimized in through-diffusion experiments conducted under confining pressures, although in situ measurements of diffusion coefficients would provide more representative diffusion coefficients. The D_p Cl⁻ values reported here provide an upper bound on the pore diffusion coefficients expected in situ.

Table 51: Estimated pore diffusion coefficient for chloride (parallel to bedding as determined at 45 °C), obtained from modelling the concentration time-series of out-diffusion experiments assuming radial diffusion.

Sample	DGR-4 189.16	DGR-4 665.41	DGR-4 730.07
Formation	Salina F Unit	Cobourg	Kirkfield
Lithology	dolomitic shale with gypsum vein	bioclastic, argillaceous limestone	Limestone with shale beds
Estimated Cl⁻ Pore Diffusion Coefficient (45 °C)	6.5E-10*	1.5E-10	6.1E-10
¹ Uncertainty in D_p Cl ⁻			
Upper bound	9.2E-10*	2.1E-10	8.6E-10
Lower bound	4.6E-10*	1.1E-10	4.3E-10

¹ Estimated uncertainty in the pore diffusion coefficient for Cl⁻ is given as a factor of 1.41 (square root of 2), corresponding to a factor of 2 in the diffusion time.

* Poorer fit of modelled diffusion profile to concentration vs. time curve, especially at early times using the homogeneous model suggests this value is only approximate; a model considering heterogeneous porosities (e.g. outer disturbed rim zone and inner, undisturbed zone) might provide a better fit to measured profile.

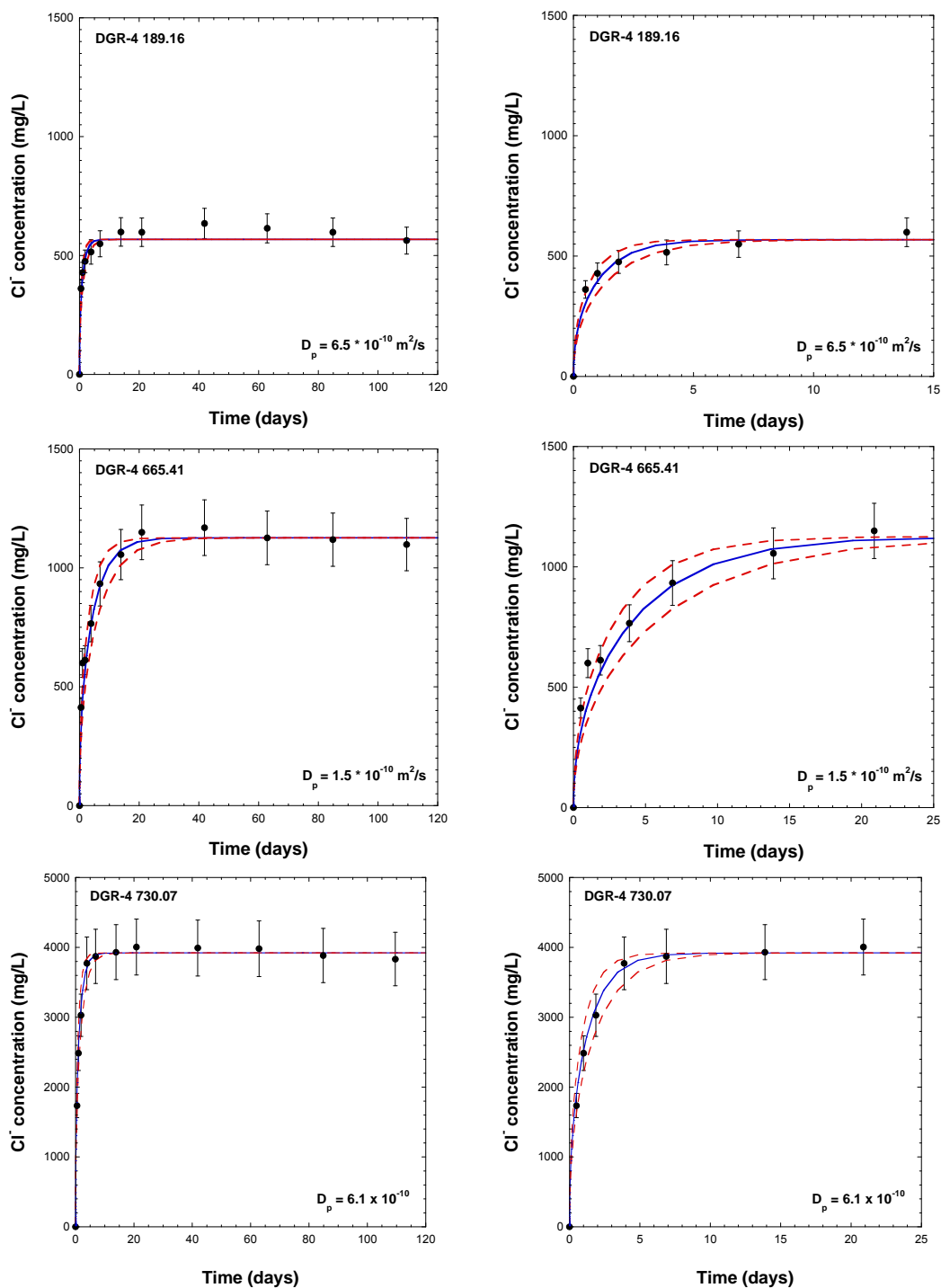


Figure 54: Fit of estimated Cl^- pore diffusion coefficient (solid line) to time series data using a radial diffusion model. The complete profile is shown in the left-hand diagram; the right-hand diagram shows the fit to early-time data. The uncertainty range for D_p Cl^- is given by the dashed lines and represents values that are smaller and larger by a factor of 1.41 (square root of 2) corresponding to a factor of 2 in the diffusion time.

Based on the results from out-diffusion experiments, Koroleva et al. (2009) estimated a pore diffusion coefficient for Cl^- of between 1.6 and $3.3\text{E-}10$ m^2/s at 45 °C for a sample of the Cobourg Formation taken in borehole DGR-2. The pore diffusion coefficient estimated for sample DGR-4 665.41 from this same formation is lower (between 1.1 and $2.1\text{E-}10$ m^2/s at 45 °C). The sample of the Cobourg Formation from DGR-4 also has a lower water-loss porosity of 1.23 vol.%, compared to 2.28 vol.% for sample DGR-2 674.73 (Koroleva et al., 2009).

Intera (2008b) determined a pore diffusion coefficient for Γ of $6.0\text{E-}11$ m^2/s parallel to bedding in the Cobourg Formation in experiments conducted at 22 °C. At temperatures between 0 and 100 °C, the temperature dependence of the self-diffusion coefficient (D^o) of an ion that diffuses faster than F^- in water (including Cl^- , Br^- and I^-) can be predicted using the following expression (Li and Gregory, 1974):

$$\frac{D_{45\text{C}}^o}{D_{22\text{C}}^o} = \frac{\eta_{22\text{C}}}{\eta_{45\text{C}}}$$

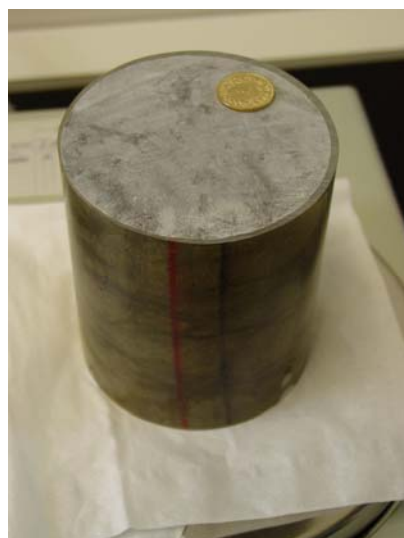
where η is the viscosity of water at a given temperature. Using this expression and values for the viscosity of water (e.g. CRC Handbook, 1987), a factor of 1.6 is estimated for the difference between the self-diffusion coefficient of Cl^- in water at 22 and 45 °C. Using this factor as a first approximation of the difference in D_p Cl^- at these two temperatures, a value of $9.4\text{E-}11$ m^2/s is predicted for D_p Cl^- at 22 °C from results of the out-diffusion experiment, which is approximately a factor of 1.6 higher than the D_p for Γ of $6.0\text{E-}11$ m^2/s measured by Intera (2008b) for the Cobourg Formation (DGR-2).

Intera (2009c) determined an average effective diffusion coefficient (D_e) for Γ of $6.5\text{E-}11$ m^2/s in the Cobourg Formation, normal to bedding. Using the rock capacity value of 0.024 reported by Intera (2009c) and assuming $K_d = 0$, a D_p Γ of $2.7\text{E-}11$ m^2/s is calculated normal to bedding. In the experiments conducted by Intera (2008b), the D_p (Γ) in the Cobourg Formation parallel to bedding was found to be approximately a factor of 3 higher than that measured normal to bedding. Considering this anisotropy, a D_p Γ of $8.1\text{E-}11$ m^2/s is predicted parallel to bedding in the Cobourg Formation from the results of Intera (2009c). This is lower than the value of $9.4\text{E-}11$ m^2/s estimated based on the results of the out-diffusion experiment for sample DGR-4 665.41, but within its estimated uncertainty ($6.7\text{E-}11$ to $1.3\text{E-}11$ m^2/s).

The D_p Cl^- values determined for the Cobourg Formation samples using out-diffusion experiments and the through-diffusion experiments conducted by Intera (2009c) are similar. The difference compared to D_p Γ from Intera (2008b) may be related to the size of the samples used for the measurements. In the through-diffusion experiments, 8 to 10 mm slices of the core (core diameter 76 mm) were used (Intera, 2009c) and in the out-diffusion experiments, samples with lengths between 85 and 110 mm and diameters of between 38 and 44 mm were used. These are much larger than the mini-cores with a diameter of 11 mm and lengths of between 15 to 20 mm required for the X-ray radiography measurements conducted by Intera (2010b, 2008b). The larger samples used in the through-diffusion and out-diffusion experiments may capture heterogeneities within the rock samples that are not captured by the mini-cores.

9 Advective Displacement – Initial results

The advective displacement experiment with core sample DGR-4 679.95 from the Cobourg Formation has been underway for over 2 months. Several stages of the set up of this experiment are illustrated in Figure 55.



A



B



C



D

Figure 55: Photographs showing A) core sample DGR-4 679.95 with its perimeter encapsulated in resin; B) after placement of a porous, Teflon disk on each end and titanium couplings; C) after wrapping core and edge of titanium couplings in Teflon and rubber-shrink tube sleeve to isolate the core from the confining medium; and D) start of experiment with core installed in advective displacement rig.

Curves showing the infiltration and confining pressure as a function of elapsed time since the start of the experiment are shown in Figure 56. The infiltration pressure was set at 4.9 MPa at the start of the experiment. After 5 minutes, approximately 1 ml of gas was discharged to the syringe. This may represent gas from within the dead volume of the porous disc and titanium end plate, which is estimated to be approximately 0.5 ml. The infiltration pressure was released and the experiment was restarted by gradually increasing the pressure to 4.4 MPa over 24 hours. This is visible as a sharp decrease followed by gradual increase in the infiltration pressure at early times in Figure 56. The confining pressure was originally 6.9 MPa and has remained stable throughout the experiment.

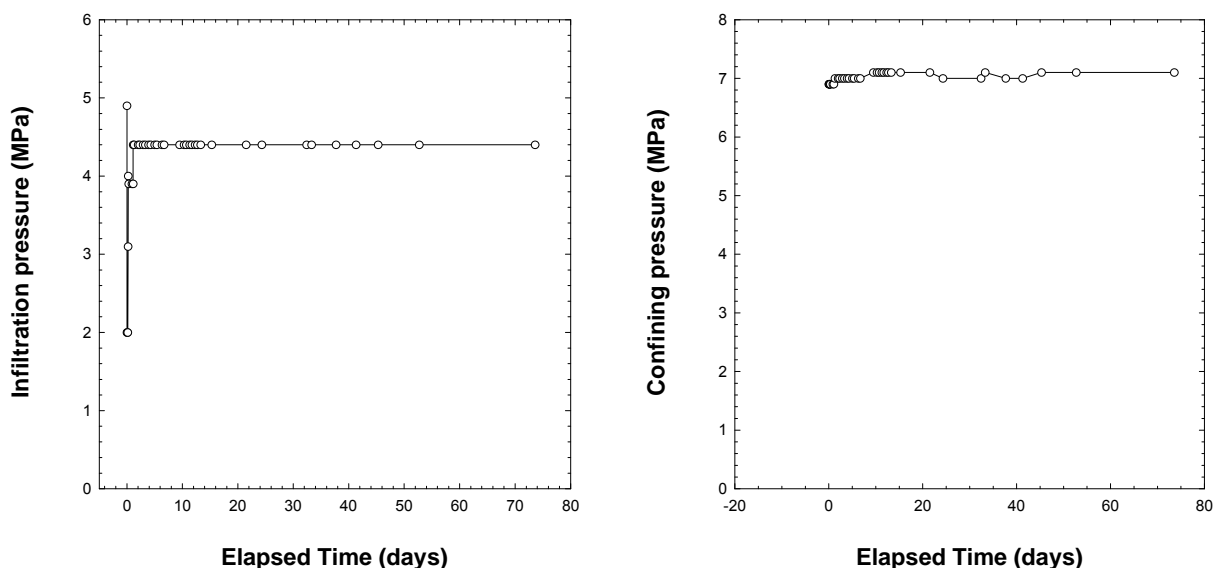


Figure 56: Plots showing the infiltration and confining pressures during the first two months of the advective displacement experiment conducted with an argillaceous limestone sample from the Cobourg Formation (DGR-4 697.95) and using TCE as the infiltrating fluid.

The gravimetric water content ($WC_{Grav.wet}$) determined based on two replicate samples of DGR-4 679.95 was 0.44 ± 0.02 wt.%. The porewater content ($PWC_{Grav.wet}$), calculated assuming that the porewater has a salinity of 28 wt.% (see section 4.2.2) is 0.61 vol.%. Assuming that the grain density is similar to that of DGR-4 672.85 (2.69 g/cm^3) and a porewater density of 1.23 g/cm^3 , the calculated porewater-loss porosity (or connected porosity) of the sample is 1.32 vol.%. Assuming the core is fully saturated and using the calculated volume of 407 cm^3 of the core segment in the advective displacement experiment, approximately 5 ml of porewater are present in the core that could potentially be extracted.

After over 2 months, no pore fluid has been extracted from the sample. Two potential explanations are:

- i) The hydraulic conductivity of the sample is so low that after 2 months, the volume displaced is not sufficient to fill the dead volume present in the system at the

upper end of the core (c.a. 0.5 ml including the Ti filter plate and the capillary tubing); or

- ii) The TCE used as the infiltration fluid has a much higher entry pressure than an electrolyte solution and therefore, no fluid has entered the core. Some support for this hypothesis is provided by the high, applied pressures of between 16.5 and 39.1 MPa required before mercury began to penetrate pores in core samples from the Cobourg Formation (as observed during high pressure mercury injection testing, Intera, 2010d).

Going forward, the infiltration pressure will first be increased to increase flow (if there is flow) or to overcome the entry pressure – this requires that the confining pressure be increased. If this is not successful, the infiltration can be reversed and an artificial porewater injected from the opposite end of the core.

10 Porewater characterisation – Status

Based on the evaluations of the aqueous extraction results presented in section 6, the current status for defining porewater chemical compositions and how this relates to the construction of geochemical conceptual models and thermodynamic codes is discussed in the following sections.

10.1 Defining porewater chemical composition

As discussed by Koroleva et al. (2009), porewater compositions can only be directly scaled up from aqueous extraction data using measured water contents if the following criteria are met:

1. No contributions to the aqueous extract solutions from cracked fluid inclusions;
2. No soluble salts are present in the rock matrix that contribute to the aqueous extract solution (other than those precipitated from the porewater);
3. Cation exchange capacity is negligible compared to the electrolyte content of the porewater (or can be quantified using selectivity coefficients);
4. No significant anion exclusion effect (i.e., the anion accessible porosity can be approximated by porewater-loss porosity).

The first three criteria must be met in order to be able to define the mass of an ion originally in the porewater of a sample. In terms of the first criteria, the contribution of fluid inclusions to the porewater has not been quantified for the sedimentary formations underlying the proposed DGR, but is generally thought to be negligible for sedimentary rocks containing highly saline porewaters. Waber et al. (2007) examined the amount of Cl^- and Br^- released from samples of the Co-bourg Formation from St. Mary's Quarry during aqueous extractions conducted on different grain-size fractions and at different solid:liquid ratios. The Cl^- and Br^- concentrations were identical within analytical uncertainty, excluding substantial contributions of salts from decrepitated fluid inclusions. Neglecting any contributions from fluid inclusions, the total mass of a cation measured in an aqueous extract solution can be formulated as a mass balance expression:

$$m\text{Me}_{\text{AqEX}} = m\text{Me}_{\text{PW}} + m\text{Me}_{\text{MIN}} + m\text{Me}_{\text{EXCH}}$$

where Me_{AqEX} is the total mass measured in the aqueous extract solution; $m\text{Me}_{\text{PW}}$ is the mass of the cation originally in the porewater, $m\text{Me}_{\text{EXCH}}$ is the mass of the cation removed from or added to the extract solution by cation exchange reactions and $m\text{Me}_{\text{MIN}}$ is the mass of the cation added to/removed from the aqueous extract solution by mineral dissolution/precipitation.

For anions, ion exchange processes are considered unimportant in clays and argillaceous limestones. The total concentration of an anion in the extract solution is the sum of the mass of ion originally in the porewater ($m\text{An}_{\text{PW}}$) plus any ions added to/removed from solution by mineral dissolution/precipitation reactions or by oxidation reactions, for example SO_4^{2-} produced due to sulphide mineral oxidation ($m\text{An}_{\text{MIN}}$):

$$mAn_{AqExt} = mAn_{PW} + mAn_{MIN}$$

In section 6, the aqueous extraction results were first examined together with mineralogical data for evidence suggesting the potential presence of soluble salts (halite and gypsum/anhydrite) in the samples. Based on this initial evaluation, aqueous extract solutions with evidence for the presence of soluble salts based on i) ion ratios, ii) predicted mineral saturation indices in the aqueous extract solutions and iii) mineralogical information were separated from those without soluble salts. For aqueous extracts without evidence for the presence of soluble salts (or the “select dataset”), the proportionality between the extracted ion concentrations and the calculated porewater content of the samples was used to evaluate whether or not the concentrations were likely primarily from the porewater, or whether additional cation exchange or mineral precipitation/dissolution reactions during the extractions may have resulted in substantial changes in their concentrations. Considering this select dataset, the evidence regarding contributions from cation exchange and mineral dissolution reactions to the aqueous extraction results are summarized for cations in Table 52 and for anions in Table 53. A qualitative assessment of the representativeness of the data for each ion in terms of its concentration in the porewater is given in the final column of each table, along with a short description of the key observations supporting this assessment.

The final criterion that must be considered prior to scaling ion concentrations to porewater concentrations is the anion-accessible porosity. In clay-rich samples, the effective porosity in which the anions reside may be reduced by anion-exclusion – in which anions are excluded from the portion of the pore space affected by diffuse double-layers associated with permanent negative layer charge. Theoretically, at high salinities, anion-exclusion would be reduced as a result of collapse of the diffuse double layer. Intera (2008b; 2010a) report Γ accessible porosities that are approximately 50% of water-loss porosities in Ordovician shale samples, whereas comparable Γ accessible and water-loss porosities were reported for limestone samples. These results suggest that anion exclusion is significant in the Ordovician shale formations, although the underlying mechanisms for this exclusion are not yet understood. In the current study, anion-accessible porosities are not considered for either chloride or bromide.

Table 52: Assessment of the sources of extractable cations determined using aqueous extraction for the select dataset (i.e. subset in which evidence for the presence of soluble salts was not observed).

Cation	Cation exchange	Mineral dissolution	Qualitative assessment Mass extracted using aqueous extracts \approx mass in porewater?
Na ⁺	Extractions conducted at multiple S:L ratios on DGR-2 samples suggested that concentrations were not significantly perturbed by ions from exchange sites.	Likely not important in selected dataset.	Strong supporting evidence: good correlation of extracted concentrations with porewater contents and with extracted Cl ⁻ concentrations.
Ca ²⁺		Contributions of Ca ²⁺ from calcite, dolomite dissolution during extraction have not been quantified. Likely reduced in DGR-3/4 samples by use of extraction time of 10 minutes.	Strong supporting evidence: good correlation of extracted concentrations with porewater contents and with extracted Cl ⁻ concentrations.
Mg ²⁺		Possible control of dolomite on Mg ²⁺ concentrations in highly dolomitised zones? Effect likely reduced in DGR-3/4 samples by use of extraction time of 10 minutes.	No evidence to support that extracted Mg ²⁺ is from porewater: no apparent (or only very weak) correlations with porewater content. Higher Mg ²⁺ concentrations noted in zones with higher degrees of dolomitisation (Queenston, Georgian Bay and Cambrian). Dolomite solubility control in these formations?
K ⁺		Likely low for most samples. Possible exceptions are samples from Shadow Lake, Cambrian and Precambrian.	Strong to moderately strong evidence for many samples: good correlation of extracted concentrations with porewater contents and with extracted Cl ⁻ concentrations. Notable exceptions are from the Shadow Lake, Cambrian, Precambrian and one sample each from the Queenston and Bass Islands formations. Na/K ratio is essentially constant from Cabot Head down through to Shadow Lake, where it increases dramatically, reflecting lower K ⁺ .
Sr ²⁺		Results for extractions conducted at multiple S:L ratios on DGR-2 samples were inconclusive. Majority of samples with lower Sr ²⁺ concentrations are from DGR-2 samples where a longer extraction time of 48 hours was used – cation exchange?	Unknown. Influence of anhydrite/gypsum or celestite dissolution cannot be completely ruled out.

Note: results of aqueous extractions conducted at multiple solid:liquid ratios on DGR-2 samples are from Koroleva et al., 2009.

Table 53: Assessment of the sources of extractable anions determined using aqueous extraction for the select dataset (i.e., subset in which evidence for the presence of soluble salts was not observed).

Anion	Mineral dissolution	Mass extracted using aqueous extracts \approx mass in porewater?
Cl ⁻	Not likely for select dataset	Strong supporting evidence: good correlation of extracted concentrations with porewater contents.
Br ⁻	Not likely for select dataset	Strong supporting evidence: good correlation of extracted concentrations with porewater contents and with extracted Cl ⁻ concentrations.
SO ₄ ²⁻	May include a contribution from oxidation of sulphide minerals (e.g. pyrite, observed in all but the oxidized, red-bed shales (Queenston and Cabot Head formations)).	Unknown. Extracted concentrations of SO ₄ ²⁻ are low for majority of samples and concentrations are similar, irrespective of porewater content. This suggests a mineral solubility control on SO ₄ ²⁻ concentrations during extractions (SO ₄ ²⁻ /pyrite?). Higher SO ₄ ²⁻ concentrations observed in specific samples from the Queenston and Georgian Bay formations are likely due to anhydrite dissolution (Queenston, Georgian Bay) or celestite dissolution (Queenston), based on the presence of these minerals in other samples from within these formations. In the Gull River Formation (2 samples) and one sample from the Cobourg Formation from DGR-2, elevated SO ₄ ²⁻ may be the result of oxidation of sulphide minerals (e.g. pyrite) prior to sample preservation, during storage or during the extraction procedure (48 hours), although all extractions were conducted under a N ₂ atmosphere in a glovebox. In DGR-3 and -4, detailed mineralogical studies including SEM/EDS were conducted on relatively few samples. Consequently, the presence of anhydrite/gypsum and/or celestite in the formations from the Cabot Head through the Shadow Lake cannot be ruled out, especially if finely dispersed in the rock matrix.
Alkalinity (HCO ₃ ⁻)	Likely low in saline porewaters; concentrations measured in aqueous extracts likely reflect dissolution of calcite/dolomite during extraction	No supporting evidence. Affected by dissolution of calcite/dolomite during aqueous extractions. Possible contributions of organic acids to measured alkalinity have not been quantified.

10.2 Apparent porewater ion concentrations

10.2.1 Apparent ion molalities in porewater

Apparent porewater concentrations in $\text{mmol/kg}_{\text{H}_2\text{O}}$ were calculated from the aqueous extraction results (at a solid:liquid ratio of 1:1) by scaling to water content. The quantity of ions extracted per kilogram of dry rock (expressed in $\text{mmol/kg}_{\text{rock}}$) is divided by the water content of the sample, reported relative to the dry mass of rock ($\text{WC}_{\text{Grav.dry}}$) and expressed as a weight fraction ($\text{kg}_{\text{H}_2\text{O}}/\text{kg}_{\text{rock}}$) (see also section 6.3.1). Summaries of the apparent porewater concentrations in $\text{mmol/kg}_{\text{H}_2\text{O}}$ determined for samples in the select dataset from DGR-3 and DGR-4 are provided in Table 54 and Table 55. Samples in which halite may be present based on geochemical modelling of the scaled aqueous extract solutions (even though no halite was actually observed) are also indicated. There is no evidence to support that the extracted Mg^{2+} concentrations are representative of porewater concentrations and therefore, the extracted concentrations were not recalculated to apparent porewater concentrations. The error on the upscaled concentrations can be roughly approximated from the sum of the error on the water content (see Table 54 and Table 55) and the error in the ion analysis (approximately 10%), some additional uncertainty (not yet quantified) due to mineral dissolution (and, less relevant, precipitation and CEC) during extraction. The apparent ion concentrations in the porewater are plotted as a function of depth in Figure 57 through Figure 62. For comparison, the concentrations of the ions determined in groundwaters sampled in the Cambrian from boreholes DGR-3 and DGR-4 (expressed in $\text{mmol/kg}_{\text{H}_2\text{O}}$) are also plotted (data from Intera, 2009).

The apparent porewater concentrations of Cl^- are plotted as a function of depth in Figure 57. The depths at which halite was identified petrographically in one sample from each of the Georgian Bay and Gull River formations in DGR-2 and in the Salina C Unit and the Guelph Formation in DGR-3 are also shown in Figure 57. Apparent porewater Cl^- concentrations are between 5500 and 6500 $\text{mmol/kg}_{\text{H}_2\text{O}}$ for the majority of samples within the Cabot Head Formation through to the top of the Cobourg Formation. The exceptions are three samples from DGR-3 with concentrations of 8000 $\text{mmol/kg}_{\text{H}_2\text{O}}$ or above, including one sample from the Manitoulin Formation and two samples from the Cobourg Formation (these samples were predicted to be close to halite saturation, as noted in Table 54). Within the Queenston Formation, sample DGR-3 502.55 has a lower apparent Cl^- concentration of 2800 $\text{mmol/kg}_{\text{H}_2\text{O}}$. The relative uncertainty in the water content determined for this core sample based on four replicate measurements is high (24%); the lower apparent chloride concentration could suggest that the water content of the core is overestimated. Apparent Cl^- concentrations between 3000 and 5000 $\text{mmol/kg}_{\text{H}_2\text{O}}$ are observed in the Cobourg through the Shadow Lake formations, with an increase in Cl^- concentrations to between 5500 and 6500 in the Cambrian. The Cl^- concentrations determined for groundwaters in the Cambrian are in the middle of the range of apparent porewater concentrations. In general, the apparent Cl^- concentrations over this profile are in the same range as those determined by Intera (2009a) using aqueous extraction with a reaction time of 60 days.

The Br/Cl ratio is also shown as a function of depth in Figure 57. Through the Ordovician shales, the Br/Cl ratio is essentially constant, with the exception of one sample from DGR-3 in the Manitoulin Formation. The lower Br/Cl ratio in this sample is consistent with the potential presence of halite in this formation; the upscaled aqueous extract solutions for this sample were also predicted to be near halite saturation. Lower Br/Cl ratios are observed in porewaters from the Ordovician limestone formations, from the Cobourg Formation through the Gull River Formation. In the

Shadow Lake Formation and in the Cambrian, the Br/Cl ratios are again higher and are similar to those observed in the Ordovician shales.

Table 54: Select dataset for DGR-3 in which presence of soluble salts was not observed petrographically. Apparent porewater concentrations (mmol/kgH₂O) have been calculated using water contents determined gravimetrically at 105 °C (WC_{Grav.dry}).

Sample ID (NWMO)	Formation	Lithology	WC _{Grav.dry}	Relative uncertainty in WC	Na ⁺	K ⁺	Ca ²⁺	Sr ²⁺	*Cl ⁻	*Br ⁻
			Wt. %	%	(mmol/ kg H ₂ O)	(mmol/ kg H ₂ O)	(mmol/ kg H ₂ O)	(mmol/ kg H ₂ O)	(mmol/ kg H ₂ O)	(mmol/ kg H ₂ O)
DGR-3 435.62	Cabot Head	Dolostone ± shale	3.75	3.1	1900	490	1430	16	6070	33
DGR-3 453.41 ^H	Manitoulin	Limestone	0.70	7.9	2970 ^H	478	2100	n.a. ¹	8980 ^H	60
DGR-3 468.76	Queenston	Shale	3.19	0.4	1690	496	1280	12	6130	33
DGR-3 502.55	Queenston	Shale	2.09	24	1090	355	767	8	2780	15
DGR-3 581.47	Georgian Bay	Shale / sandstone	3.33	2.3	2130	489	1110	14	5300	27
DGR-3 621.63	Blue Mountain	Shale	3.07	0.8	2270	528	1240	16	5780	30
DGR-3 646.29	Blue Mountain	Shale	2.83	1.0	2170	427	1130	13	5170	28
DGR-3 665.29	Cobourg – CM	Argill. Limestone	0.54	4.9	1800	637	434	8	3560	16
DGR-3 676.21 ^H	Cobourg – LM	Argill. Limestone	0.89	13	3530 ^H	n.a. ²	1250	n.a. ¹	8020 ^H	36
DGR-3 678.92	Cobourg – LM	Limestone	0.59	53	1640	493	570	8	3660	16
DGR-3 685.52	Cobourg – LM	Limestone	0.64	5.7	2040	548	723	9	4570	22
DGR-3 690.12 ^H	Cobourg – LM	Limestone	0.28	27	3640 ^H	823	1300	20	7910 ^H	33
DGR-3 692.82	Cobourg – LM	Limestone	0.86	10	2300	492	712	11	4860	22
DGR-3 697.94	Cobourg – LM	Argill. Limestone	0.64	5.7	2380	602	802	10	5120	24
DGR-3 710.38	Sherman Fall	Argill. Limestone	0.31	19	1990	364	867	12	4260	18
DGR-3 725.57	Sherman Fall	Argill. Limestone	0.88	6.6	3100	785	802	10	5780	29
DGR-3 744.27	Kirkfield	Argill. Limestone	0.90	11	2860	742	675	8	5000	22
DGR-3 777.33	Coboconk	Limestone / shale	0.46	4.1	2140	523	374	4	3100	12
DGR-3 807.43	Gull River	Limestone	0.33	3.9	2140	396	600	7	3680	14
DGR-3 843.92	Gull River	Limestone	0.48	27	2110	422	395	5	3150	12
DGR-3 852.18	Shadow Lake	Limestone	3.15	1.9	1750	248	590	n.a. ¹	3500	17
DGR-3 856.06 ^H	Cambrian	Sandy limestone	0.49	15	2790 ^H	367	699	10	6520 ^H	26

*For all ions including Cl⁻ and Br⁻, it was assumed that ion accessible porosity (i.e. geochemical porosity) is equal to the porewater-loss porosity.

¹n.a.: not applicable due to evidence that extracted concentration may not represent porewater concentration

^H predicted to be at or above saturation with respect to halite when upscaled aqueous concentrations were modelled using PHREEQC and Pitzer thermodynamic database.

Table 55: Select dataset for DGR-4 in which presence of soluble salts was not observed petrographically. Apparent porewater concentrations (mmol/kgH₂O) have been calculated using water contents determined gravimetrically at 105 °C (WC_{Grav.dry}).

Sample ID (NWMO)	Formation	Lithology	WC _{Grav.dry}	Relative un- certainty in WC	Na ⁺	K ⁺	Ca ²⁺	Sr ²⁺	*Cl ⁻	*Br ⁻
			Wt. %	%	(mmol/ kg H ₂ O)	(mmol/ kg H ₂ O)	(mmol/ kg H ₂ O)	(mmol/ kg H ₂ O)	(mmol/ kg H ₂ O)	(mmol/ kg H ₂ O)
DGR-4 154.60	Bass Islands	Dolomitic shale	1.60	3.9	n.a. ¹	n.a. ¹	n.a. ¹	n.a. ¹	n.a. ¹	n.a. ¹
DGR-4 422.21 ^H	Cabot Head	Red-green shale with carbonate/black shale beds	4.21	1.7	2080 ^H	530	1590	19	6310 ^H	35
DGR-4 520.42	Georgian Bay	Shale with sandstone/siltstone/limestone beds	1.64	12	1880	465	1210	8	4970	25
DGR-4 662.83	Cobourg – LM	Bioclastic limestone/ argillaceous limestone	0.63	19	2810	713	969	12	5140	25
DGR-4 665.41 ^H	Cobourg – LM	Bioclastic limestone/ argillaceous limestone	0.57	27	2760 ^H	707	1000	13	6690 ^H	33
DGR-4 672.85	Cobourg – LM	Bioclastic limestone/ argillaceous limestone	0.40	17	2390	662	881	12	4870	23
DGR-4 717.12	Sherman Fall	Bedded argillaceous limestone/calcareous shale	1.15	41	1830	444	448	4	2900	13
DGR-4 730.07	Kirkfield	Limestone with shale beds	1.53	19	1830	417	468	5	3380	15
DGR-4 841.06	Shadow Lake	Sandy mudstone, siltstone and sandstone	2.04	6.9	2180	210 (n.a. ¹)	852	6	4390	20
DGR-4 847.48	Cambrian	Sandstone/dolostone	0.73	11	2510	98 (n.a. ¹)	726	9	5170	24

*For all ions including Cl⁻ and Br⁻, it was assumed that ion accessible porosity (i.e. geochemical porosity) is equal to the porewater-loss porosity.

¹n.a. not applicable; evidence that ion concentration may not represent porewater compositions.

^H predicted to be at or above saturation with respect to halite when upscaled aqueous concentrations were modelled using PHREEQC and Pitzer thermodynamic database.

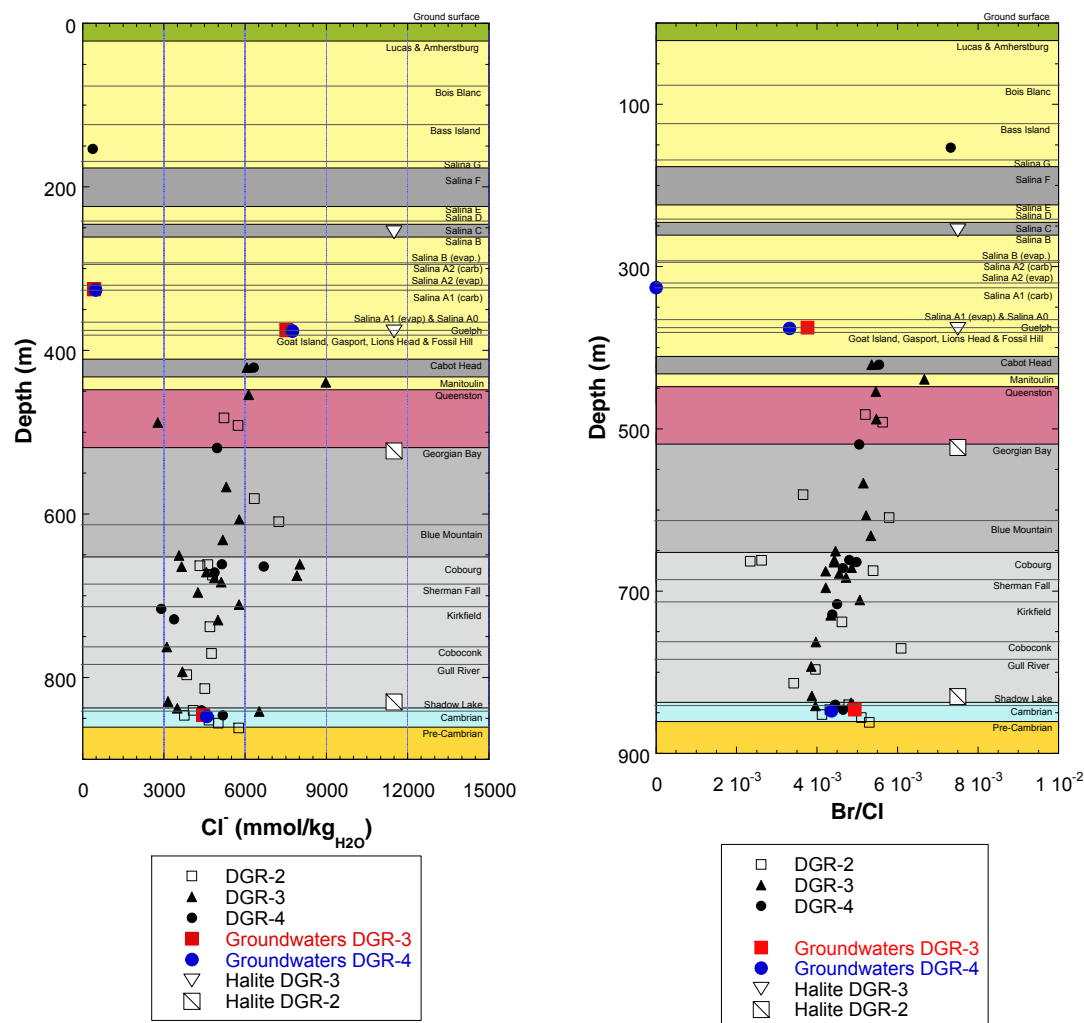


Figure 57: Apparent porewater concentration of Cl^- (mmol/kg_{H₂O}) and Br/Cl ratio as a function of depth for select dataset (Br/Cl ratio of modern seawater is also shown). Depths of DGR-3 and -4 samples are plotted relative to DGR-1/2. Depth positions in boreholes DGR-2 and DGR-3 where halite was observed petrographically are also shown (note that Cl^- concentrations and Br/Cl ratios plotted for these samples are meaningless).

The apparent Br^- concentrations in the porewaters are plotted as a function of depth in Figure 58 (the Br/Cl ratio is also shown for comparison). Bromide concentrations in the porewaters show essentially the same trend as Cl^- , with higher concentrations present in the Ordovician shales, decreasing to lower concentrations through the Ordovician limestones and then increasing in concentration again in the Shadow Lake and Cambrian. In DGR-3 and DGR-4, porewaters within the Cambrian have apparent Br^- concentrations between 24 and 26 mmol/kg_{H₂O}, in good agreement with its concentration in the groundwaters (20 to 22 mmol/kg_{H₂O}).

Greater scatter is observed in the Br/Cl ratios determined for the DGR-2 samples than in those from DGR-3 and DGR-4. For the DGR-2 samples, it was noted that the Br^- concentrations are subject to larger analytical uncertainties at low concentrations, where close to detection in the

aqueous extract solutions (Koroleva et al., 2009). In DGR-3 and DGR-4, improved confidence was obtained in Br^- concentrations measured in aqueous extract solutions that were at or near the detection limit in aqueous extracts by cross-checking using ICP-MS (see also section 6).

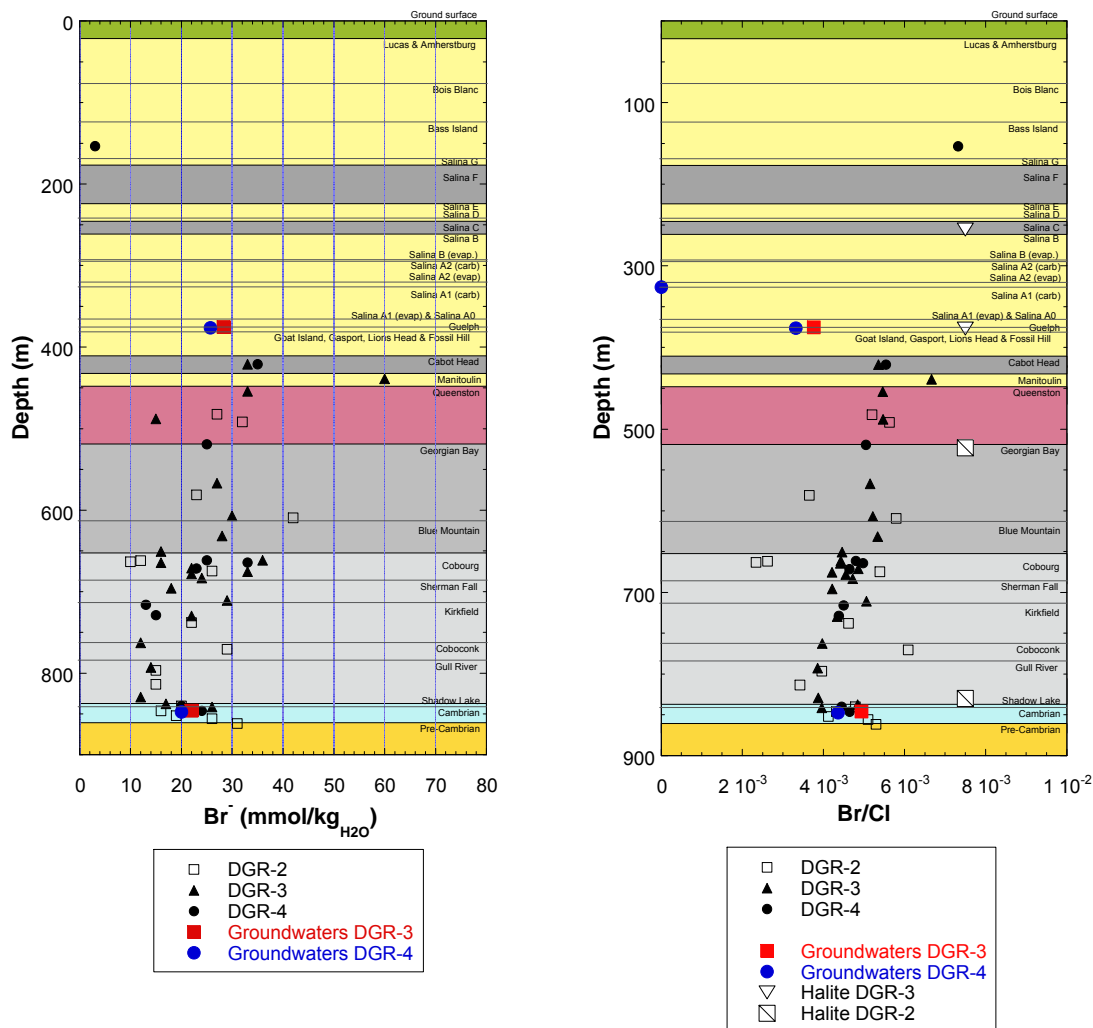


Figure 58: Apparent porewater concentration of Br^- (mmol/kg_{H2O}) and Br/Cl ratio as a function of depth for select dataset (Br/Cl ratio of modern seawater is also shown). Depths of DGR-3 and -4 samples are plotted relative to DGR-1/2. Depth positions in boreholes DGR-2 and DGR-3 where halite was observed petrographically are also shown (note that Br^- concentrations and Br/Cl ratios plotted for these samples are meaningless).

In Figure 59, the apparent Na^+ concentrations and the Na/Cl ratios in the porewater are shown as a function of depth. In the porewaters of the Ordovician shales, the apparent Na^+ concentrations are approximately 2000 mmol/kg_{H2O} in the majority of samples. A wider range of values is observed through the underlying limestones, with apparent porewater Na^+ between 1500 and 3000 mmol/kg_{H2O}. As was observed for Cl^- , the Na^+ concentrations are higher in one sample from the

Manitoulin Formation and two from the Cobourg Formation, consistent with predictions that the scaled aqueous extracts were near saturation with respect to halite. The Na/Cl ratio is approximately 0.3 in the Cabot Head Formation and increases to approximately 0.4 in Queenston Formation and remains constant at this value down through the Blue Mountain Formation. From the top of the Cobourg Formation, the Na/Cl ratio increases from 0.5 to 0.7 in the Coboconk Formation and decreases gradually again to approximately 0.4 in the Cambrian. The range of Na^+ concentrations and Na/Cl ratios determined in this study are similar to those reported for DGR-3 and DGR-4 samples by Intera (2009a) for the same interval. Within the Cambrian, the concentration of Na^+ and the Na/Cl ratio in the groundwaters from DGR-3 and DGR-4 are below the range of values determined for the porewaters; substantial variation in both parameters is observed in the porewaters.

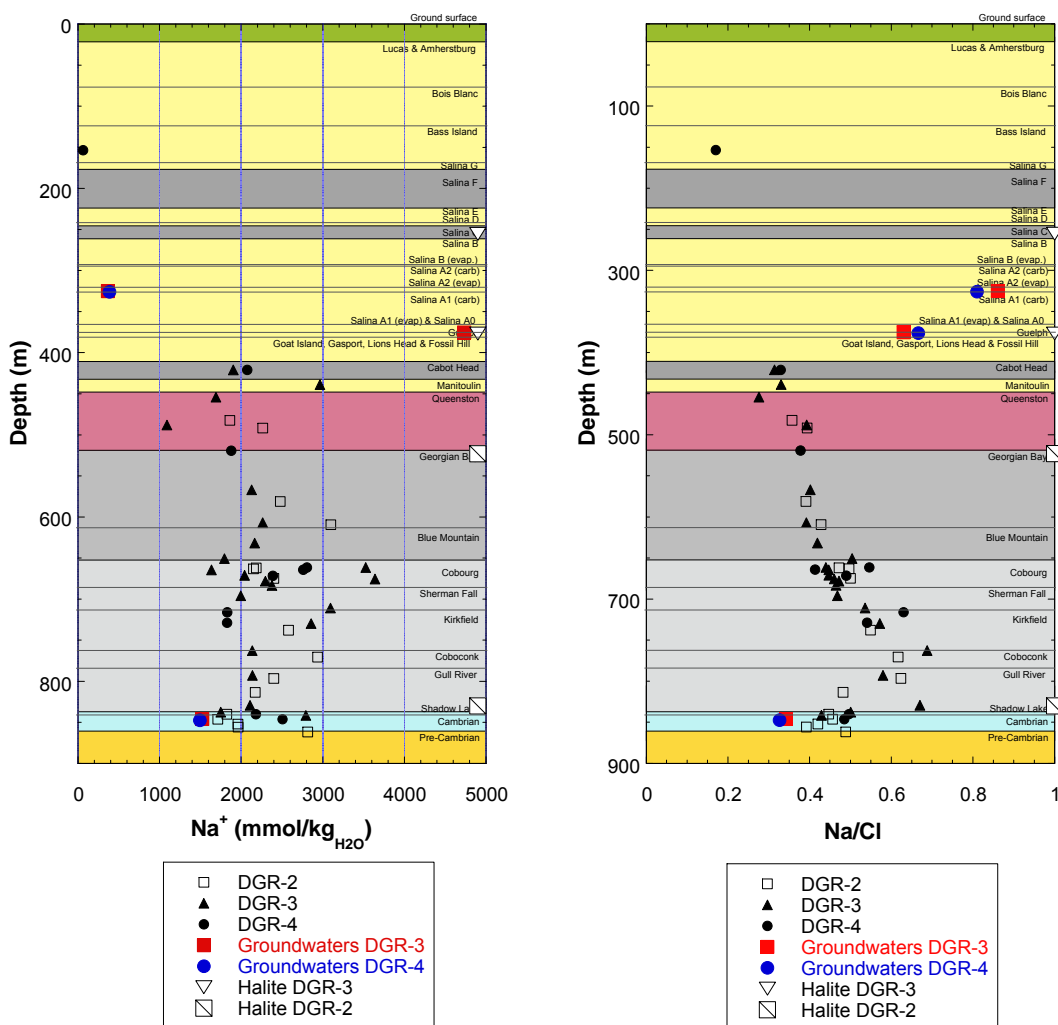


Figure 59: Apparent porewater concentration of Na^+ (mmol/kg_{H2O}) and Na/Cl ratio as a function of depth for select dataset. Depths of DGR-3 and DGR-4 samples are plotted relative to DGR-1/2. Depth positions in boreholes DGR-2 and DGR-3 where halite was observed petrographically are also shown (note that Na^+ concentrations plotted for these samples are meaningless).

The apparent concentrations of Ca^{2+} and the Ca/Cl ratio in the porewaters are plotted in Figure 60. From the Cabot Head Formation and through the Ordovician shales, the apparent porewater Ca^{2+} ranges between 1000 and 1500 $\text{mmol}/\text{kg}_{\text{H}_2\text{O}}$. Although there is scatter over a relatively wide range in the Cobourg Formation (500 to 1500 $\text{mmol}/\text{kg}_{\text{H}_2\text{O}}$), Ca^{2+} in the porewaters appears to decrease to approximately 500 $\text{mmol}/\text{kg}_{\text{H}_2\text{O}}$ through the Ordovician limestones. In the porewaters within the Shadow Lake and Cambrian, apparent Ca^{2+} concentrations range from 500 to 1200 $\text{mmol}/\text{kg}_{\text{H}_2\text{O}}$; calcium concentrations in the groundwaters are within this range (approximately 1000 $\text{mmol}/\text{kg}_{\text{H}_2\text{O}}$). The Ca/Cl ratio is between 0.20 and 0.28 from the Cabot Head Formation through the Ordovician shales, where the aqueous extraction solutions suggest that the porewaters are predominantly Ca-Na-Cl type porewaters. In the Ordovician limestones, the Ca/Cl ratios decrease to ratios between 0.1 and 0.2, where the porewaters are Na-Ca-Cl type. In the Shadow Lake and Cambrian, Ca/Cl ratios from 0.10 to 0.24 are recorded in the porewaters; the groundwaters in DGR-3 and DGR-4 have a Ca/Cl ratio of 0.22.

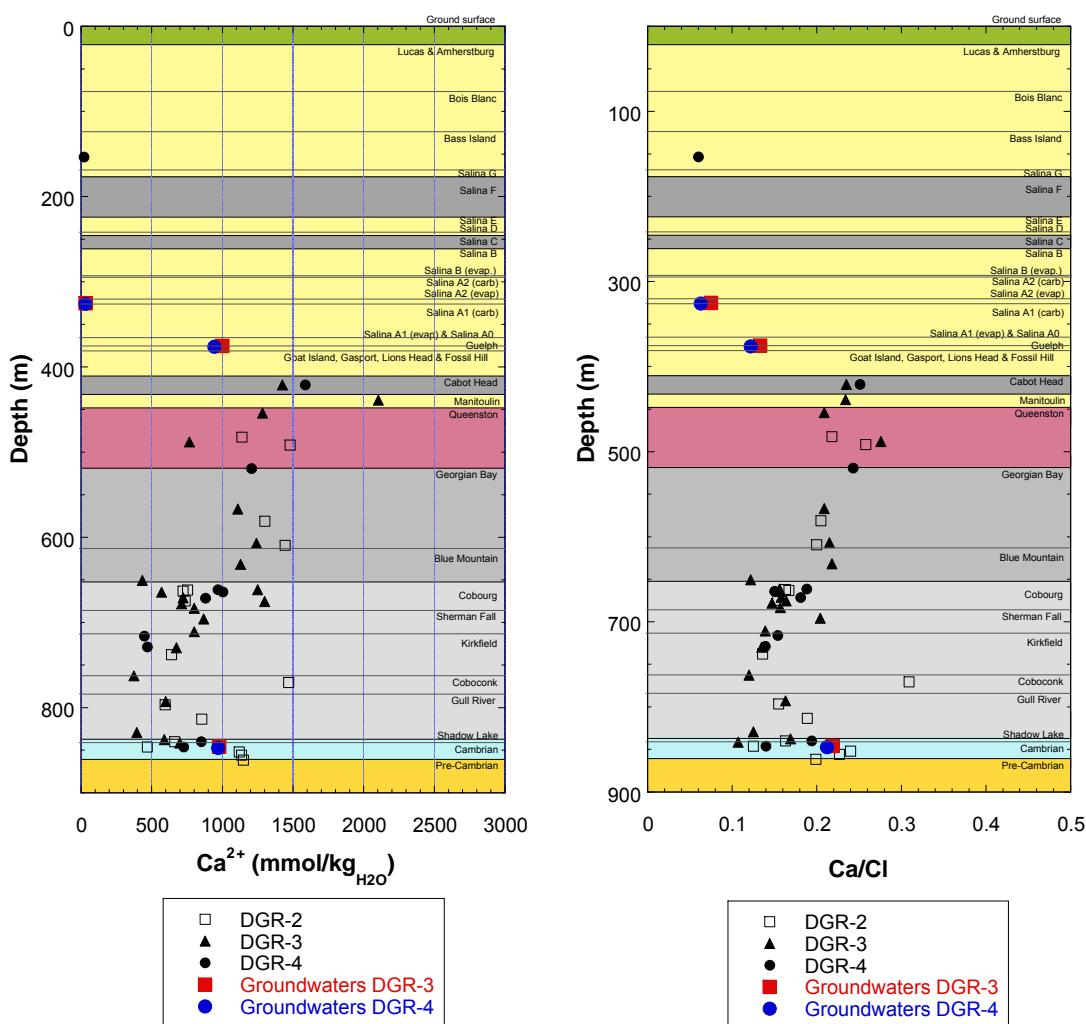


Figure 60: Apparent porewater concentrations of Ca^{2+} ($\text{mmol}/\text{kg}_{\text{H}_2\text{O}}$) and Ca/Cl ratio as a function of depth for select dataset. Depths of DGR-3 and -4 samples are plotted relative to DGR-1/2.

In Figure 61, the ratio Na/Ca in the porewaters as a function of depth is compared to the stable oxygen composition determined over the profile in boreholes DGR1/2 (Intera, 2008c) and in boreholes DGR-3 and DGR-4 (Intera, 2009a and this study, section 5.3). As discussed in section 6.2, the aqueous extract solutions through the Ordovician shales are Ca-Na-Cl type, and predominantly Na-Ca-Cl type through the Ordovician limestones and into the Cambrian. The low Na/Ca ratio of 1.5 calculated for porewaters through the Ordovician reflects this dominance of more Ca-rich porewaters through the shales. As shown by the data from Intera (2008c, 2009a), the stable oxygen isotope signatures determined for the porewaters are also relatively constant through the Cabot Head Formation and the Ordovician shales. As the Na/Ca ratio increases in the Ordovician limestones to approximately 4 in the middle of the limestones (Kirkfield and Gull River formations), this trend is also recorded as a shift towards lighter oxygen isotopic signatures in the stable isotope values determined for the porewaters in datasets from Intera (2008c, 2009a) and in the data from this study (section 5.3). The Cambrian groundwaters record a trend back to lower Na/Ca ratios (1.5), similar to those observed in the Ordovician shales, whereas a wider range of Na/Ca ratios (1.5 to 4) are observed in the apparent porewater compositions. Through the lower part of the Gull River Formation and into the Shadow Lake and Cambrian, the stable isotopic composition determined in the porewaters by Intera (2008c, 2009a) shifts back towards heavier signatures of approximately -5%, in agreement with the stable oxygen values determined for the Cambrian groundwaters from boreholes DGR-2, DGR-3 and DGR-4.

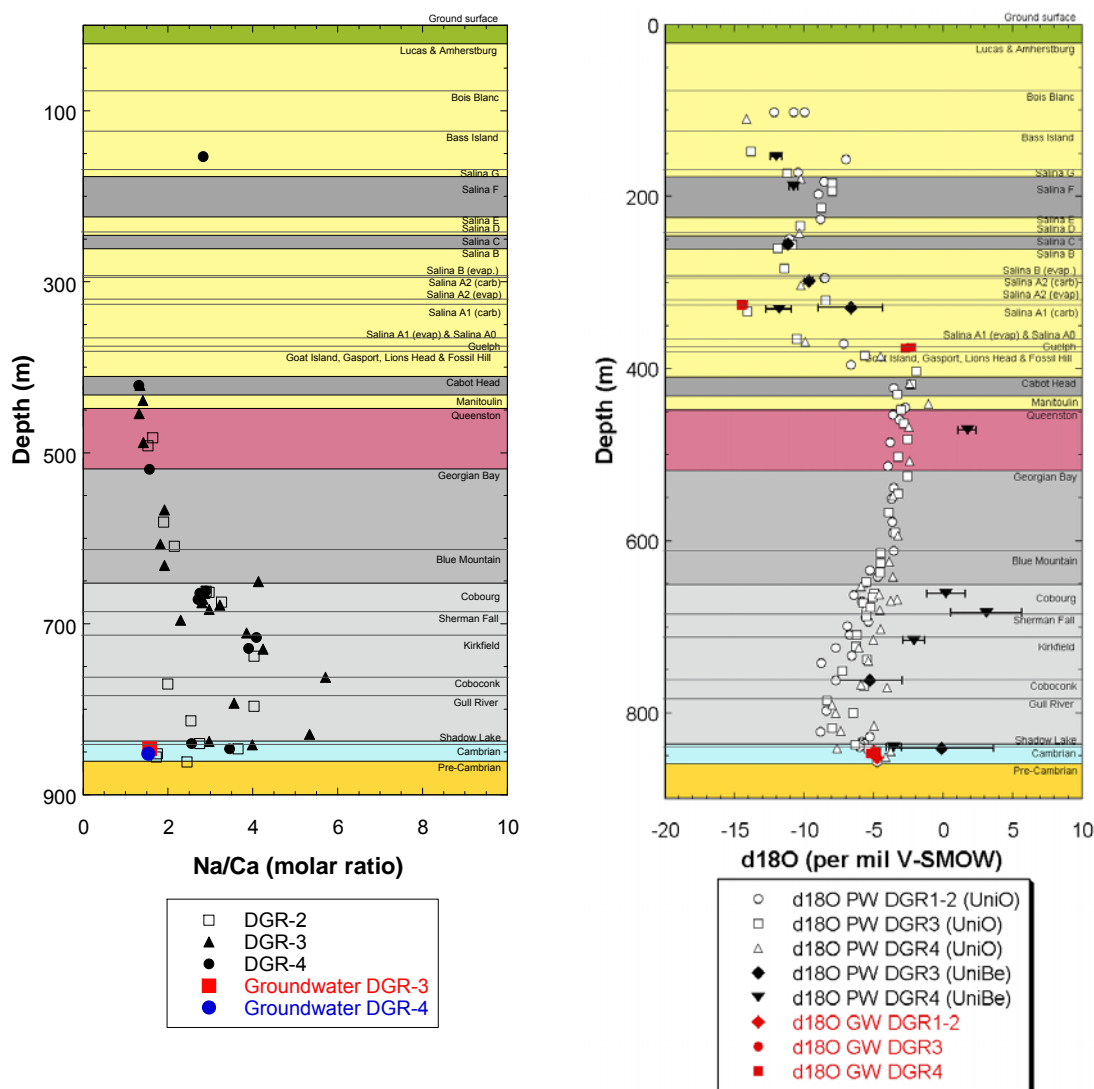


Figure 61: Na/Ca ratio and $\delta^{18}\text{O}$ determined for porewaters as a function of depth in boreholes DGR-1/2, DGR-3 and DGR-4 (see section 5.4 for additional details on stable isotope profiles).

The stable oxygen compositions for the porewaters in DGR-3 and DGR-4 obtained using the adapted diffusive exchange technique (this study) show the same general trend to the vacuum distillation results of Intera (2008c, 2009a) through the Ordovician limestones and into the Cambrian. However, the $\delta^{18}\text{O}$ signatures determined using the adapted diffusive exchange technique are enriched in ^{18}O relative to those determined by vacuum distillation through the Ordovician shales and limestones. In the Cambrian, the stable oxygen isotopic signatures are again the same within error; this is most convincing for the sample from DGR-4, given that the uncertainty in the $\delta^{18}\text{O}$ value determined for the DGR-3 is large. In the upper part of the sedimentary sequence, within the units of the Salina Formation, the stable isotopic signatures determined by both methods are the same within error (see also section 5.4). There is at the moment no definitive explanation for the isotopically more positive signatures obtained for the porewaters using the isotope

diffusive exchange method compared to those determined using vacuum distillation, but two possible explanations are proposed:

- Vacuum distillation at 150°C recovers all the water from the sample in the case of NaCl-dominated porewater (i.e., in the upper part of the DGR profile) but not when more complex brines are involved (lower part of the DGR profile, from Guelph Formation down; see section 6.2), where the presence of CaCl₂ and MgCl₂ might impede the complete vacuum distillation of the porewater, even at 150°C (see de Haller et al., 2008). Incomplete vacuum distillation would produce water with lighter isotopic composition than the original porewater. Intera (2010c) reached the conclusion that, if any, the effect of incomplete distillation was below analytical error for DGR samples;
- the isotope diffusive exchange method is sensitive to differences in the chemical compositions between the porewater and the testwater used in the experiments. As described previously, the upper part of the profile was investigated with NaCl test waters, while deeper samples had lower water activities and required the use of CaCl₂ test waters. Although the water activities of the test solutions are matched to those measured for the porewaters, the relatively simple compositions of these test waters do not reflect the complex chemical composition of the porewaters (see also section 5.4; section 6.2). The potential influence of an isotopic fractionation effect due to differences in chemical composition is being investigated in an NWMO methodology study (GS85).

The apparent K⁺ concentrations and Na/K ratios are presented in Figure 62. There are seven samples in the Cobourg, Sherman Fall and Kirkfield formations that have high K⁺ concentrations of between 600 and 1000 mmol/kg_{H₂O}. The remainder of the samples from the Cabot Head Formation down through the Coboconk Formation have K⁺ concentrations ranging between 400 and 600 mmol/kg_{H₂O}. From the Gull River Formation into the Shadow Lake and Cambrian, apparent K⁺ concentrations in the porewaters range from approximately 400 mmol/kg_{H₂O} down to approximately 50 mmol/kg_{H₂O}. There appears to be some consistency between decreasing apparent porewater K⁺ concentrations observed in these lowermost formations and the lower K⁺ are approximately 25 mmol/kg_{H₂O} determined in the Cambrian groundwaters from DGR-3 and DGR-4. However, as discussed in section 6.2 and highlighted in section 10.1, Table 54 and Table 55, the extracted K⁺ concentrations measured for these samples may not reflect porewater concentrations, but rather, may be controlled by mineral solubility reactions occurring during the extractions. Aqueous extractions on these specific samples conducted at multiple solid:liquid ratios are required to test this hypothesis.

A constant Na/K ratio of approximately 4 is observed in the porewaters is from the Cabot Head Formation down through to the top of the Shadow Lake for DGR-3 and DGR-4 samples. In the DGR-2 samples, a trend towards higher Na/K ratios appears to begin in the Coboconk. However, in the Shadow Lake and Cambrian, a range of higher Na/K ratios between 8 and 40 observed in the porewaters reflect the lower K⁺ concentrations determined in the aqueous extracts of these samples. As discussed in above, these may not reflect true ratios in the porewaters, because mineral solubility reactions may have impacted the aqueous extracts for these samples (i.e. measured K⁺ concentrations reflect the solubility of a mineral phase, not porewater concentrations). The highest Na/K ratios of approximately 60 are observed in the Cambrian groundwaters from DGR-3 and DGR-4.

Ziegler and Longstaffe (2000a, 2000b) have investigated diagenetic alteration of the uppermost Precambrian and the overlying Cambrian and Ordovician sedimentary rocks. The diagenetic as-

semblage includes secondary K-feldspar, chlorite, illite and some kaolinite; the secondary clay minerals occur within fractures and within the rock matrix as grain-coatings or as in-filling minerals between grains. In the current study, secondary K-feldspar adularia was identified in sample DGR-3 856.06 from the Cambrian during mineralogical investigations (section 3.1). An evaluation of the clay minerals as a potential mineralogical control on K^+ and/or Na^+ concentrations in the Cambrian groundwater and/or porewaters is not currently possible, because aluminosilicate minerals including K-feldspars and clay minerals are not yet included in the PHREEQC Pitzer thermodynamic database (e.g. Waber et al., 2007).

In summary, similar trends are observed as a function of depth in the apparent porewater concentrations of Cl^- , Br^- and Ca^{2+} and in the corresponding Br/Cl , Ca/Cl and Na/Ca ratios. All are relatively constant through the Ordovician shales, decrease in the underlying Ordovician limestones and then increase again in the Gull River Formation through the Cambrian. For these parameters, the values measured in the Cambrian groundwater samples are within the range of the apparent porewater values. Apparent porewater concentrations of Na^+ (and also Na/Cl ratios) are also relatively constant through the Ordovician shales, but then increase in the underlying Ordovician limestone formations, where Na-Ca-Cl porewaters become dominant. This trend is mirrored in the $\delta^{18}O$ values, which are relatively constant within the Ordovician shales, decrease towards more negative signatures in the Ordovician limestones and then increase again in the Shadow Lake and Cambrian to values similar to those observed in the overlying Ordovician shales. The profile of apparent K^+ porewater concentrations and Na/K is unusual in comparison to the other parameters examined. The concentration range observed for K^+ and the Na/K ratio is relatively constant throughout the sequence (Cabot Head Formation through the Coboconk Formation), but then the K^+ concentrations decrease (and Na/K ratios increase) gradually in the bottom of the profile – from approximately 400 mmol/kg_{H₂O} in the Gull River Formation to very low K^+ concentrations (20 mmol/kg_{H₂O}) in the Cambrian. One hypothesis for this decrease is that K^+ concentrations may be related to the presence of secondary potassium feldspar in these lower formations, as identified in mineralogical investigations in one sample from the Cambrian in this study, and more widely identified in the lower Ordovician/Cambrian in southern Ontario (e.g. Ziegler and Longstaffe, 2000a; 2000b). However, additional information from aqueous extractions at multiple solid:liquid ratios are required for the select samples from DGR-2 and DGR-4, where low K^+ concentrations were observed, to determine whether or not these concentrations are controlled by mineral dissolution/precipitation reactions during the extraction procedure.

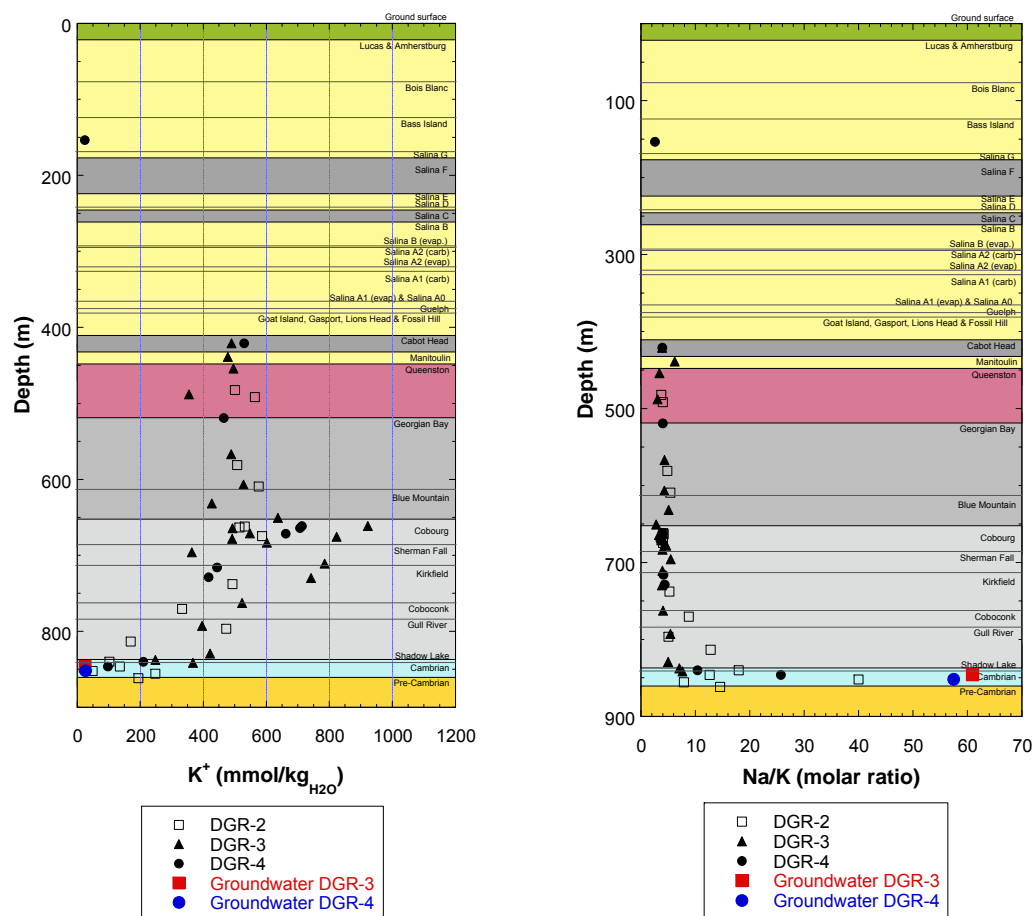


Figure 62: Apparent porewater concentration of K^+ (mmol/kg_{H2O}) and Na/K ratio as a function of depth for select dataset. Depths of DGR-3 and -4 samples are plotted relative to DGR-1/2.

10.2.2 A starting point to account for ion-accessible porosity

The scaling of the aqueous extracts using water content to define apparent porewater concentrations in mmol/kg_{H2O} as presented in the previous section provides an estimate that may be sufficient for the majority of cations that will have access to the entire porewater-filled porosity. Anions, on the other hand, may be excluded from a portion of the porewater-filled porosity, as discussed in section 10.1.

To account for the proportion of the porosity (ion-accessible or geochemical porosity) in which ions such as Cl^- and Br^- are transported or undergo water-rock reactions, porewater concentration is expressed in terms of mass of an ion per unit volume. The molar concentration of an ion in porewater can be calculated from aqueous extraction data using the following expression:

$$C_{PW}^i = \frac{C_{rock}^i * \rho_{b.dry}}{\phi_{PWL}} \quad (20)$$

where C_{pw}^i is the concentration of the ion in mol/L porewater, C_{rock}^i is the extracted ion concentration in mol/kg_{rock} determined using aqueous extraction, $\rho_{b,dry}$ is the bulk dry density of the rock in kg_{rock}/L and ϕ_{PWL} = the porewater-loss porosity (see also section 4.4), expressed as a volume fraction. In this expression, it is assumed that the ion has access to the total volume of porewater in the rock. The apparent porewater concentrations in units of mmol/L porewater for samples from DGR-3 and DGR-4 are given in Table 56 and Table 57, respectively.

Pearson (1999) defined geochemical porosity as the ratio of the volume of fluid in which transport and water-rock reactions occur to the total volume of the rock. For rocks in which transport is dominated by diffusion, the geochemical porosity for a given ion will likely be similar to its diffusion porosity (or ion accessible porosity). Considering the results of Intera (2008b; 2010c) for I⁻, it appears that the anion accessible porosity may be approximately 50% of the porewater porosity in shales such as the Cabot Head, Queenston, Georgian Bay and Blue Mountain formations. The concentration of an ion in the porewater, taking into account this ion accessible porosity, can be calculated as follows (Pearson, 1999):

$$C_{pw}^i = \frac{C_{rock}^i * \rho_{b,dry}}{\phi^i} \quad (21)$$

where C_{pw}^i is the concentration of the ion in mol/L porewater, C_{rock}^i is the extracted ion concentration in mol/kg_{rock} determined using aqueous extraction, $\rho_{b,dry}$ is the bulk dry density of the rock in kg_{rock}/L and ϕ^i is the geochemical (or ion-accessible porosity) for species *i*, expressed as a volume fraction. The apparent porewater concentrations for samples from shale formations in DGR-3 and -4 have been calculated using equation 21 and assuming that Cl⁻ has access to 50% of the porewater-loss porosity, as suggested for I⁻ by the results of Intera (2008b, 2010c). The results are tabulated in Table 58. For comparison, the upscaled concentrations (in mmol/kg_{H2O}) given in Table 54 and Table 55 were speciated using PHREEQC and the Pitzer thermodynamic database and equilibrium with halite was stipulated. The Cl⁻ concentrations predicted at equilibrium with halite are also tabulated for these samples. With the exception of one sample from the Georgian Bay Formation (DGR-3 581.47), the apparent porewater Cl⁻ concentrations are much higher than predicted at halite saturation. This may suggest that:

- the anion accessible porosity for Cl⁻ is greater than 50% of the porewater-loss porosity observed for I⁻ in diffusion studies (Intera, 2008b; 2010a).
- halite is present throughout the formation and was dissolved during the aqueous extraction experiments. This interpretation is not consistent with the mineralogical information available (i.e., halite identified in only a limited number of samples), although the number of samples on which detailed studies were conducted is limited.

Table 56: Select dataset for DGR-3 in which presence of soluble salts was not observed petrographically. Apparent porewater concentrations in mmol/L of porewater, calculated using bulk dry densities and porewater-loss porosity.

Sample ID (NWMO)	Formation	Lithology	Porewater -loss porosi- ty (ϕ_{PWL}) (vol. %)	Uncertainty in ϕ_{PWL} (vol. %)	Na ⁺	K ⁺	Ca ²⁺	Sr ²⁺	*Cl ⁻	*Br ⁻
					(mmol/L)	(mmol/L)	(mmol/L)	(mmol/L)	(mmol/L)	(mmol/L)
DGR-3 435.62	Cabot Head	Dolostone ± shale	10.3	0.53	1730	446	1300	14.8	5520	29.6
DGR-3 453.41 ^H	Manitoulin	Limestone	2.09	0.19	2630 ^H	425	1870	n.a. ¹	7970 ^H	53.2
DGR-3 468.76	Queenston	Shale	8.98	0.40	1520	446	1150	11.1	5510	30.1
DGR-3 502.55	Queenston	Shale	6.03	1.36	976	318	686	7.14	2480	13.6
DGR-3 581.47	Georgian Bay	Shale / sandstone	5.41	0.55	1870	430	975	12.2	4660	24.0
DGR-3 621.63	Blue Mountain	Shale	8.72	0.39	2010	468	1100	13.8	5130	26.8
DGR-3 646.29	Blue Mountain	Shale	7.95	0.37	1960	386	1020	12.0	4670	25.0
DGR-3 665.29	Cobourg –C M	Argill. Limestone	1.55	0.11	1590	565	386	7.52	3160	14.1
DGR-3 676.21 ^H	Cobourg – LM	Argill. Limestone	2.63	0.35	3150 ^H	n.a. ¹	1120	n.a. ¹	7170 ^H	31.7
DGR-3 678.92	Cobourg – LM	Limestone	1.74	0.90	1470	442	511	6.78	3280	14.5
DGR-3 685.52	Cobourg – LM	Limestone	1.90	0.14	1800	483	637	7.83	4020	19.6
DGR-3 690.12 ^H	Cobourg – LM	Limestone	0.83	0.23	3220 ^H	728	1150	17.3	7000 ^H	29.5
DGR-3 692.82	Cobourg – LM	Limestone	2.54	0.28	2050	440	637	10.0	4350	19.8
DGR-3 697.94	Cobourg – LM	Argill. Limestone	1.90	0.14	2110	535	713	8.62	4550	21.5
DGR-3 710.38	Sherman Fall	Argill. Limestone	0.92	0.18	1750	320	762	10.6	3750	15.8
DGR-3 725.57	Sherman Fall	Argill. Limestone	2.58	0.21	2820	715	731	8.67	5260	26.6
DGR-3 744.27	Kirkfield	Argill. Limestone	2.64	0.30	2560	665	605	6.86	4480	19.4
DGR-3 777.33	Coboconk	Limestone / shale	1.36	0.09	1920	470	336	3.91	2790	11.1
DGR-3 807.43	Gull River	Limestone	0.98	0.06	1940	359	545	5.96	3350	12.9
DGR-3 843.92	Gull River	Limestone	1.42	0.38	1870	375	351	4.00	2800	10.8
DGR-3 852.18	Shadow Lake	Limestone	8.57	0.44	1570	222	529	n.a. ¹	3140	15.2
DGR-3 856.06 ^H	Cambrian	Sandy limestone	1.46	0.27	2550 ^H	335	638	8.84	5950 ^H	23.6

*For all ions including Cl⁻ and Br⁻, it was assumed that ion accessible porosity (i.e. geochemical porosity) is equal to the porewater-loss porosity.

¹n.a. not applicable; evidence that ion concentration may not represent porewater compositions.

^H predicted to be at or above saturation with respect to halite when upscaled aqueous concentrations were modelled using PHREEQC and Pitzer thermodynamic database (section 6.3).

Table 57: Select dataset for DGR-3 in which presence of soluble salts was not observed petrographically. Apparent porewater concentrations in mmol/L of porewater, calculated using bulk dry densities and porewater-loss porosity.

Sample ID (NWMO)	Formation	Lithology	Porewater -loss poros- ity (ϕ_{PWL})	Uncertainty in ϕ_{PWL}	Na ⁺	K ⁺	Ca ²⁺	Sr ²⁺	*Cl ⁻	*Br ⁻
			(vol. %)	(vol. %)	(mmol/L)	(mmol/L)	(mmol/L)	(mmol/L)	(mmol/L)	(mmol/L)
DGR-4 154.60	Bass Islands	Dolomitic shale	4.36	0.26	n.a. ¹	n.a. ¹	n.a. ¹	n.a. ¹	n.a. ¹	n.a. ¹
DGR-4 422.21^H	Cabot Head	Red-green shale with carbonate/black shale beds	11.8	0.51	1840 ^H	469	1410	17.0	867 ^H	30.9
DGR-4 520.42	Georgian Bay	Shale with sandstone/siltstone/limestone beds	4.83	0.39	1670	414	1070	6.90	5590	22.3
DGR-4 662.83	Cobourg – LM	Bioclastic limestone and argillaceous limestone	1.87	0.22	2510	637	867	11.0	4420	22.1
DGR-4 665.41^H	Cobourg – LM	Bioclastic limestone and argillaceous limestone	1.73	0.28	2410 ^H	618	877	11.3	4600 ^H	29.1
DGR-4 672.85	Cobourg – LM	Bioclastic limestone and argillaceous limestone	1.19	0.14	2170	602	801	11.2	5850	20.6
DGR-4 717.12	Sherman Fall	Bedded argillaceous limestone and calcareous shale	3.33	0.80	1670	406	410	3.95	4430	11.9
DGR-4 730.07	Kirkfield	Limestone with shale beds	4.32	0.54	1690	386	433	4.73	2660	13.7
DGR-4 841.06	Shadow Lake	Sandy mudstone, siltstone and sandstone	5.83	0.40	2010	194	787	5.58	3120	18.0
DGR-4 847.48	Cambrian	Sandstone/dolostone	2.22	0.22	2210	86.4	643	8.04	4050	21.3

* For all ions including Cl⁻ and Br⁻, it was assumed that ion accessible porosity (i.e. geochemical porosity) is equal to the porewater-loss porosity.

¹n.a. not applicable; evidence that ion concentration may not represent porewater compositions.

^H predicted to be at or above saturation with respect to halite when upscaled aqueous concentrations were modelled using PHREEQC and Pitzer thermodynamic database.

Table 58: Apparent porewater concentrations of Cl⁻ in shale samples from DGR-3 and DGR-4 calculated using ion accessible porosity.

Sample ID (NWMO)	Formation	Lithology	Porewater-loss porosity (ϕ_{PWL}) (vol. %)	Uncertainty in ϕ_{PWL} (vol. %)	¹ Anion accessible porosity = $(\phi_{PWL}) * 0.5$ (vol frac)	² Cl ⁻ conc. calculated using anion accessible porosity (mmol/L)	³ Cl ⁻ at halite saturation (mmol/L)
DGR-3 435.62	Cabot Head	Dolostone ± shale	10.3	0.26	0.052	11045	6487
DGR-3 468.76	Queenston	Shale	8.98	0.40	0.045	15938	6589
DGR-3 502.55	Queenston	Shale	6.03	1.36	0.030	11027	3887
DGR-3 581.47	Georgian Bay	Shale / sandstone	5.41	0.55	0.027	4967	5952
DGR-3 621.63	Blue Mountain	Shale	8.72	0.39	0.044	9324	6277
DGR-3 646.29	Blue Mountain	Shale	7.95	0.37	0.040	10259	5850
DGR-4 422.21^H	Cabot Head	Red-green shale with carbonate/black shale beds	11.8	0.51	0.059	11174	6366
DGR-4 520.42	Georgian Bay	Shale with sandstone/siltstone/limestone beds	4.83	0.39	0.024	8845	5588

¹Calculated as 50% of the porewater-loss porosity.

²Calculated according to equation 2.

³The Cl⁻ concentration at halite saturation, predicted by simulating the concentrations given in Table 56 and Table 57 using the geochemical code PHREEQC and the Pitzer thermodynamic database and then equilibrating the solutions with halite.

10.3 Reconstructive geochemical modelling

Porewater characterisation studies conducted by Koroleva et al. (2009) and Intera (2008c) on core from DGR-2 and those reported here for samples from DGR-3 and -4 and by Intera (2009a) have involved the application of indirect methods to characterise the chemical composition of porewater (i.e. aqueous extraction, determination of cation exchange capacity, etc.). In the short term, development and testing of geochemical conceptual and numerical models of porewater compositions can provide an increased understanding of reactions between minerals and dissolved solid or gas phases in the porewater. These models may also be used to delineate bounds on parameters such as porewater pH that cannot be determined using indirect methods. Once a reconstructive geochemical model has been established and demonstrated to provide reasonable predictions of porewater composition, then the model can be used to develop an understanding of how perturbations might affect the system (e.g. Gaucher et al., 2009; Pearson et al., 2003).

The challenges in developing a conceptual and numerical geochemical model to reconstruct porewater compositions within the sedimentary sequence at the DGR site were discussed by Waber et al. (2007) and Koroleva et al. (2009) and include the following:

- Identifying for which ions the concentrations determined using aqueous extraction are representative of porewater compositions, as described in the previous section (10.2);
- The highly saline porewater compositions require application of a code with appropriate means to calculate activities coefficients. In this report, PHREEQC has been used with the Pitzer thermodynamic database. This includes only a limited number of elements, but captures the major ions in the porewater observed in this study. It does not include Si and Al or many of the relevant minerals for shales or argillaceous limestones (Waber et al., 2007).
- The ion exchange model, as it is implemented in PHREEQC with the Pitzer thermodynamic database, is not yet tested and proven, but could be used as a first approach to modelling ion exchange processes (Waber et al., 2007);
- Further development of databases will be required if redox reactions are to be implemented using PHREEQC and the Pitzer thermodynamic database.

10.3.1 How does current information measure up?

The development of a thermodynamic geochemical model to reconstruct porewater compositions requires that the concentrations of the major elements present can be constrained using either mass balance expressions (e.g. specifying the total concentration of the element present in the porewater), or using mass action expressions such as mineral solubility or exchange controls. The porewater composition will be uniquely defined if the number of constraints is equal to the number of unknowns (Gibbs' phase rule). In the following sections, the information available on the major ion compositions of the porewaters is reviewed in this context, considering first the subset of samples without evidence for soluble salts and then those with evidence for the presence of soluble salts.

In terms of defining cation exchange capacities, Waber et al. (2007) and Koroleva et al. (2009) determined that Ni-consumption could be used as reasonable proxy for cation exchange capacity. Initial measurements of CEC are available for several of the Ordovician formations in the sequence including the Queenston, Georgian Bay, Cobourg, Gull River and Shadow Lake formations and the Cambrian (Table 7-1 in Koroleva et al., 2009). The CEC values range from approximately 3 to 45 meq/kg_{rock}. For these formations, cation exchange capacities could be used together with generic selectivity coefficients from the literature as a constraint on porewater cation concentrations.

The potential for constructing geochemical conceptual/numerical models for formations within the sedimentary sequence is discussed in general terms in the following sections, for formations without and with evidence for the presence of soluble salts. However, in developing a geochemical model to refine porewater composition, it is envisioned that efforts would begin with the host rock, the Cobourg Formation. Geochemical models to refine porewater compositions within other formations such as the shales of the Ordovician shales (Queenston, Georgian Bay and Blue Mountain formations) for example, could be developed at a later stage, if required.

10.3.1.1 No petrographic evidence for soluble salts

For the select dataset without evidence for the presence of soluble salts, Na⁺, Ca²⁺ and Cl⁻ are the dominant ions extracted from all formations examined. The only exception is the Cambrian, where Mg²⁺ also appears to be a dominant species. Other species are relatively minor in terms of their concentrations in meq/kg_{rock}, including K⁺, Sr²⁺, SO₄²⁻, alkalinity (as HCO₃⁻) and Br⁻. In this simplified system (elements not yet measured or considered include Fe, Si and Al), there are a total of 9 elements for which the total concentrations in the porewater must be either given or constrained by mineral solubility or ion exchange controls. As described in section 10.1, apparent porewater concentrations were calculated assuming that the ion accessible porosity is equal to the porewater-loss porosity for these ions (i.e. no anion exclusion for Cl⁻ or Br⁻).

Consider first the subset of samples for which there is strong to good evidence that the concentrations of K⁺ and Sr²⁺ can be constrained based on their concentrations determined in the aqueous extractions, in addition to Na⁺, Ca²⁺, Cl⁻ and Br⁻. In this case, mass balance expressions can be used to constrain the concentrations of 6 out of the 9 elements and pH can be constrained using the expression for solution electroneutrality. Constraints are still required for the remaining 3 elements – magnesium, carbon and sulphur.

All aqueous extract solutions were predicted to be at or supersaturated with respect to calcite. Taken together with the ubiquitous presence of calcite throughout the sedimentary sequence, equilibrium with respect to calcite could be used to constrain carbon in the geochemical model. In order to use the solubility of calcite as a constraint on carbon, the pH and alkalinity of the porewater or the partial pressure of carbon dioxide (PCO_2) is required to fully constrain the system. Currently, there are no constraints on the pH of the porewaters and alkalinity may reflect contributions from organic acids, in addition to HCO_3^- , in some formations. Based on the high salinities of the porewaters, it is likely that the PCO_2 will be below the atmospheric value of $10^{-3.5}$ bars (also suggested by geochemical modelling performed for samples of the Cobourg Formation by Waber et al., 2007). Until another estimate is available, a literature value of PCO_2 could be used.

In terms of magnesium concentrations, many of the aqueous extract solutions from both DGR-3 and DGR-4 were predicted to be at or above saturation with respect to dolomite, despite the fact that a very short extraction time of 10 minutes was used. However, it was noted that, in general, higher concentrations of Mg^{2+} are observed in more highly dolomitised formations, including the Queenston, Georgian Bay, Blue Mountain and Cambrian, whereas lower concentrations are observed in less heavily dolomitised formations. As a first approach, dolomite could be used to constrain the concentrations of Mg^{2+} in these more highly dolomitised formations. For the remaining formations, total concentrations of magnesium could be constrained using measured cation exchange capacities (where available) and generic selectivity coefficients from the literature.

The only remaining element is sulphur. As noted in section 6.2 and section 10.1, the extracted sulphate concentrations are low and relatively constant, regardless of porewater content for the majority of samples in the subset. However, as seen in section 6.3, even these low concentrations of sulphate are predicted to result in oversaturation with respect to anhydrite/gypsum and celestite in the scaled aqueous extract solutions. Detailed mineralogical studies including SEM/EDS were conducted on relatively few samples from DGR-3 and -4; the presence of anhydrite/gypsum and/or celestite in the formations from the Cabot Head through the Shadow Lake, especially if finely dispersed in the rock matrix, cannot be ruled out. An alternative explanation is that the sulphate concentrations determined using aqueous extraction include sulphate generated as a result of sulphide oxidation. Trace sulphide minerals (e.g. pyrite, marcasite) were identified in all formations except those that are heavily oxidised (i.e. red shales of the Cabot Head and Queenston Formations).

In summary, for the subset of samples in which there is some supporting evidence that extracted K^+ and Sr^{2+} concentrations may be representative of porewater concentrations, 8 of the 9 elements could be constrained. There is currently no clear control to constrain sulphur concentrations when modelling the porewater compositions. In the Queenston and Georgian Bay formations where anhydrite or anhydrite/celestite have been identified in several samples, exploratory modelling using anhydrite or celestite as controls on sulphate and Na-Ca or Na-Sr exchange could be performed. For the remaining formations where lower sulphate concentrations have been determined using aqueous extraction, the apparent porewater concentrations could be used in exploratory modelling, together with sensitivity analyses of the saturation indices to the apparent sulphate concentrations.

For the remainder of the samples in the select dataset, potassium and/or strontium are likely not representative of porewater compositions. A first approach to constraining these element concentrations would be to try using CEC values and generic selectivity coefficients in exploratory geo-

chemical modelling. The potential constraints that could be applied in both cases explored here are summarized in Table 59.

10.3.1.2 *Samples with petrographically identified soluble salts*

As with the case where no salts were identified (previous section), there are still nine elements in the simplified system that must be constrained. Two simplified cases are considered here:

- i) Halite is present but there is no gypsum/anhydrite present;
- ii) Gypsum/anhydrite is present, but no halite.

Where halite has been identified, the solubility of halite could be used as a mineralogical constraint on the concentration of either Na or Cl, but not both. If halite were used to constrain the concentration of Cl⁻ then another constraint would be required to constrain Na⁺ (e.g., Na-Ca exchange). In the case where gypsum or anhydrite is present, one of these minerals could be added as a mineralogical control (equilibrium constraint) on sulphate concentrations; a second constraint, such as cation exchange, would be required to constrain calcium.

Table 59: Potential constraints on major elements for the next stage in exploratory modelling of apparent porewater compositions.

Element	Constraint on element concentration	
	Case 1 (K ⁺ and Sr ²⁺ from porewater)	Case 2: K ⁺ and Sr ²⁺ not exclusively from porewater
Cl ⁻	Fix at apparent porewater concentration ¹ , assuming $\phi_i = \phi_{PWL}$. Include trials with apparent porewater concentrations in Ordovician shales* calculated using $\phi_i = 0.5\phi_{PWL}$ based on iodide accessible porosity reported by Intera (2008b, 2010c).	Same as Case 1
Br ⁻	Fix at apparent porewater concentration ¹ , assuming $\phi_i = \phi_{PWL}$. Include trials with apparent porewater concentrations in Ordovician shales* calculated using $\phi_i = 0.5\phi_{PWL}$ based on iodide accessible porosity reported by Intera (2008b, 2010c).	Same as Case 1
SO ₄ ²⁻	Use anhydrite and Na-Ca exchange OR celestite and Na-Sr exchange for predictions within Ordovician shales*; For remainder of formations, trials with concentrations fixed at apparent porewater concentrations, including sensitivity analysis.	Same as Case 1
Carbonate	CO ₃ ²⁻ from calcite saturation OR PCO ₂ from literature value	Same as Case 1
Pe	Not included - set at 4.0 for initial exploratory modelling; eventually consider use of SO ₄ ²⁻ /pyrite pair	Same as Case 1
pH	Solution electroneutrality	Same as Case 1
Na ⁺	Fix at apparent porewater concentration ¹	Same as Case 1
K ⁺	Fix at apparent porewater concentration ¹	Na-K exchange
Ca ²⁺	Fix at apparent porewater concentration ¹	Same as Case 1
Mg ²⁺	Dolomite saturation in highly dolomitised formations (Ordovician shales plus Cambrian); Na-Mg ²⁺ exchange in formations composed primarily of limestone.	Same as Case 1
Sr ²⁺	Fix at apparent porewater concentration ¹	Na-Sr exchange

*Queenston, Georgian Bay and Blue Mountain formations

¹Calculated using concentrations determined using aqueous extraction (mmol/kg_{rock}), bulk dry density and assuming the ion accessible porosity is equal to the porewater-loss porosity ($\phi_i = \phi_{PWL}$).

10.4 Porewater characterisation - Recommendations

In low permeability and porosity rocks such as those from the Ordovician shales and limestone underlying southern Ontario, it is likely that indirect methods such as aqueous extraction, combined with supporting mineralogical and petrophysical information, will continue to form an important part of the approach for characterising porewaters. Especially for rocks containing soluble mineral phases (e.g., halite, gypsum/anhydrite), further understanding regarding the importance of the processes affecting samples during aqueous extraction (mineral-water reactions, ion exchange) and improved constraints on porewater compositions will be gained by:

- Conducting all aqueous extractions at multiple solid:liquid ratios to provide evidence on the importance of cation exchange processes or mineral solubility controls on extracted concentrations of various ions in different lithologies. Ideally, this would be done for every sample examined. This procedure was followed for a selection of samples from DGR-2, but was not included in the DGR-3 and -4 studies. This information is particularly important in evaluating whether or not the extracted concentrations are representative of porewater concentrations, or whether they reflect water-mineral interaction processes that occurred during the extraction procedure. The shorter aqueous extraction time of 10 minutes implemented with DGR-3 and -4 extractions is also recommended. This change reduced the impact of ion exchange reactions on extracted Sr^{2+} concentrations, in particular.
- Determining a range of total cation exchange capacities (CECs) for each different lithology (ideally, determine the total CEC for each individual core sample examined). This will enable at least a first attempt at implementing cation exchange controls in geochemical modeling, by using the CEC values together with generic selectivity coefficients from the literature.
- Whole-rock mineralogical analyses should be performed on all samples on which aqueous extractions are conducted to provide information on clay content of the sample. This information is required to enable correlations with calculated porewater contents and the measured CEC values for various formations.
- Detailed follow-up mineralogical studies (SEM-EDS) on samples for which aqueous extractions/scaled porewater compositions indicate soluble mineral phases such as halite are present. Where positively identified, these minerals can be used as a constraint in the geochemical model.
- Geochemical porosity/anion exclusion: develop independent arguments on the pore-space fraction accessible to anions.

11 Summary and conclusions

The following sections summarise the findings and advances from this work, subdivided into the following four key areas:

- i. Evidence for the saturation state of the samples based on a comparison between porewater-loss porosities and total porosities;
- ii. Chemical compositions of porewaters and status of knowledge in terms of reconstructive geochemical equilibrium modelling;
- iii. Stable isotope compositions of porewaters determined using the adapted diffusive exchange technique; and
- iv. Pore diffusion coefficients for Cl^- from the out-diffusion experiments.

11.1 Evidence for the saturation state of DGR samples

Petrophysical measurements provide evidence regarding the saturation state of preserved samples from boreholes DGR-2, -3 and -4. In the majority of samples, the calculated porewater-loss and physical porosities are the same within the calculated uncertainty of these parameters, suggesting that the pore space is completely filled with porewater and interconnected. However, approximately 25% of all samples investigated have porewater-loss porosities that are lower than their total physical porosities - beyond the uncertainty associated with the calculated values. In the upper portion of the sedimentary sequence, this group includes some samples from the Salina A2 Unit, Salina A1 Unit, Salina A1 Evaporite and from the Manitoulin Formation. From the lower part of the sequence, some samples from the Cobourg, Georgian Bay, Sherman Fall, Kirkfield, Gull River and Cambrian had porewater-loss porosities less than their physical porosities. Three possible hypotheses that could be consistent with these observations are proposed:

- a) The rocks are fully saturated, but the entire porosity within the rock is not interconnected.
- b) The porosity of the rock is fully connected, but is not completely saturated with porewater.
- c) Experimental artefacts affect the measurements. For example, not all porewater may be retrieved by heating to 105 °C, such that the water content (and consequently, the porewater-loss porosity) may be slightly underestimated. Alternatively, partially unsaturated conditions within the core may have developed during sample handling prior to core preservation (e.g. some evaporation of porewater, prior to sealing of the core, despite the stringent core handling protocols applied).

If there is a separate gas phase present in situ, it is expected that gas would preferentially accumulate in larger pores that occur mainly within carbonate units, whereas pore apertures within shale units are likely too small. Many of the samples (but not all) that have porewater-loss porosities lower than their physical porosities are from carbonate units. Furthermore, the potentially under-saturated samples are distributed over the entire profile; there are no specific depth intervals to which this phenomenon is restricted.

11.2 Chemical composition of porewaters

Porewater investigations conducted for DGR-3 and DGR-4 focused on developing a thorough understanding and interpretation of results from the aqueous extractions conducted at a solid:liquid ratio of 1:1, in combination with supporting detailed mineralogical information. Porewater compositions can only be directly scaled up from aqueous extraction data using measured water contents if the following criteria are met:

1. No contributions to the aqueous extract solutions from cracked fluid inclusions;
2. No soluble salts are present in the rock matrix that contribute to the aqueous extract solution (other than those from the porewater);
3. Cation exchange capacity is negligible compared to the electrolyte content of the porewater (or can be quantified using selectivity coefficients from the literature);
4. No significant anion exclusion effect (i.e., the anion accessible porosity can be approximated by water-loss porosity).

The first three criteria must be met in order to be able to define the mass of an ion originally in the porewater of a sample. The contribution of fluid inclusions to the porewater is negligible in DGR rocks containing highly saline porewaters (criterion 1).

Compositions of aqueous extracts were examined together with mineralogical information to qualify whether or not the solutions may have been impacted by dissolution of halite or calcium sulphate phases (criterion 2). On the basis of this evaluation, samples were sorted into a group likely to contain soluble salts and a group without any evidence for presence of these salts. Further evaluations were limited to the latter group.

For Cl^- and Br^- ions, a strong correlation was observed between the mass of the ions extracted and the quantity of porewater in the sample, suggesting that these ions are predominantly from the porewater in the majority of samples (this applies only to the portion of the dataset without evidence for presence of soluble salts). This relationship between the mass of extracted ion (expressed in $\text{meq}/\text{kg}_{\text{rock}}$) and porewater content was applied as a tool to investigate whether other ions could also be attributed to the porewater or, alternatively, if the extracted masses were affected by ion-exchange or mineral dissolution/precipitation reactions during the extraction procedure (criterion 3). The cation exchange capacities measured for samples from DGR-2 were low (3 to 45 $\text{meq}/\text{kg}_{\text{rock}}$) and, therefore, are not expected to have a marked effect on measured ion concentrations, with the possible exception of the ratios between mono- and divalent cations (dilution effect due to water added in the aqueous extractions).

Strong correlations were observed between the extracted mass of Na^+ and Ca^{2+} for the majority of samples and the porewater content, suggesting that the extracted mass of these ions is predominantly from the porewater. For K^+ and Sr^{2+} , a good correlation between the mass of ion extracted and porewater content was observed for many samples. Notable exceptions were from the Queenston, Georgian Bay, Shadow Lake and Cambrian, which may reflect ion exchange or mineral dissolution/precipitation reactions during the aqueous extractions. For magnesium, no evidence was found to support that extracted Mg^{2+} is from the porewater; rather, ion-exchange and mineral dissolution reactions likely control the masses extracted. In particular, higher extracted Mg^{2+} (and also Sr^{2+}) concentrations were observed in formations with higher degrees of dolomitisation (Queenston, Georgian Bay and Cambrian). The extracted SO_4^{2-} concentrations were low (1 to 3 $\text{meq}/\text{kg}_{\text{rock}}$) and similar, irrespective of porewater content, suggesting a mineral solubility control on sulphate during

the extractions (SO_4^{2-} /pyrite?). Contributions from oxidation of sulphide minerals, observed in all but the oxidized red bed shales (Queenston and Cabot Head formations), cannot be completely ruled out.

Using the approach outlined above, significant progress was made in terms of identifying, on a sample-by-sample basis, the ions for which there is evidence suggesting that the extracted masses are predominantly from the porewater and separating them from those which may have been impacted by ion exchange or mineral dissolution/precipitation reactions during the aqueous extractions. The state of knowledge on porewater compositions was then examined with respect to the application of geochemical equilibrium codes to reconstruct porewater compositions. In developing a conceptual and/or numerical geochemical model to reconstruct porewater compositions, it is envisioned that efforts would begin with the host rock, the Cobourg Formation.

In the geochemical model, each major element in the system needs to be constrained using either a mass balance or mass action (such as ion exchange or solubility controls) expression. For a subset of samples from DGR-3 and DGR-4, there is strong to good evidence that the concentrations of K^+ and Sr^{2+} can be constrained based on their concentrations determined in the aqueous extractions, in addition to Na^+ , Ca^{2+} , Cl^- and Br^- . Mass balance expressions can therefore be used to constrain the concentrations of 6 out of the 9 elements and pH can be constrained using the expression for solution electroneutrality. Constraints are still required for the remaining 3 elements – magnesium, carbon and sulphur. In first attempts, it may be possible to constrain magnesium concentrations using dolomite solubility and carbon by stipulating a PCO_2 (to be assumed based on a literature value). There is currently no clear control to constrain sulphur concentrations when modelling the porewater compositions.

The final criterion in determining porewater concentrations of ions is knowledge of the anion accessible porosity. Results from diffusion experiments in the shale formations (Intera, 2008b; 2010a) suggest that the I^- accessible porosity is approximately 50% of the porewater-loss porosity. Assuming that the Cl^- accessible porosity is similar to that of I^- , preliminary calculations of apparent Cl^- concentrations were made for DGR-3 and -4 samples from the Cabot Head, Queenston, Georgian Bay and Blue Mountain shale formations. With the exception of one sample from the Georgian Bay Formation, the apparent porewater Cl^- concentrations are higher than those predicted at halite saturation. This may suggest that:

- the anion accessible porosity for Cl^- is greater than 50% of the porewater-loss porosity.
- halite is present throughout the formation and was dissolved during the aqueous extraction experiments. This interpretation is not consistent with the mineralogical information available to date (i.e. halite identified in only a limited number of samples), although the number of samples on which detailed studies were conducted is limited.

In the future, development of independent arguments on the pore-space fraction accessible to anions may be particularly useful to better constrain the geochemical porosity/anion exclusion.

11.3 Testing of other methodologies for porewater extractions

Ethanol-water extractions were investigated in this study as a potential method to improve estimations of ion concentrations in porewater by reducing, or if possible, eliminating contributions of ions due to the dissolution of highly soluble mineral phases present in the rock matrix (e.g. gypsum, anhydrite, halite) during aqueous extractions. In tests with DGR-3 samples, the highest ethanol:water ratios were designed to exactly replicate the amount of pure water originally in the rock material determined gravimetrically at 105 °C. This ratio was selected on the premise that only salts precipitated from the porewater during drying would be redissolved during the extractions and therefore the ion concentrations in the extract solutions would be equal to those originally present in the porewater. Unfortunately, alcohols do not act as purely neutral liquids when added to a system containing pure water and salts and determining the effect of the alcohol on the activity of ions in solution is quite complex. Theoretically, the ion concentrations measured in the ethanol-water extracts could be corrected to a concentration in the original aqueous phase, if the ethanol interaction coefficient (γ^N) could be predicted. However, unlike the situation for aqueous solutions where it is possible to predict activity coefficients (γ^S) for ion-ion interactions (e.g. Pitzer parameters), for mixed ethanol/water/salt systems, there is currently no similar method for predicting ion-ethanol interactions (γ^N). Ethanol activity coefficients (γ^N) for specific salt/water mineral systems over a range of ethanol-water compositions could be predicted using a semi-empirical approach similar to that proposed by Kan et al. (2003), if experiments were conducted to obtain the required supporting data. In any future testing of the ethanol-water extraction method, extract solutions containing different alcohols and lower alcohol:water ratios are recommended. Replicate extractions conducted on multiple samples would also be required to establish more firmly the analytical uncertainty associated with the extractions.

In the current study, further development of the advective displacement method for application to rocks containing highly saline porewaters was undertaken on a sample of the Cobourg Formation from borehole DGR-4. In an effort to minimize interactions between the infiltrating fluid and the porewater within the core, the experiment was conducted using trichloroethylene (TCE) as the infiltrating fluid. After over 2 months, no pore fluid had been extracted from the sample. Two potential explanations are i) the hydraulic conductivity of the sample is so low that the volume displaced was not sufficient to fill the dead volume present in the system at the upper end of the core (c.a. 0.5 ml); or ii) the TCE used as the infiltration fluid has a much higher entry pressure than an electrolyte solution and therefore, no fluid entered the core.

11.4 Stable isotope composition of porewaters

Stable isotope compositions were determined for samples from several formations in the DGR-3 and DGR-4 boreholes using protocols of the diffusive exchange technique adapted for rocks containing highly saline porewaters. Improvements to the technique from DGR-3 to DGR-4 included:

1. Development of a screening procedure to evaluate the quality of the data obtained;
2. Optimisation of the rock:test water mass ratio used in the experiments; and
3. Improved matching of the water activities measured for rock samples by addition of either NaCl for samples with $a_w > 0.75$ or CaCl₂ to achieve $a_w < 0.75$. This was

made possible by the development of a NaF treatment process used to convert CaCl_2 test waters to NaCl solutions prior to low temperature distillation.

The latest adaptation of the experimental protocol from DGR-3 to DGR-4, in which the isotope diffusive exchange technique is adapted to the range of measured water activities for rocks from the DGR boreholes (a_w between 0.6 and 1.0), is a major step forward. These improvements, in particular the optimisation of the porewater/test water mass ratio by increasing the amount of rock used in the experiment, greatly reduced the experimental error associated with the stable isotope compositions determined for porewaters in DGR-4 samples compared to DGR-3 samples.

Although the number of data points is limited, the $\delta^{18}\text{O}$ and $\delta^2\text{H}$ depth profiles for DGR-3 and for DGR-4 determined using the diffusive exchange technique are similar. The general shape of the profiles is also similar to profiles obtained at the University of Ottawa using vacuum distillation at 150 °C. Absolute values are similar in both data sets in the upper part of the profile (down to the Salina Formation) and nearly constant values of $\delta^2\text{H}$ are observed from the Cabot Head down to the Cambrian groundwater in both profiles. However, compared to the vacuum distillation data, more enriched values of both $\delta^{18}\text{O}$ and $\delta^2\text{H}$ are determined using diffusive exchange for samples from the Queenston through the Coboconk formations. The isotopic compositions of porewaters in both datasets converge towards similar values in the Shadow Lake and Cambrian at the bottom of the profile and towards the Cambrian groundwater composition, although the obtained $\delta^{18}\text{O}$ values tend to be higher than the corresponding groundwater. Currently, there is no definitive explanation for the isotopically more positive signatures obtained for the porewaters using the isotope diffusive exchange method compared to those determined using vacuum distillation, but two possible explanations are proposed:

- Vacuum distillation at 150°C recovers all the water from the sample in the case of NaCl-dominated porewater (i.e. in the upper part of the DGR profile) but not when more complex brines are involved (lower part of the DGR profile, from Guelph Formation downwards), where the presence of CaCl_2 and MgCl_2 might impede the complete vacuum distillation of the porewater, even at 150°C; and/or
- The isotope diffusive exchange technique is sensitive to differences in the chemical compositions between the porewater and the testwater used in the experiments. Although the water activities of the test solutions are matched to those measured for the porewaters, the relatively simple compositions of these test waters do not reflect the complex chemical composition of the porewaters. Research is on-going to evaluate the potential influence of an isotopic fractionation effect due to differences in chemical composition between the test waters and in situ porewaters.

Acknowledgements

We are grateful to Dr. H. Niklaus Waber (Rock-Water Interaction, University of Bern) for his thoughtful and thorough review of several sections of this report. We also extend our thanks to Drs. Dru Heagle and Richard E. Jackson (Intera Engineering Ltd., Ottawa, Canada) and to Laura Kennell (Nuclear Waste Management Organization) for their helpful review comments and suggestions.

References

- Altinier, M.V., Savoye, S., Michelot, J.-L., Beaucaire, C., Massault, M., Tessier, D., Waber, H.N. 2007. The isotopic composition of pore-water from Tournemire argillite (France): An inter-comparison study. *Physics and Chemistry of the Earth* 32, 209-218.
- Blum, P., 1997. Physical properties handbook: a guide to the shipboard measurement of physical properties of deep-sea cores. ODP Tech. Note 26.
- Bradbury, M.H. and Baeyens, B., 1998. A physicochemical characterization and geochemical modeling approach for determining porewater chemistries in argillaceous rocks. *Geochimica et Cosmochimica Acta* 62, 783-795.
- Deer W.A., R.A. Howie and J. Zussman. 1985. An introduction to the rock forming minerals. Longman Group Ltd., Essex, England.
- de Haller, A., Spangenberg, J., and Koroleva, M. 2008. Analysis of stable water isotopes in brines: Methodology study. Progress Report PR 08-02, Rock-Water Interaction Group, Institute of Geological Sciences, University of Bern, Switzerland.
- de Haller, A., Spangenberg J., Smuda J., and Koroleva, M. 2009. The stable H and O isotope analysis of small highly saline water samples: a methodological study. *Goldschmidt Conference Abstract 2009, Geochimica et Cosmochimica Acta*, v. 73, A274.
- Gaucher, E. C., Tournassat C., Pearson F.J., Blanc P., Crouzet C., Lerouge C. and Altmann, S. 2009. A robust model for pore-water chemistry of a clayrock. *Geochimica et Cosmochimica Acta*, Vol. 73, 6470-6487.
- Hardie, L.A. 1967. The gypsum-anhydrite equilibrium at one atmosphere pressure. *The American Mineralogist*, Vol. 52, 171-200.
- Herwegh M. and Mazurek M. 2008. Feasibility SEM study: Primary and secondary salts and sulphates in the Paleozoic of the DGR-2 borehole, Bruce, southwestern Ontario. Progress Report PR-08-03, Institute of Geological Sciences, University of Bern, Switzerland.
- Hobbs, M.Y., Frape S.K., Shouakar-Stash O. and Kennell L.R. 2008. Phase I Regional Hydrogeochemistry, Southern Ontario. OPG's Deep Geologic Repository for Low & Intermediate Level Waste. Supporting Technical Report, November 30, 2008. OPG 00216-REP-01300-00006-R00.
- Hobbs, M.Y. and Waber H.N. 2002. Pore Water Chemistry (PC) Experiment: Evaluation of the diffusive exchange method for the determination of $\delta^{18}\text{O}$ and $\delta^2\text{H}$ in Opalinus Clay pore water from Mont Terri. Mont Terri Project, Technical Note 2002-24.
- Horita, J., Wesolowski, D.J., Cole, D.R. 1993a. The activity-composition relationship of oxygen and hydrogen isotopes in aqueous salt solutions: I. vapor-liquid water equilibration of single salt solutions from 50 to 100°C. *Geochimica et Cosmochimica Acta*, v. 57(12), p. 2797-2817.
- Horita, J., Cole, D.R., Wesolowski, D.J. 1993b. The activity-composition relationship of oxygen and hydrogen isotopes in aqueous salt solutions: II. Vapor-liquid water equilibration of mixed salt solutions from 50 to 100°C and geochemical implications. *Geochimica et Cosmochimica Acta*, v. 57(19), p. 4703-4711.
- Husain M. M., Cherry, J.A. and Frape, S.K. 2004. The persistence of a large stagnation zone in a developed regional aquifer, southwestern Ontario. *Can. Geotech. J.*, 41, 943-958.

- Intera, 2010a. Assessment of Porosity Data and Gas Phase Presence in DGR Cores. TR-08-34. Revision 0E, November 26, 2010. DGR Site Characterization Document, Intera Engineering Project 08-200.
- Intera, 2010b. Measurement of diffusion properties by X-ray radiography and by through-diffusion techniques using iodide and tritium tracers: Core samples from DGR-3 and DGR-4. TR-08-27. Revision 0B, May 7, 2010. DGR Site Characterization Document, Intera Engineering Project 08-200.
- Intera, 2010c. Vacuum distillation experiments on DGR core. TR-08-37. Revision 0, May 21, 2010. DGR Site Characterization Document, Intera Engineering Project 08-200.
- Intera, 2010d. Petrophysical testing of DGR-2 core. TR-07-18. Revision 2, May 20, 2010. DGR Site Characterization Document, Intera Engineering Project 06-219.
- Intera, 2009a. Porewater and gas analyses in DGR-3 & DGR-4 core. Draft Technical Report TR-08-19, Revision 0E, November 19, 2009. DGR Site Characterization Document, Intera Engineering Project 08-200.
- Intera, 2009b. Opportunistic groundwater sampling in DGR-3 and DGR-4. Draft Technical Report TR-08-18, Revision 0B, August 20th, 2009. DGR Site Characterization Document, Intera Engineering Project 08-200.
- Intera, 2009c. Diffusion of ¹²⁵I in Limestone and Red Shale Samples from DGR-2. Draft Technical Report TR-07-22, Revision 0A, April 9, 2009. DGR Site Characterization Document, Intera Engineering Project 08-200.
- Intera, 2008a. Phase 2 Geoscientific Site Characterization Plan, OPG's Deep Geologic Repository for Low and Intermediate Level Waste, Report INTERA 06-219-50-Phase 2 GSCP-R0, OPG 00216-PLAN-03902-00002-R00, April, Ottawa.
- Intera, 2008b. Measurement of diffusion properties by X-ray radiography and by through-diffusion techniques using iodide and tritium tracers: Core samples from OS-1 and DGR-2. TR-07-17. Revision 0, July 21, 2008. DGR Site Characterization Document, Intera Engineering Project 08-200.
- Intera Engineering Ltd., 2008c. Technical Report: Pore Water and Gas Analyses in DGR-1 and DGR-2 Core, TR-07-21, Revision 0, July 4, Ottawa. DGR Site Characterization Document, Intera Engineering Project 08-200.
- Intera Engineering Ltd., 2008c. Pore Water and Gas Analyses in DGR-1 and DGR-2 Core, TR-07-21, Revision 0, July 4, Ottawa. DGR Site Characterization Document, Intera Engineering Project 08-200.
- Intera, 2006. Geoscientific Site Characterization Plan, OPG's Deep Geologic Repository for Low and Intermediate Level Waste, Report INTERA 05-221-1, OPG 00216-REP-03902-00002-R00, April, Ottawa.
- Jarrett, M.A., Gusler B., Xiang T. and Clapper, D. 2004. Improved competence in water activity measurement. Paper presented at the AADE (American Association of Drilling Engineers) Technology Conference, Houston, Texas, April 6-7, 2004. AADE-04-DF-HO-31.
- Jury, W.A., Gardner W.R. and Gardner, W.H. 1991. Soil Physics, 5th Edition. John Wiley & Sons Inc.
- Kan, A. T., Fu, G. and Tomson, M.B. 2002. Effect of methanol on carbonate equilibrium and calcite solubility in a gas/methanol/water/salt mixed system. *Langmuir*, 18, 9713-9725.
- Kan, A. T., Fu, G. and Tomson, M.B. 2003. Effect of methanol and ethylene glycol on sulphates and halite scale formation. *Ind. Eng. Chem. Res.*, 42, 2399-2408.

- Kharaka Y. K. and Hanor, J.S. 2005. Deep fluids in the continents: 1. Sedimentary Basins. In: Treatise on Geochemistry, Vol. 5, Surface and groundwater, weathering and soils. J. I. Drever, (ed.), 499-540.
- Koroleva, M., de Haller, A., Mäder, U., Waber, H.N., and Mazurek, M., 2009. Borehole DGR-2: Pore-water investigations. Rock-Water Interaction (RWI), Institute of Geological Sciences, University of Bern, Switzerland, TR-08-02, 127 p.
- Li Y.-H. and Gregory, S. 1974. Diffusion of ions in sea water and deep sea sediments. *Geochimica et Cosmochimica Acta*, Vol. 38, 703-714.
- Mäder, U., Waber H.N. & Gautschi, A. 2004. New method for porewater extraction from claystone and determination of transport properties with results for Opalinus Clay (Switzerland). In: R. B. Wanty & R.R. Seal II (eds), Proceedings of the 11th International Symposium on Water-Rock Interaction, Saratoga Springs (N.Y.), 445-449. Balkema.
- Mäder, U. 2005. Porewater chemistry, porosity and hydraulic conductivity of Callovo-Oxfordian claystone at the EST-322 deep drilling site sampled by the method of advective displacement (Laboratoire de Recherche Souterrain de Meuse / Haute-Marne). Nagra, Wettingen, Switzerland, Nagra Arbeitsbericht NAB 05-04, 43 p.
- Mazurek, M. and Meier, D. *in prep.* Mont Terri Technical Note, Working title: WS-H experiment: Characterisation of drillcores from borehole BHG-11.
- Patriarche, D., Michelot, J.L., Ledoux, E., and Savoye, S., 2004, Diffusion as the main process for mass transport in very low water content argillites: I. Chloride as a natural tracer for mass transport - Diffusion coefficient and concentration measurements in interstitial water. *Water resources Research* 40, W01517
- Pearson, F. J. 1999. What is the porosity of a mudrock? In: Apalin, A. C., Fleet, A. J. & MacQuaker, J. H. S. (eds). *Muds and Mudstones: Physical and Fluid Flow Properties*. Geological Society, London, Special Publications, 158, 9-21.
- Pearson, F.J., Arcos D., Bath, A., Boisson, J.Y., Fernandez, A.M., Gaebler, H.E., Gaucher, E.C., Gautschi, A., Griffault, L., Hernan, P. & Waber, H.N., 2003. Mont Terri Project - Geochemistry of Water in the Opalinus Clay Formation at the Mont Terri Rock Laboratory. Reports of the Federal Office of Water and Geology (FOWG), Geology Series No. 5, 321p.
- Parkhurst, D.L. & Appelo, C.A.J., 1999. User's guide to PHREEQC, a computer program for speciation, batch-reaction, one-dimensional transport, and inverse geochemical calculations: - U.S. Geol. Surv. Water-Resour. Invest. Rep.: 99-4259.
- Robinson, R. A., and Stokes, R.H. 1959. *Electrolyte Solutions*. Butterworth & Co., Ltd., London, England, 559 p.
- Rübel, A.P., Sonntag, C., Lippmann, J., Pearson, F.J., and Gautschi, A. 2002. Solute transport in formations of very low permeability: Profiles of stable isotope and dissolved noble gas contents of pore water in the Opalinus Clay, Mont Terri, Switzerland. *Geochimica et Cosmochimica Acta*, v. 66(8), p. 1311-1321.
- Spangenberg, J.E., Dold, B., Vogt, M.L. and Pfeifer, H.R. 2007. The stable hydrogen and oxygen isotope composition of waters from porphyry copper mine tailings. *Environmental Science & Technology* 41, 1870-1876.
- Spangenberg, J.E. and Vennemann, T.W. 2008. The stable hydrogen and oxygen isotope variation of water stored in polyethylene terephthalate (PET) bottles. *Rapid communications in mass spectrometry* 22, 672-676.
- Sposito G. 1990. Molecular Models of Ion Adsorption on Mineral Surfaces. In: M.F. Hochella and A.F. White (Eds.). *Mineral-Water Interface Geochemistry*. Reviews in Mineralogy Vol. 23, Min. Soc. America, Washington D.C., 261-279.

- Waber, H.N., Mäder, U.K., Koroleva, M., and de Haller, A. 2007. Testing Methods for the Characterisation of Saline Pore Water in an Ordovician Limestone (Cobourg Formation, St. Mary's Quarry, Ontario). Rock-Water Interaction (RWI), Institute of Geological Sciences, University of Bern, Switzerland, TR-07-01, 112 p.
- Ziegler K. and Longstaffe, F.J. 2000a. Multiple episodes of clay alteration at the Precambrian/Paleozoic unconformity, Appalachian Basin: Isotopic evidence for long-distance and local fluid migrations. *Clay. Clay Miner.*, 48(4): 474-493.
- Ziegler K. and Longstaffe, F.J. 2000b. Clay mineral authigenesis along a mid-continental scale fluid conduit in Palaeozoic sedimentary rocks from southern Ontario, Canada. *Clay Miner.*, 35, 239-260.

APPENDIX A: Supplementary information for the diffusive exchange technique

A1.0 Diffusive Isotope Exchange Technique

The diffusive isotope-exchange technique is used to determine the stable isotope composition of porewater. The technique was originally developed at the University of Heidelberg (Rübel et al., 2002). It is based on the diffusive exchange of water isotopes via the vapour phase between the porewater of a rock sample and two test waters of known isotopic composition in two sealed containers at room temperature. If the masses and the isotopic compositions ($\delta^{18}\text{O}$ and $\delta^2\text{H}$ values) of the test waters are known, then the isotopic composition of the porewater can be calculated from the measurement of the modified compositions of the test waters once isotopic equilibrium is reached. The original $\delta^2\text{H}$ and $\delta^{18}\text{O}$ values of porewater and the mass of porewater are related by the mass-balance equation:

$$m_{pw} * c_{pw(t=0)} + m_{tw} * c_{tw(t=0)} = (m_{pw} + m_{tw}) * c_{tw(t=\infty)} \quad (1)$$

where m_{pw} and m_{tw} are the masses of pore and test water, c_{pw} is the original (in situ) isotopic composition of porewater, and c_{tw} is the isotopic composition of the test water at the beginning ($t=0$) and at the end ($t=\infty$) of the experiment. This formulation assumes that equilibration between the test water and porewater is complete at the end of the experiment, such that both have the same isotopic composition (ie. right hand side of equation 1).

Each equilibration experiment yields two independent equations, one for $\delta^{18}\text{O}$ and one for $\delta^2\text{H}$, but there are three unknowns, namely the mass of porewater and the hydrogen and oxygen isotope composition of the porewater ($\delta^{18}\text{O}$ and $\delta^2\text{H}$). Therefore, two different exchange experiments have to be performed for each sample to obtain a set of four equations. The two isotopically different test waters used are laboratory tap water (referred to here as "LAB") and a standard water ("TEW"), prepared with water from an ice core from Greenland at the Institute of Physics, University of Bern.

A1.1 Isotopic composition of porewater

Equation 1 can be rearranged to give an expression for the mass of porewater present in each experiment (LAB or TEW):

$$m_{pw} = \frac{m_{tw} * c_{tw(t=\infty)} - m_{tw} * c_{tw(t=0)}}{c_{pw(t=0)} - c_{tw(t=\infty)}} \quad (2)$$

where m_{tw} is the mass of the test waters (LAB or TEW), c_{tw} is the isotope composition ($\delta^{18}\text{O}$ or $\delta^2\text{H}$) of the test waters (LAB or TEW) at the beginning ($t=0$) and at the end ($t=\infty$) of equilibration in the two experiments "LAB" and "TEW" and c_{pw} is the original (in situ) isotope composition of the porewater.

To solve for the isotopic composition of the porewater, the assumption is made that the water contents of the rock material used in the LAB and TEW experiments are identical:

$$WC = \frac{m_{pwLAB}}{m_{rockLAB}} = \frac{m_{pwTEW}}{m_{rockTEW}} \quad (3)$$

where m_{rock} is the mass of the porewater-saturated rock and the water content (WC) is expressed as a fraction. Equation 2 is used to derive expressions for the mass of porewater in both the LAB (m_{pwLAB}) and TEW (m_{pwTEW}) experiments and then substituted into equation 3 to give two equivalent expressions for water content:

$$\frac{m_{twLAB} * c_{twLAB(t=\infty)} - m_{twLAB} * c_{twLAB(t=0)}}{m_{rockLAB} * (c_{pw(t=0)} - c_{twLAB(t=\infty)})} = \frac{m_{twTEW} * c_{twTEW(t=\infty)} - m_{twTEW} * c_{twTEW(t=0)}}{m_{rockTEW} * (c_{pw(t=0)} - c_{twTEW(t=\infty)})} \quad (4)$$

The only unknown in the expression given by equation 4 is the initial (in situ) isotopic composition of the porewater ($\delta^{18}\text{O}$ or $\delta^2\text{H}$), $C_{pw(t=0)}$, which can be solved by rearranging equation 4 as follows:

$$c_{pw(t=0)} = \frac{m_{twLAB} * c_{twTEW(t=\infty)} * m_{rockTEW} (c_{twLAB(t=\infty)} - c_{twLAB(t=0)}) - m_{twTEW} * m_{rockLAB} * c_{twLAB(t=\infty)} * (c_{twTEW(t=\infty)} - c_{twTEW(t=0)})}{m_{rockTEW} * (m_{twLAB} * c_{twLAB(t=\infty)} - m_{twLAB} * c_{twLAB(t=0)}) - m_{rockLAB} * (m_{twTEW} * c_{twTEW(t=\infty)} + m_{twTEW} * c_{twTEW(t=0)})} \quad (5)$$

The $\delta^{18}\text{O}$ value of the porewater is calculated according to equation 5 using the initial and final $\delta^{18}\text{O}$ values of the test waters; similarly, the $\delta^2\text{H}$ value of the porewater is solved using the initial and final $\delta^2\text{H}$ values of the test waters.

A1.2 Water content by the diffusive isotope-exchange technique

The initial or in situ $\delta^{18}\text{O}$ and $\delta^2\text{H}$ values of porewater ($C_{pw(t=0)}$) in the rock material at the beginning of both experiments (LAB and TEW) are the same, such that:

$$c_{pw(t=0)} = c_{pw(t=0)LAB} = c_{pw(t=0)TEW} \quad (6)$$

Rearranging equation 1 to give an expression for the isotopic composition of the porewater ($C_{pw(t=0)}$) yields:

$$c_{pw(t=0)} = \frac{(m_{pw} + m_{tw}) * c_{tw(t=\infty)} - m_{tw} * c_{tw(t=0)}}{m_{pw}} \quad (7)$$

The mass of porewater in the rock material (m_{pw}) can be expressed as a function of water content and the mass of rock used in each experiment (equilibrated with LAB or TEW) by rearranging equation 3:

$$m_{pw} = WC * m_{rock} \quad (8)$$

Expressions for mass of porewater from each experiment (m_{pwLAB} and m_{pwTEW}) are then substituted into equation 7 and the initial isotopic compositions of the porewater in the LAB and TEW experiments are equated (as per equation 6) to yield the following expression:

$$\frac{(WC * m_{rockLAB} + m_{twLAB}) * c_{tw(t=\infty)LAB} - m_{twLAB} * c_{tw(t=0)LAB}}{WC * m_{rockLAB}} = \frac{(WC * m_{rockTEW} + m_{twTEW}) * c_{tw(t=\infty)TEW} - m_{twTEW} * c_{tw(t=0)TEW}}{WC * m_{rockTEW}} \quad (9)$$

Equation 9 is then rearranged to solve for water content:

$$WC = \frac{(c_{tw(t=\infty)TEW} - c_{tw(t=0)TEW}) * m_{twTEW} * m_{rockLAB} - (c_{tw(t=\infty)LAB} - c_{tw(t=0)LAB}) * m_{twLAB} * m_{rockTEW}}{m_{rockLAB} * m_{rockTEW} * (c_{tw(t=\infty)LAB} - c_{tw(t=\infty)TEW})} \quad (10)$$

This expression is solved twice: once using the initial and final $\delta^{18}\text{O}$ values of the test waters (WC_{d18O}) and once using the $\delta^2\text{H}$ values (WC_{d2H}).

A1.3 Error calculation

The relative error of the equilibration experiment for the determination of the water content of the rock samples and the original $\delta^2\text{H}$ and $\delta^{18}\text{O}$ values of the porewater can be calculated applying Gauss's law of error propagation:

$$\sigma_f = \sqrt{\sum_{i=1}^n \left(\frac{\partial f}{\partial p_i} * \sigma_{p_i} \right)^2} \quad (11)$$

where the P_i represents the analytical errors attached to the measurements of the mass of test water (m_{tw}) and of the mass of rock (m_{rock}) and the analytical error of the isotope analyses of the test water at the beginning ($c_{tw(t=0)}$) and the end ($c_{tw(t=\infty)}$) of the two experiments "LAB" and "TEW".

A2.0 Protocol for the adapted diffusive-isotope exchange technique (saline porewaters)

Saturated rock pieces from the central part of the drillcore and approximately 2 cm in diameter were placed in a vapour-tight container together with a small crystallisation dish containing a known mass of test water with known isotopic composition. Approximately 170 ± 40 g (DGR-3) and 300 ± 50 g (DGR-4) of rock material were used for the individual experiments.

In the original method, a minor amount of NaCl was added to the test solution (0.3 molal) to avoid condensation to the container walls. In order to prevent mass transfers and isotopic fractionation (e.g. Horita et al., 1993a and b) between the test water and the porewater of the rock through desiccation-condensation mechanisms, the activity of the test water must be adjusted to fit the rock sample water activity, which depends on the type and concentration of salts and on the proportion of bound water. The activity of pure water is 1, while water activities of brines saturated with NaCl and CaCl_2 are 0.75 and 0.32 at 25°C , respectively (Robinson & Stokes, 1959). Therefore, NaCl can be added to the test water to fit porewater activities down to 0.75, but CaCl_2 has to be used if porewater activity is below this value. The majority of samples from borehole DGR-4 have water activities between 0.6 and 0.7, thus requiring CaCl_2 addition to the test waters.

The equilibration time of the three-reservoir system (porewater in rock sample, test water in crystallisation dish, air inside the container) depends on the size of the rock pieces, the rock permeability and the distance of the rock piece to the test water. Typical equilibration times for the Opalinus Clay range between about 2.5 and 20 days (Rübel et al. 2002, Hobbs and Waber, 2002). An extended equilibration time of 30 days was chosen for use in the current study.

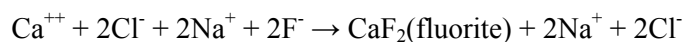
The test water, rock material and the container were weighed before and after the equilibration experiment to check the tightness of the container and to have a control on possible mass transfers between the test water and the sample. No transfer occurred if the masses of the test water and rock material are the same at the beginning and end of experiment (initial masses of rock material, initial and final masses of test waters, and salinities of the test solutions used in the isotope diffusive exchange experiments with DGR-3 and DGR-4 samples are given in Table A-1 and Table A-3, respectively). After equilibration, the test water was removed from the crystallisation dish, and stored in a small vapour-tight PE-bottle for further water stable isotope ($\delta^2\text{H}$, $\delta^{18}\text{O}$) analyses. The rock material was dried in an oven to constant mass at 105°C in order to determine the gravimetric water content of the sample. When the presence of gypsum was suspected, the gravimetric water content was also determined at 40°C, in an attempt to avoid removing structural water from gypsum during drying (see section 4.2.1).

A2.1 Protocol for analysis of oxygen and hydrogen isotopes in saline waters

The determination of the hydrogen and oxygen isotope composition of saline waters using the common procedure of Cr-reduction in a Thermo Fisher (former Thermo Finnigan, Bremen, Germany) H-Device and CO_2 equilibration in a GasBench (for $\delta^{18}\text{O}$ determination) is not possible; the saline solutions used as test waters need to be distilled before analysis (de Haller et al., 2008). As part of the adaptation of the diffusive exchange technique for application to rocks containing saline porewaters, a new protocol was developed and tested for analysing saline (NaCl or CaCl_2) test waters. Development and testing of this protocol is on-going as part of collaborative research between the University of Bern and the University of Lausanne within the frame of a NWMO project (GS85).

In the current protocol, the NaCl -bearing test water samples (up to 6.1M NaCl at saturation) are distilled to remove the salt from the solution. Distillation involves heating the ~5 ml for > 4 hours at 90 °C followed by 1 hour at 110-130 °C in a Savillex-vial connected by a screw-closed L-tube to a PTF vial cooled in ambient air (~25 °C). The condensed water is recovered and filled into a 5 ml sealed glass bottle and stored at +4 °C for isotopic analysis. This distillation procedure was originally developed at the University of Lausanne for hydrogen and oxygen isotope analyses of highly mineralised porewaters from mine tailings impoundments (Spangenberg et al., 2007). A methodology study based on synthetic NaCl brines showed that the isotopic composition of water recovered by this technique was undistinguishable from the known composition of the standard water used to prepare the solution within 0.2 and 1‰ 1σ errors, respectively, for $\delta^{18}\text{O}$ and $\delta^2\text{H}$ values (de Haller et al., 2008).

Such distillation procedure is not adapted for CaCl_2 solutions because it is not possible to completely dehydrate this salt at 120-130 °C. This problem has been solved by converting CaCl_2 into NaCl and solid CaF_2 (fluorite) through the addition of NaF , following the aqueous reaction:



The solubility of fluorite at the relevant temperatures and pH is low enough to limit the remaining Ca^{++} content in the water to amounts that are negligible in terms of isotope salt effect (< 0.001 molal; Rimstidt, 1997). This development of the distillation technique has been successfully tested, as reported by de Haller et al. (2008, 2009). Errors induced by the distillation technique are similar for NaCl solutions, $\text{CaCl}_2 + \text{NaF}$ solutions and pure water.

Distillation of the test waters and hydrogen and oxygen isotope analyses of aliquots of the distilled test water samples were conducted at the Stable Isotopes Laboratory of the University of Lausanne, Switzerland (e.g., Spangenberg et al., 2007; Spangenberg and Venneman, 2008). The stable hydrogen isotope composition was measured using a Thermo Fischer H-Device connected to a Delta V isotope ratio mass spectrometer (IRMS). In this method, the H_2 gas is produced by reduction of a volume of 1.2 μl of water over hot (840 °C) chromium within a quartz reactor connected to the dual inlet of the IRMS. Oxygen isotope analyses were conducted by equilibration of 0.5% CO_2 in He with 1.2 ml of water for 24 hours at room temperature, followed by extraction in a continuous He flow using a Thermo Fisher GasBench II connected to a Delta Plus XL IRMS.

The stable hydrogen and oxygen isotope ratios are reported in delta (δ) notation as the per mil (‰) deviation relative to the Vienna Standard Mean Ocean Water (VSMOW). The standardization of the $\delta^2\text{H}$ and $\delta^{18}\text{O}$ values relative to the international VSMOW scale was done by calibration of the reference gases and working standards with IAEA VSMOW, Standard Light Antarctic Precipitation (SLAP) and Greenland Ice Sheet Precipitation (GISP) standards. The calibration and assessment of the reproducibility of the isotopic analyses is based on replicate analyses of four working water standards prepared and distilled between 1999 and 2003 in the Stable Isotopes Laboratory of the University of Lausanne (Spangenberg et al., 2007). These include tap water (UNIL-INH, working values $\delta^2\text{H} = -114.0\text{‰}$, $\delta^{18}\text{O} = -17.0\text{‰}$), two bottled mineral waters that were mixed in different proportions (UNIL-LIPE, working values $\delta^2\text{H} = -54.8\text{‰}$, $\delta^{18}\text{O} = -8.5\text{‰}$; UNIL-SCH, working values $\delta^2\text{H} = -123.7\text{‰}$, $\delta^{18}\text{O} = -17.7\text{‰}$), water from Lake Geneva (UNIL-LEMAN, working values $\delta^2\text{H} = -83.9\text{‰}$, $\delta^{18}\text{O} = -10.2\text{‰}$), Mediterranean ocean water (UNIL-MOW, working values $\delta^2\text{H} = 3.4\text{‰}$, $\delta^{18}\text{O} = 0.4\text{‰}$), and water produced by combustion of natural gas (UNIL-TOCH, working values $\delta^2\text{H} = -142.2\text{‰}$, $\delta^{18}\text{O} = 27.4\text{‰}$). All water samples were analyzed in duplicate. The reproducibility, assessed by the within-run replicate analyses of laboratory standards, was better than 0.1‰ and 0.3‰ (1σ) for $\delta^{18}\text{O}$ and $\delta^2\text{H}$, respectively. The total analytical errors (1σ) are 0.15‰ and 0.7‰, respectively for $\delta^{18}\text{O}$ and $\delta^2\text{H}$. The accuracy of the analyses was checked every fourth run using the IAEA standard waters.

A2.2 Data screening criteria for the adapted diffusive isotope exchange technique

The method has been significantly improved in the DGR-3 and DGR-4 programs, with an increasing number of samples analysed successfully when compared to early trials on samples from borehole DGR-2 (where no reliable data could be obtained). The quality of the data can be affected by many parameters and, therefore, a screening procedure has been developed. In the following, we explore the main sources of error in the calculated isotopic composition of the porewater and the calculated water content and list the criteria that are used to evaluate analytical problems. Because the adapted diffusive isotope exchange technique for highly saline porewaters (de Haller et al., 2008 and 2009) is still undergoing development and testing, some potential sources of error have not yet been fully evaluated.

At the time of DGR-3 sample preparation, the 120 °C distillation procedure worked well for NaCl standard solutions, but was not adapted for CaCl₂ standard solutions (CaCl₂ cannot be fully dehydrated at 120 °C). For this reason, only NaCl solutions were used in diffusive exchange experiments with DGR-3 samples. Consequently, for rock samples with measured water activities below 0.75 (NaCl-saturated solution), the activities of the test solutions were not closely matched to the rock samples (see Figure 23 in section 5.1). Before the DGR-4 campaign began, the procedure in which CaCl₂ test solutions are treated after equilibration with NaF to remove the Ca⁺⁺ was developed (section A2.1). The resulting NaCl solutions could then be distilled following the same procedure applied to the DGR-3 samples. This allowed the test solutions used in the experiments with DGR-4 samples to be more closely matched to the water activities measured for rock samples by addition of either NaCl or CaCl₂. As a result of this latest improvement, the diffusive isotope-exchange technique has been adapted to the range of water activities (0.6 to 1.0) measured to date for rocks from the DGR project boreholes (DGR-2, -3 and -4).

Independent of the developments related to the water activity adjustment (use of saline test waters) for the isotope diffusive exchange technique, the precision of the calculated isotopic composition and water content depends on the ratio between the masses of test water and porewater, with errors being minimized when both masses are similar. For samples with low water contents, errors can be minimised by maximising the mass of rock and minimizing the mass of test water. The mass of rock used in the diffusive isotope-exchange experiments has been increased from 170 ± 40 g in DGR-3 to 300 ± 50 g in DGR-4, which significantly improved the errors (Figure A-1), in particular for low water content samples. Technically, the smallest mass of test water that can be analyzed is approximately 3 ml and with the current experimental setup, the maximum mass of rock that can be used is approximately 400 g. Consequently, rock samples with water contents below 0.5 wt% will yield high errors, as illustrated in Figure A-1.

Mass transfer between the test water and the porewater might affect the precision of the results, although this has not been quantified. The importance of mass transfer between the test water and the sample depends on the water activity matching of the test water with the sample (Figure 23 in section 5.1) and on the mass ratio of the test water and porewater (Figure A-2). Aside from the chemical composition of the porewater, the presence of hydrophilic minerals (e.g., anhydrite, halite, smectite) may also lower the measured water activity of a rock sample. From a theoretical viewpoint, mass transfer between the test water and the sample should not affect the calculated isotopic composition of the porewater or the calculated water contents because, at equilibrium, both test and porewaters have the same isotopic composition. However, as an interim measure until the errors associated with mass transfers can be quantified, data are rejected when the change in the mass of

the test water is >1 0% of the gravimetric water content (WC_{grav}) obtained by drying of the corresponding LAB or TEW subsample.

The water content of the sample can be calculated independently from the results obtained for $\delta^{18}\text{O}$ and $\delta^2\text{H}$ as described in section A1.1. Both water contents ($WC_{\delta^{18}\text{O}}$ and $WC_{\delta^2\text{H}}$) should be similar within analytical error if both the isotope diffusive exchange experiment and the distillation-analysis procedures are successful. For this reason, data from samples that give two distinct water contents are rejected (see Table 21, Table 22, Table 24 and Table 26 in section 5 of the main body of the report). Ultimately, $WC_{\delta^{18}\text{O}}$ and $WC_{\delta^2\text{H}}$ should coincide with and, in any case, should not be lower than the WC obtained gravimetrically. Samples with $WC_{\delta^{18}\text{O}}$ and $WC_{\delta^2\text{H}}$ lower than $WC_{\text{Grav.wet}}$ were rejected during the screening procedure because such behaviour might indicate that full equilibrium was not achieved during the experiment time.

Figure A-3 shows $WC_{\delta^{18}\text{O}}$ versus $WC_{\delta^2\text{H}}$ plots for DGR-3 and DGR-4 samples. Data for almost all DGR-4 samples overlap within error with the 1:1 line, suggesting that there were no major perturbations during the isotope diffusive exchange experiments or during the distillation-analysis procedures. In contrast, many DGR-3 samples show a poor correlation, which indicates perturbations either during the equilibration experiments or during the distillation-analysis procedures.

In the present study, the consistency of the distillation procedure was controlled on aliquots of the LAB and TEW standard water solutions (NaCl or $\text{CaCl}_2 + \text{NaF}$) used for each series of isotope exchange experiments. Data obtained for DGR-3 standard solutions are given in Table A-2 and plotted in Figures A-4 and A-5, while those obtained from DGR-4 standard solutions are given in Table A-5 and shown in Figures A-6 and A-7. Results must be similar within analytical error when the distillation-analysis and standard solution preparation procedures are correct. This is the case for all DGR-3 and DGR-4 standard solutions, with the exception of the results obtained for the two TEW standard CaCl_2 solutions prepared for DGR-4, which show significant deviation to higher $\delta^{18}\text{O}$ and $\delta^2\text{H}$ values. This may indicate that a problem occurred during the distillation of these two samples (e.g., vapor loss). Therefore, although the distillation does normally not induce significant perturbation, careful examination of the data using the screening procedure is required to identify problems with the distillation or analysis of standards and samples. It has to be stressed here that only values obtained from pure standard waters (no salts) are used as initial test water composition in the calculation of pore water isotopic compositions and water contents.

Based on this examination of the results obtained from isotope diffusive exchange experiments on DGR-3 and DGR-4 samples, the following conclusions are drawn:

- Reliable data can be obtained using the adapted isotope diffusive exchange method for rock samples with water activities between 0.5 and 1.0. Either NaCl or CaCl_2 is added to the test water to adjust the water activity to closely match the measured water activity of the sample. The main limitation is the water content of the rock sample. When the water content is ≤ 0.5 wt%, the errors on the calculated porewater isotopic composition and water content become unacceptably large ($> 2\%$ for $\delta^{18}\text{O}$ and $> 10\%$ for $\delta^2\text{H}$; see Figure A-1).
- The quality of data obtained using the isotope diffusive exchange technique is assessed using the following screening criteria: 1) the total mass of the system (container + rock sample + test water) has to remain constant during experiment (< 0.1 g difference between start and end of the experiment); 2) the mass transfer between the test water and the sample pore water during experiment has to be minimal (currently an upper limit of 10% weight change relative to the corresponding gravimetric water content of the sample is used); 3) the WC contents calculated from both isotopic systems ($\delta^2\text{H}$ and $\delta^{18}\text{O}$) have to be identical within error; and 4) these calculated water contents cannot be lower (within error) than the measured gravimetric water content $WC_{\text{Grav.wet}}$ as this could indicate incomplete equilibration be-

tween the test water and sample (calculated water contents higher than $WC_{Grav.wet}$ are not eliminatory because they might be due to the presence of $CaCl_2$ or $MgCl_2$ in the porewater, which can impede the total drying of the rock during the gravimetric experiment).

- The transfer of water between the test water and the sample is greatly reduced when the test water activity is properly adjusted using $CaCl_2$ when required (especially below the Salina Formation). In this sense, the adaptation of the experimental protocol from DGR-3 (where only NaCl was used for water activity matching) to DRG-4 (where NaCl or $CaCl_2$ were used for the water activity matching) is a major step forward.

Future improvements of the method will include systematic sealing of the distillation vials with Teflon® tape to minimize the risk of possible vapour loss.

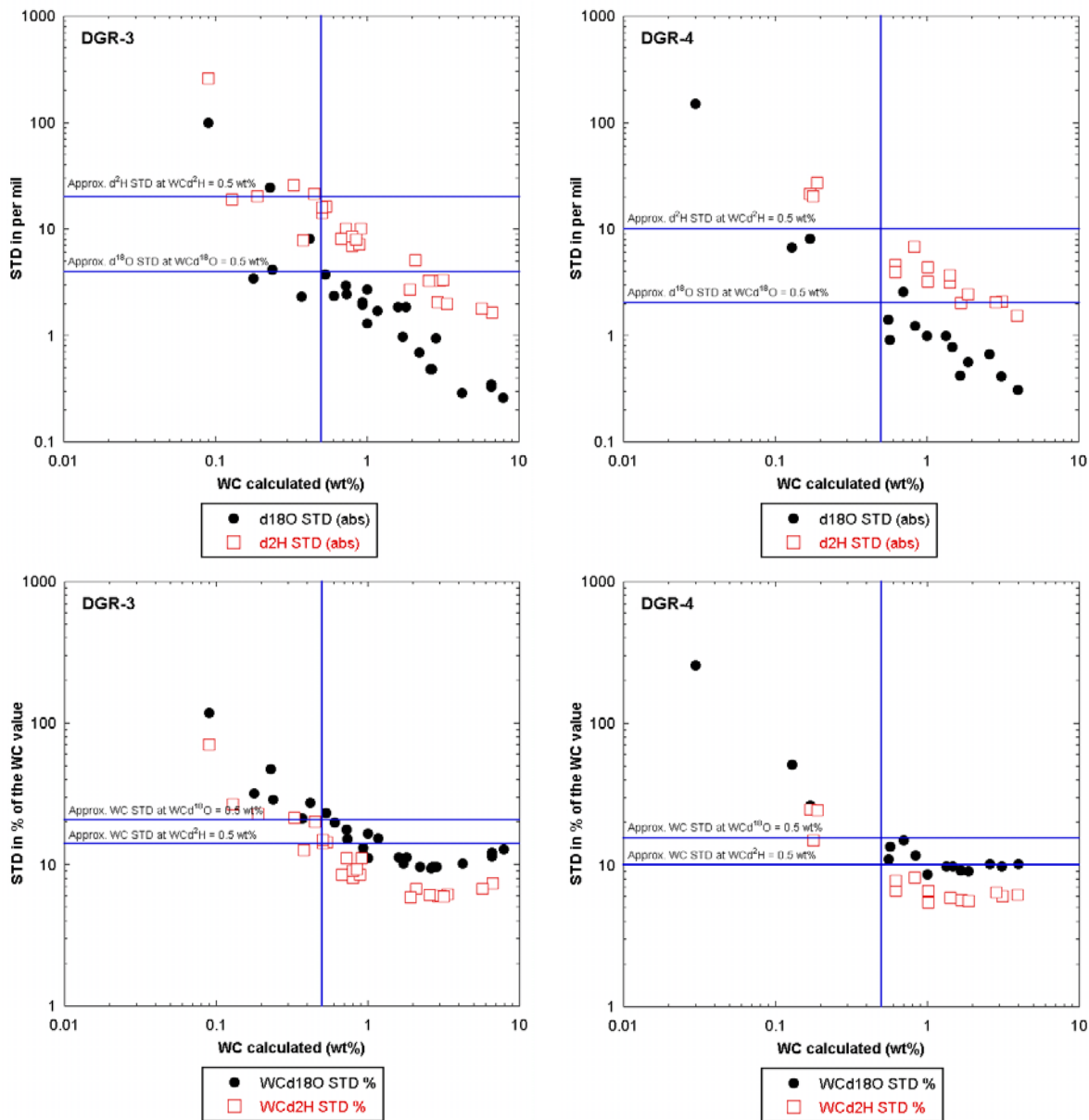


Figure A-1: Errors (STD = standard deviation) in stable isotopic composition (top diagrams) and water content (lower diagrams) determined by the diffusive exchange technique as a function of the calculated water content (WC) (from diffusive isotope-exchange data). The errors plotted for $\delta^{18}\text{O}$ and $\delta^2\text{H}$ are absolute (two upper diagrams), while the error for the WC is relative (two lower diagrams). Errors are approximately two times less for DGR-4 results than for DGR-3. In the DGR-4 experiments, care was taken to maximize the rock mass and minimize the test water mass, especially when low water content was suspected.

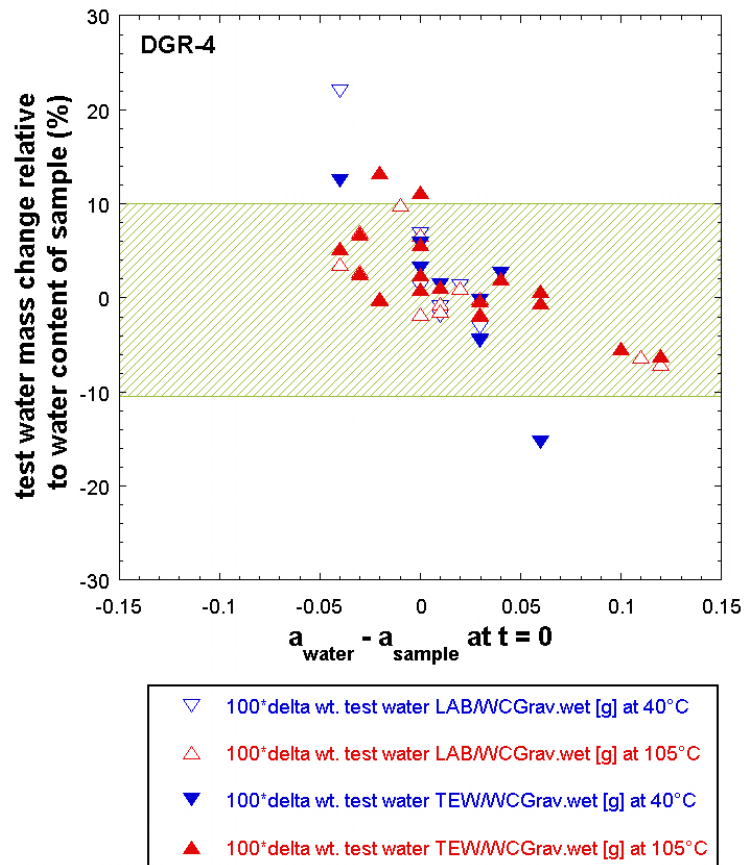


Figure A-2: Change in the mass of test water during experiment (delta mass test water) relative to the sample water content determined gravimetrically ($WC_{Grav.wet}$) as a function of the a_w mismatch between test water and sample for DGR-4. The a_w of test water was calculated from its salinity (Table A-4). The hatched area indicates the range of results that were accepted (test water mass change < 10% of the sample water content).

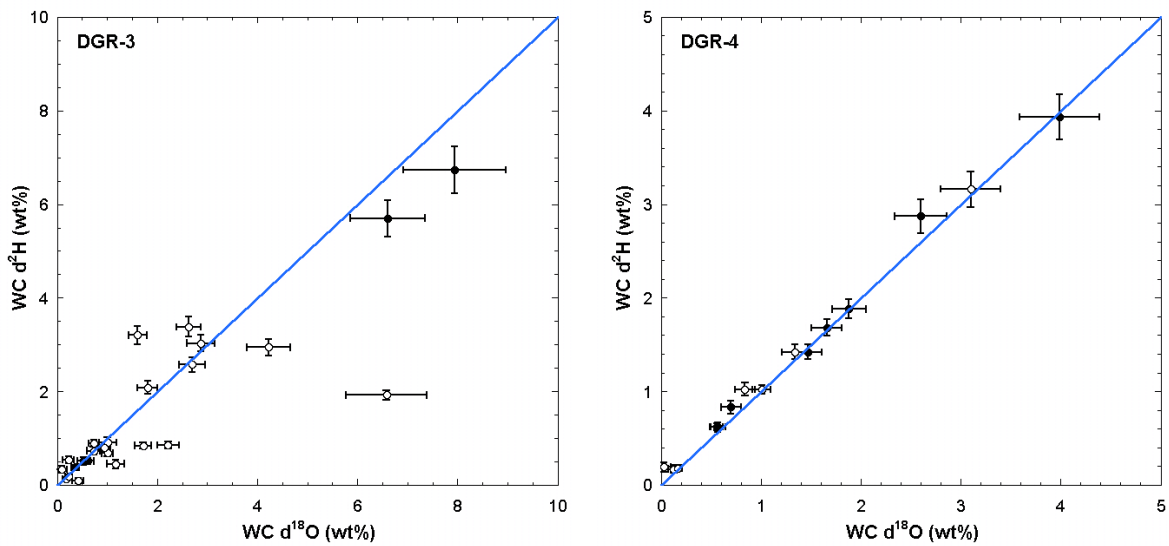


Figure A-3: Comparison of water content (WC) values calculated with both $\delta^2\text{H}$ and $\delta^{18}\text{O}$ data. If the experiment and isotopic analyses are sound, both isotopic systems should give the same value for water content (within the analytical error). Filled black symbols correspond to results that successfully met all four data screening criteria.

Table A-1: DGR-3. Isotope diffusive exchange experiments: Masses of rock material, masses and salinities of the two test waters (LAB and TEW).

Sample ID (NWMO) ¹	Formation	NaCl in test solu- tion	Test solution “LAB” (tap water)					Test solution “TEW” (glacial meltwater)			
			Initial mass of saturated rock ²	Date of test solution Preparation ³	Initial mass of test solution ²	Final mass of test so- lution ²	Initial mass of test water (without NaCl) ²	Initial mass of saturated rock ²	Initial mass of test solu- tion ²	Final mass of test so- lution ²	Initial mass of test water (without NaCl) ²
			(molal)	(g)	(d.m.y.)	(g)	(g)	(g)	(g)	(g)	(g)
DGR-3 198.72	Salina – F Unit	0.3	261.871	23.06.2008	5.074	4.665	4.987	268.554	5.074	4.653	4.987
DGR-3 208.41 ^A	Salina - F Unit	0.3	224.803	23.06.2008	5.052	4.027*	4.965	216.384	5.076	4.187 ^A	4.989
DGR-3 248.71	Salina – E Unit	2.5	235.883	20.06.2008	5.461	5.311	4.765	239.000	5.359	5.206	4.676
DGR-3 270.06	Salina – C Unit	2.5	232.728	20.06.2008	5.784	5.932	5.047	233.487	5.761	5.970	5.027
DGR-3 289.36	Salina – B Unit	5.0	160.990	20.06.2008	6.444	5.681	4.987	177.127	6.965	6.383	5.390
DGR-3 312.53	Salina – A2 Unit	2.5	175.925	20.06.2008	5.413	5.274	4.723	190.045	5.259	5.057	4.589
DGR-3 335.22	Salina – A2 Evaporite	5.0	260.828	20.06.2008	5.798	5.778	4.487	279.421	5.788	5.695	4.479
DGR-3 344.06	Salina -A1 Unit	2.5	236.655	20.06.2008	5.430	5.456	4.738	235.390	5.412	5.375	4.722
DGR-3 380.88	A1 Evaporite	5.0	226.168	20.06.2008	5.772	5.746	4.467	225.143	5.783	5.691	4.475
DGR-3 391.34 ^A	Guelph	5.0	168.168	20.06.2008	5.783	4.639 ^A	4.475	185.005	5.680	4.540 ^A	4.396
DGR-3 435.62 ^A	Cabot Head	6.1	173.103	01.07.2008	5.721	5.428 ^A	4.218	162.772	5.761	4.388 ^A	4.247
DGR-3 453.41	Manitoulin	6.1	167.742	01.07.2008	5.783	5.240	4.263	161.654	5.774	5.263	4.257
DGR-3 468.76 ^A	Queenston	6.1	182.446	01.07.2008	5.779	4.601 ^A	4.260	182.793	5.775	4.595 ^A	4.257
DGR-3 484.58 ^A	Queenston	6.1	183.770	01.07.2008	5.774	4.674 ^A	4.257	170.458	5.754	4.712 ^A	4.242
DGR-3 502.55 ^A	Queenston	6.1	176.480	01.07.2008	5.818	4.724 ^A	4.289	175.065	5.754	4.719 ^A	4.242
DGR-3 531.65	Georgian Bay	6.1	112.923	01.07.2008	5.779	4.914	4.260	106.643	5.861	5.141	4.321
DGR-3 581.47	Georgian Bay	6.1	161.363	01.07.2008	5.776	4.842	4.258	172.784	5.828	4.857	4.296
DGR-3 621.63 ^A	Blue Mountain	6.1	181.821	01.07.2008	5.791	4.621 ^A	4.269	180.025	5.782	4.681 ^A	4.262
DGR-3 646.29 ^A	Blue Mountain	6.1	192.911	01.07.2008	5.747	4.604 ^A	4.237	189.193	5.805	4.745 ^A	4.279
DGR-3 665.29	Cobourg – C M	6.1	128.324	01.07.2008	5.771	5.514	4.254	129.599	5.784	5.535	4.264

¹ Depth of sample in meters below ground surface is given by the second half of the NWMO sample ID

² The analytical error associated with the reported mass is 0.002g. The initial mass of the test solution without NaCl is calculated from the molality of the test solution and the initial mass of test solution. No record of the weight of the NaCl added to the LAB and TEW solutions was made at the time of DGR3 standard solutions preparation (error on the salinity is considered to be <0.05 molal). Salinity at 6.1 molal refers to NaCl saturation.

³ The isotopic composition of the tap water used to prepare the LAB standard is not constant and may depend on the date of preparation of the standard. Because all LAB waters were prepared in about 10 days (from 20.06.2008 to 1.07.2008), this variation is below the analytical uncertainty (see Table A-2).

^A Using only NaCl standard solutions, it was not possible to match the activity of the test water to the low water activity of these rock samples (see Table 7, section 4.1). This resulted in a significant (>1 g) transfer of water from the test water to the rock. For this reason, the stable water isotopic compositions of these samples were not measured (see Table 21, section 5.3).

Table A-1 (Cont'd): DGR-3. Isotope diffusive exchange experiments: Masses of rock material, masses and salinities of the two test waters (LAB and TEW).

Sample ID (NWMO) ¹	Formation	NaCl in test solu- tion (molal)	Test solution "LAB" (tap water)					Test solution "TEW" (glacial meltwater)			
			Initial mass of saturated rock ²	Date of test so- lution Prepara- tion ³	Initial mass of test so- lution ²	Final mass of test solution ²	Initial mass of test water (without NaCl) ²	Initial mass of saturated rock ²	Initial mass of test solu- tion ²	Final mass of test so- lution ²	Initial mass of test water (without NaCl) ²
			(g)	(d.m.y.)	(g)	(g)	(g)	(g)	(g)	(g)	(g)
DGR-3 676.21	Cobourg – LM	6.1	108.024	01.07.2008	5.782	5.447	4.262	109.411	5.788	5.425	4.267
DGR-3 678.92	Cobourg – LM	6.1	104.544	01.07.2008	5.733	5.548	4.226	101.843	5.772	5.589	4.255
DGR-3 685.52	Cobourg – LM	6.1	146.505	01.07.2008	5.767	5.349	4.251	140.928	5.809	5.434	4.282
DGR-3 690.12	Cobourg – LM	6.1	131.676	01.07.2008	5.764	5.481	4.249	135.281	5.755	5.607	4.243
DGR-3 692.82	Cobourg – LM	6.1	203.956	01.07.2008	5.788	5.231	4.267	204.770	5.778	5.244	4.260
DGR-3 697.94	Cobourg – LM	6.1	135.342	01.07.2008	5.729	5.356	4.223	126.525	5.787	5.437	4.266
DGR-3 710.38	Sherman Fall	6.1	174.800	01.07.2008	4.590	4.318	3.384	173.168	4.595	3.830	3.387
DGR-3 725.57	Sherman Fall	6.1	134.807	01.07.2008	4.584	4.264	3.379	147.503	4.599	4.276	3.390
DGR-3 744.27	Kirkfield	6.1	176.205	01.07.2008	4.586	4.220	3.381	177.007	4.600	4.327	3.391
DGR-3 761.56	Kirkfield	6.1	133.123	01.07.2008	4.586	4.330	3.381	127.975	4.595	4.373	3.387
DGR-3 777.33	Coboconk	6.1	141.697	01.07.2008	5.898	5.870	4.348	141.234	5.862	5.806	4.321
DGR-3 807.43	Gull River	6.1	129.840	01.07.2008	5.893	5.845	4.344	137.334	5.911	5.869	4.358
DGR-3 843.92	Gull River	6.1	156.001	01.07.2008	5.932	5.912	4.373	149.662	5.889	5.841	4.341
DGR-3 852.18	Shadow Lake	6.1	142.396	01.07.2008	5.922	6.013	4.366	145.098	5.905	5.948	4.353
DGR-3 856.06	Cambrian	5.0	138.949	20.06.2008	5.842	5.840	4.521	133.760	5.817	5.789	4.502

¹Depth of sample in meters below ground surface is given by the second half of the NWMO sample ID.

²The analytical error associated with the reported mass is 0.002g. The initial mass of the test solution without NaCl is calculated from the molality of the test solution and the initial mass of test solution. No record of the weight of the NaCl added to the LAB and TEW solutions was made at the time of DGR3 standard solutions preparation (error on the salinity is considered to be < 0.05 molal). Salinity at 6.1 molal refers to NaCl saturation.

³The isotopic composition of the tap water used to prepare the LAB standard is not constant and might depend on the date of preparation of the standard. Because all LAB waters were prepared in about 10 days (from 20.06.2008 to 1.07.2008), this variation is below the analytical uncertainty (see Table A-2).

Table A-2: DGR-3. Isotope diffusive exchange experiments: Stable isotope values measured for standard water solutions analyzed using 120 °C distillation at the University of Lausanne, as described by de Haller et al. 2008.

Standard Identification	Date of preparation (d.m.y)	NaCl in Standard (molal)	$\delta^2\text{H}$ (‰VSMOW)	STD (1 σ , abs.)	$\delta^{18}\text{O}$ (‰VSMOW)	STD (1 σ , abs.)
Standard 1 LAB ^{1,3}	20.06.2008	2.5	-80.7	1	-11.1	0.2
Standard 2 LAB ^{1,3}	20.06.2008	5.0	-80.8	1	-11.1	0.2
Standard 3 LAB ^{1,3}	20.06.2008	2.5	-81.2	1	-11.2	0.2
Standard 4 LAB ^{1,3}	23.06.2008	0.3	-80.8	1	-11.1	0.2
Standard 5 LAB ^{1,3}	01.07.2008	6.1	-80.4	1	-11.1	0.2
Standard 6 LAB ^{1,3}	01.07.2008	6.1	-80.4	1	-11.4	0.2
Standard 7 LAB ^{1,3}	20.06.2008	0	-80.2	1	-11.1	0.2
Standard 8 LAB ^{1,3}	23.06.2008	0	-80.7	1	-11.2	0.2
Standard 9 LAB ^{1,3}	01.07.2008	0	-80.6	1	-11.1	0.2
Average of Std 7 LAB to Std 9 LAB ^{1,3}		0	-80.5	1	-11.1	0.2
Standard 1 TEW ³	20.06.2008	2.5	-187.3	1	-24.3	0.2
Standard 2 TEW ³	20.06.2008	5.0	-187.3	1	-24.6	0.2
Standard 3 TEW ³	20.06.2008	2.5	-188.1	1	-24.5	0.2
Standard 4 TEW ³	23.06.2008	0.3	-188.3	1	-24.6	0.2
Standard 5 TEW ³	01.07.2008	6.1	-188.2	1	-24.6	0.2
Standard 6 TEW ³	01.07.2008	6.1	-188.2	1	-24.4	0.2
Standard 7 TEW ²	20.06.2008	0	-188.1	0.7	-24.8	0.15
Standard 7 TEW ³	20.06.2008	0	-188.0	1	-24.5	0.2
Long-term average composition of the TEW water ⁴			-187.94	0.3	-24.56	0.1

¹ The isotopic composition of the tap water used to prepare the LAB standard is not constant and depends on the date of preparation of the standard. However, this variation is less than the analytical error and a single value for the LAB water has been considered for the calculations based on the average of Standards 7 LAB to 9 LAB.

² Not distilled

³ Estimated error based on a limited number of analyses (a long-term evaluation of the standard deviation is not yet available).

⁴ KUP, Institute of Physics, University of Bern

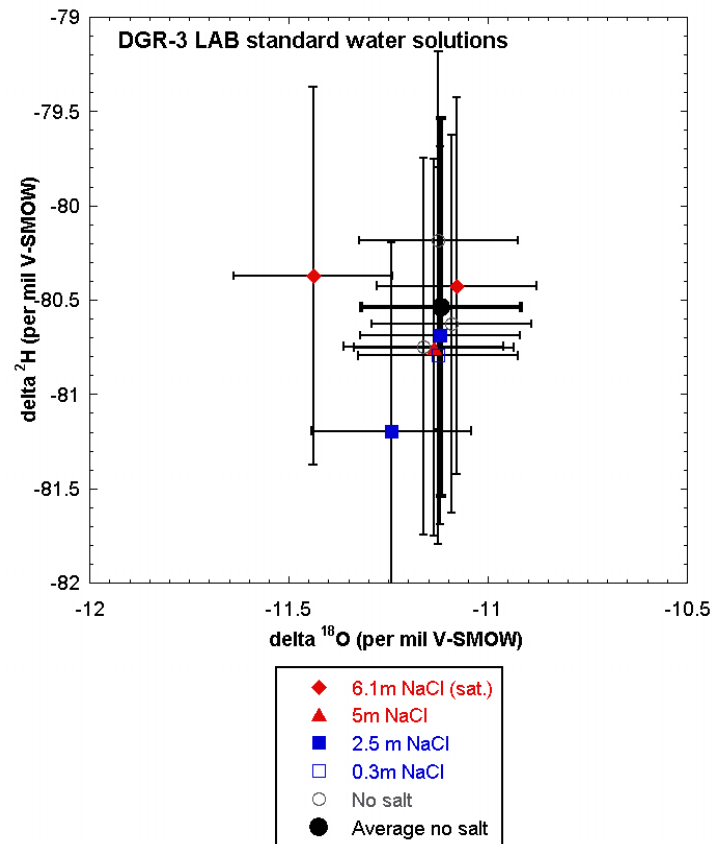


Figure A-4: DGR-3 program. Isotopic compositions of distilled NaCl solutions prepared with LAB standard water (data are in Table A-2). Some standards were distilled in duplicate or triplicate. Considering the average of the three results obtained for 0 molal NaCl (labelled "no salt" in the legend) as the true LAB water composition, the results obtained at salinities up to NaCl saturation are similar within errors of 0.2 ‰ and 1‰ for $\delta^{18}\text{O}$ and $\delta^2\text{H}$, respectively. There is no correlation of the isotopic composition with the salinity, which rules out any salt effect.

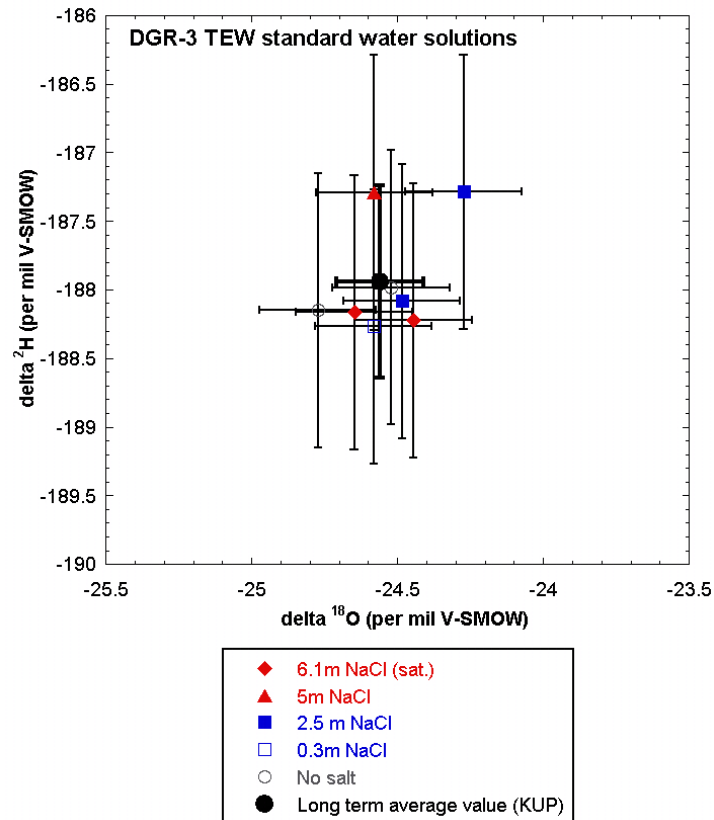


Figure A-5: DGR-3 program. Isotopic compositions of distilled NaCl solutions prepared with TEW standard water (data are in Table A-2). Some standards were distilled in duplicate. Samples labelled "no salt" had 0 mole NaCl. Results obtained at salinities up to NaCl saturation (6.1 molal) are similar to the long term isotopic composition of the TEW standard (KUP, Institute of Physics, University of Bern), considering errors of 0.2 ‰ and 1‰ for $\delta^{18}\text{O}$ and $\delta^2\text{H}$, respectively. There is no correlation of the isotopic composition with the salinity, which rules out any salt effect.

Table A-3: DGR-4. Isotope diffusive exchange experiments: Masses of rock material, masses and salinities of the two test waters (LAB and TEW).

Sample ID (NWMO) ¹	Formation	Test solution "LAB" (tap water) ³						Test solution "TEW" (glacial meltwater)					
		NaCl in test solution	CaCl ₂ in test solution	Initial mass of saturated rock ²	Initial mass of test solution ²	Final mass of test solution ²	Initial mass of test water (without NaCl) ²	NaCl in test solution	CaCl ₂ in test solution	Initial mass of saturated rock ²	Initial mass of test solution ²	Final mass of test solution ²	Initial mass of test wa- ter (without NaCl) ²
		(molal)	(molal)	(g)	(g)	(g)	(g)	(molal)	(molal)	(g)	(g)	(g)	(g)
DGR-4 154.60	Bass Islands	0.30	0	298.237	5.068	5.389	4.980	0.30	0	293.354	5.133	5.392	5.044
DGR-4 189.16	Salina - F	0.30	0	272.171	5.006	4.62	4.919	0.30	0	272.671	5.02	4.585	4.933
DGR-4 229.32	Salina - E	3.00	0	216.35	6.46	7.462	5.497	3.00	0	263.68	6.481	7.351	5.514
DGR-4 322.68	A2 Evaporite	0	4.11	312.691	9.068	9.064	6.228	0	3.87	303.068	9.046	9.026	6.213
DGR-4 332.13	Salina - A1	5.00	0	274.761	5.746	5.849	4.447	4.99	0	272.735	5.741	5.842	4.443
DGR-4 369.43	A1 Evaporite	0	4.11	258.232	9.161	9.158	6.292	0	3.87	311.314	9.275	9.279	6.371
DGR-4 422.21	Cabot Head	Failed experiment						Failed experiment					
DGR-4 472.78	Queenston	0	2.88	367.118	5.907	5.221	4.477	0	2.96	377.604	5.994	5.366	4.542
DGR-4 520.42	Georgian Bay	0	4.00	413.111	5.762	5.752	3.991	0	4.00	413.119	6.342	6.339	4.393
DGR-4 662.83	Cobourg - LM	0	4.11	379.528	6.244	6.237	4.289	0	3.87	286.361	6.093	6.103	4.185
DGR-4 665.41	Cobourg - LM	0	4.00	361.544	6.372	6.39	4.414	0	4.00	360.77	6.298	6.313	4.362
DGR-4 672.85	Cobourg - LM	Failed experiment						Failed experiment					
DGR-4 685.14	Cobourg - LM	0	4.11	265.973	9.175	9.16	6.302	0	3.87	290.809	9.293	9.286	6.383
DGR-4 717.12	Sherman Fall	0	2.88	336.005	5.948	5.658	4.508	0	2.96	369.712	5.911	5.652	4.480
DGR-4 730.07	Kirkfield	0	4.00	241.995	6.287	6.407	4.355	0	4.00	242.714	6.301	6.41	4.364
DGR-4 841.06	Shadow Lake	0	2.88	260.607	4.029	4.091	3.053	0	2.96	249.26	4.041	4.096	3.062
DGR-4 847.48	Cambrian	0	2.88	329.272	7.971	8.193	6.041	0	2.96	249.413	8.093	8.358	6.133

¹Depth of sample in meters below ground surface is given by the second half of the NWMO sample ID. Some of the samples were not measured (n.m.).

²The analytical error associated with the reported mass is 0.002g. The initial mass of the test solution without NaCl is calculated from the molality of the test solution and the initial mass of test solution.

³All LAB solutions were prepared from a single 5L bottle filled with laboratory tap water on 23.03.2009.

Table A-4: DGR-4. Salinity and calculated water activity of the standard water solutions used for isotope diffusive-exchange experiments.

Standard water solution ¹	Date of standard preparation ² (d. m. y)	NaCl	CaCl ₂	H ₂ O	NaCl salinity	CaCl ₂ salinity	Calculated water activity
		(g)	(g)	(ml at ~20°C)	(molal)	(molal)	
LAB 0.3m NaCl	23.03.2009	0.881	0	50	0.301	0	0.99
LAB 3m NaCl	23.03.2009	8.764	0	50	2.999	0	0.89
LAB 5m NaCl	23.03.2009	14.613	0	50	5.001	0	0.80
LAB 3m CaCl ₂	23.03.2009	0	15.976	50	0	2.879	0.76
LAB 4m CaCl ₂	23.03.2009	0	22.795	50	0	4.108	0.62
LAB 4m CaCl ₂	18.08.2009 ²	0	22.197	50	0	3.998	0.63
TEW 0.3m NaCl	23.03.2009	0.878	0	50	0.300	0	0.99
TEW 3m NaCl	23.03.2009	8.772	0	50	3.002	0	0.89
TEW 5m NaCl	23.03.2009	14.587	0	50	4.992	0	0.80
TEW 3m CaCl ₂	23.03.2009	0	16.429	50	0	2.961	0.75
TEW 4m CaCl ₂	23.03.2009	0	21.480	50	0	3.871	0.65
TEW 4m CaCl ₂	18.08.2009 ²	0	22.212	50	0	3.997	0.63

¹ LAB is tap water from the laboratory of the University of Bern, and TEW is a standard water prepared at the Physical Institute of the University of Bern with glacial melt water. All LAB solutions were prepared from a single 5L bottle filled with laboratory tap water on 23.03.2009.

² 4 molal CaCl₂ standards prepared the 18.08.2009 were used for samples DGR4-520.42, DGR4-665.41, and DGR4-730.07.

Table A-5: DGR-4. Isotope diffusive exchange experiments: Stable isotope values measured for standard water solutions analyzed using 120 °C distillation at the University of Lausanne, as described by de Haller et al. 2008.

Standard ID	Date of prep. (d.m.y)	NaCl or CaCl ₂	Distilled sample $\delta^2\text{H}$ (‰VSMOW)	Estimated error ¹	Not distilled $\delta^2\text{H}$ (‰VSMOW)	STD (1 σ , abs.)	Distilled sample $\delta^{18}\text{O}$ (‰VSMOW)	Estimated error ¹	Duplicate analysis $\delta^{18}\text{O}$ (‰VSMOW)	Not distilled $\delta^{18}\text{O}$ (‰VSMOW)	STD (1 σ , abs.)
UB-101-LAB	23.03.2009	0	-76.7	1	-76.3	0.7	-10.6	0.2	-10.8	-10.9	0.15
UB-102-LAB	“	0	-76.5	1	-75.9	0.7	-10.9	0.2	-10.9	-10.9	0.15
UB-105-LAB	“	0.3 molal NaCl	-76.4	1	n.a.	0.7	-10.9	0.2	-10.9	-10.9	0.15
UB-107-LAB	“	3 molal NaCl	-76.2	1			-10.8	0.2	-10.8		
UB-109-LAB	“	3 molal CaCl ₂	-76	1			-10.9	0.2			
UB-111-LAB	“	4 molal CaCl ₂	-77.6	1			-10.8	0.2			
Average UB-101-LAB and 102-LAB	“	0			-76.1	0.7				-10.9	0.15
UB-103-TEW		0	-187.1	1	-188.3	0.7	-24.4	0.2	-24.6	-24.8	0.2
UB-104-TEW		0	-186.9	1	-187.9	0.7	-24.6	0.2	-24.6	-24.7	0.2
UB-106-TEW		0.3 molal NaCl	-187.9	1	n.a.	n.a.	-24.5	0.2		-24.7	0.2
UB-108-TEW		3 molal NaCl	-188.0	1			-24.6	0.2			0.2
UB-110-TEW		3 molal CaCl ₂	-182.5	1			-24.5	0.2			0.2
UB-112-TEW		4 molal CaCl ₂	-184.2	1			-24.2	0.2			0.2
Long-term average composition of the TEW water ²					-187.94	0.7				-24.56	0.15

¹Estimated error based on a limited number of analyses (a long-term evaluation of the standard deviation is not yet available).

²KUP, Institute of Physics, University of Bern

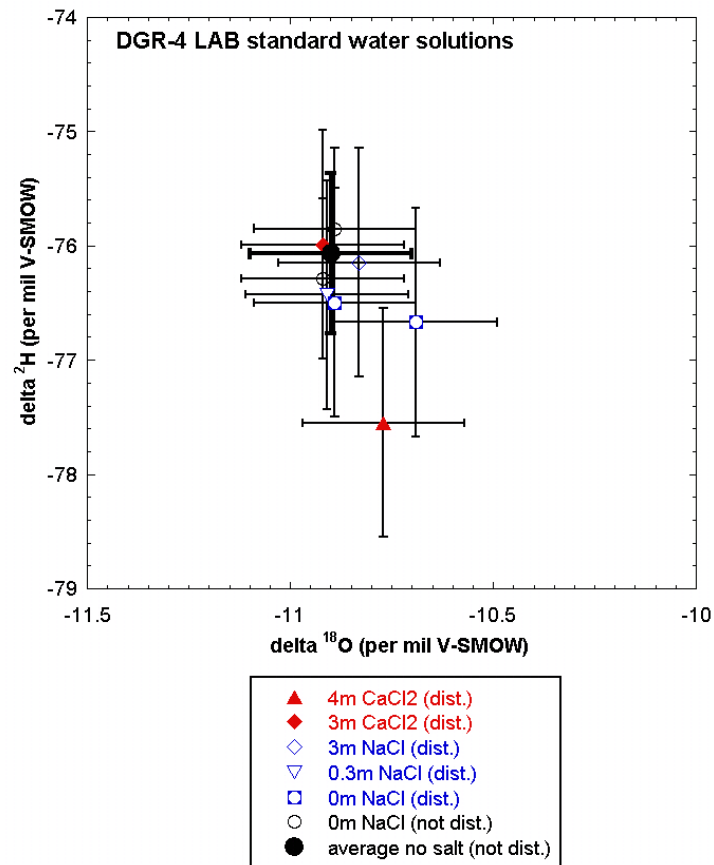


Figure A-6: DGR-4 program. Isotopic compositions of distilled NaCl and NaF-treated CaCl₂ solutions prepared with LAB standard water (data are in Table A-5). Solutions range from pure water to 4 molal CaCl₂ or 3 molal NaCl. Some standards were distilled in duplicate. Considering the average of the duplicate results obtained for the undistilled pure LAB water (labelled "0m NaCl (not dist.)") as its true isotopic composition, the results obtained from salt solutions at any concentration are similar within errors of 0.2 ‰ and 1‰ for δ¹⁸O and δ²H values, respectively. There is no correlation of the isotopic composition with the salinity, ruling out any salt effect.

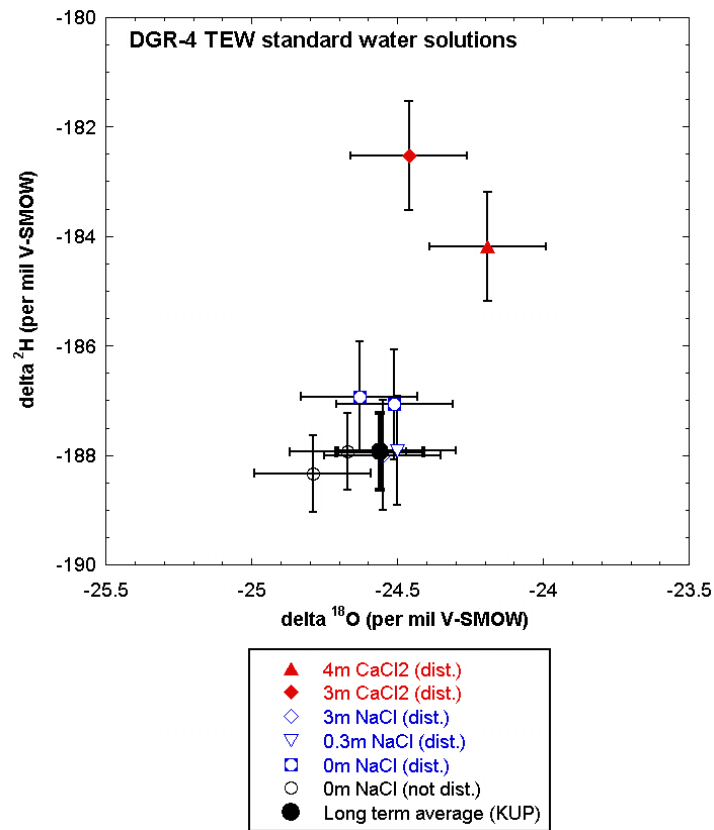


Figure A-7: DGR-4 program. Isotopic compositions of distilled NaCl and CaCl₂ solutions prepared with TEW standard water (data are in Table A-5). Some standards were distilled in duplicate. Results obtained from distilled pure water and NaCl solutions are similar to the long-term isotopic composition of the TEW standard (KUP, Institute of Physics, University of Bern), considering errors of 0.2 ‰ and 1‰ for $\delta^{18}\text{O}$ and $\delta^2\text{H}$, respectively. In contrast, values obtained from the NaF treated 3M and 4M CaCl₂ solutions are significantly disturbed (e.g., vapour loss, see text).

APPENDIX B: Supplementary Information on gravimetric water content measurements

Table B-1: DGR-4 samples - criteria used to designate constant mass for gravimetric water content measurements at 40 °C.

Sample ID	Formation	Lithology (short)	Replicate	Criterion Applied Mass change (wt. %)	¹ Time to constant mass (days)	Additional information on selection of end point
DGR-4 154.60	Bass Islands	Dolomitic shale with Ca-sulphate	LAB TEW	<0.005 <0.005	87 87	
DGR-4 189.16*	Salina - F Unit	Dolomitic shale with Ca-sulphate	A B LAB TEW	<0.03 <0.03 <0.01 <0.01	85 85 120 120	
DGR-4 229.32*	Salina - E Unit	Dolomitic shale with Ca-sulphate	LAB TEW	<0.005 <0.005	87 87	
DGR-4 322.68*	Salina – A2 Unit	Massive Ca-sulphate	LAB TEW	<0.005 <0.005	48 48	
DGR-4 332.13	Salina – A1 Unit	Argillaceous dolostone with Ca-sulphate	A B	<0.02 <0.01	85 85	
DGR-4 369.43	A1 Evaporite	Anhydritic dolostone	LAB TEW	<0.005 <0.005	75 75	
DGR-4 422.21	Cabot Head	Red-green shale with carbonate/ Black shale beds	LAB TEW	<0.05 <0.05	108 108	
DGR-4 472.78	Queenston	Red-green shale with carbonate beds	A B	<0.005 <0.01	135 135	
DGR-4 520.42	Georgian Bay	Shale with sandstone/siltstone/ limestone beds	A B	<0.05 <0.05	85 85	

A and B indicate measurements were made on subsamples taken immediately after preserved core was unpacked.

LAB and TEW indicate measurements were made on subsamples used in the diffusive exchange experiments. Final water contents determined on these subsamples were corrected to the original water content of the sample at the beginning of the experiments (also taken immediately after unpacking preserved core) as described in section 2.1.1 of the main body of the report.

¹After first month of drying, samples were weighed every two weeks.

Shading indicates that a less stringent criterion was applied for attainment of constant mass.

Table B-1 (Cont'd): DGR-4 samples – criteria used to designate constant mass for gravimetric water content measurements at 40 °C.

Sample ID	Formation	Lithology (short)	Replicate	Criterion Applied Mass change (wt. %)	¹ Time to constant mass (days)	Additional information on selection of end point
DGR-4 662.83	Cobourg	Bioclastic limestone/argillaceous limestone	A	<0.005	135	
			B	<0.005	135	
DGR-4 665.41	Cobourg – LM	Bioclastic limestone/argillaceous limestone	A	<0.02	85	
			B	<0.02	85	
DGR-4 672.85	Cobourg – LM	Bioclastic limestone/argillaceous limestone	A	<0.005	135	
			B	<0.005	135	
DGR-4 717.12	Sherman Fall	Bedded argillaceous limestone/calcareous shale	A	<0.005	135	
			B	<0.005	135	
DGR-4 730.07	Kirkfield	Limestone with shale beds	A	<0.03	85	
			B	<0.04	85	
DGR-4 841.06	Shadow Lake	Sandy mudstone, siltstone and sandstone	LAB	<0.01	108	Large decrease in mass at 42 days followed by large increase
			TEW	<0.005	108	
DGR-4 847.48	Cambrian	Sandstone/dolostone	A	<0.005	135	
			B	<0.005	135	

A and B indicate measurements were made on subsamples taken immediately after preserved core was unpacked.

LAB and TEW indicate measurements were made on subsamples used in the diffusive exchange experiments. Final water contents determined on these subsamples were corrected to the original water content of the sample at the beginning of the experiments (also taken immediately after unpacking preserved core) as described in section 2.1.1 in the main body of the report.

¹After first month of drying, samples were weighed every two weeks.

Shading indicates that a less stringent criterion was applied for attainment of constant mass.

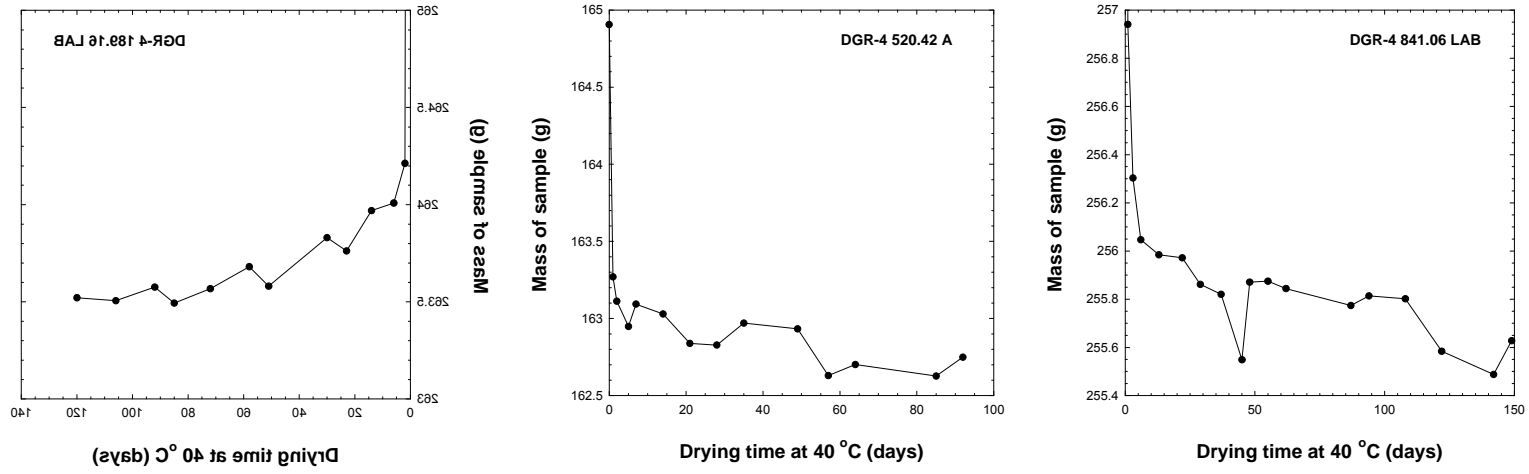


Figure B-1: Example drying curves for samples from DGR- 4 during gravimetric water content determinations at 40 °C.

Table B-2: DGR-4 samples - criteria used to designate constant mass for gravimetric water content measurements at 105 °C.

Sample ID	Formation	Lithology (short)	Replicate	Criterion Applied Mass change (wt. %)	¹ Time to constant mass (days)	Additional information on selection of end point
DGR-4 154.60	Bass Islands	Dolomitic shale with Ca-sulphate	A	<0.005	61	
			B	<0.005	61	
			LAB	<0.005	87	
			TEW	<0.005	87	
DGR-4 189.16*	Salina - F Unit	Dolomitic shale with Ca-sulphate	A	<0.005	63	
			B	<0.01	63	
			LAB	<0.005	120	
			TEW	<0.01	120	
DGR-4 229.32*	Salina - E Unit	Dolomitic shale with Ca-sulphate	A	<0.03	174	
			B	<0.04	174	
			LAB	<0.005	98	
			TEW	<0.01	77	
DGR-4 322.68*	Salina – A2 Unit	Massive Ca-sulphate	A	<0.005	119	
			B	<0.005	119	
			LAB	<0.02	34	
			TEW	<0.03	34	
DGR-4 332.13	Salina – A1 Unit	Argillaceous dolostone with Ca-sulphate	A	<0.005	12	*Low value
			B	<0.005	12	
			LAB	<0.005	23	
			TEW	<0.005	23	
DGR-4 422.21	Cabot Head	Red-green shale with carbonate/ black shale beds	A	<0.005	119	
			B	<0.02	174	
			LAB	<0.005	77	
			TEW	<0.005	77	

A and B indicate measurements were made on subsamples taken immediately after preserved core was unpacked.

LAB and TEW indicate measurements were made on subsamples used in the diffusive exchange experiments. Final water contents determined on these subsamples were corrected to the original water content of the sample at the beginning of the experiments (also taken immediately after unpacking preserved core) as described in section 2.1.1 in the main body of the report.

Shading indicates that a less stringent criterion was applied for attainment of constant mass.

Table B-2 (Cont'd): DGR-4 samples – criteria used to designate constant mass for gravimetric water content measurements at 105 °C.

Sample ID	Formation	Lithology (short)	Replicate	Criterion Applied Mass change (wt. %)	¹ Time to constant mass (days)	Additional information on selection of end point
DGR-4 472.78	Queenston	Red-green shale with carbonate beds	A	<0.005	119	
			B	<0.01	119	
			LAB	<0.01	135	
			TEW	<0.01	135	
DGR-4 520.42	Georgian Bay	Shale with sandstone/siltstone/ limestone beds	A	<0.005	63	
			B	<0.01	63	
			LAB	<0.005	113	
			TEW	<0.005	113	
DGR-4 662.83	Cobourg	Bioclastic limestone/argillaceous limestone	A	<0.005	91	
			B	<0.005	91	
			LAB	<0.005	101	
			TEW	<0.005	101	
DGR-4 665.41	Cobourg – LM	Bioclastic limestone/argillaceous limestone	A	<0.005	63	
			B	<0.005	63	
			LAB	<0.005	127	
			TEW	<0.005	113	
DGR-4 672.85	Cobourg – LM	Bioclastic limestone/argillaceous limestone	A	<0.005	91	
			B	<0.005	91	
			LAB	<0.005	106	
			TEW	<0.005	80	
DGR-4 717.12	Sherman Fall	Bedded argillaceous limestone/calcareous shale	A	<0.005	91	
			B	<0.005	91	
			LAB	<0.005	80	
			TEW	<0.005	80	

A and B indicate measurements were made on subsamples taken immediately after preserved core was unpacked.

LAB and TEW indicate measurements were made on subsamples used in the diffusive exchange experiments. Final water contents determined on these subsamples were corrected to the original water content of the sample at the beginning of the experiments (also taken immediately after unpacking preserved core) as described in section 2.1.1 in the main body of the report.

¹After first month of drying, samples were weighed every two weeks.

Shading indicates that a less stringent criterion was applied for attainment of constant mass.

Table B-2 (Cont'd): DGR-4 samples – criteria used to designate constant mass for gravimetric water content measurements at 105 °C.

Sample ID	Formation	Lithology (short)	Replicate	Criterion Applied Mass change (wt. %)	¹ Time to constant mass (days)	Additional information on selection of end point
DGR-4 730.07	Kirkfield	Limestone with shale beds	A	<0.005	63	
			B	<0.005	63	
			LAB	<0.005	127	
			TEW	<0.005	127	
DGR-4 841.06	Shadow Lake	Sandy mudstone, siltstone and sandstone	A	<0.005	119	
			B	<0.005	140	
			LAB	<0.005	77	
			TEW	<0.005	77	
DGR-4 847.48	Cambrian	Sandstone/dolostone	A	<0.005	105	
			B	<0.005	105	
			LAB	<0.005	80	
			TEW	<0.005	80	

A and B indicate measurements were made on subsamples taken immediately after preserved core was unpacked.

LAB and TEW indicate measurements were made on subsamples used in the diffusive exchange experiments. Final water contents determined on these subsamples were corrected to the original water content of the sample at the beginning of the experiments (also taken immediately after unpacking preserved core) as described in section 2.1.1 in the main body of the report.

¹After first month of drying, samples were weighed every two weeks.

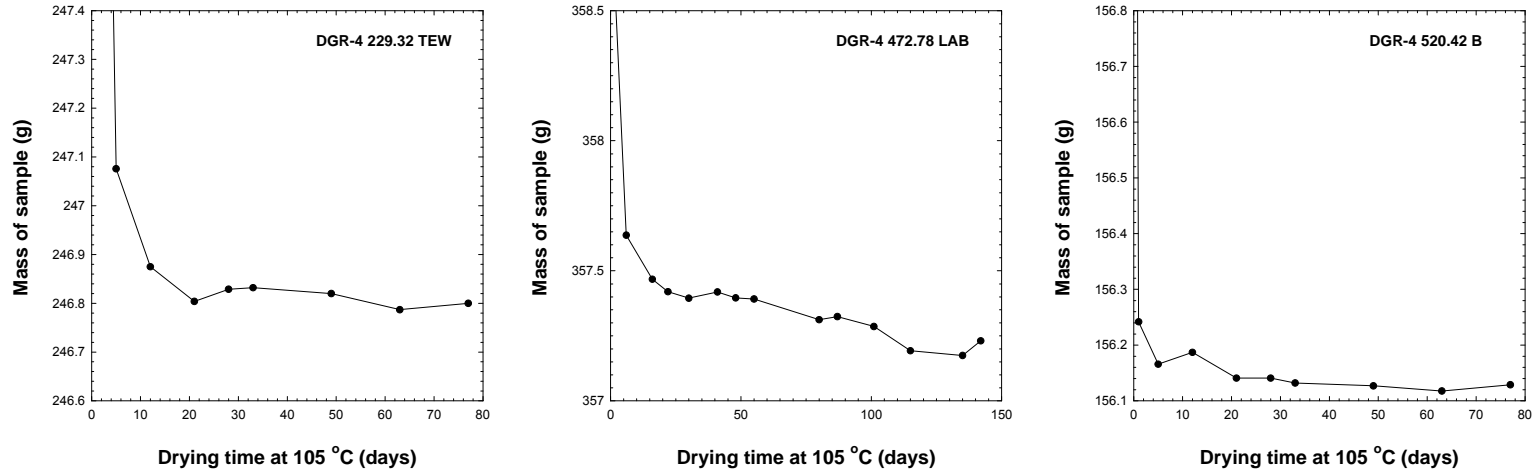


Figure B-2: Example drying curves for samples from DGR- 4 during gravimetric water content determinations at 105 °C.

APPENDIX C: Results for duplicate aqueous extractions, DGR-3 and DGR-4 samples

Table C1: Borehole DGR-3: Chemical composition of aqueous extract solutions from experiments conducted at a solid:liquid ratio of 1:1.

Sample ID ¹ (NWMO)	Formation	Replicate	pH	Na ⁺	K ⁺	Mg ²⁺	Ca ²⁺	Sr ²⁺	¹ F ⁻	Cl ⁻	Br ⁻	SO ₄ ²⁻	NO ₃ ⁻	Total Alkalinity	Charge Balance ²
				(mg/l)	(mg/l)	(mg/l)	(mg/l)	(mg/l)	(mg/l)	(mg/l)	(mg/l)	(mg/l)	(mg/l)	(mg/l)	(meq/l)
DGR-3 198.72*	Salina – F Unit	A	8.16	585	162	55.2	604	5.5	5.8	712	2.4	2170	<1	0.83	-1.53%
		B	8.19	577	158	54.1	594	5.0	5.8	715	2.2	2160	<1	0.82	-2.34%
DGR-3 208.41*	Salina – F Unit	A	8.40	726	109	35.7	582	3.6	4.7	1250	2.1	2040	<1	0.67	-8.50%
		B	8.25	836	121	40.7	658	4.3	4.7	1250	3.4	2040	<1	0.66	-1.85%
DGR-3 248.71*	Salina – E Unit	A	8.37	1520	131	45.2	720	5.0	5.7	2040	2.7	2400	<1	0.88	0.26%
		B	8.63	1480	127	43.1	718	5.2	5.6	2020	2.6	2400	<1	0.91	-0.55%
DGR-3 270.06*	Salina – C Unit	A	8.28	6410	210	46.8	1130	13.1	3.6	10400	10.0	2920	4.3	0.42	-1.00%
		B	8.43	6490	211	46.6	1150	13.2	3.6	10400	10.2	2920	4.3	0.41	-1.15%
DGR-3 289.36*	Salina – B Unit	A	8.34	3900	135	75.9	1090	6.6	5.8	6430	7.5	2740	2.6	0.76	-1.15%
		B	8.52	3800	129	75.7	1040	6.2	5.7	6432	14.0	2740	4.9	0.76	-2.83%
DGR-3 312.53	Salina – A2 Unit	A	8.28	2570	107	131	346	26.9	5.8	4136	5.4	1440	<1	0.80	-1.59%
		B	8.39	2230	114	131	353	26.4	5.8	4180	5.5	1440	8.0	0.82	-7.30%
DGR-3 335.22*	Salina – A2 Evaporite	A	8.71	53.5	13.1	5.4	799	18.7	<1	105	1.0	1878	1.8	0.35	1.06%
		B	8.77	50.1	10.3	5.0	791	15.8	<1	100	0.5	1910	1.5	0.35	-0.23%
DGR-3 344.06	Salina – A1 Unit	A	8.99	181	25.0	2.9	17.8	<1	2.9	230	1.0	112	<1	0.92	-1.34%
		B	8.97	182	30.3	3.7	16.0	<1	3.0	230	1.2	110	<1	0.94	-0.52%
DGR-3 380.88*	A1 Evaporite	A	8.82	61.2	16.0	3.5	1180	<1	<1	189	1.2	2560	<1	0.44	2.76%
		B	8.49	63.0	13.9	3.4	990	<1	<1	185	1.2	2470	<1	0.41	-3.90%
DGR-3 391.34*	Guelph	A	8.61	10700	120	113	1290	4.2	<1	20000	56.7	2100	23.6	0.71	-5.76%
		B	8.79	10500	120	111	1260	4.3	<1	19900	39.9	2090	17.7	0.74	-6.34%
DGR-3 435.62	Cabot Head	A	7.92	1640	718	274	2140	53.4	2.2	8060	97.4	12.1	12.1	0.49	-2.03%
		B	7.98	1530	713	275	2000	53.7	2.1	8030	97.4	10.6	11.2	0.46	-4.64%

*Soluble sulphates and/or halite identified in sample.

¹Data for F⁻ are considered semi-quantitative due to overlap with peaks for organic acids in the ion chromatograms.

Shading of Br⁻ value indicates that it is the average of measurements made on the two replicate extraction solutions using ICP-MS at the British Geological Survey.

Table C1 (Cont'd): Borehole DGR-3: Chemical composition of aqueous extract solutions from experiments conducted at a solid:liquid ratio of 1:1.

Sample ID (NWMO)	Formation	Replicate	pH	Na ⁺	K ⁺	Mg ²⁺	Ca ²⁺	Sr ²⁺	¹ F ⁻	Cl ⁻	Br ⁻	SO ₄ ²⁻	NO ₃ ⁻	Total Alkalinity	Charge Balance ²
				(mg/l)	(mg/l)	(mg/l)	(mg/l)	(mg/l)	(mg/l)	(mg/l)	(mg/l)	(mg/l)	(mg/l)	(mg/l)	(meq/l)
DGR-3 453.41	Manitoulin	A	8.01	489	134	129	593	14.4	<1	2260	33.3	17.7	2.7	0.35	0.13%
		B	8.13	466	128	126	589	14.4	<1	2190	33.8	16.8	2.3	0.35	0.50%
DGR-3 468.76	Queenston	A	7.90	1330	614	204	1750	33.4	2.0	6940	85.2	19.9	8.1	0.39	-5.06%
		B	7.95	1150	623	208	1530	35.8	1.9	6920	85.3	19.1	7.8	0.38	-10.30%
DGR-3 484.58*	Queenston	A	8.04	1070	489	155	1750	29.5	1.8	5190	64.8	1150	6.5	0.43	-3.57%
		B	8.06	975	488	156	1600	30.2	1.7	5160	64.2	1160	6.5	0.42	-7.20%
DGR-3 502.55	Queenston	A	8.08	526	293	73.3	649	15.3	1.1	2070	25.3	444	1.4	0.48	0.43%
		B	8.15	524	289	71.5	639	13.9	<1	2050	25.5	435	1.3	0.47	0.46%
DGR-3 531.65*	Georgian Bay	A	8.05	836	276	95.9	778	17.0	<1	2850	32.2	330	1.5	0.50	1.31%
		B	8.17	853	283	97.4	786	16.4	<1	2840	32.1	324	1.4	0.50	2.22%
DGR-3 581.47	Georgian Bay	A	7.88	1630	656	113	1510	40.2	1.3	6360	74.2	9.4	6.3	0.41	-2.26%
		B	7.95	1640	618	110	1440	40.7	1.2	6160	71.1	9.4	5.8	0.40	-1.86%
DGR-3 621.63	Blue Mountain	A	7.86	1620	638	118	1540	41.6	1.2	6300	74.2	19.0	6.1	0.42	-1.60%
		B	7.88	1590	630	116	1520	42.4	1.3	6300	73.9	19.7	6.1	0.42	-2.29%
DGR-3 646.29	Blue Mountain	A	7.98	1390	475	92.1	1260	32.1	1.2	5180	62.2	28.9	4.7	0.42	-1.61%
		B	7.97	1430	470	91.8	1300	33.9	1.2	5190	62.8	28.7	4.8	0.41	-0.45%
DGR-3 665.29	Cobourg –C M	A	8.64	221	136	21.8	93.0	3.8	1.1	679	6.8	54.8	<1	0.74	-3.86%
		B	8.58	221	131	22.8	93.6	4.2	1.1	675	6.8	54.9	<1	0.79	-3.69%
DGR-3 676.21	Cobourg – LM	A	8.25	722	321	85.5	443	14.2	<1	2530	26.2	27.3	<1	0.51	-2.55%
		B	8.24	720	320	85.1	448	14.8	<1	2530	24.3	25.5	<1	0.50	-2.45%
DGR-3 678.92	Cobourg – LM	A	8.40	222	112	25.9	135	4.1	<1	758	7.6	41.4	<1	0.58	-3.33%
		B	8.39	218	115	25.1	133	3.7	<1	763	7.6	41.3	<1	0.58	-4.33%

*Soluble sulphates and/or halite identified in sample.

¹Data for F⁻ are considered semi-quantitative due to overlap with peaks for organic acids in the ion chromatograms.

Shading of Br⁻ value indicates that it is the average of measurements made on the two replicate extraction solutions using ICP-MS at the British Geological Survey.

Table C2: Borehole DGR-3: Chemical composition of aqueous extract solutions from experiments conducted at a solid:liquid ratio of 1:1.

Sample ID (NWMO)	Formation	Replicate	pH	Na ⁺	K ⁺	Mg ²⁺	Ca ²⁺	Sr ²⁺	F ⁻	Cl ⁻	Br ⁻	SO ₄ ²⁻	NO ₃ ⁻	Total Alkalinity	Charge Balance ²
				(mg/l)	(mg/l)	(mg/l)	(mg/l)	(mg/l)	(mg/l)	(mg/l)	(mg/l)	(mg/l)	(mg/l)	(mg/l)	(meq/l)
DGR-3 685.52	Cobourg – LM	A	8.31	296	137	33.2	183	4.9	<1	1030	11.8	37.4	<1	0.57	-3.86%
		B	8.32	301	136	33.2	186	5.1	<1	1030	10.8	34.2	<1	0.56	-2.89%
DGR-3 690.12	Cobourg – LM	A	8.53	232	90.9	26.3	145	4.8	<1	791	7.5	33.6	<1	0.46	-3.67%
		B	8.49	230	86.8	26.0	143	4.7	<1	758	7.2	31.1	<1	0.45	-2.32%
DGR-3 692.82	Cobourg – LM	A	8.44	420	151	39.9	226	7.9	<1	1500	15.3	28.3	<1	0.46	-8.52%
		B	8.40	493	181	47.1	268	9.1	<1	1480	15.3	28.7	<1	0.45	0.56%
DGR-3 697.94	Cobourg – LM	A	8.23	346	148	36.2	203	5.4	<1	1140	12.9	25.5	<1	0.47	-1.96%
		B	8.46	354	153	37.5	208	5.5	<1	1180	11.8	29.2	<1	0.47	-2.61%
DGR-3 710.38	Sherman Fall	A	8.60	142	43.6	18.2	106	3.1	<1	468	4.4	18.7	1.3	0.38	0.26%
		B	8.65	140	43.7	19.0	107	3.4	<1	459	4.4	18.7	<1	0.36	1.48%
DGR-3 725.57	Sherman Fall	A	8.39	620	268	50.5	281	7.1	1.4	1810	23.4	29.2	<1	0.51	-0.31%
		B	8.14	595	265	36.8	244	6.2	1.4	1610	15.6	27.9	<1	0.55	1.40%
DGR-3 744.27	Kirkfield	A	8.14	595	265	36.8	244	6.2	1.4	1600	15.6	27.9	<1	0.55	1.40%
		B	8.36	592	259	36.9	244	5.9	1.4	1600	15.6	27.8	<1	0.54	1.37%
DGR-3 761.56	Kirkfield	A	8.91	61.6	19.5	8.9	70.5	<1	<1	179	1.5	93.7	1.00	0.35	0.16%
		B	8.67	63.3	18.9	9.4	74.4	<1	<1	177	1.4	88.5	<1	0.35	3.24%
DGR-3 777.33	Coboconk	A	8.56	221	91.2	12.7	66.8	1.5	1.3	508	4.5	55.2	1.3	0.63	0.32%
		B	8.73	232	97.5	13.5	71.4	2.0	1.2	507	4.6	53.7	1.3	0.62	3.32%
DGR-3 807.43	Gull River	A	8.63	157	49.3	14.4	77.4	1.8	<1	425	3.7	45.4	1.3	0.43	-1.14%
		B	8.86	171	53.9	16.1	83.0	2.1	<1	445	3.9	48.8	1.4	0.42	0.68%
DGR-3 843.92	Gull River	A	8.55	232	80.9	14.7	76.6	2.0	1.7	534	4.6	55.2	1.4	0.66	0.61%
		B	8.63	232	76.8	15.2	74.8	1.8	1.7	534	4.7	54.0	1.4	0.59	0.32%
DGR-3 852.18	Shadow Lake	A	7.97	1290	298	111	728	9.8	3.5	3910	42.6	64.6	2.7	0.40	-1.60%
		B	7.99	1260	313	118	762	10.1	3.4	3900	42.8	63.9	2.6	0.39	-0.91%
DGR-3 856.06	Cambrian	A	8.89	314	68.4	121	136	4.2	<1	1120	10.9	18.9	<1	0.60	-0.94%
		B	9.16	314	72.1	119	138	4.1	<1	1140	9.3	14.7	<1	0.60	-1.19%

¹Data for F⁻ are considered semi-quantitative due to overlap with peaks for organic acids in the ion chromatograms.

Shading of Br⁻ value indicates that it is the average of measurements made on the two replicate extraction solutions using ICP-MS at the British Geological Survey.

Table C2: Borehole DGR-4: Chemical composition of aqueous extract solutions from experiments conducted at a solid:liquid ratio of 1:1.

Sample ID ¹ (NWMO)	Formation	Replicate	pH	Na ⁺	K ⁺	Mg ²⁺	Ca ²⁺	Sr ²⁺	¹ F ⁻	Cl ⁻	Br ⁻	SO ₄ ²⁻	NO ₃ ⁻	Total Alkalinity	Charge Balance ²
				(mg/l)	(mg/l)	(mg/l)	(mg/l)	(mg/l)	(mg/l)	(mg/l)	(mg/l)	(mg/l)	(mg/l)	(mg/l)	(meq/l)
DGR-4 154.60	Bass Islands	A	9.51	23.2	15.6	109	15.8	<1	<2	209	3.44	32.34	<1	3.78	3.53%
		B	9.44	23.1	14.9	114	12.7	<1	<2	210	3.48	50.06	<1	3.72	2.71%
DGR-4 189.16*	Salina - F Unit	A	8.71	287	92.5	34.5	642	3.8	5.1	442	1.40	1890	<2	0.75	-2.38%
		B	8.73	297	96.8	34.1	638	4.4	5.2	438	1.40	1880	<2	0.76	-1.80%
DGR-4 229.32*	Salina - E Unit	A	8.69	301	101	42.5	643	4.45	5.59	261	0.97	1950	<1	0.70	2.23%
		B	8.63	283	109	43.7	645	4.25	5.67	249	1.05	1950	<1	0.67	2.29%
DGR-4 322.68*	A2 Evaporite	A	8.56	57.4	4.71	2.55	856	16.4	<2	106	0.32	1880	<1	0.32	3.55%
		B	8.50	57.5	8.39	2.27	844	16.9	<2	110	0.28	1870	<1	0.31	3.08%
DGR-4 332.13	Salina A1 Unit	A	9.08	300	43.3	3.7	19.1	<1	2.70	416	1.36	129	<2	1.11	0.04%
		B	9.09	289	47.1	4.1	20.3	<1	2.70	418	1.43	128	<2	1.13	-0.99%
DGR-4 422.21	Cabot Head	A	7.93	2030	868	427	2690	69.1	2.79	9520	114	55.7	<1	0.34	1.47%
		B	7.89	1990	879	426	2670	73.1	3.57	9340	121	49.1	<1	0.31	1.94%
DGR-4 472.78*	Queenston	A	8.01	1260	576	200	1980	31.0	2.55	5560	71.4	946	<1	0.51	1.91%
		B	7.92	1270	590	224	2000	32.9	2.73	5550	71.2	963	<1	0.51	2.87%
DGR-4 520.42	Georgian Bay	A	8.07	708	306	101	776	10.6	<2	2920	33.1	388	<2	0.54	-3.10%
		B	8.12	704	289	97.1	805	11.7	<2	2850	32.4	413	<2	0.52	-1.87%
DGR-4 662.83	Cobourg – LM	A	8.43	403	175	41.1	245	6.51	<2	1150	12.1	39.2	<1	0.54	5.26%
		B	8.36	410	176	42.2	245	7.07	<2	1150	12.8	39.3	<1	0.53	5.57%
DGR-4 665.41	Cobourg – LM	A	8.29	363	159	51.7	231	6.9	<2	1350	15.8	37.3	<2	0.49	-4.83%
		B	8.34	365	158	51.3	230	6.2	<2	1370	14.7	32.9	<2	0.48	-5.46%
DGR-4 672.85	Cobourg – LM	A	8.50	219	102	28.3	142	4.51	<2	693	7.28	34.3	<1	0.59	1.47%
		B	8.48	225	107	29.2	143	4.24	<2	703	7.32	34.6	<1	0.59	1.90%

*Soluble sulphates and/or halite identified in sample.

¹Data for F⁻ are considered semi-quantitative due to overlap with peaks for organic acids in the ion chromatograms.

Shading of Br⁻ value indicates that it is the average of measurements made on the two replicate extraction solutions using ICP-MS at the British Geological Survey.

Table C2 (Cont'd): Borehole DGR-4: Chemical composition of aqueous extract solutions from experiments conducted at a solid:liquid ratio of 1:1.

Sample ID (NWMO)	Formation	Replicate	pH	Na ⁺	K ⁺	Mg ²⁺	Ca ²⁺	Sr ²⁺	¹ F ⁻	Cl ⁻	Br ⁻	SO ₄ ²⁻	NO ₃ ⁻	Total Alkalinity	Charge Balance ²
				(mg/l)	(mg/l)	(mg/l)	(mg/l)	(mg/l)	(mg/l)	(mg/l)	(mg/l)	(mg/l)	(mg/l)	(mg/l)	(meq/l)
DGR-4 717.12	Sherman Fall	A	8.54	461	189	28.1	198	4.31	0.61	1150	11.9	24.0	<1	0.50	4.80%
		² B	8.54	503	209	33.7	214	4.37	0.66	1210	12.1	23.8	<1	0.50	6.91%
		C	8.54	454	194	30.6	202	5.3	1.3	1240	12.4	24.4	<2	0.42	1.83%
		D	8.66	392	163	31.1	174	4.5	<2	1230	12.2	23.7	<2	0.42	-4.47%
DGR-4 730.07	Kirkfield	A	8.55	655	248	38.4	288	6.9	<2	1820	17.5	35.9	<2	0.42	-0.02%
		B	8.60	628	251	38.2	285	6.8	<2	1840	18.6	33.6	<2	0.44	-1.84%
DGR-4 841.06	Shadow Lake	A	8.41	1030	164	180	706	9.59	2.78	3180	31.2	36.4	<1	0.72	3.77%
		B	8.46	1010	170	183	685	12.0	2.69	3160	32.3	36.0	<1	0.71	3.28%
DGR-4 847.48*	Cambrian	A	8.74	422	28.1	171	212	5.91	<2	1340	14.0	16.9	<1	0.48	5.92%
		B	8.77	420	27.6	169	213	5.71	<2	1340	14.1	17.2	<1	0.47	5.79%

*Soluble sulphates and/or halite identified in sample.
¹Data for F⁻ are considered semi-quantitative due to overlap with peaks for organic acids in the ion chromatograms.
²Data for B replicate was excluded from average due to poor charge balance.

APPENDIX D: Supporting Petrophysical Data, University of New Brunswick samples

Table D-2: Results for DGR-3. Standard deviations of density values relate to the variability among measurements of two (occasionally three) subsamples but exclude any other methodological or analytical errors. The error on physical porosity is calculated from assumed total errors on the bulk dry and grain density measurements of $\pm 0.05 \text{ g/cm}^3$ each.

Sample ID	Formation	Bulk dry density		Grain density		Phys. porosity		CS-Mat		
		Average g/cm ³	StDev g/cm ³	Average g/cm ³	StDev g/cm ³	Value %	Error %	S wt. %	C(inorg) wt. %	C(org) wt. %
DGR-3 188.36	Salina - G Unit	2.533	0.081	2.827	0.005	10.4	2.4	3.3	10.5	<0.1
DGR-3 200.07	Salina - F Unit	2.436	0.010	2.741	0.003	11.1	2.4	2.9	5.0	<0.1
DGR-3 204.05	Salina - F Unit	2.578	0.005	2.829	0.023	8.9	2.4	<0.1	5.9	<0.1
DGR-3 273.98	Salina - C Unit	2.316	0.011	2.770	0.003	16.4	2.4	3.5	3.2	<0.1
DGR-3 308.05	Salina - A2 Unit	2.349	0.014	2.796	0.021	16.0	2.3	9.8	5.2	<0.1
DGR-3 334.44	A2 Evaporite	2.322	0.017	2.684	0.011	13.5	2.5	13.6	6.1	<0.1
DGR-3 381.40	A1 Evaporite	2.821	0.000	2.745	0.024	<0.5	2.6	9.2	7.0	0.1
DGR-3 386.04	Salina - A0 Unit	2.692	0.005	2.729	0.015	1.3	2.6	<0.1	12.1	0.1
DGR-3 408.19	Goat Island	2.672	0.017	2.711	0.027	1.4	2.6	<0.1	10.4	0.1
DGR-3 506.64	Queenston	2.604	0.004	2.832	0.033	8.1	2.4	0.5	3.2	<0.1
DGR-3 563.49	Georgian Bay	2.518	0.012	2.833	0.028	11.1	2.4	<0.1	1.1	<0.1
DGR-3 589.21	Georgian Bay	2.681	0.000	2.706	0.006	0.9	2.6	0.1	9.3	0.1
DGR-3 608.42	Georgian Bay	2.595	0.001	2.794	0.033	7.1	2.4	1.3	1.4	0.1
DGR-3 641.23	Blue Mountain	2.572	0.000	2.778	0.034	7.4	2.5	1.3	1.4	0.3
DGR-3 672.42	Cobourg - Collingwood	2.672	0.002	2.697	0.001	1.0	2.6	0.1	10.4	0.1
DGR-3 688.43	Cobourg - Lower	2.689	0.001	2.750	0.032	2.2	2.5	0.1	10.7	0.1
DGR-3 703.84	Sherman Fall	2.699	0.007	2.756	0.009	2.1	2.5	0.2	10.7	0.1
DGR-3 758.16	Kirkfield	2.673	0.000	2.650	0.022	<0.5	2.7	0.2	10.7	<0.1
DGR-3 776.57	Coboconk	2.681	0.003	2.733	0.041	1.9	2.6	0.5	10.8	<0.1
DGR-3 845.00	Gull River	2.695	0.005	2.765	0.008	2.5	2.5	0.2	11.0	0.2

Table D-2: Results for DGR-4. Standard deviations of density values relate to the variability among measurements of two (occasionally three) subsamples but exclude any other methodological or analytical errors. The error on physical porosity is calculated from assumed total errors on the bulk dry and grain density measurements of $\pm 0.05 \text{ g/cm}^3$ each.

Sample ID	Formation	Bulk dry density		Grain density		Phys. porosity		CS-Mat		
		Average g/cm^3	StDev g/cm^3	Average g/cm^3	StDev g/cm^3	Value %	Error %	S wt. %	C(inorg) wt. %	C(org) wt. %
DGR-4 229.54	Salina - E Unit	2.659	0.001	2.811	0.001	5.4	2.4	0.8	7.3	0.5
DGR-4 287.62	Salina - B Unit	2.522	0.020	2.816	0.025	10.4	2.4	5.1	4.2	0.0
DGR-4 337.11	Salina - A1 Unit	2.629	0.000	2.768	0.017	5.0	2.5	0.2	11.2	0.2
DGR-4 387.42	Goat Island	2.689	0.000	2.695	0.017	0.2	2.6	<0.1	11.3	<0.1
DGR-4 422.43	Cabot Head	2.579	0.000	2.866	0.052	10.0	2.3	<0.1	0.6	<0.1
DGR-4 516.89	Queenston	2.612	0.008	2.824	0.048	7.5	2.4	<0.1	2.9	<0.1
DGR-4 520.12	Georgian Bay	2.642	0.001	2.757	0.022	4.2	2.5	<0.1	5.5	<0.1
DGR-4 559.70	Georgian Bay	2.762	0.013	2.742	0.004	<0.5	2.6	0.2	9.8	0.2
DGR-4 681.32	Cobourg - Lower	2.646	0.004	2.767	0.006	4.4	2.5	0.2	8.5	0.3
DGR-4 719.15	Kirkfield	2.685	0.006	2.677	0.024	<0.5	2.6	0.1	11.3	0.1

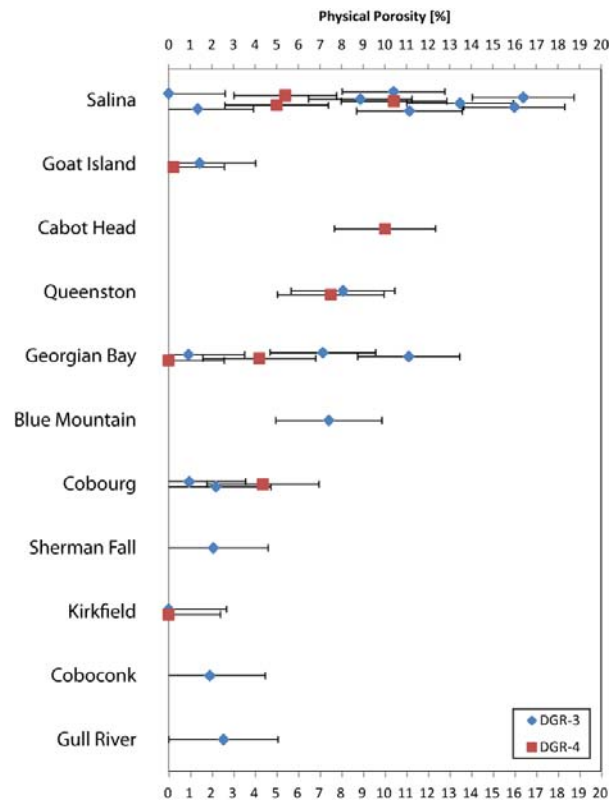


Figure D-1: Physical porosities of the studied formations.

The error in the physical porosity is calculated according to the Gaussian law of uncertainty propagation, which is defined by the following formulae:

Let y be calculated from measured parameters x_1, x_2, \dots with uncertainties u_1, u_2, \dots the uncertainty of y is defined by:

$$u_y = \sqrt{\sum_{i=1}^n \left(\frac{\partial y}{\partial x_i} u_i \right)^2}$$

Then, the uncertainty in the physical porosity is given by:

$$u_n = \sqrt{\left(-\frac{u_{\rho_{\text{bulk,dry}}}}{\rho_{\text{grain}}} \right)^2 + \left(\frac{\rho_{\text{bulk,dry}} u_{\rho_{\text{grain}}}}{\rho_{\text{grain}}^2} \right)^2}$$

Where $u_{\rho_{\text{bulk,dry}}} = u_{\rho_{\text{grain}}}$ were chosen as 0.05 g/cm^3 each.

APPENDIX E: Revised DGR-2 Data

Table E-1: Revised average gravimetric water contents ($WC_{Grav.}$) of DGR-2 samples determined by drying to constant mass at 105 °C. The water contents are calculated relative to the wet ($WC_{Grav. wet}$) or dry ($WC_{Grav. dry}$) mass of the rock sample. Includes correction for original water content of two replicate water content samples from diffusive exchange experiments; correction is not applicable to water content values reported at 40 °C samples in Koroleva et al. (2009).

Sample ID ¹	Formation ²	Lithology (short) ²	Average	STD	Average	STD
			$WC_{Grav. wet}$ 105°C ² (n = 4) (wt.%)	(±1σ) (wt.%)	$WC_{Grav. dry}$ 105°C ² (n = 4) (wt.%)	(±1σ) (wt.%)
DGR-2 473.19	Queenston	argillaceous marl	2.92	0.06	3.01	0.06
DGR-2 482.69	Queenston	argillaceous marl	2.78	0.09	2.87	0.10
DGR-2 491.83	Queenston	calcareous marl	1.16	0.33	1.18	0.33
DGR-2 510.12	Queenston	argillaceous marl	2.81	0.10	2.89	0.11
DGR-2 523.08	Georgian Bay	calcareous marl / limestone-dolostone	0.98	0.25	0.99	0.26
DGR-2 562.92	Georgian Bay	calcareous marl	1.11	0.29	1.12	0.30
DGR-2 581.32	Georgian Bay	clay rock	2.95	0.11	3.05	0.12
DGR-2 609.39	Georgian Bay	clay rock	2.23	0.21	2.27	0.22
DGR-2 662.09	Cobourg	Limestone	0.51	0.02	0.51	0.02
DGR-2 663.46	Cobourg	Limestone	0.71	0.06	0.72	0.07
DGR-2 674.73	Cobourg	Limestone	0.69	0.04	0.70	0.04
DGR-2 738.00	Kirkfield	limestone-dolostone	0.62	0.12	0.62	0.13
DGR-2 770.60	Coboconk	limestone-dolostone	0.14	0.03	0.14	0.03
DGR-2 796.54	Gull River	Limestone	0.33	0.09	0.33	0.09
DGR-2 813.70	Gull River	limestone-dolostone	0.35	0.06	0.35	0.06
DGR-2 830.05	Gull River	limestone-dolostone	0.29	0.16	0.29	0.16
DGR-2 840.06	Shadow Lake	limestone-dolostone	2.69	0.04	2.76	0.04
DGR-2 846.31	Cambrian	sandy limestone-dolostone	1.24	0.11	1.26	0.11
DGR-2 852.39	Cambrian	Sandstone	7.40	0.06	8.00	0.08
DGR-2 855.89	Cambrian	Sandstone	6.22	0.47	6.62	0.51
DGR-2 861.90	Precambrian	granitic gneiss	1.34	0.25	1.36	0.26

¹ Sample depth in mBGS is given by second half of sample ID.

² From Koroleva et al. 2009.

Corrections for original water contents of samples prior to start of the diffusive exchange experiments is described in section 2.1.1 of the main report.

Table E-2: Revised porewater contents for DGR-2 samples calculated relative to wet ($PWC_{Grav.wet}$) or dry ($PWC_{Grav.dry}$) mass of rock using porewater salinity and density estimates consistent with those applied to DGR-3 and DGR-4 samples (see section 4.2.2 in main report).

Sample ID ¹	Formation ²	Lithology (short) ²	Measured a_w ²	Estimated porewater salinity ³	$PWC_{Grav.wet}$ ¹	Uncertainty $PWC_{Grav.wet}$ ²	$PWC_{Grav.dry}$ ¹	Uncertainty $PWC_{Grav.dry}$ ²	Recalculated Bulk Dry Density ⁴ (using $PWC_{Grav.dry}$)
			-	(%)	(wt.%)	(± wt.%)	(wt.%)	(± wt. %)	(g/cm ³)
DGR-2 473.19	Queenston	argillaceous marl	0.62	28	4.06	0.30	4.18	0.30	2.57
DGR-2 482.69	Queenston	argillaceous marl	0.67	28	3.87	0.30	3.98	0.31	2.55
DGR-2 491.83	Queenston	calcareous marl	0.60	28	1.62	0.47	1.63	0.48	2.65
DGR-2 510.12	Queenston	argillaceous marl	0.64	28	3.90	0.31	4.02	0.32	2.56
DGR-2 523.08	Georgian Bay	calcareous marl / limestone-dolostone	0.56	28	1.36	0.36	1.37	0.37	2.68
DGR-2 562.92	Georgian Bay	calcareous marl	0.66	28	1.54	0.42	1.56	0.43	2.56
DGR-2 581.32	Georgian Bay	clay rock	0.64	28	4.10	0.33	4.23	0.34	2.51
DGR-2 609.39	Georgian Bay	clay rock	0.62	28	3.09	0.36	3.16	0.37	2.56
DGR-2 662.09	Cobourg	Limestone	0.62	28	0.71	0.06	0.71	0.06	2.64
DGR-2 663.46	Cobourg	Limestone	0.60	28	0.99	0.11	1.00	0.11	2.64
DGR-2 674.73	Cobourg	Limestone	0.67	28	0.96	0.09	0.97	0.09	2.65
DGR-2 738.00	Kirkfield	limestone-dolostone	0.66	28	0.86	0.18	0.86	0.18	2.66
DGR-2 770.60	Coboconk	limestone-dolostone	0.68	28	0.19	0.04	0.19	0.04	2.68
DGR-2 796.54	Gull River	Limestone	0.69	28	0.46	0.13	0.46	0.13	2.66
DGR-2 813.70	Gull River	limestone-dolostone	0.62	28	0.49	0.09	0.49	0.09	2.65
DGR-2 830.05	Gull River	limestone-dolostone	0.65	28	0.40	0.22	0.40	0.22	2.69
DGR-2 840.06	Shadow Lake	limestone-dolostone	0.80	20	3.36	0.22	3.45	0.22	2.61
DGR-2 846.31	Cambrian	sandy limestone-dolostone	0.80	20	1.56	0.17	1.58	0.17	2.68
DGR-2 852.39	Cambrian	Sandstone	0.81	20	9.25	0.58	10.00	0.63	2.12
DGR-2 855.89	Cambrian	Sandstone	0.81	20	7.78	0.77	8.28	0.82	2.14
DGR-2 861.90	Precambrian	granitic gneiss	0.81	20	1.68	0.33	1.70	0.34	2.50

¹ Sample depth in mBGS is given by second half of sample ID.

² From Koroleva et al. 2009

³ Revised salinity and density estimates for porewaters are described in section 4.2.2 of main report.

⁴ Calculated using revised porewater contents for DGR-2 samples given in this table; calculations are described in section 4.2.2 of main report.

Table E-3: Comparison of porewater contents for DGR-2 samples calculated relative to wet ($PWC_{Grav.wet}$) mass of rock using estimated porewater salinities and densities from this study and from Intera, 2010a.

Sample ID	Formation	This study (Table 12 and Table E-2)				From Intera, 2010		
		Measured a_w -	Porewater Salinity (%)	$PWC_{Grav.wet}$ (wt.%)	Uncertainty $PWC_{Grav.wet}$ ¹ (± wt.%)	Pore fluid salinity ² (%)	Estimated liquid density ² (kg/m ³)	$PWC_{Grav.wet}$ ³ (wt.%)
DGR-2 473.19	Queenston	0.62	28	4.06	0.30	28.8	1210	4.11
DGR-2 482.69	Queenston	0.67	28	3.87	0.30	28.8	1210	3.91
DGR-2 491.83	Queenston	0.60	28	1.62	0.47	28.8	1210	1.63
DGR-2 510.12	Queenston	0.64	28	3.90	0.31	28.8	1210	3.94
DGR-2 523.08	Georgian Bay	0.56	28	1.36	0.36	25.9	1177	1.32
DGR-2 562.92	Georgian Bay	0.66	28	1.54	0.42	25.9	1177	1.50
DGR-2 581.32	Georgian Bay	0.64	28	4.10	0.33	25.9	1177	3.98
DGR-2 609.39	Georgian Bay	0.62	28	3.09	0.36	25.9	1177	3.00
DGR-2 662.09	Cobourg	0.62	28	0.71	0.06	19.9	1128	0.64
DGR-2 663.46	Cobourg	0.60	28	0.99	0.11	19.9	1128	0.89
DGR-2 674.73	Cobourg	0.67	28	0.96	0.09	19.9	1128	0.86
DGR-2 738.00	Kirkfield	0.66	28	0.86	0.18	23.3	1157	0.80
DGR-2 770.60	Coboconk	0.68	28	0.19	0.04	20.4	1132	0.17
DGR-2 796.54	Gull River	0.69	28	0.46	0.13	22.3	1148	0.42
DGR-2 813.70	Gull River	0.62	28	0.49	0.09	22.3	1148	0.45
DGR-2 830.05	Gull River	0.65	28	0.40	0.22	22.3	1148	0.37
DGR-2 840.06	Shadow Lake	0.80	20	3.36	0.22	18.3	1115	3.29
DGR-2 846.31	Cambrian	0.80	20	1.56	0.17	18.1	1113	1.52
DGR-2 852.39	Cambrian	0.81	20	9.25	0.58	18.1	1113	9.03
DGR-2 855.89	Cambrian	0.81	20	7.78	0.77	18.1	1113	7.60
DGR-2 861.90	Precambrian	0.81	20	1.68	0.33	19.4	1146	1.67

⁴Average of values for the Salina A1 Upper and Salina A1 Lower reported in Intera, 2010.

¹Calculated using an estimated uncertainty of ±5% for the porewater salinity.

²Salinity and density for pore fluids from Table 2 in Intera, 2010a.

³Calculated using equation 4 or 5 and average water contents determined at 105 °C.

Table E-4: Calculated porewater-loss (ϕ_{PWL}) and physical porosities (ϕ_{tot}) of DGR-2 samples using revised porewater contents presented in Table E-2.

Sample ID	Formation	Lithology (short)	Porewater-loss Porosity ¹	Uncertainty Porewater-loss porosity ²	Physical Porosity ¹	Uncertainty in Physical Porosity ²	Difference between ϕ_{PWL} and ϕ_{tot}
			(vol.%)	(± vol. %)	(vol.%)	(± vol. %)	(vol.%)
DGR-2 473.19	Queenston	argillaceous marl	8.56	0.42	5.42	1.1	3.1
DGR-2 482.69	Queenston	argillaceous marl	8.36	0.43	8.66	1.1	-0.3
DGR-2 491.83	Queenston	calcareous marl	3.57	0.65	4.45	1.2	-0.9
DGR-2 510.12	Queenston	argillaceous marl	8.29	0.43	6.67	1.1	1.6
DGR-2 523.08	Georgian Bay	calcareous marl / limestone-dolostone	2.98	0.51	2.07	1.2	0.9
DGR-2 562.92	Georgian Bay	calcareous marl	3.42	0.59	7.91	1.2	-4.5
DGR-2 581.32	Georgian Bay	clay rock	8.64	0.45	7.59	1.1	1.0
DGR-2 609.39	Georgian Bay	clay rock	6.57	0.49	5.57	1.2	1.0
DGR-2 662.09	Cobourg	Limestone	1.54	0.09	2.18	1.2	-0.6
DGR-2 663.46	Cobourg	Limestone	2.14	0.17	1.73	1.2	0.4
DGR-2 674.73	Cobourg	Limestone	2.08	0.14	1.69	1.2	0.4
DGR-2 738.00	Kirkfield	limestone-dolostone	1.86	0.26	1.22	1.2	0.6
DGR-2 770.60	Coboconk	limestone-dolostone	0.42	0.06	0.56	1.2	-0.1
DGR-2 796.54	Gull River	Limestone	1.01	0.19	3.00	1.1	-2.0
DGR-2 813.70	Gull River	limestone-dolostone	1.05	0.13	0.49	1.3	0.6
DGR-2 830.05	Gull River	limestone-dolostone	0.89	0.32	2.21	1.2	-1.3
DGR-2 840.06	Shadow Lake	limestone-dolostone	7.80	0.37	6.79	1.1	1.0
DGR-2 846.31	Cambrian	sandy limestone-dolostone	3.60	0.29	1.55	1.2	2.1
DGR-2 852.39	Cambrian	Sandstone	18.60	0.71	17.90	1.1	0.7
DGR-2 855.89	Cambrian	Sandstone	15.85	0.94	16.63	1.2	-0.8
DGR-2 861.90	Precambrian	granitic gneiss	3.70	0.52	3.57	1.2	0.1

*¹Porewater-loss and physical porosities were calculated using equations 12 and 13, respectively; section 4.4 of main report.

²Uncertainty determined using Gaussian error propagation applied to equations 12 or 13; section 4.4 of main report.

³Positive value indicates porewater-loss porosity is larger than physical porosity; Shading indicates difference is greater than the uncertainty in the physical porosity.